Isoprenoid biosynthesis, specificities and homeostasis in plants : genetic approach for the identification of regulators by screening for suppressors of growth defect

Claire Villette

UNIVERSITÉ DE STRASBOURG

ÉCOLE DOCTORALE DES SCIENCES DE LA VIE ET DE LA SANTE

Institut de Biologie Moléculaire des Plantes (CNRS)

THÈSE présentée par

Claire VILLETTE

soutenue le 11 mai 2017

pour obtenir le grade de **Docteur de l'université de Strasbourg**

Discipline/ Spécialité : Aspects moléculaires et cellulaires de la biologie.

Isoprenoid biosynthesis, specificities and homeostasis in plants. Genetic approach for the identification of regulators by screening for suppressors of growth defect.

THÈSE dirigée par :
Dr. SCHALLER Hubert — Directeur de recherche, IBMP Strasbourg

RAPPORTEURS :
Pr. HANSSON Mats — Professeur, Université de Lund
Dr. LI-BEISSON Yonghua — Chercheur, CEA Cadarache

EXAMINATEUR :
Pr. SCHMIT Anne-Catherine — Professeur, Université de Strasbourg

Acknowledgement

I would like to thank the Carlsberg Company and the Region Alsace for funding this thesis, and CNRS and IBMP where my work was hosted. Many thanks to the members of the Carlsberg Research Center for their precious advice.

Thanks to Mats Hansson, Yonghua Li-Beisson and Anne-Catherine Schmit for accepting to review this thesis work, and thanks to Luc Didierjean for his participation to the jury.

Sincere thanks to Hubert Schaller for his confidence and the liberty he gave me in my work.

Thanks to the members of the team, Monique Schmitz for the help in *in vitro* cultivation, Anne Berna and Andréa Hemmerlin for the help in the experiments. Thanks to Thomas Bach for the careful reading of the manuscript. Pierre Mercier, thank you for your involvement in the many projects of the team.

Muito obrigada to Sylvain Darnet and Elaine Pessoa, who welcomed me as a precious gest in Brazil and made a huge work on the sequencing part. Obrigada to “las meninas” too! You were right: no final, tudo dá certo…

A special though for the team of Daniele Werck and the members of the metabolomic platform with whom I had nice relations. Dimitri, merci pour ta diligence !
Thanks to the sequencing platform of IGBMC for the nice collaboration and interesting talks. Thanks to Louwrance Right and Diego Gonzalez for the measurements of metabolic intermediates of the MEP pathway. Thanks to Malek Alioua for the sequencing, and to the gardeners’ team for the many plants they provided for such screens. Marta, merci beaucoup pour ton implication, ta patience et ta motivation dans la mise en place de la culture d’orges, en plus de l’énorme travail sur *Arabidopsis* et *Nicotiana*. Merci également à l’équipe du Jardin Botanique de Strasbourg pour sa collaboration sur le sujet de l’orge.

Gratitude to the students who joined the lab during my thesis work and helped me, Marie-Angélique Schott, Saretta Paramita, and particularly to Caroline Mercier who made an amazing work on the pollen part.

Extended summary (in French) of the thesis validated by the doctoral school.

Objectifs de la thèse

Chez les plantes, la croissance est influencée des facteurs génétiques ou environnementaux, par des processus tels que l'assimilation des nutriments et la photosynthèse, ou par des produits issus du métabolisme, comme les hormones, ou les pigments intervenant dans la photosynthèse. Beaucoup de ces produits appartiennent à la famille des isoprénoïdes. Citons par exemple les cytokinines, les gibbérellines, l'acide abscissique ou les brassinostéroïdes dans le cas des hormones ; les caroténoïdes, chlorophylles et tocophérols impliqués dans la photosynthèse, et les stérols dont le rôle de structurants membranaires est bien documenté.

Deux voies de biosynthèse distinctes sont décrites chez les plantes pour produire les isoprénoïdes : la voie cytosolique du mévalonate (MVA) mène à la production de stérols et de brassinostéroïdes ; la voie plastidiale du méthylérythritol phosphate (MEP) aboutit aux pigments photosynthétiques. Les enzymes impliquées dans ces deux voies ainsi que les intermédiaires biosynthétiques produits sont connus, mais les informations concernant leur régulation sont manquantes. Pour élucider les mécanismes de cette régulation des voies de biosynthèse du MVA et du MEP, une étude génétique a été engagée avec comme matériel biologique deux mutants d'*Arabidopsis thaliana*, présentant un déficit de synthèse de précurseurs isopréniques dans l'une et l'autre des voies biosynthétiques. Le mutant *hmg1-1* présente un défaut partiel de synthèse de mévalonate et de stérols. En effet, l'allèle *hmg1-1* du gène codant la 3-hydroxy-3-méthylglutarylcoenzyme A réductase 1 (HMGR1) est porteur d'une insertion de T-DNA invalidante chez ce mutant ; seule l'enzyme HMGR2 est fonctionnelle. Par ailleurs, le mutant *chs5* (*chilling sensitive 5*) présente une production réduite

de chlorophylle et de pigments photosynthétiques. Il porte une mutation ponctuelle dans le gène codant la 1-deoxy-D-xylulose 5-phosphate synthase 1 (DXS1), conférant un défaut partiel de 1-deoxy-D-xylulose 5-phosphate dans la voie du MEP. Ces mutants montrent des phénotypes caractéristiques : diminution de la croissance et du remplissage des siliques chez *hmg1-1*, feuilles albinos ou présentant des marbrures jaunes chez *chs5*. Une première partie de la thèse est une étude génétique visant à identifier les régulateurs (ou contrôleurs) de la synthèse et de l'accumulation d'isoprénoïdes. Cette étude a consisté à isoler et caractériser des mutants porteurs d'allèles suppresseurs des phénotypes déficitaires causés par *hmg1-1* ou *chs5*.

Le rôle des hormones issues du métabolisme d'isoprénoïdes est essentiel pour le développement des plantes. Des applications importantes en découlent dans le domaine de l'agriculture. Ainsi, des mutants de blé (*Triticum aestivum*) de taille réduite, dits « semi-nains », sont porteurs d'une mutation au locus *Rht-1* (*Reduced height*), qui a pour effet de diminuer la réponse aux gibbérellines en termes d'élongation des entre-nœuds tout en maintenant des rendements élevés en production de grains. Ce caractère a été introgressé dans des variétés de céréales d'intérêt agronomique, particulièrement pour contrer les phénomènes de verse des cultures, et ainsi obtenir de meilleurs rendements en réduisant les pertes dues aux intempéries. L'exploitation de telles variétés en agriculture a défini une période appelée « révolution verte », à partir des années 1960. Les brassinostéroïdes constituent une autre classe d'hormones agissant sur l'élongation cellulaire et par conséquent sur la taille des plantes. Une deuxième partie de la thèse a porté sur la génétique de la réponse aux brassinostéroïdes chez une céréale modèle, l'orge (*Hordeum vulgare*), en collaboration avec un partenaire industriel. Afin d'identifier de nouveaux loci impliqués dans cette réponse, et plus généralement dans le but de détailler le rôle des isoprénoïdes dans les mécanismes de la croissance végétale, des suppresseurs du phénotype « semi-nain » d'un mutant d'orge partiellement déficitaire dans la réponse au brassinostéroïdes ont été recherchés. Le mutant « semi-nain » *ert-ii.79* est affecté par une double substitution sur le récepteur de brassinostéroïdes (BRI1), empêchant une perception correcte du signal hormonal.

Enfin, dans une troisième partie de la thèse, nous nous sommes intéressés à une étape particulière de la fécondation chez les angiospermes, à savoir, l'élongation du tube pollinique, dans le contexte de la spécificité de la biosynthèse des stérols, une catégorie essentielle de lipides isopréniques. Le pollen ou gamétophyte mâle émet lors de sa germination

un type cellulaire présentant une croissance rapide et polarisée : le tube pollinique. Lors de cette élongation cellulaire, nous avons observé une accumulation de composés intermédiaires de la voie de biosynthèse des stérols, et l'absence des produits typiques du sporophyte. Ces composés, principalement le cycloeucalénol, présentent un motif 9β,19-cyclopropanique sur le noyau tétracyclique stérolique, ce qui indique l'arrêt de la chaîne biosynthétique au niveau de l'étape d'isomérisation du cycloeucalénol en obtusifoliol par l'enzyme cycloeucalenol obtusifoliol isomerase (CPI). Les travaux engagés dans cette partie de la thèse ont consisté en une analyse fonctionnelle de la biosynthèse des stérols chez le gamétophyte mâle.

Ainsi, les travaux réalisés dans cette thèse m'ont amenée à m'intéresser à des plantes modèles distinctes, à leur génétique, à un organisme haploïde, le pollen, donnant un type cellulaire particulier, en ciblant des gènes importants de la biosynthèse d'isoprénoïdes, pour ouvrir la voie à l'identification des régulateurs centraux ou « master switches » du métabolisme d'isoprénoïdes.

Résultats

Isolement de mutants suppresseurs d'un défaut de biosynthèse de précurseurs isopréniques chez *Arabidopsis thaliana*.

Les criblages des lignées d'*Arabidopsis thaliana hmg1-1* et *chs5* mutagénisées à l'EMS ont permis d'identifier dans les générations M2, des individus suppresseurs caractérisés par une restauration de la croissance et du remplissage des siliques d'une part (*sup hmg1-1*), et une restauration du phénotype chlorophyllien d'autre part (*sup chs5*). Ces individus ont été caractérisés d'un point de vue phénotypique sur deux générations successives. Les caractères choisis pour l'identification des individus suppresseurs sont le remplissage des siliques (poids des siliques de la hampe principale) et la taille des plantes (*sup hmg1-1*) ou le reverdissement des feuilles et une croissance restaurée en conditions *in vitro* (*sup chs5*). Un croisement avec la lignée parentale a permis d'obtenir des populations F2 dans lesquelles la ségrégation des caractères d'intérêt est étudiée. Les résultats obtenus permettent d'identifier plusieurs types de mutations : allèles récessifs, allèles dominants, en particulier. Au cours de la thèse, 14 lignées *sup hmg1-1* et 6 lignées *sup chs5* ont été étudiées plus particulièrement. Les mutations sélectionnées sont en cours d'identification par séquençage profond du génome d'individus des populations recombinantes F2 (analyse NGM « next-generation-mapping »). Pour cela, ces

populations ont été échantillonnées en « bulk-segregants », de façon à regrouper les individus suppresseurs et les individus non suppresseurs. Le séquençage du génome a été réalisé en collaboration avec la plateforme de séquençage de l'IGBMC (B. Jost). L'analyse des données obtenues est faite actuellement avec la participation de Sylvain Darnet (Laboratório de Biotecnologia Vegetal, Instituto de Ciências Biológicas, Universidade Federal do Pará (UFPA), Belém, Brazil), dans la cadre d'une collaboration cadrée par un LIA-CNRS (Laboratoire International Associé), et permettra d'identifier un ou plusieurs gènes responsables de la restauration du phénotype recherché dans les lignées suppresseurs d'un défaut de biosynthèse d'isoprénoïdes.

Sélection de mutants d'orge « overgrowth » et « early maturity » dans un fond génétique *bri1* déficitaire dans la perception du signal brassinostéroïde.

La lignée d'orge semi naine *ert-ii.79* a été mutagénisée à l'azide de sodium. La population d'individus M2, obtenue des caryopses M1, a été criblée afin d'identifier des individus présentant une taille comparable à celle d'une orge de fond génétique sauvage. Lors de ce crible, quatre candidats suppresseurs de défaut de taille ont été identifiés, appelés *sup ert-ii.79* (mutant « overgrowth »). De plus, six individus *sup ert-ii.79 em* présentant une maturité précoce (*em*, « early maturity ») ont été isolés. Ce caractère lié au développement de l'épi est intéressant à étudier dans le contexte de la régulation hormonale de la croissance et du développement des céréales. Les lignées candidates sélectionnées ont été caractérisées d'un point de vue phénotypique : date de maturité, taille des plantes, morphométrie des épis. Le phénotype chimique a été détaillé, particulièrement pour ce qui concerne le contenu en hormones végétales. Pour cela, une méthode d'extraction a été mise au point à partir de tissus foliaires en vue d'analyser en une seule fois jusqu'à 10 hormones, par chromatographie liquide ultra performance et spectrométrie de masse (UPLC-MS), sur la plateforme de métabolomique de l'IBMP (D. Heintz). Un croisement avec la lignée parentale a été réalisé afin d'obtenir des populations F2, dans lesquelles ségrégent des individus suppresseurs et non suppresseurs, permettant de définir ainsi la génétique formelle des mutations sélectionnées. Une analyse du génome en « exome capture », ainsi qu'une analyse du transcriptome, sont actuellement projetées. En effet, ces approches sont plus appropriées qu'un séquençage profond du génome comme dans le cas d'*Arabidopsis thaliana*, pour l'identification des mutations responsables des phénotypes sélectionnés, en raison de la grande taille du génome. Des prélèvements ont été réalisés sur les populations F2 disponibles, en vue de ces analyses.

Spécificités de la biosynthèse des stérols chez le gamétophyte mâle.

Le profil stérolique des grains de pollen et des tubes polliniques a été caractérisé chez différentes espèces de plantes par chromatographie gazeuse couplée à la spectrométrie de masse. Les tubes polliniques ont été cultivés *in vitro* en milieu liquide, avec apport de glucose non marqué (^{12}C) ou marqué (^{13}C) dans le milieu. Les stérols présents dans un extrait brut et séparés en chromatographie gazeuse sont identifiés par la détection d'ions fils de valeur masse/charge caractéristique, obtenus après ionisation par impact électronique et fragmentation de l'ion moléculaire. Les produits néo synthétisés par les tubes polliniques en croissance, à partir du glucose marqué, sont identifiés par l'enrichissement isotopique de leurs spectres de masse. Les produits préexistants dans le grain de pollen non germé sont quant à eux caractérisés par un spectre de masse reflétant l'abondance naturelle du ^{13}C. De ce fait, il est possible d'identifier les stérols nouvellement synthétisés au sein des tubes polliniques. L'accumulation d'un produit, le cycloeucalénol, est ainsi révélée. Ce produit est dans le cas du sporophyte, un intermédiaire de la synthèse des phytostérols. Ainsi, ces expériences ont montré que la voie de biosynthèse des stérols est tronquée chez le tube pollinique. En effet, les produits situés en aval de l'enzyme CPI (cycloeucalénol obtusifoliol isomérase) ne présentent pas d'enrichissement isotopique (ils préexistent dans le grain de pollen avant germination du tube pollinique), tandis que les produits situés en amont de cette étape enzymatique sont enrichis, jusqu'à hauteur de 20% de l'enrichissement en abondance naturelle. Ces observations ont été répétées chez plusieurs espèces végétales et montrent que la présence d'une voie de biosynthèse de stérols tronquée chez le gamétophyte mâle lors de la germination du tube pollinique est conservée. Chez *Nicotiana tabacum*, l'analyse de tubes polliniques prélevés en conditions semi *in vivo* a confirmé la présence exclusive de cycloeucalénol dans les parties apicales de ces tubes.

Afin de caractériser un avantage sélectif potentiel conféré par cette voie de biosynthèse de stérols tronquée, nous avons cherché pour documenter cette hypothèse, à restaurer une voie de biosynthèse de type sporophytique chez le gamétophyte mâle, pour en évaluer les conséquences biologiques sur la fécondation. Pour cela, des disques foliaires de *Nicotiana tabacum* et *Nicotiana benthamiana* ont été transformés avec un T-DNA porteur d'un cDNA codant une enzyme de fusion CPI-GFP (cycloeucalénol-obtusifoliol isomérase fusionnée à la « green fluorescent protein ») sous contrôle du promoteur LAT52 spécifique du pollen. Les tubes polliniques des plantes ainsi générées ont été analysés. Leur profil stérolique a montré la conversion totale du cycloeucalénol en obtusifoliol, indiquant que l'étape enzymatique

manquante avait été restituée dans la voie de biosynthèse. En fait, l'obtusifoliol obtenu par l'action de l'enzyme CPI-GFP s'accumule comme un produit final, suggérant l'absence de toutes les enzymes suivantes normalement présentes chez le sporophyte. Une étude de ségrégation est en cours de finalisation afin de déterminer si les tubes polliniques accumulant de l'obtusifoliol sont affectés dans leur capacité à transmettre leur patrimoine génétique, comparé à la capacité de tubes de génotype sauvage (non transformés). En effet, la modification du profil stérolique des tubes polliniques pourrait altérer leur capacité d'élongation rapide au travers du tissu transmetteur du style des fleurs, et la stabilité de leur membrane. Ce dernier point est en cours d'analyse grâce à l'utilisation de sondes ratiométriques fournies par Andrey Klymchenko (laboratoire de biophotonique, UMR 7213, Faculté de Pharmacie, Université de Strasbourg), ciblant spécifiquement le feuillet externe des membranes pour l'une, et les systèmes endomembranaires pour l'autre.

Conclusion

Les différents criblages génétiques effectués chez *Arabidopsis thaliana* et *Hordeum vulgare* ont permis de sélectionner plusieurs lignées présentant un phénotype suppresseur des effets phénotypiques causés par les mutations parentales (*hmg1-1*, *chs5*, *ert-ii.79*). Les phénotypes de réversion ont été détaillés sur le plan phénotypique : mesures morphométriques, dosages de produits d'intérêt (pigments, hormones, intermédiaires biosynthétiques), mesures de l'expression de gènes impliqués dans les voies de biosynthèse étudiées. Les populations F2 recombinantes analysées montrent la présence d'allèles suppresseurs dominants ou récessifs, indiquant l'existence probable de différents mécanismes de compensation de défauts de production de précurseurs d'isoprénoïdes ou de signalisation par des produits finaux (brassinostéroïdes). Les échantillons d'ADN génomiques issus de classes phénotypiques d'individus de populations recombinantes d'*Arabidopsis thaliana* sont en cours d'analyse par séquençage profond ; les premiers résultats permettent de mettre en évidence quelques mutations dans des allèles de gènes potentiellement impliqués dans des mécanismes de régulation des voies du MVA et du MEP.

La culture de l'orge a été démarrée et adaptée au sein de l'IBMP et fonctionne maintenant en routine, de même que le protocole d'extraction et d'analyse permettant d'identifier plus de dix hormones végétales simultanément. La génétique de l'orge nécessite une organisation particulière, de par les surfaces de culture nécessaires et les temps de génération, bien plus longs

que chez *Arabidopsis thaliana*. Un partenariat avec le Jardin Botanique de Strasbourg a permis de mettre en place des parcelles d'essai en conditions extérieures, intéressantes pour travailler avec des plantes cultivées. La prochaine étape de ce projet consiste à analyser les transcriptomes ou les exomes des lignées sélectionnées dans ce travail de thèse en vue d'identifier les mutations impliquées dans les évènements de réversion.

L'analyse des profils stéroliques de grains de pollen et de tubes polliniques chez différentes espèces végétales et la mise en évidence d'une voie de biosynthèse tronquée a donné lieu à la publication d'un article (Villette et al. (2015) Lipids 50:749-60). La suite du projet visant à rétablir une CPI fonctionnelle dans les tubes polliniques de tabac et à analyser leur capacité à transmettre leur patrimoine génétique donnera lieu à un second article (en cours de rédaction).

Table of contents

List of abbreviations

2iP: 6-(γ,γ-dimethylallylamino)purine

ABA: abscisic acid

ACN: acetonitrile

AF: allelic frequency

BAP: 6-benzylaminopurine

BL: brassinolide

BIN2: brassinosteroid insensitive 2

BRI1: brassinosteroid insensitive 1

CAS: cycloartenol synthase

CDP-ME: 4-(cytidine 5'diphospho)-2-*C*-methyl-D-erythritol

CDP-MEP: 2-phospho-4-(cytidine 5'diphospho)-2-*C*-methyl-D-erythritol

chs5: chilling sensitive 5

Col-0: Columbia-0 ecotype

CPI: cyclopropylsterol isomerase

CS: castasterone

CT: cathasterone

CTAB: cetyltrimethylammonium bromide

CMK: 4-(cytidine 5'-diphospho)-2-*C*-methylerythritol kinase

CPI: cyclopropyl isomerase

DMAPP: dimethylallyl diphosphate

DXP: 1-deoxy-D-xylulose 5-phosphate

DXR: 1-deoxy-D-xylulose 5-phosphate reductoisomerase

DXS: 1-deoxy-D-xylulose 5-phosphate synthase

EDTA: ethylenediaminetetraacetic acid

EMS: ethyl methanesulfonate

FDS: farnesyl diphosphate synthase

FPP: farnesyl diphosphate

GA: gibberellin A

GAP: glyceraldehyde 3-phosphate

GC-MS: gas chromatography and mass spectrometry

GFP: green fluorescent protein

GGPP: geranylgeranyl diphosphate

HDR: 4-hydroxy-3-methylbut-2-enyl diphosphate reductase

HDS: 4-hydroxy-3-methylbut-2-enyl diphosphate synthase

HMGR: 3-hydroxy-3-methylglutaryl coenzyme A reductase

HMGS: 3-hydroxy-3-methylglutaryl-coenzyme A synthase

IAA: indole-3-acetic acid

IDI: isopentenyl diphosphate:dimethylallyl diphosphate isomerase

INDELS: insertions and deletions

IPP: isopentenyl diphosphate

JA: jasmonic acid

KIN: kinetin

LAS: lanosterol synthase

LAT52: *Solanum lycopersicum* pollen specific promotor

LRR: leucine-rich repeat

LRR-RLK: leucine-rich repeat receptor-like kinase

MCT: MEP cytidyltransferase

MEcDP: 2-*C*-methylerythritol 2,4-cyclodiphosphate

MEcPP: 2-*C*-methyl-D-erythritol 2,4-cyclopyrophosphate

MDC: mevalonate diphosphate decarboxylase

MDS: 2-*C*-methylerythritol 2,4-cyclodiphosphate synthase

MEP: 2-*C*-methyl-D-erythritol 4-phosphate

MVK: mevalonate kinase

MVA: mevalonic acid

NaCl: sodium chloride

NaN_3: sodium azide

NGS: next generation sequencing

PMVK: 5-phosphomevalonate kinase

SNP: single nucleotide polymorphism

SQE: squalene epoxydase

SQS: squalene synthase

TIC: total ion current

UPLC-MS/MS: ultra-performance liquid chromatography and tandem mass spectrometry

VEP: variant effect predictor

WS2: wassilewskja ecotype

List of tables

List of figures

List of supplemental figures

Introduction

I. Isoprenoid diversity, chemical structures and functions.

1. Isoprenoid diversity in the biological world.

Isoprenoids are widely represented and diversified among living organisms, from animals to bacteria, algae, fungi and plants. Various isoprenoids play a role as end products in many biological processes such as cell division and elongation (sterols), photosynthesis (carotenoids), and respiration (ubiquinones) in plants, and for this reason must be considered as primary metabolites. Some of these pathway end products are in turn precursors for the synthesis of oxidized compounds that define specialized (so-called "secondary") metabolic pathways. This is for instance the case of cholesterol, an abundant isoprenoid lipid in the solanaceae (*Solanum tuberosum*, *Solanum lycopersicum*), where it serves as precursor for the biogenesis of the steroidal alkaloids solanine and tomatine (Sonawane et al., 2016). More generally speaking, mammals, algae, fungi and plants use sterols as membrane constituents, but also as precursors for the production of other biologically active molecules such as the hormone brassinosteroids in plants (Clouse, 2011) or the steroid hormones estradiol (**Figure 1, A**), progesterone and testosterone that are essential in mammalian development and reproduction. Cholesterol in mammals leads also to the synthesis of bile acids, a series of steroid acids involved in fat absorption or stress response (Wollam and Antebi, 2011).

Among the isoprenoid lipids, carotenoid pigments are precursors of vitamin A, which plays a role in vision, growth, reproduction and neural development. Isoprenoids are frequently accumulated and stored, for example as oil in the liver of some fishes that are rich in squalene, a C_{30} linear isoprenoid (Huang et al., 2009).

Although being essential to normal developmental processes, some isoprenoids are not synthesized by all organisms. In fact, insects are unable to synthesize cholesterol but its uptake as a nutrient is mandatory for growth and development (Urich, 2013). Sterols are precursors of ecdysteroids (**Figure 1, B**), which act on larval development as a hormone and play a role in mating behaviors and reproduction (Wollam and Antebi, 2011).

In fungi, ergosterol (**Figure 1, C**) is the end product of the sterol pathway. It is a component of cell membranes, as it is the case of cholesterol in animals. In addition to its membrane-related

functions, ergosterol plays a role in the cell cycle (Gaber et al., 1989). The ergosterol pathway has been well studied and is a target of antifungal agents to be used in medicine or agriculture (Lees et al., 1995).

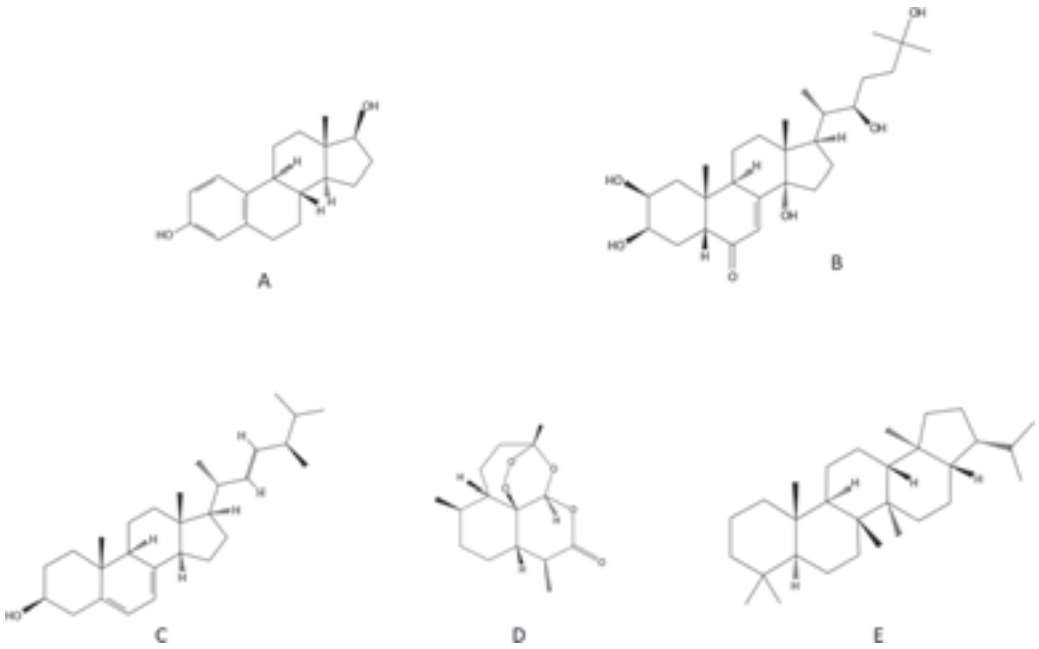

Figure 1. Isoprenoid diversity across the biological world. Examples of the structural and functional isoprenoid diversity in animals (A, estradiol), insects (B, ecdysone), fungi (C, ergosterol), plants (D, artemisinin) and bacteria (E, hopane). Structures from PubChem.

In plants, a wealth of isoprenoids act as signal molecules produced by semio-terpene synthases or traumato-terpene synthases (Bouvier et al., 2005). These isoprenoids play a role in plant-environment interactions, to attract pollinators or as a protection against herbivores and pathogens (Rodríguez-Concepción and Boronat, 2015). Plants are sessile organisms and had to develop ways to face biotic and abiotic stresses, which could explain the huge diversity of isoprenoids found in plants. This diversity has been valorized for human use: biofuels, agrochemicals and polymers in industry; aromas and pigments for food or cosmetics; bioactive compounds in pharmacy. In the medical field, isoprenoid compounds are used to treat human diseases. For example, paclitaxel (also called Taxol) extracted from *Taxus brevifolia* acts as an anticancer agent (Strobel et al., 1993), and artemisinin (**Figure 1, D**) from *Artemisia annua L.* is efficient as antimalarial drug and against parasitic protozoa (Shi Ni Loo et al., 2016).

Marine organisms often show the same series of isoprenoid compounds as found in plants, the major isoprenoids depending on the species considered. As in other organisms, they play a role

in membrane structure and fluidity, stress response and defense against pathogens (Kumari et al., 2013). Algal sterols are beneficial for human health as antioxidants, antidiabetic, and anti-inflammatory compounds for example. Algae also synthesize pigments like carotenoids or chlorophylls. Soft corals and sponges are known to contain diterpenes specific to sea organisms. The biosynthesis pathways of marine isoprenoids are not well studied because of the difficulty to isolate and grow these organisms (Kashman and Rudi, 2004).

Most of the bacteria do not produce sterols, but hopanoids (**Figure 1, E**). These are bacterial membrane lipids that fulfill the same role in the regulation of membrane fluidity and stability (Kannenberg and Poralla, 1999; Sáenz et al., 2015). Bactoprenol (undecaprenyl phosphate, C_{55}-P) is described as an important lipid for the establishment of bacterial cell walls as it is involved in the biosynthesis of peptidoglycans and cell-wall polysaccharides. Because of its vital functions, C_{55}-P is a target of bacitracin antibiotic (Bouhss et al., 2008). Chlorophototrophic bacteria possess bacteriochlorophylls harvesting light energy, and are able to synthesize the isoprene pigments carotenoids (Maresca et al., 2008), which are photoprotective too. Archaea are unicellular microorganisms often living in extreme environments like salt lakes and hot springs. They contain specific lipids (archaeol and caldarchaeol for example), differing in their stereostructure, the presence of ether linkages, the type of side chains, and their bipolarity allowing the formation of monolayers (Koga and Morii, 2007; Jain et al., 2014).

2. Chemical structures of plants isoprenoids.

Isoprenoids are diversified across the biological world, as much by their structure as by their function, as it has been exemplified above in the case of sterols and steroids. This study focuses on plant isoprenoids. Their structure and nomenclature are described by the International Union of Pure and Applied Chemistry (IUPAC). The structural basis of isoprenoids, also called terpenoids, is a five-carbone building unit. All isoprenoids derive from isopentenyl diphosphate (IPP) and its isomer dimethylallyl disphosphate (DMAPP) (**Figure 2**).

Figure 2. Isoprene units are derived from isopentenyl diphosphate (IPP, A) or its isomer dimethylallyl disphosphate (DMAPP, B).

Isoprenoids are classified according to the number of C_5 isoprene units added head-to-tail or head-to-head: monoterpenes (C_{10}, citral, geraniol), diterpenes (C_{20}, side chain of chlorophylls), triterpenes (C_{30}, squalene), tetraterpenes (C_{40}, carotenoids), polyterpenes (C_{5n}, polyprenols, dolichols, natural rubber).

3. Isoprenoids as membrane constituants in plants.

Plant membranes consist of phospholipid bilayers that need to be maintained in a microfluidic state to keep their properties and biological functions. Sterols are involved in the regulation of membrane fluidity and permeability as membrane components. They are inserted between phospholipids with the hydroxyl group of carbon 3 facing the hydrophilic environment, and the aliphatic side chain into the hydrophobic structure formed by acyl chains (**Figure 3**). The ordering effect is due to their capacity to restrict the mobility of the fatty acyl chains of phospholipids (Hartmann, 1998). Apart from the free hydroxyl group and the side chain, the planar geometry of sterols is another essential structural property needed for their role in ordering lipid bilayers (Sáenz et al., 2015; Miller et al., 2012).

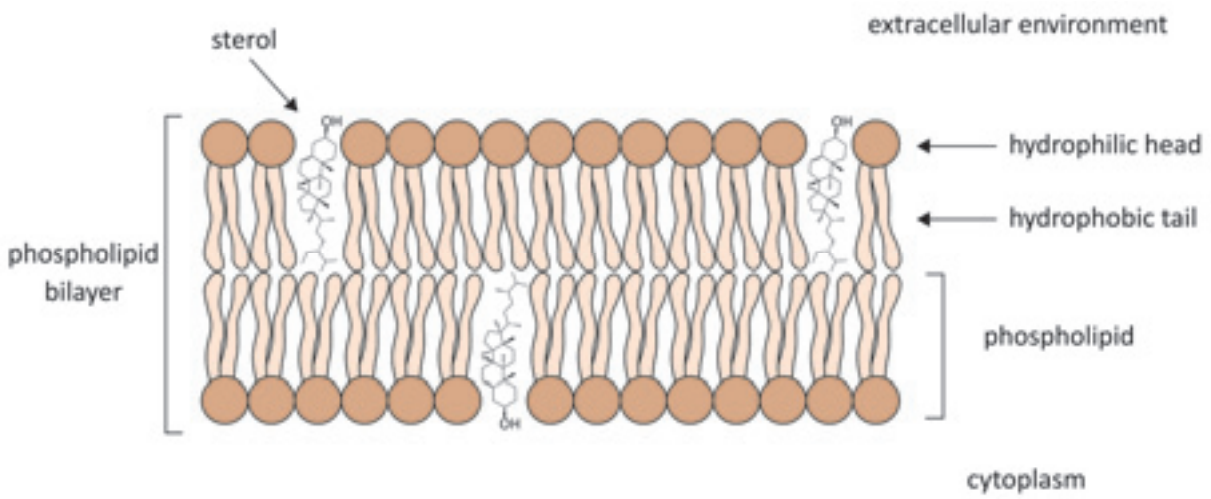

Figure 3. Sterols maintain membrane integrity when inserted between phospholipids of the bilayer.

The sterol structure is composed of four rings (A, B, C, D), carrying a hydroxyl group on carbon 3, a double bond at C5-6 and a side chain on carbon 17. Carbon numbering has been defined by the International Union of Pure and Applied Chemistry (Moss, 1989) as presented in **Figure 4**.

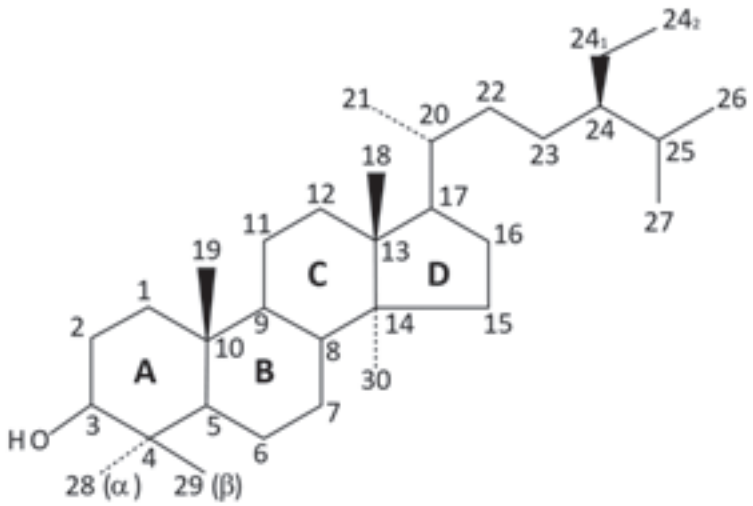

Figure 4. Carbon numbering nomenclature of sterols as defined by the International Union of Pure and Applied Chemistry (IUPAC).

While many organisms (mammals, fungi) present one main end-product, plants use a mixture of different sterols. More than 200 phytosterols have been described (Moreau et al., 2002), but three major end products are found in almost all plant species: campesterol, sitosterol and stigmasterol (**Figure 5**). The ratio between 24-methyl sterols (campesterol) and 24-ethyl sterols (sitosterol) depends on the plants species considered. The majority of plant sterols are found as free sterols and serve as membrane components, but they can also be conjugated, for example esterified with fatty acids and stored in lipid droplets (Schaller et al., 1995) or glycosylated to exert specialized functions like for instance steroidal saponins or alkaloids (Bouvier-Navé et al., 2010). Campesterol is in most plants the precursor for the biosynthesis of other important molecules as the brassinosteroids hormones (Fujioka and Yokota, 2003).

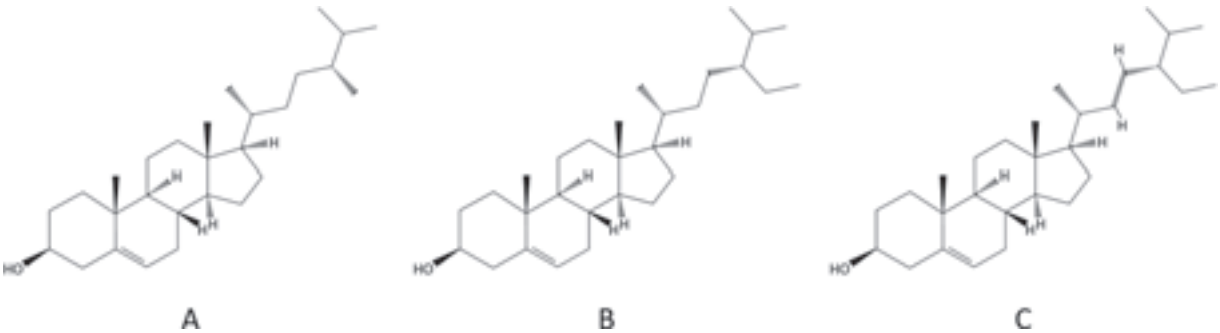

Figure 5. Three major sterols are found in almost all plant species: campesterol (A), sitosterol (B) and stigmasterol (C).

4. Many plant hormones are isoprenoids.

Brassinosteroids, gibberellins and abscisic acid are plant hormones and are part of the isoprenoid group of compounds. They are involved in the regulation of plant growth.

Brassinolide (BL) (**Figure 6, A**) is the first brassinosteroid discovered from the pollen of *Brassica napus* (Grove et al., 1979). It is the end-product of the brassinosteroid biosynthesis pathway, and the most bioactive product together with castasterone among the 65 free brassinosteroids and five conjugates described (Bishop and Koncz, 2002; Bajguz, 2007). Brassinosteroids are hydroxylated compounds derived from campesterol (Fujioka and Yokota, 2003). They act as plant growth regulators and are involved in cell division and mostly in cell elongation. Mutants affected in brassinosteroids biosynthesis or signaling, display dwarf phenotypes. Brassinosteroids play a role in other processes throughout the plant life, in seed germination, flowering, maturation, stress resistance and senescence. As hormones, they also interact in synergy with auxins (Bajguz, 2007) and regulate the biosynthesis of gibberellins (Unterholzner et al., 2015).

Numerous gibberellins (GA) (**Figure 6, B**) have been described that are involved in plant growth promotion by acting on cell division and elongation. Plants treated with exogenous gibberellins show an increase in shoot growth, internode elongation and leaf expansion and enhanced apical dominance. This growth promoting role is due to the gibberellin induction of DELLA-proteins degradation, which are responsible for growth inhibition. Gibberellins also act in the breaking of seed and tuber dormancy (Brian, 1959). In plants, these hormones are synthesized from diterpenes produced in the plastids and were first discovered in the fungus *Gibberella fujikuroi* in Japan (for review, Hedden and Sponsel, 2015).

Figure 6. Structures of isoprenoid plant hormones: brassinolide (A), gibberellin A_4 (B), abscisic acid (C).

Abscisic acid (ABA), as a hormone (**Figure 6, C**) acts on stomatal closure to regulate plant transpiration, and thereby prevents water content. It is up-regulated when the plant is facing water stress, and prevents water loss. Root growth, hydraulic conductivity in shoots and roots, cell turgor maintenance and desiccation tolerance are also modulated by abscisic acid (Wilkinson et al., 2012). The action of abscisic acid is closely related to the environmental conditions (water availability) and the action of other hormones (cytokinins, auxins). More generally, abscisic acid is synthesized in the plants in response to abiotic stresses: heat, cold, drought, salinity, wounding (Verma et al., 2016). Abscisic acid is synthesized by the rate limiting cleavage of carotenoids (violaxanthin or neoxanthin) in chloroplasts and several steps in the cytoplasm (Hauser et al., 2011). Abscisic acid levels are controlled by conjugation for storage in the vacuole and deconjugation when ABA is needed (Verslues, 2016).

5. Compounds of the photosynthetic machinery.

Photosynthetic pigments are compounds capable of capturing solar energy to convert it into chemical energy, and display antioxidant and photoprotective activities. Chlorophyll side chains and carotenoids are plastid isoprenoids synthesized by the specific plastidial biosynthetic route.

Chlorophyll is bound to photosystems I and II to take part in the photosynthesis process in thylakoid membranes (for review, Wang and Grimm, 2015). Chlorophylls absorb light of the solar spectrum in the visible and near-infrared regions. Two types or chlorophylls have been described, chlorophyll *a* and *b*. Chlorophyll *a* (**Figure 7, A**) is found in photosynthesis reaction

centers but also in the light harvesting complexes, and can absorb light around 670nm. Chlorophyll *b* is situated in the light-harvesting complexes and has an absorption spectrum situated near 650nm, which allows flexibility in the plant adaptation to light quality changes during the day (Croce et al., 2014).

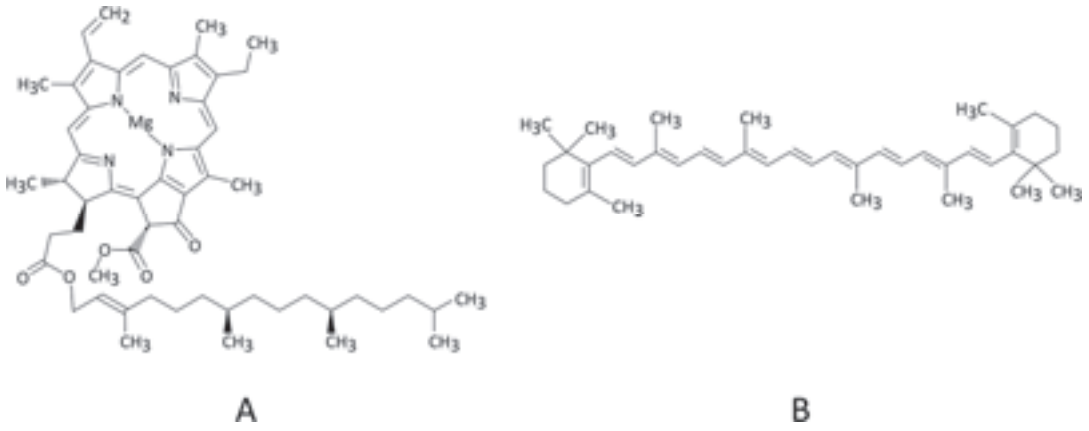

Figure 7. Chlorophyll a (A) and β-carotene (B) are compounds of the photosynthetic machinery.

Carotenoids (**Figure 7, B**) are C_{40} isoprenoids that play an important role in the photoprotection mechanism. These pigments are situated close to the chlorophylls in the light harvesting complexes. They avoid the formation of lethal reactive oxygen species that could derive from photosynthesis (Croce et al., 2014). In flowers, carotenoids bring color and are precursors for aromas and fragrances (like for instance β-ionones), thus attracting pollinators. They are essential in the diet of animals, which are unable to synthesize it *de novo* (Zhai et al., 2016). As we have seen previously, carotenoids are also precursors of abscisic acid, an important hormone in the plant life cycle.

II. Two distinct isoprenoid biosynthetic pathways occur in plants.

Plants exhibit a specificity in the biosynthesis of isoprenoids as they present two distinct pathways to synthesize isopentenyl diphosphate (IPP) and the diversity of its derivatives (**Figure 8**). One pathway occurs in the cytoplasm, it is called the mevalonate pathway, due to the production of mevalonic acid (MVA) as an important intermediate. The second pathway was described later, first in bacteria then in the plastids of plants and green algae, it is called the 2-*C*-methyl-D-erythritol 4-phosphate (MEP) pathway, also named after the key intermediate of this pathway (for review, Rohmer, 1999). In an evolutionary point of view, the MVA

pathway seems to be the ancestral route to produce IPP in archaebacteria, while eubacteria developed the MEP pathway to synthesize IPP (Lange et al., 2000). The MEP pathway is not found in insects, fungi and animals. Limited exchanges of IPP and prenyl diphosphates (C_5-C_{15}) are possible between the cytosol and plastids (Hemmerlin et al., 2003), but they are not sufficient to compensate the blockage of one or the other pathway by the remaining one (Pulido et al., 2012; Rodríguez-Concepción and Boronat, 2015). Moreover, it seems that the two pathways are not supposed to work synergistically, since the up-regulation of the gene expression of one pathway is concomitant with the down-regulation of the gene expression of the second pathway. The reason why plants retained the two pathways is yet not clear. These two pathways have been studied, genes and proteins involved in the IPP synthesis in the cytoplasm or in plastids are well described, but molecular, biochemical and genetic elements of their regulation are still missing (Rodríguez-Concepción and Boronat, 2015). An interesting way to explore a pathway and its key steps is to study different mutants affected on the successive genes, and to see which ones are the most affected in their phenotypes. In the following parts of this introduction, we will focus on the MVA and MEP pathways, and investigate some key features and plant mutants affected in these pathways.

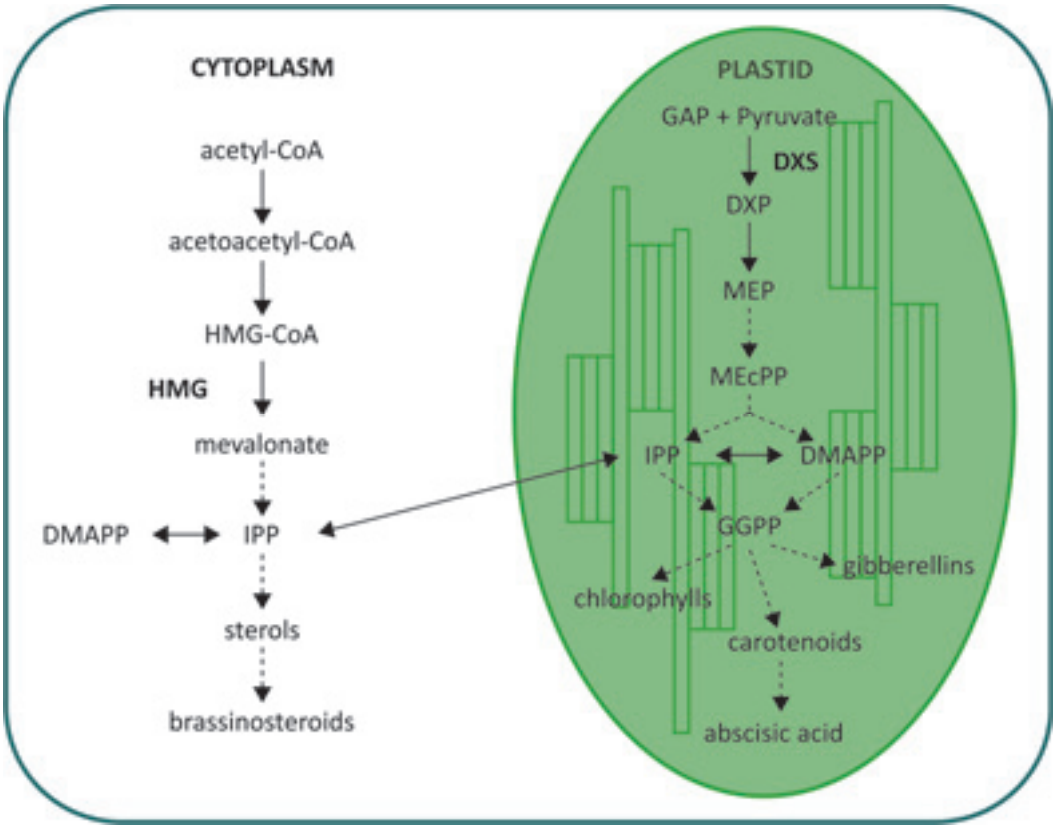

Figure 8. Simplified scheme of the mevalonate (MVA) and 2-*C*-methyl-D-erythritol 4-phosphate (MEP) pathways. The MVA pathway occurs in the cytoplasm and involves the 3-hydroxy-3-methylglutaryl CoA reductase (HMG) as a key enzyme. The MEP pathway is specific of the plastids and necessitates the 1-deoxy-D-xylulose 5-phosphate synthase (DXS) enzyme. Both pathways lead to the production of IPP (isopentenyl diphosphate), precursor of a diversity of end products. Full arrows indicate single steps, dashed arrows indicate multiple steps. GAP: glyceraldehyde 3-phosphate; DXP: 1-deoxy-D-xylulose 5-phosphate; MEcPP: 2-*C*-methyl-D-erythritol 2,4-cyclodiphosphate; DMAPP: dimethylallyl diphosphate; GGPP: geranylgeranyl diphosphate. For an exhaustive overview of isoprenoid biosynthetic schemes and enzymes see Bouvier et al., 2005; Hemmerlin et al., 2012.

1. Focus on the MVA biosynthetic pathway: synthesis of sterols from mevalonate, and brassinosteroids from sterols.

Key enzymes of the MVA biosynthetic pathway.

All the enzymes of the mevalonate pathway are found in the endoplasmic reticulum/peroxisome/cytosol compartments of plant cells (Lange et al., 2000). The pathway is schematically represented in **Figure 9** and starts with the condensation of acetoacetyl-CoA with acetyl-CoA by 3-hydroxy-3-methylglutaryl-CoA synthase (HMGS) to obtain HMG-CoA, further reduced to mevalonate by 3-hydroxy-3-methylglutaryl-CoA reductase (HMGR).

HMGR is a key enzyme in the synthesis of isoprenoids. Indeed, a double mutant for *HGM1* and *HMG2* genes in *Arabidopsis thaliana* is lethal (Suzuki et al., 2009). Mevalonate is phosphorylated at C_5 by mevalonate kinase (MVK), and the conversion of mevalonate phosphate to IPP is catalyzed in two consecutive steps by phosphomevalonate kinase (PMVK) and mevalonate diphosphate decarboxylase (MDC). Thus, the mevalonate pathway uses 3 molecules of acetyl-CoA for the synthesis of 1 molecule of IPP, which can be further isomerized to DMAPP by isopentenyl diphosphate:dimethylallyl diphosphate isomerase (IDI). Subsequent addition of 2 IPPs on the active isoprenic unit that is DMAPP yields farnesyl diphosphate (FPP), produced by farnesyl diphosphate synthase (FDS). Two molecules of FPP condensed head-to-head by squalene synthase (SQS) form squalene, which is then oxidized by the squalene epoxidase responsible for the production of 2,3-squalene oxide. This C_{30} linear triterpenoid is the cyclized into the sterol precursors lanosterol and/or cycloartenol, the latter being the first committed intermediate in the biosynthesis of plant sterols (Enfissi et al. 2005).

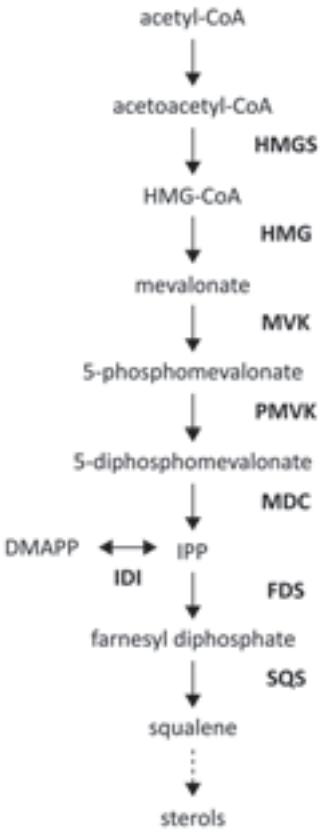

Figure 9. Mevalonate biosynthetic pathway. The mevalonate (MVA) pathway occurs in the cytoplasm and leads to the production of IPP, further converted into essential end products as sterols. Full arrows indicate single steps, dashed arrows indicate multiple steps. HMGS, 3-hydroxy-3-methylglutaryl coenzyme A synthase; HMGR, 3-hydroxy-3-methylglutaryl coenzyme A reductase; MVK, mevalonate kinase; PMVK, 5-phosphomevalonate kinase; MDC, mevalonate diphosphate decarboxylase; IDI, isopentenyl diphosphate:dimethylallyl diphosphate isomerase; FDS, farnesyl diphosphate synthase; SQS, squalene synthase. IPP: isopentenyl diphosphate; DMAPP: dimethylallyl diphosphate.

Plants use a specific detour in the sterol biosynthesis pathway when compared to animals and fungi. The first steps of sterol biosynthesis in plants involves 9β,19-cyclopropylsterols, bearing a cyclopropane ring on cycle B (**Figure 10**). This structure in conserved among the plant species, and is opened by the cyclopropylsterol isomerase enzyme (CPI) later in the biosynthetic pathway to give Δ^8-sterols, further converted into Δ^5-sterols. We can assume that a specific and conserved feature as the use of cyclopropylsterols must confere an advantage at some point in the plant life cycle.

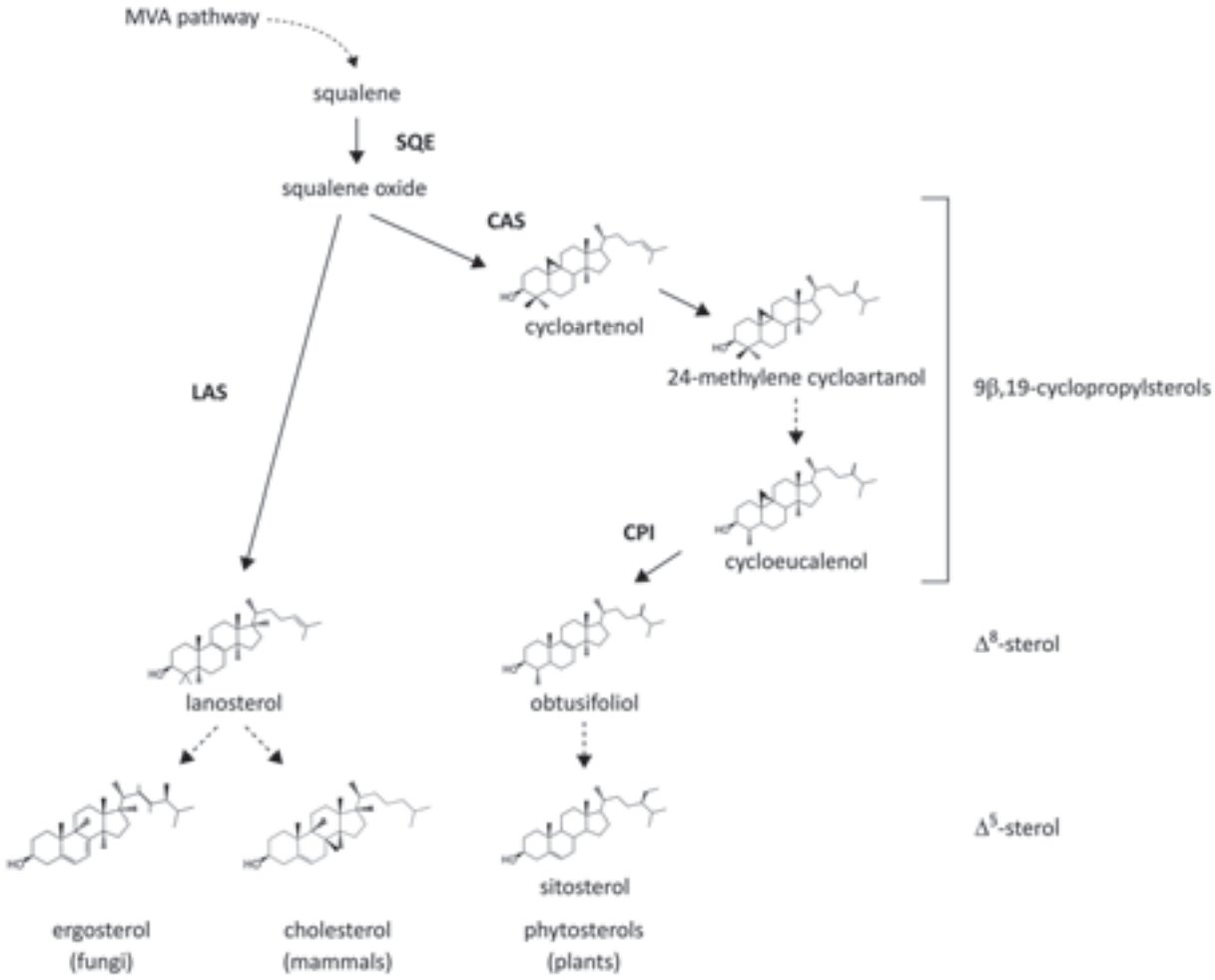

Figure 10. Schematic representation of the sterol biosynthetic pathways in fungi, mammals and plants. Squalene is provided by the mevalonate pathway and converted into squalene oxide, the common precursor of sterols for fungi, mammals and plants. Plants use a specific pathway involving 9β,19-cyclopropylsterols bearing a cyclopropane ring on cycle B, opened by the cyclopropylsterol isomerase (CPI) enzyme. Full arrows indicate single steps, dashed arrows indicate multiple steps. SQE: squalene epoxidase; LAS: lanosterol synthase; CAS: cycloartenol synthase.

Mutants affected in the sterol biosynthetic pathway.

The first requirement for sterol biosynthesis is a functional mevalonate pathway leading to squalene and 2,3-oxidosqualene. As already stated above, a key step of this pathway is the production of mevalonate, mediated by HMGR1 and HMGR2. In *Arabidopsis thaliana*, the *hmg1 hmg2* double mutant is lethal, showing the crucial role of these genes (Suzuki et al., 2009). The *hmg1-1* mutant (**Figure 11, A**) is viable but its size is reduced compared to the wild type, and it produces less seeds in small siliques (Suzuki et al., 2004). Later in the sterol pathway, squalene oxide is converted by the cycloartenol synthase (CAS1) into the first 9β,19-cyclopropylsterol, cycloartenol. In *Arabidopsis thaliana*, plants carrying a *cas1-1* hypomorphic mutant allele develop albino stems and inflorescences (**Figure 11, B**). Strong *cas1* alleles are characterized by a male gametophytic lethality; conditional alleles display leaf albinism and abnormal leaf growth due to a deficiency in the activity of marginal meristems (Babiychuk et al., 2008). The 9β,19-cyclopropyl ring of sterol precursors is isomerized in a subsequent step of the pathway *en route* to the synthesis of the end product campesterol and sitosterol. Indeed, the cyclopropylsterol isomerase CPI is an essential enzyme necessary for the conversion of 9β,19-cyclopropylsterols into Δ^8-sterols. A *cpi1-1* null mutant in *Arabidopsis thaliana* is extremely dwarf (to seedling lethal) and sterile, with small rounded dark leaves (**Figure 11, C**), a short hypocotyl and a defect in root gravitropism, indicating that the plants cannot go through their whole life cycle using only 9β,19-cyclopropylsterols (Men et al., 2008). Downstream the sterol pathway, the conversion of Δ^8-sterols to Δ^7-sterols (and finally, to the Δ^5-sterols usually called “end product”) is in general compatible with the completion of the plant’s life cycle. In fact, *Arabidopsis* mutant that bear weak or even strong alleles of genes encoding enzymes at play in the above-mentioned conversion display a reduced growth and a low fertility. These type of mutants can be rescued by the exogenous supply of brassinosteroids (Schaller, 2003; Fujioka and Yokota, 2003; Schaeffer et al., 2001). In a general point of view, mutants being affected in early sterol biosynthesis have severe embryogenesis and growth defects that cannot be rescued by the application of brassinosteroids. Therefore, it can be stated that sterols play a vital role in the plant life cycle.

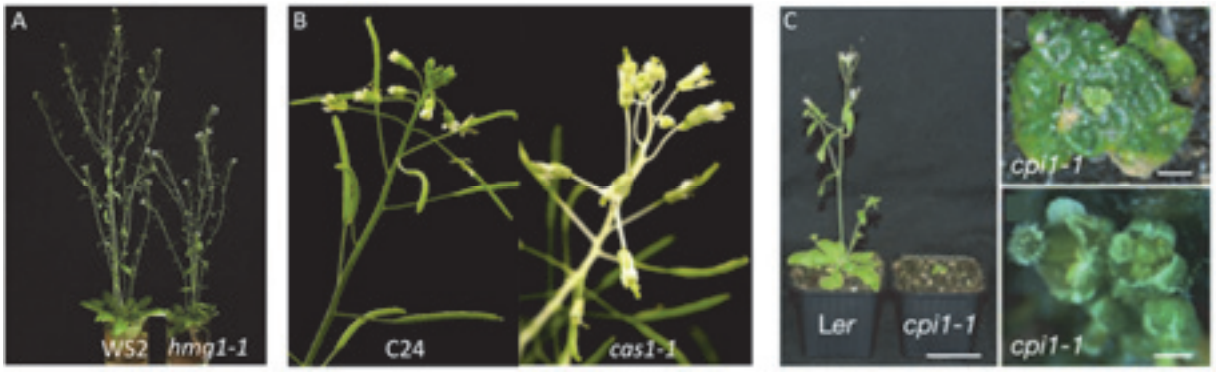

Figure 11. Sterol mutants in *Arabidopsis thaliana*. Mutants affected in the mevalonate and sterol biosynthetic pathways are touched on essential biological functions and show a diversity of phenotypes as reduced height and fertility (**A**), albinism (**B**) or dwarfism (**C**). Adapted from **(A)**, Heintz et al., 2012**; (B)**, Babiychuk et al., 2008**; (C)**, Men et al., 2008**.**

Specific sterol biosynthetic pathway in the male gametophyte.

The pollen grain is the male gametophyte, a haploid organism, in charge of carrying the male genetic material (the sperm cells) to the female gametophyte for fertilization, the important step of plant sexual reproduction together with meiosis. The pollen grain is produced in the anthers, and released when mature at anthesis. At this point, depending on the species considered, the pollen grain is disseminated by the wind, water, insects or animals. Once on the stigmas, the pollen grains produce a pollen tube that germinates (or elongates) through the transmitting tract of the style (**Figure 12**), guided by female signals to the embryonic sac, the female gametophyte (Dresselhaus and Márton, 2009; Palanivelu et al., 2006). This germination is a fast-apical growth, permitted by a supply of the necessary elements through a cytoplasmic streaming to build up cell wall and membrane components (Qin and Yang, 2011).

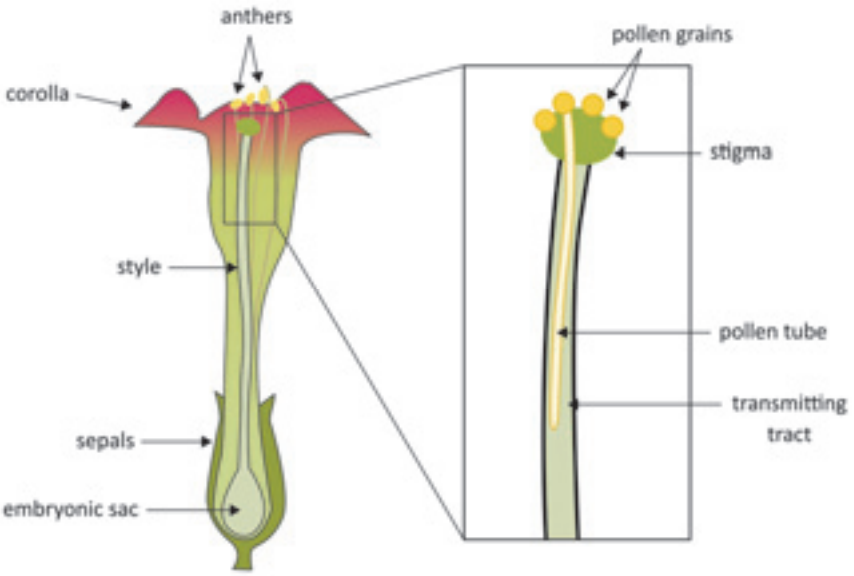

Figure 12. ***Nicotiana tabacum*** **flower morphology and germination of the pollen tube through the transmitting tract.**

This apical growth necessitates lipids, among which sterols play an essential role, since sterol mutants in *Arabidopsis thaliana* are often sterile or display a male gametophyte lethality (Suzuki et al., 2009).

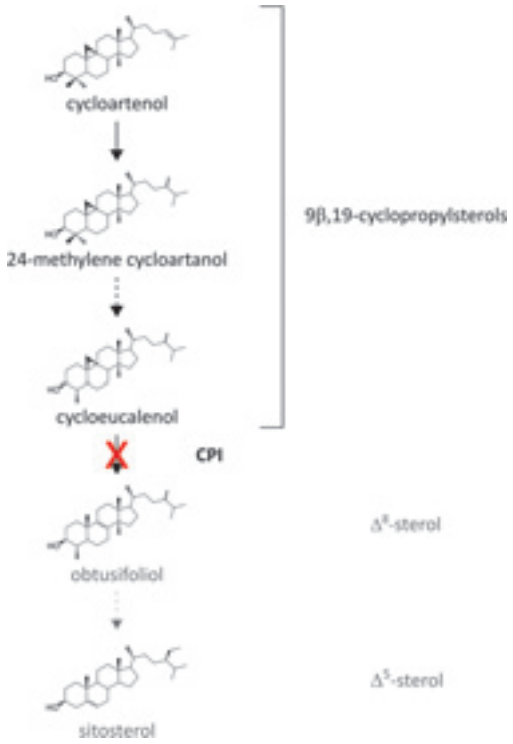

Figure 13. Hypothetic sterol pathway in germinating pollen tubes. At the beginning of this study, the working hypothesis was in favor of a truncated pathway in the germinating pollen tubes. Full arrows indicate single steps, dashed arrows indicate multiple steps. CPI: cyclopropylsterol isomerase.

Mutants affected in brassinosteroid biosynthesis and signaling.

Hormonal mutants can be divided into two classes: biosynthesis mutants (hormone deficient), which are not capable of synthesizing the hormones, and signaling mutants (hormone insensitive), that are unable to correctly integrate the hormonal signal. Mutants affected in the biosynthesis can be identified by exogenous application of the hormones, thus restoring a wild type-like phenotype. Signaling mutants do not show the wild type phenotype when treated with physiological doses of the hormone (Chandler and Robertson, 1999). Typical phenotypes of brassinosteroid and gibberellin mutants are dwarf plants, with phenotypes ranging from semi-dwarf to severe dwarfism in the light, and deetiolated phenotypes in the dark. Brassinosteroids have been shown to act as regulators of gibberellin biosynthesis in *Arabidopsis thaliana* (Unterholzner et al., 2015) and metabolism in *Oryza sativa* (Tong et al., 2014).

The brassinosteroid signal is mediated in a phosphorylation dependent mode of action. Hormones are perceived at the cell surface by a receptor complex including the receptor kinase BRASSINOSTEROID INSENSITIVE 1 (BRI1), from the family of the leucine-rich repeat receptor-like kinase (LRR-RLK) (**Figure 14**). Several *bri1* mutants have been described in *Arabidopsis thaliana* and in crops that show a dwarf phenotype, delayed flowering and senescence, and reduced male fertility (Fujioka and Yokota, 2003). The analysis of these mutants shows that BRI1 is essential for the perception of brassinosteroids and the subsequent plant growth. BRI1 exhibits an extracellular domain composed of 24 leucine-rich repeats (LRR) and a 70 amino acid island domain essential for ligand binding. Furthermore, a single-pass transmembrane sequence followed by a juxtamembrane domain and a cytoplasmic sequence bearing the catalytic kinase and C-terminal domains have been described (Clouse, 2011; Kim and Wang, 2010). The binding of brassinosteroids to the extracellular island domain of BRI1 receptor initiates a phosphorylation cascade causing the inactivation of the negative regulator BRASSINOSTEROID INSENSITIVE 2 (BIN2) kinase. The inhibition of BIN2 allows the activity of transcription factors of brassinosteroid target gene expression (Unterholzner et al., 2015). Brassinosteroids, and genes acting on their synthesis and signaling have been considered as potential targets for crop improvement with respect to yields and tolerance to biotic and abiotic stresses (Vriet et al., 2012). In addition, the brassinosteroids as major growth regulators of cereals have provided an impetus on the genetic characterization of specific loci, such as BRI1, the brassinosteroid receptor (Dockter et al., 2014).

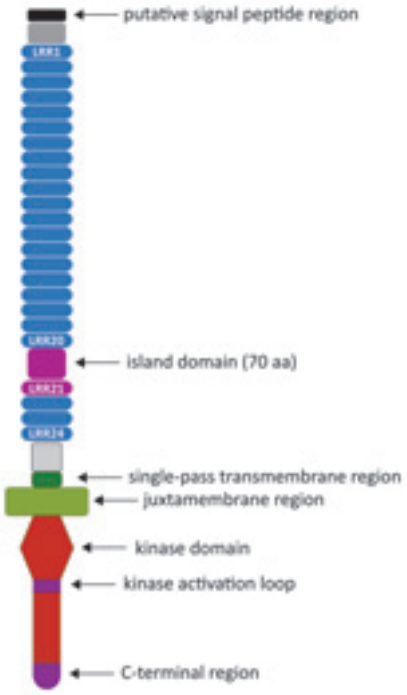

Figure 14. Structure of BRI1 brassinosteroid receptor, adapted from (Kim and Wang, 2010). LLR: leucine reach repeat.

2. Focus on the MEP pathway: leading to plastidial compounds.

The MVA pathway was long believed to be the only source of IPP synthesis in all organisms, further isomerized to DMAPP. The MEP pathway was discovered lately in bacteria and plastids, leading to the synthesis of both IPP and DMAPP (for review, Rohmer, 2007).

Key enzymes of the MEP pathway.

The synthesis of plastidial IPP (**Figure 15**) starts with the condensation of pyruvate and glyceraldehyde 3-phosphate, catalyzed by 1-deoxy-D-xylulose 5-phosphate synthase (DXS), to form 1-deoxy-D-xylulose 5-phosphate (DXP). DX is then reduced to 2-*C*-methylerythritol 4-phosphate (MEP) by 1-deoxy-D-xylulose 5-phosphate reductoisomerase (DXR). MEP is conjugated with cytidine diphosphate by MEP cytidyltransferase (MCT) and forms 4-(cytidine 5'-diphospho)-2-*C*-methylerythritol, further phosphorylated by 4-(cytidine 5'-diphospho)-2-*C*-methylerythritol kinase (CMK), a member of the same family of metabolite kinases as MVK and PMVK from the mevalonate pathway. The product of CMK phosphorylation is then converted to 2-*C*-methylerythritol 2,4-cyclodiphosphate by 2-*C*-methylerythritol-2,4-cyclodiphosphate synthase (MDS). IPP and DMAPP are formed by two final steps catalyzed by 4-hydroxy-3-methylbut-2-enyl diphosphate synthase (HDS) and reductase (HDR) (Lange et al., 2000; Phillips et al., 2008).

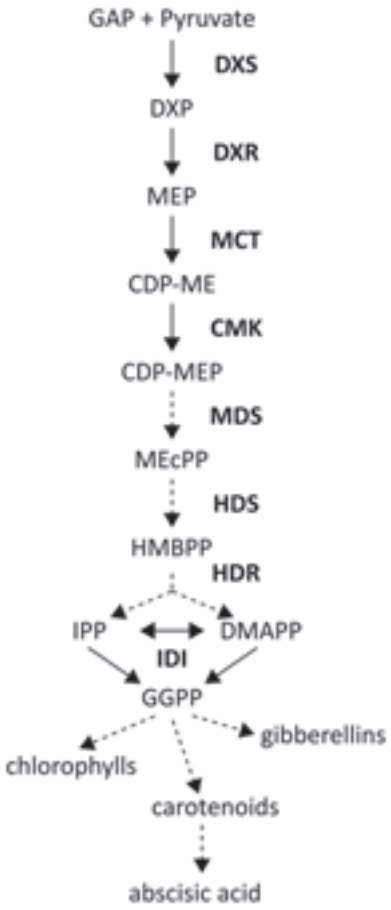

Figure 15. MEP biosynthetic pathway. The MEP pathway occurs in plastids and leads to the production of IPP, a common precursor for essential compounds as hormones or pigments. Full arrows indicate single steps, dashed arrows indicate multiple steps. DXS, 1-deoxy-D-xylulose 5-phosphate synthase; DXR, 1-deoxy-D-xylulose 5-phosphate reductoisomerase; MCT, 2-*C*-methyl-D-erythritol 4-phosphate cytidyltransferase; CMK, 4-(cytidine 5'-diphospho)-2-*C*-methyl-D-erythritol kinase; MDS, 2-*C*-methyl-D-erythritol 2,4-cyclodiphosphate synthase; HDS, (E)-4-hydroxy-3-methylbut-2-enyl 4-diphosphate synthase; HDR, (*E*)-4-hydroxy-3-methylbut-2-enyl 4-diphosphate reductase. GAP: glyceraldehyde 3-phosphate; DXP: 1-deoxy-D-xylulose 5-phosphate; MEP: 2-*C*-methyl-D-erythritol 4-phosphate; CDP-ME: 4-(cytidine 5'diphospho)-2-*C*-methyl-D-erythritol; CDP-MEP: 2-phospho-4-(cytidine 5'diphospho)-2-*C*-methyl-D-erythritol; MEcPP: 2-*C*-methyl-D-erythritol 2,4-cyclodiphosphate; DMAPP: dimethylallyl diphosphate; GGPP: geranylgeranyl diphosphate.

Mutants affected in the biosynthesis of plastidial compounds.

Plastidial compounds are essential to the plant survival, and this is emphasized by the fact that mutants lacking any of the MEP pathway steps are lethal. Null mutants display an albino phenotype, independently of the gene affected (**Figure 16**). In these mutants, chloroplast development is stopped at an early stage (Phillips et al., 2008).

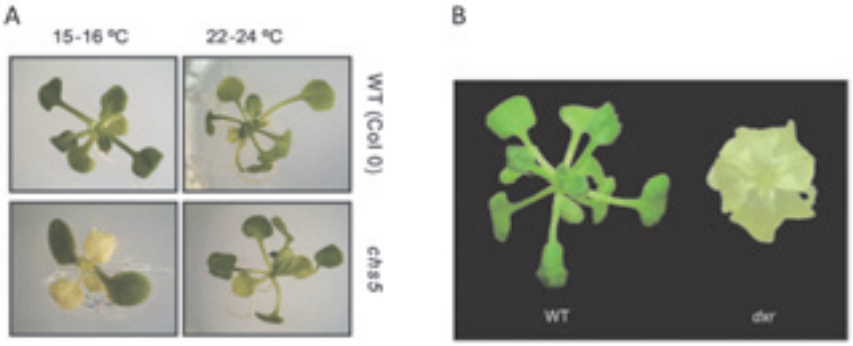

Figure 16. *Arabidopsis thaliana* mutants affected in the MEP pathway. Mutants of the MEP pathway display an albino phenotype, sometimes accompanied by seedling lethality or severe dwarfism, as it is the case for *dxr*. The *chs5* mutant is a conditional mutant sensitive to the temperature, showing the albino phenotype at low temperatures. Adapted from (**A**), (Carretero-Paulet et al., 2013) and (**B**), (Xing et al., 2010).

As already mentioned, isoprenoids are essential for cell viability and plant reproduction, and are involved in diverse processes at play during plant growth, cell division, hormonal regulation, photosynthesis, and so forth. Over the last decades, the biosynthesis of isoprenoid compounds has been described, the genes and enzymes involved in the MVA and MEP pathways were functionally characterized, and biosynthetic mutants were isolated as allelic series (Rodríguez-Concepción and Boronat, 2015; Hemmerlin et al., 2012). At present, the description of the isoprenoid metabolism as a component of plant integrative physiology suffers from lack of information regarding gene, enzyme, and pathway regulation. Except phosphorylation-mediated regulation of the enzyme 3-hydroxy-3-methylglutaryl coenzyme A reductase (HMGR, (Antolín-Llovera et al., 2011)) or the chaperone-mediated degradation of the DXS enzyme (Pulido et al., 2016), we have a limited knowledge of biochemical regulation at enzyme levels (for example, allosteric regulations). We do not know the nature of the master switches at play in isoprenoid homeostasis, we do not know the transcription factors that govern the expression of sets of isoprenoidogenic genes, and we do not know how metabolic interactions proceed in the cell, between the MVA and the MEP pathways, and between isoprenoid pathways and other tremendously important pathways like for instance lipid and fatty acid synthesis.

III. Genetic screens and new tools for bioinformatic analysis of whole genomes.

1. A brief history of genetic selection in crops.

In the process of crop selection during domestication of wild species, dwarfism or semi-dwarfism has naturally been a trait that was sought by farmers. Among other interesting traits as drought or disease resistance, semi-dwarfism was the most important in modern breeding programs (Maluszynski and Szarejko, 2005). First, spontaneous mutations were observed, causing a defect in gibberellin metabolism or a malfunctioning of brassinosteroid signaling, as it is the case for the spontaneous *uzu* mutant in barley (Gruszka et al., 2011). Then, chemical or physical mutation techniques were used as a source of genetic variation, to screen for new mutants presenting interesting agronomical traits. As an example, semi-dwarf rice cultivars Reimei and Calrose76 carrying a mutation in the *semi-dwarf1* (*sd1*) gene were used as a source of semi-dwarfism in breeding programs (Maluszynski and Szarejko, 2005). In wheat, the discovery of the reduced height (*Rht*) genes causing semi-dwarfism by acting on gibberellin signaling contributed to the Green Revolution, a period of strong development of agriculture productivity. The Green Revolution started in the 1940s in Mexico, with preliminary research led by Norman Borlaug to obtain disease resistant and high yield varieties of wheat. These varieties combined with new agricultural technics as mechanization technologies and the use of fertilizers, herbicides and pesticides, helped producing larger amounts of grains on the same land surface. The Green Revolution expanded to other countries as the USA, India and China, and helped fight against starvation, aiming at feeding a world population constantly growing.

2. Forward Genetics: the principle of suppressor screens.

A suppressor screen aims at identifying individuals capable of suppressing a parental phenotype, while carrying the parental mutation causative of the phenotype (for review, Page and Grossniklaus, 2002a). The suppressor individual can display a wild type-like phenotype or any other phenotype diverging from the original parental phenotype, to allow the plant growth and reproduction (this, in the case of a severe of deficient parental phenotype). Seeds of the parental lines are mutagenized to generate genetic diversity in the parental background. Suppressor individuals are selected in a M2 generation and phenotypes are assessed in further

generations before a first backcross. The F1 individuals obtained from the backcross are self-fertilized to generate F2 populations in which the suppressor and non-suppressor individuals segregate. The analysis of the segregation pattern gives clues on the mutations selected, causative of the suppressor phenotype. In this study, parental lines affected on key genes of isoprenoid biosynthesis (*hmg1-1*, *dxs1/chs5*) or signaling (*bri1*) have been chosen.

3. Mutagenesis

Mutagenesis is a precious tool for forward genetics, which goes from traits to genes. Plant mutagenesis can be done using physical treatments as radiation, or chemical treatments. The most frequently used chemical treatments are ethyl methanesulfonate (EMS) and sodium azide (NaN_3), inducing modifications of nucleotides resulting in mispairing and base changes.

EMS mutations induce alkylation of guanine residues (G) that can only pair with thymidine (T) and not cytosine (C) anymore. By natural DNA repair mechanisms, the G/C pair originally present can be replaced by a A (adenine)/T pair (Kim et al., 2006). The C/G to A/T substitutions are found in 99% of EMS mutations, in all mutation classes: silent, missense and truncated (Greene et al., 2003). In *Arabidopsis thaliana*, EMS mutations are randomly distributed across the genome, allowing for the search of loss- or gain-of-function mutants. The mutation frequency for a given gene depends on the position of the gene in the genome and the mutagenesis conditions. Only few insertion or deletion mutations are produced by EMS mutagenesis as compared to physical mutagenesis techniques like gamma ray irradiation (Kim et al., 2006). High concentrations of EMS can lead to 50% lethality, which is defined according to the seed germination rate after treatment (Lundqvist, 1992).

Sodium azide is known as a non-persistent respiration inhibitor, commonly used as a herbicide, nematicide, fungicide and preservative in clinical laboratories, which has a low toxicity for human health (Lundqvist, 1992). Sodium azide induces a high frequency of mutations, only base substitutions and single-strand breaks. No chromosome breaks or frameshift mutations were reported (Owais et al., 1978). Previous experiments on barley anthocyanin and proanthocyanin mutant collection treated with sodium azide showed that mostly transitions were obtained compared to transversions (Jende-Strid, 1993; Owais et al., 1978), with a preference for A/T to G/C transitions (3/4) compared to G/C to A/T transitions (1/4)

(Maluszynski and Szarejko, 2005; Salvi et al., 2014). Parental lines used for mutagenesis were selected because of their central role in their respective biosynthetic pathways.

4. Bioinformatic tools and Next Generation Sequencing.

Suppressor screens aim at identifying one or several mutations responsible for the suppressor phenotype selected and confirmed over generations. The analysis of F1 and F2 generations and segregating populations provides valuable information about the type of mutation selected (dominant or recessive, one or several mutations causative of the phenotype). With more and more genomes being available in public databases, bioinformatics tools are of great help in identifying new genes of interest. Whole genome sequencing, also known as next generation sequencing (NGS), is becoming accessible, and the quality of the sequences obtained now only relies on the quality of the sample provided for the analysis. High quality genomic DNA (high molecular weight, $A_{260}/A_{280}>1.8$) is used for library preparation prior to sequencing. The most commonly used platforms for sequencing are the HiSeq from Illumina and the Ion Proton from ThermoFisher. For larger genomes as *Hordeum vulgare*, it is also possible to sequence only the coding sequences, with the "exome capture" technic. Another way is to perform transcriptome (or RNAseq) analysis (Takahagi et al., 2016), providing data on the gene expression and possibly on sequence polymorphisms (Feuillet et al., 2012).

IV. Objectives of the thesis

As multiple mechanisms are at play, isoprenoid homeostasis research cannot rely on the individual study of genes of interest. In this context, **the first objective of my thesis work was to perform genetic screens in order to isolate novel plant lines and beyond, identify new key regulators of isoprenoid homeostasis**. Considering the important role of isoprenoids in growth and development, I have been focusing on the suppressor screens in my thesis. Novel plant lines isolated from the screens will certainly lead to the identification of new genes acting on isoprenoid homeostasis, metabolic interactions or compensations, or metabolite transport. For this, I worked on two *Arabidopsis thaliana* mutants defective in isoprenoid biosynthesis, leading to growth defects. Furthermore, in an attempt to identify novel loci implicated in growth and culm height, I conducted a suppressor screen on a *Hordeum vulgare* mutant being deficient in brassinosteroid signaling, causing a dwarf phenotype. This work allowed me to contribute to

the characterization of mutants with the help of emerging techniques collectively called “Next Generation Sequencing (NGS)”.

The investigation of the sterol biosynthetic pathway was pushed further with the use of pollen tubes, to understand why the plant kingdom developed a specific mandatory detour that is conserved in plants, involving 9β,19-cyclopropylsterols. **The second objective of my thesis was to study the sterol pathway that occurs in the pollen tubes during their germination** (Figure 13) **and to explain the biological relevance of such metabolic peculiarities**, an aspect of plant metabolic biology that was never described. Preliminary data available in the host laboratory suggested strongly that pollen tubes required specifically 9β,19-cyclopropylsterols for growth. The scientific objective was to perform sterol biosynthetic and functional studies in the pollen tube of angiosperms.

Chapter I. Genetic screens for suppressors of growth defects in two isoprenoid *Arabidopsis thaliana* biosynthesis mutants.

Materials and Methods

I. Plant material

1. *hmg1-1* (WS2 genetic background)

Seeds of the wild type ecotype Wassilewskija (WS2) and of the *hmg1-1* line in the WS2 background were obtained from Prof. Toshiya Muranaka (Osaka University). The *hmg1-1* line is carrying a T-DNA insertion in the first exon of the gene coding for 3-hydroxy-3-methylglutaryl coenzyme A reductase 1 (*HMG1*, At1g76490). The mutant line was originally screened by PCR-based reverse genetics (*Arabidopsis* T-DNA insertional mutant facility of Madison University, Wisconsin, USA). The *HMG1* gene expression is very low in *hmg1-1*, leading to a defect in growth and fertility associated to a decrease of metabolites downstream of squalene, sterols and terpenoids (Suzuki et al., 2004; Heintz et al., 2012).

2. *chs5* (Col-0 genetic background)

Seeds of the *chilling sensitive 5* line (*chs5*) were obtained from Dr. Koh Iba, Kyushu University. The *chs5* line in Columbia-0 ecotype (Col-0) was originally isolated from a genetic screen for chilling sensitive mutants that display a normal wild type phenotype at 22°C and a chlorotic phenotype when temperature is shifted to lower temperature (15°C) (Schneider et al., 1995; Hugly and Somerville, 1992). The *chs5* mutant presents a missense mutation in the gene coding for the 1-deoxy-D-xylulose 5-phosphate synthase (*DXS1*, At4g15560): a GAC to AAC mutation in exon 8 is changing an aspartic acid (D) to an asparagine (N) residue at position 627 (D627N) of the encoded protein. This mutation causes a chlorotic phenotype due to a defect of plastidial DXP biosynthesis (Araki et al., 2000). The Columbia-0 seeds were of initially ordered from the ABRC stock center (*Arabidopsis* Biological Resource Center, https://abrc.osu.edu/), then multiplied at the IBMP by the gardeners.

Arabidopsis thaliana lines used in this study were called WS2 VIL, *hmg1-1* VIL, Col-0 VIL and *chs5* VIL and were called so since their genome is entirely sequenced for the purpose of

the Next Generation Sequencing (NGS) project started during this thesis. The lines were maintained by self-fertilization to ensure a constant use of the same genetic backgrounds.

II. Methods

1. Plant culture conditions in soil

All lines of *Arabidopsis thaliana* were cultivated in 7cm diameter pots in soil (LAT-Terra Standard Topferde, Awita). Seeds were kept at -20°C for 48h before sowing. WS2, *hmg1-1* and suppressor lines of *hmg1-1* were cultivated in a 12-hour light regime under fluorescent tubes (4 Biolux T8 tubes, Osram) and 12-hour dark regime. Temperature was set at 19°C-21°C during the light phase and 17°C-18°C during the dark phase. Phenotyping and sampling of plants occurred after 3 months of growth. Col-0, *chs5* and suppressor lines of *chs5* were grown in a 12-hour light and 12-hour dark regime at 18°C during the light phase under fluorescent tubes (6 Lumilux tubes T5, Osram), and 15°C during the dark phase. Phenotyping was performed on one-month-old plants to assess a phenotypic class to each individual plant within a given population. Samplings of fresh plant tissues or organs for analytical purposes were made according to the appropriate developmental stage for a given measurement or experiment.

2. Plant culture conditions *in vitro*

Col-0, *chs5* and suppressor lines of *chs5* were sown *in vitro* on MS medium to score WT and *chs5* phenotypes. Seeds were surface sterilized in 25% commercial liquid bleach containing 0.1% SDS (Sodium Dodecyl Sulfate, Euromedex) for 10 minutes, and washed three times with sterile water. Sowing was made by pipetting seeds individually on the surface of the medium. For the screening of M2 generations or F2 populations, 150 seeds of each M2 or F2 were sown, together with 30 seeds of each control lines Col-0 and *chs5* sown on the same plate divided in sectors. The plates were kept for 2 days at 4°C before transferring them to a plant incubator (Sanyo MLR-351). The photoperiodic regime was 16h of light at 16,5°C and 8h of darkness at 18°C. Plantlets phenotypes were scored two to three weeks after transfer of the MS plates in the incubator.

Composition of MS medium: Murashige & Skoog Medium M0221 (Duchefa Biochemie) 4.3g.L^{-1}, sucrose 10g.L^{-1} (Euromedex), myo-inositol 100mg.L^{-1} (Duchefa Biochemie), thiamine

HCl 1mg.L^{-1} (Duchefa), pyridoxine HCl 0.5mg.L^{-1} (Duchefa), nicotinic acid 0.5mg.L^{-1} (Duchefa), agar 8g.L^{-1} (Bio-Rad), pH=5.7.

3. Crossings

Crossings of *Arabidopsis thaliana* were performed under a magnifying lens. Sepals, petals and stamens from the female parent were removed before anthesis. Pistils from such flowers were pollinated the same day using fresh pollen from the male plant, applied directly on the stigma. Pollinated plants were then grown as described above to let the siliques develop before colleting the F1 seeds.

4. Plant mutagenesis

Seeds of *Arabidopsis thaliana* L. *hmg1-1* or *chs5* were treated with 0.25% ethyl methanesulfonate (EMS, Sigma Aldrich) in water under gentle stirring in an Erlenmeyer flask (250 mL) for 12h at 23°C. Treated batches of seeds were sown in standard growth chamber conditions, to measure an approximately 50% survival rate of EMS treatment.

5. Screening of mutagenized populations

hmg1-1

Suppressor lines of *hmg1-1* were selected based on their phenotype when grown in soil. The full size of the plant, the seeds or siliques weights and the number of siliques were recorded. Candidate lines were genotyped to ensure the presence of the T-DNA insertion in the *HMG1* gene.

chs5

Suppressor lines of *chs5* were screened *in vitro* on MS medium in order to select plants with a wild type-like phenotype (green leaves) or capable of restoring a normal growth as compared to the parental line, which was chlorotic and small. Candidate lines were genotyped to check for the presence of the SNP G to A substitution in exon 8 of the *DXS1* gene.

6. DNA extraction

From plant material for PCR genotyping

DNA was extracted from leaf samples. Leaf material was ground in 750µL of grinding buffer with metal beads for 2 minutes on a Tissue Lyser (Quiagen) at 30Hz. Samples were incubated for 30 minutes at 65°C, then DNA was extracted with 700µL of chloroform/isoamyl alcohol (24/1, v/v, Carlo Erba Reagents, Merck). After a centrifugation step (5 minutes, 10000rpm, room temperature), the aqueous phase was collected and added to 550µL of isopropanol (Carlo Erba Reagents). Precipitated DNA was pelleted by centrifugation (5 minutes at 10000rpm, room temperature) then pellets were washed with 70% ethanol (Sigma Aldrich) and dried at room temperature before resuspension in 20µL of sterile water.

Composition of grinding buffer:
25mL DNA extraction buffer, 25mL Nuclei lysis buffer, 10mL Sarkosyl 5% (Sigma).
DNA extraction buffer:
sorbitol 0.35M (Roth), Tris base 0.1M (Sigma), EDTA 0.005M (Euromedex), pH=7.5.
Nuclei lysis buffer:
Tris base 0.2M (Sigma), EDTA 0.05M (Euromedex), NaCl 2M (Sigma-Aldrich), CTAB 2% (Sigma).

From plantlets for NGS analysis

F2 populations of *chs5* suppressor lines were cultivated *in vitro* on growth medium for 2 weeks. After phenotyping, 30 suppressor and 30 non-suppressor plantlets were collected as a bulk for each phenotypical category. Samples were ground with a pestle in a 1,5mL tube with 800µL of grinding buffer, and incubated 30 minutes at 65°C in a water bath. Then, 700µL of chloroform/isoamyl alcohol (24/1, v/v, Carlo Erba Reagents, Merck) were added and mixed by inverting the tubes. The supernatant was recovered in a new tube after a centrifugation step for 5 minutes at 10000rpm, 16°C. RNA was digested with 50µL of RNAse A/T1 (10mg.mL^{-1}, Thermo Scientific) at 37°C for 45 minutes. Once again, 700µL of chloroform/isoamyl alcohol (24/1, v/v, Carlo Erba Reagents, Merck) were added to the samples, mixed, and the tubes were centrifuged 5 minutes at 10000rpm, 16°C. In new tubes, samples were added to 1/2 volume of NaCl 5M, 3 volumes of cold ethanol, mixed and stored at -20°C for one hour before 20 minutes of centrifugation at 5500rpm, 16°C. The pellets were washed three times with 1mL 70% ethanol

(Sigma Aldrich) and dried at room temperature before resuspension in 20µL of water. At this stage, samples from the same line and same phenotypic category coming from different crossing events (candidate line as male or female) were pooled together and DNA was quantified using the Qubit dsDNA BR Assay kit (Thermo Fisher Scientific).

From leaf disks for NGS analysis

Leaf disks from 3 months old suppressor or non-suppressor plants were sampled as punches of identical size from physiologically identical leaves, with 16 to 50 plants per line and the same number of plants in each phenotypical category. Leaf disks were immediately frozen in liquid nitrogen and stored at -80°C before DNA extraction.

For DNA extraction, 1mL of grinding buffer was added to the leaf disks, and samples were ground with metal beads for 2 minutes on a Tissue Lyser (Quiagen) at 30Hz. Samples were incubated for 30 minutes at 65°C and extracted with 800µL of chloroform/isoamyl alcohol (24/1, v/v, Carlo Erba Reagents, Merck). The supernatant was recovered in a new tube after a centrifugation step for 5 minutes at 10000rpm, 20°C. RNA was digested with 10µL of RNAse A/T1 (10mg.mL^{-1}, Thermo Scientific) at 37°C for 30 minutes. DNA was precipitated by addition of 600µL of isopropanol (Carlo Erba Reagents) and a centrifugation step for 5 minutes at 10000rpm, 20°C. Pellets were washed with 500µL of 70% ethanol (Sigma Aldrich), dried at room temperature and resuspended in 15µL of sterile water. DNA was quantified using the Qubit dsDNA BR Assay kit (Thermo Fisher Scientific).

7. Genotyping by PCR

Plants were genotyped by PCR using the following mix for one sample: 4µL of GoTaq 5X buffer (Promega), 2,4µL of $MgCl_2$ (25mM, Promega), 0,4µL of dNTP (10mM, Promega), 0,48µL of each primer (20µM, Integrated DNA Technologies), 0,24µL of GoTaq (Promega), water up to 19,5µL, and 0,5µL of DNA sample obtained as described. Primers used for each line are listed in **Table 1**.

Table 1 Primers used for genotyping by PCR

Target gene	Primer name	Primer sequence
AtHMG1	HMGR784	GAGCGGCGTCGATTCGTCGTGAGGCGTTG
	JL202	CATTTTATAATAACGCTGCGGACATCTAC
	HMGR3'	CCAACAGACATGCGAGTTCGTCTCCTATA
AtDXS1	DXR F2N	GTTTTGCAAGCCATTGGA
	DXR F2M	GTTTTGCAAGCCATTGAA
	DXR R1	GCACCGTGATCAATGTATCG

Samples were placed in a thermocycler (Eppendorf Mastercycler) for PCR amplification with a specific cycle according to the line (**Table 2**), and placed on a 1% agarose gel (Sigma Life Science) in TAEX1 with Sight DNA stain (Euromedex) for migration at 100V during 30 minutes.

Table 2 PCR cycles used for genotyping of *Arabidopsis thaliana* and *Hordeum vulgare* suppressor lines.

	AtHMG1			*AtDXS1*		
	Temperature		*Time*	*Temperature*		*Time*
Denaturation	95°C		5 min	94°C		3min
PCR Cycle	X30	95°C	30 sec	X35	94°C	30sec
		58°C	30 sec		61°C	40sec
		72°C	15 sec		72°C	1min
Final elongation	72°C		20 min	72°C		5min
Hold	15°C		1 min	4°C		/

8. DNA sequencing by NGS (Illumina)

DNA samples were analyzed and processed by the IGBMC Microarray and Sequencing Platform (Strasbourg). Libraries were prepared according to the protocol of TruSeq DNA sample prep kit (Illumina). Sequencing was made on the Illumina Hiseq 2500 (*in vitro* F2BC1 G2.10 and L8.4 samples) or Illumina Hiseq 4000 (other samples) sequencer as paired-end 100 base reads following the Illumina's instructions. Reads forming adapter dimer were removed by the platform using an in-house script.

9. Bioinformatic analysis of NGS datasets

Bioinformatics analysis was performed in collaboration with Sylvain Darnet (Laboratório de Biotecnologia Vegetal, Instituto de Ciências Biológicas, Universidade Federal do Pará (UFPA), Belém, Brazil), who created a specific pipeline for the analysis of *Arabidopsis thaliana* sequencing datasets. I was trained to this bioinformatic analysis during a stay in the team of Sylvain Darnet in the University of Para in November 2016. The reads datasets were preprocessed using the trimmomatic tool in order to trim and remove adapter sequences, low quality read ends and unpaired reads (Bolger et al., 2014). The mapping step was performed using gsnap mapper with default parameters and Col-0 genome, TAIR10 version 30 (Wu and Nacu, 2010; Yates et al., 2016). The output BAM file from gsnap mapper was filtered with samtools rmdup and samtools view with the flag -f 0x0002 in order to remove PCR duplicated reads and not properly paired mapped reads respectively. SNPs calling was based on SAMtools mpileup and BCFtools view as described in SHOREmap methods (Li et al., 2009; Sun and Schneeberger, 2015). The VCF file was converted with convert tool from SHOREmap package in order to obtain for each SNP the position, the reference base, the variant base, the SNP calling quality of the variant base, number of reads that support the variant, and the allelic frequency (AF) (Sun and Schneeberger, 2015). In order to identify the unique high quality EMS SNPs, three successive filtering steps were applied for each SNP dataset: i) removing SNPs with quality inferior to 25 and with read coverage of variant base inferior to 6 (James et al., 2013) removing SNPs that are separated by a distance inferior to 50 bp (James et al., 2013) removing SNPs that are not corresponding to EMS mutation spectrum (CT:GA). In the unique high quality SNPs dataset, were selected homozygous SNPs, SNPs with a AF equal to 1 or superior to rf value (James et al., 2013). The rf value is calculated using the read coverage and sequencing error frequency and indicates the minimum AF to consider to select a SNP as homozygous (James et al., 2013). In order to identify homozygous SNP mutation associated with *chs5* phenotype suppression, homozygous SNPs common to four set of plants (2 sets with *chs5* suppression phenotype and 2 with *chs5* phenotype) were subtracted to homozygous SNPs from 2 sets with *chs5* suppression phenotype. After subtraction, the homozygous SNPs specific from each set of *chs5* suppressor plants were annotated to Variant Effect Predictor (VEP) tool from ENSEMBL server, in order to evaluate the position and effect of each mutation in coding and intergenic sequences (Yates et al., 2016).

10. RNA extraction

Plant material was ground in liquid nitrogen before adding 1mL of Trizol (Molecular Research Center). Samples were incubated at room temperature for 4 minutes and centrifuged for 10 minutes at 13500rpm, 4°C. The supernatant was collected and added to 200µL of chloroform (Carlo Erba Reagents) for incubation at room temperature during 4 minutes. Aqueous phase was collected after centrifugation (10 minutes at 13500rpm, 4°C), mixed with 500µL isopropanol (Carlo Erba Reagents) and incubated at room temperature for 10 minutes. The RNA pellets were obtained after centrifugation for 10 minutes, 13500rpm, 4°C and washed with 70% ethanol (Sigma Aldrich) before resuspension in 10 to 50µL of water. Samples were stored at -20°C.

11. Reverse transcription

RNA samples were quantified on a NanoDrop 2000 (Thermo Scientific) and diluted to obtain a 1µg.µL^{-1} solution in water. DNA from 1µL of sample was digested with 2µL of DNAse (Thermo Scientific, diluted to 1/50^{e}) at 37°C for 15 minutes. On ice, 1µL of random primers (200ng.µL^{-1}, Promega), 1µL of dNTP (10mM, Promega) and 10µL of RNAse free water were added. Samples were incubated at 65°C for 5 minutes, and put back at 4°C. Then, 4µL of RT buffer 5X (Invitrogen) and 1µL of reverse transcriptase (Super Script III, Invitrogen) were added to the samples, placed in a thermocycler for 10 minutes at 25°C, 30 minutes at 50°C and 5 minutes at 85°C to obtain cDNA samples.

12. qPCR analysis of MVA and MEP pathways gene expression in *Arabidopsis thaliana* leaves

cDNA samples as 20µL of RT reaction final mixture were filled up to 100µL with water. On a 96 wells plate, each sample was prepared as follows: 5µL of cDNA solution, 7,5µL of primer pool (1µM, Integrated DNA Technologies), 12,5µL of SYBR Green (Roche). The plate was sealed and centrifuged for 10 minutes at 3000rpm before reading on light cycler 480 (Roche) following the cycle : denaturation (95°C, 5min, 4,8°C/s), PCR 45 x (95°C, 10s, 4,8°C/s ; 60°C, 15s, 2,5°C/s ; 72°C, 15s, 4,8°C/s), melting curve (95°C, 5s, 4,8°C/s ; 55°C, 1min, 2,5°C/s ; 95°C, 0,11°C/s, 5 acquisitions/°C), cooling (40°C, 30s, 2,5°C/s). Primers used are listed in

Table 3 and **Table 4**. For *chs5* suppressor lines, three biological replicates were sampled. For *hmg1-1* suppressor lines, technical triplicates were made from one sample.

Table 3 Primers used for qPCR analysis of MEP pathway gene expression in *Arabidopsis thaliana*, from Wright et al., 2014. DXS, 1-deoxy-D-xylulose 5-phosphate synthase; DXR, 1-deoxy-D-xylulose 5-phosphate reductoisomerase; MCT, MEP cytidyltransferase; CMK, 4-(cytidine 5′-diphospho)-2-*C*-methylerythritol kinase; MDS, 2-*C*-methylerythritol-2,4-cyclodiphosphate synthase; HDS, 4-hydroxy-3-methylbut-2-enyl diphosphate synthase; HDR, 4-hydroxy-3-methylbut-2-enyl diphosphate reductase.

Target gene	Primer name	Primer sequence
AtRP21s	RP21sF	GAAGGCAAAGGAAGGCAGAATCAG
	RP21sR	GCAATACTCCACGGAACACCAAG
AtAPT1	APT1F	GTTGCAGGTGTTGAAGCTAGAGGT
	APT1R	TGGCACCAATAGCCAACGCAATAG
AtDXS	DXSF	TCGCAAAGGGTATGACAAAG
	DXSR	CAGTCCCGCTTATCATTCC
AtDXR	DXRF	AGTAGCGGATGCGTTGAAGC
	DXRR	GCGGATGAATGACAATCTCTATATCG
AtMCT	MCTF	TTCTGATTCGCTTGTGGTG
	MCTR	AACTGGATGCTTGAGGTATTC
AtCMK	CMKF	TCGGTGGTGGAAGTAGTAATG
	CMKR	AGGAAGGTCTTGGACAATCTC
AtMDS	MDSF	CATCGTTTAGAGCCAGGGTATCC
	MDSR	TGAAGTAACACATCGCCATCGG
AtHDS	HDSF	CAGAATGCGTAACACTAAGAC
	HDSR	GAGAACCACCTACATATCCG
AtHDR	HDRF	TCGTGCGGGAGAATCATC
	HDRR	TCTTACGGAACACCTTGGC

Table 4 Primers used for qPCR analysis of MVA pathway gene expression in *Arabidopsis thaliana*. HMG, 3-hydroxy-3-methylglutaryl coenzyme A reductase; MVK, mevalonate kinase; PMVK, 5-phosphomevalonate kinase; MDC, mevalonate diphosphate decarboxylase; IDI, isopentenyl diphosphate:dimethylallyl diphosphate isomerase; FDS, farnesyl diphosphate synthase; SQS, squalene synthase; SQE, squalene epoxidase; CAS, cycloartenol synthase.

Target gene	Primer name	Primer sequence
AtHMG1	HMG1F	GTCACTATGCCATCTATCGAGGTG
	HMG1R	GCTCCTTTAACTCCGAGCAGGT
AtHMG2	HMG2F	TCCCGATGGTGACGACCTT
	HMG2R	GCTGCTTGTGATGCAAGTTGTG
AtMVK	MVKF	AACCACGGTCAAGCACAAGC
	MVKR	GCTCCTCCACCACTTTGTCCA
AtPMVK	PMVKF	TGTAGTGTGCTTACTTCTGAAAAGTGG
	PMVKR	CCTCAACATAGCTTCTCTTGCCTCTA
AtMDC1	MDC1F	CCCTCCTAAGCCTGACACAGAC
	MDC1R	TTCCTTGTGGAAGCTCTCCTTC
AtMDC2	MDC2F	TTCTGAAGGGACACCACAGGTT
	MDC2R	TGTTGCGTGCAATCAGTACAGC
AtIDI1	IDI1F	ATGGGGAGAGCACGAAGTTG
	IDI1R	CTTAAGCTCTTCCCTGCTCACG
AtIDI2	IDI2F	AAATGGGGAGAGCATGAACTTG
	IDI2R	TGCTTTCTTCACCAGCTCCTTC
AtFDS1	FDS1F	CGCTTGGCAAGATAGGAACAG
	FDS1R	CGATGGGTCGGGTTTACCAT
AtFDS2	FDS2F	TGTGCTCTTGGTTGGTGCATT
	FDS2R	TGTGACAGAGTTGTCCATGATGTC
AtSQS1	SQS1F	CATTGCTTCGGAATTAGAAATACTGAC
	SQS1R	GCGCGACTTTGGTCTCTCAT
AtSQS2	SQS2F	TGGCCAAGTTTATCTGCCAAGA
	SQS2R	TGCAGCGAGGAAGAGTTTCG
AtSQE1	SQE1F	TCCCTTCCCCAAAACGAATC
	SQE1R	CGGAAATATTATCCCCGATGC
AtSQE2	SQE2F	CCATTTCCTTCGATTGAGAGCTT
	SQE2R	CTGCTTTAATTATTGGAAAGATGATGC

AtSQE3	SQE3F	GCGTCGATCTCTCTGCAAACC
	SQE3R	CGCAATTCTCCAATACCAGACC
AtSQE4	SQE4F	TCGCTTTTGGCATAGCCTCA
	SQE4R	AAATGTGCACCCAACATTTGC
AtSQE5	SQE5F	TGGCATAGCCTTCGACTTTTTG
	SQE5R	GCGGCGTTGACTGGAAACA
AtSQE6	SQE6F	GGCATAGCCTCAAGCTTTTTGG
	SQE6R	CATTTGCTGGAAACAACATTTGG
AtCAS1	CAS1F	TGAATTTCTATTGTCGAAACAACAACC
	CAS1R	TGTTGCCATCAAGGTTTGAATAGA

13. Imaging and measurement of *Arabidopsis thaliana* seeds

Imaging of *Arabidopsis thaliana* seeds was made on a TM-100 electronic tabletop microscope (Hitachi) under vacuum. Measurements of the size of the seeds were also performed with ImageJ from pictures of seeds populations to get statistical data (Jérôme Mutterer, IBMP).

14. Measurement of chlorophyll and carotenoid content from leaf material.

Fresh leaf samples of approximately 40mg were collected in liquid nitrogen. Leaf material was ground with a metal bead for 1 min at 30Hz (Tissue Lyser, Qiagen) in 1mL of freshly prepared 80% acetone (Sigma Aldrich) in water (v/v). Samples were incubated in the dark at 4°C for 24h. After incubation, 200µL of the supernatant were transferred to a 96 well microplate (96 Well ELISA Microplates, PS, U-bottom, MICROLON®, Greiner Bio-one). For each sample, 3 wells were prepared for measurement. Optical density was measured for each well at 470nm, 646nm and 663nm on FLUOstar Omega spectrometer (BMG Labtech). The concentration of chlorophylls and carotenoids in the samples was determined with the equations given by (Lichtenthaler and Buschmann, 2001), with c_a: concentration of chlorophyll a; c_b: concentration of chlorophyll b; $c_{(x+c)}$: concentration of xanthophylls and carotenes.

c_a (µg/mL) = 12.25 $A_{663.2}$ – 2.79 $A_{646.8}$

c_b (µg/mL) = 21.50 $A_{646.8}$ – 5.10 $A_{663.2}$

$c_{(x+c)}$ (µg/mL) = (1000 A_{470} – 1.82 c_a – 85.02 c_b)/198

15. Extraction of total sterols, sterol esters, fatty acids from plant tissues

Lyophilised material (ground whole plant material) was saponified in 12,5mL of 6% KOH in methanol (Carlo Erba) at 75°C for 2h. After addition of water to 15mL total volume, samples were extracted 3 times with 15mL n-hexane (Roth). The hexane phase was evaporated, and acetylation was performed on the dried residue with 50µL of toluene (Carlo Erba), 30µL of acetic anhydride (Fluka) and 20µL of pyridine (Fluka) in a glass vial at 70%C for 30 minutes. The extracts were spiked with lupenyl-3,28-diacetate (20µg, Sigma) as a standard for chromatography, and resuspended in 300µl of n-hexane.

16. Sterol analysis by gas chromatography and mass spectrometry (GC-MS)

Plant extracts were analysed by gas chromatography (GC instrument, Agilent 6890) and mass spectrometry (MS analyser, Agilent 5973) to identify the different sterol species in their composition. A HP-5MS column (5% PhenylMethyl Siloxane, 30mx250µmx0,25µm, Agilent J&W) was used, on which 2µL of sample were injected, and transported with a helium flux of 1mL.min^{-1}. The column temperature was hold at 60°C for 1min, heated to 200°C at 30°C.min^{-1} before reaching a maximum of 300°C at 2°C.min^{-1}, for a total run time of 56,33min per sample. The separated molecules were ionized by electronic impact at 70eV. The identification of each species was made by the detection of specific daughter ions obtained after ionization (Rahier and Benveniste, 1989).

Results

I. Genetic screening for *hmg1-1* suppressor alleles.

1. Size of the mutagenesis experiment.

Seeds from the *hmg1-1* line (1 gram, approximately 50000 seeds) were treated with 0.3% EMS at 23°C for 12 hours then rinsed several times with 0.1M sodium thiosulfate. This mutagenic treatment resulted in a 50% survival rate of seedlings. About ten thousand plantlets were further grown in culture conditions described above, and half of this batch gave well-rooted rosettes that constituted a M1 population. To favor seed setting of these *hmg1-1* individuals otherwise characterized by a low fertility, rosette leaves at the pre-bolting stage were spread with squalene to perform a biochemical complementation of the mevalonate pathway deficiency leading to phytosterols (Suzuki et al., 2004; Heintz et al., 2012). The final size of the mutagenesis experiment was of 4500 M1. M2 seeds were harvested for each plant and organized in 225 pools of 20 M2 families, each M2 family being represented by 50 seeds (Rédei and Koncz, 1992). The screening of M2 families (about 2000 trays of 96 wells of soil) consisted in selecting plants that displayed an improved growth phenotype, silique filling and seed setting with respect to *hmg1-1* parental phenotype and also compared to the wild type WS2 background of the *hmg1-1* allele. The screen was conducted by Vincent Compagnon and Hubert Schaller over several months. I joined the laboratory at the time the last batches of M2 pools were screened.

2. Details of screening conditions.

The screening for suppressors of *hmg1-1* phenotype in *Arabidopsis thaliana* Wassilewskija (WS2) background and the study of sup *hmg1-1* lines was carried out under horticultural conditions, with plants growing in soil. The temperature conditions in the growth room were recorded on weekly basis. They showed a stable alternation between the coldest temperature set at 17°C during the dark phase, and the warmest temperature set at 21°c during the light phase (**Figure 17**). A small increase of the temperature in the light phase was observed, until

23.6°C at maximum. The temperature and light conditions were stable for all series of plants from which materials were sampled for nucleic acid extraction and phenotypic measurements (morphometry, chemical analysis).

Figure 17. Temperature conditions in the growth room for *Arabidopsis thaliana hmg1-1* suppressor and parental lines.

3. Genotyping of *hmg1-1* insertional mutation.

The *hmg1-1* mutant is carrying a T-DNA insertion in the first exon of the *HMG1* gene. The screen aims at identifying individuals that show a suppressor phenotype while carrying the defective *HMG1* gene. Selected individuals were genotyped by multiplex PCR using 3 primers in the same reaction. Two primers are situated on the exon 1 of *HMG1*; the forward primer before the T-DNA insertion site, the reverse primer after the T-DNA insertion site; and the last reverse primer is situated on the T-DNA sequence (**Figure 18, A**). PCR fragments were separated by gel electrophoresis, which allows the identification of plants carrying the T-DNA insertion. The amplification of a fragment with the forward primer on *HMG1* sequence (HMG1-784) and the reverse primer on the T-DNA sequence (JL202) gave a product of 700bp length. The fragment amplified between the forward (HMG1-784) and reverse (HMG-3') primers situated on the *HMG1* sequence was found at 500bp. Thus, it was possible to identify *HMG1-1/HMG1-1* individuals (wild type) with one amplification product at 700bp, *HMG1-1/hmg1-1* heterozygous individuals showing two products of 700bp and 500bp, and *hmg1-1/hmg1-1* homozygous individuals showing one amplification product at 500bp (**Figure 18, B**). While screening the M2 families, individuals with a *HMG1-1/hmg1-1* genotype were discarded; in

fact, many of these heterozygotes (that displayed a true wild type phenotype) were found among M2 families, indicative of a genetic contamination (about 0.1-1 %) expected when low fertility genotypes are considered for large scale mutagenesis experiments. Individuals of the *hmg1-1/hmg1-1* genotype were selected for further experiment and phenotypic characterization on several generations.

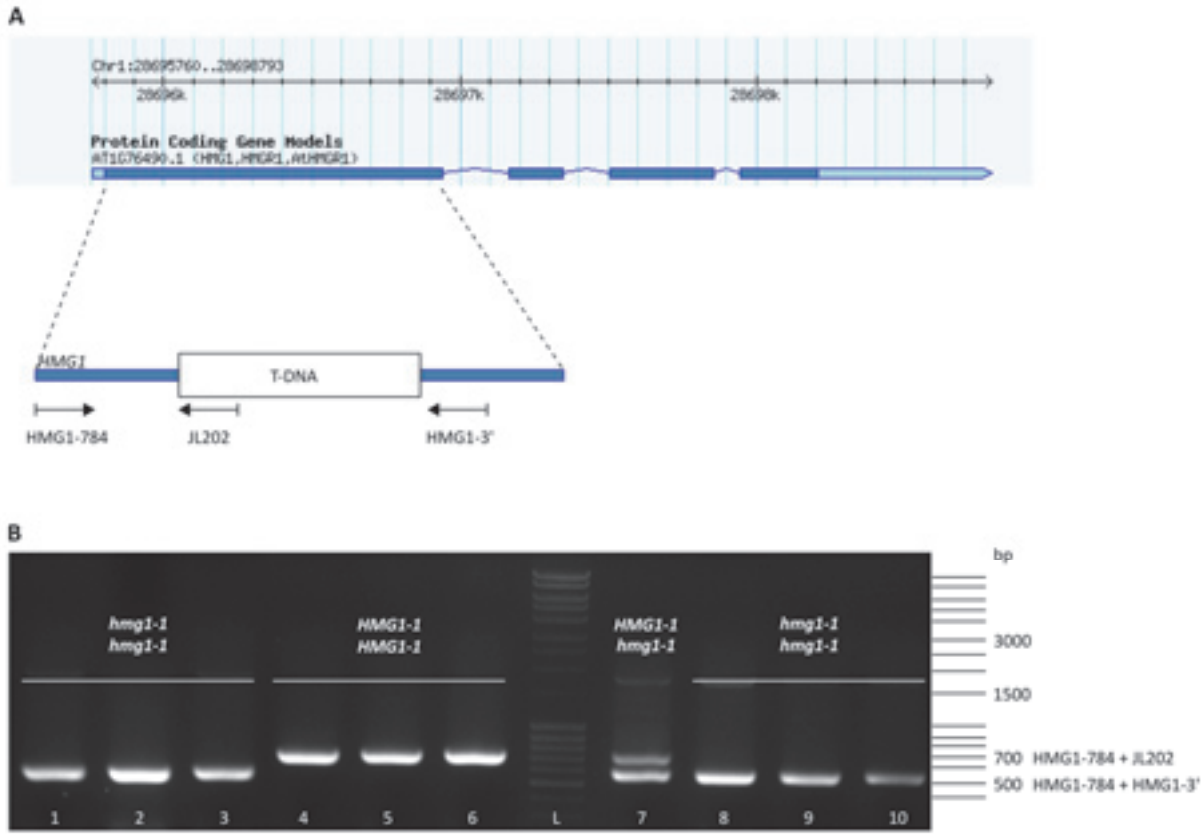

Figure 18. Genotyping of a T-DNA insertion in the *HMG1* gene. (**A**), *hmg1-1 Arabidopsis thaliana* is carrying a T-DNA insertion in the first exon of the *HMG1* gene. Exons are represented as blue boxes, introns as blue lines (Gene map from TAIR, The *Arabidopsis* Information Resource, http://www.*Arabidopsis*.org/). Genotyping is made by multiplex PCR amplification of a gene-specific product using primers HMG1-784 (forward) and HMG1-3' (reverse) and/or of a T-DNA specific product with primers HMG1-784 and JL202 (reverse). (**B**), Electrophoretic separation of PCR fragments amplified from genomic DNA from *hmg1-1*/*hmg1-1* individuals (*hmg1-1* parental line, lanes 1-3), *HMG1-1*/*HMG1-1* individuals (wild type of the WS2 ecotype, lanes 4-6), a mix of *hmg1-1* and WS2 gDNA (lane 7), and individuals from *hmg1-1* suppressor lines demonstrating the *hmg1-1*/*hmg1-1* genotype (lanes 8-10). L: MassRuler DNA Ladder Mix, Thermo Fischer Scientific.

4. Phenotypic characterization of *hmg1-1* suppressor candidates in M2, M3 and backcrossed generations.

The selection of *hmg1-1* suppressor individuals in M2 generations was performed in horticultural conditions ensuring autotrophic growth, as described above. Individuals showing an improved growth phenotype, when compared to *hmg1-1* parental line and WS2 wild type grown in the same conditions as controls were given special attention for a phenotypic characterization. In fact, the key point for the success of such a risky screening based on growth is the definition of a robust criteria. The *hmg1-1* mutant is smaller than the wild type and semi-sterile. Thus, suppressors were selected according to their size and their seed filling capacity. The morphology of an *Arabidopsis thaliana* adult plant at seed filling and flowering stage is represented in **Figure 19.** The phenotypical traits that were observed and quantified were the size of the main stem, the number of siliques and their filling, in relation with the capability to produce seeds.

Figure 19. Representative scheme of *Arabidopsis thaliana* morphology at seed filling and flowering stage. Plants were grown in soil as described in Materials and Methods section. To maximize reproducibility of the sampling for phenotyping, a WS2 *Arabidopsis* plant shown in (**A**) is schematically drawn as a standard individual shown in (**B**). Roots are not represented in this illustration. Plant size was measured from the soil to the top of the main stem, the number of siliques was counted on the main stem, and siliques of the main stem were sampled for weight measurements. Genomic DNA for Illumina sequencing was prepared from cauline leaf disks. Whole plants ground in liquid nitrogen were used for the identification of unsaponifiable lipids and gene expression analysis by qPCR.

Suppressor individuals selected in a M2 generation were self-fertilized and phenotypes were carefully analyzed in M3 for confirmation, with the measurement of the total size of the plants, the number of siliques on the main stem and the weight of the seeds from the siliques of the main stem (**Figure 20**). First, 83 candidate lines were screened in M3. For this, 6 plants were grown per candidate line. Among these, 64 lines did not further show a suppressor phenotype and were discarded. Of 19 lines, 5 lines showed two phenotypic classes of suppressors (*sup*) and non-suppressor (*SUP*) individuals in segregating M3 populations. This could be indicative of dominant mutations represented in M2 generations as heterozygotes. These lines were kept aside. Fourteen lines showing a homogenous population of suppressor individuals in M3 were chosen for a further analysis. Measurements were made to assess the suppressor phenotype. No statistical difference was found between the suppressor candidates and *hmg1-1* line for the size measurement, the number of siliques and the weight of the seeds. The weight of the seeds in the WS2 wild type control was statistically higher than in *hmg1-1*. No other statistical difference was found for the number of siliques and the weight of the seeds between the suppressor lines and the control lines.

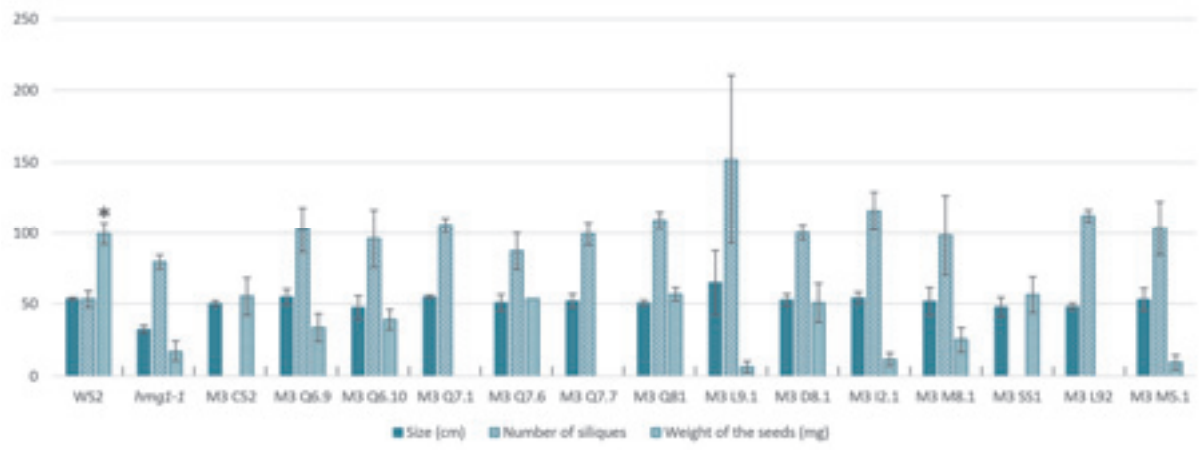

Figure 20. Measurement of phenotypical traits on *Arabidopsis thaliana hmg1-1* suppressor lines in a M3 generation. Bars show the size of the main stem (dark blue) and the number of siliques (striped bars) on the main stem (N_i=2-7). Light blue bars are the weight of mature seeds from the main stem (N_i=1-7). Statistical analysis was made using Kruskal-Wallis rank sum test, no statistical difference was found between suppressor candidates and *hmg1-1* for the size and the number of siliques. A two-tailed multiple comparison test after Kruskal-Wallis was applied for the weight of the seeds, with a p-value=0.05 (single asterisk).

The fourteen lines with a homogenous suppressor population in M3 generation were backcrossed to *hmg1-1*. Crossings were made using the suppressor individuals as a male and the parental *hmg1-1* line as a female. Crossings using *hmg1-1* as a male failed most of the time

as this line does not produce a lot of pollen. For lines L92 and M5.1, the crossings did not work. The F1BC1 individuals obtained from the crossings of the twelve candidate lines were treated with squalene, a precursor of sterol biosynthesis, to allow the plants to produce as much seeds as possible. This was done to avoid a possible low fertility or sterility of F1 plants that would carry a recessive *sup hmg1-1* allele. Thus, it was not possible to identify if the phenotype of F1 individuals was suppressor or non-suppressor. After self-fertilization, one F1 individual was selected for each candidate line, and the seeds of this unique plant were used for a segregation analysis in F2BC1 populations. In these populations, two distinct phenotypes were observed: suppressor plants (*sup*) were identified by a tall size and the filling of their siliques; non-suppressor plants (*SUP*) were displaying a smaller size and did not fill their siliques. Pictures of representative individuals of each candidate line at flowering stage are shown in **Figure 21, A**. The size of the main stem was measured on *sup* and *SUP* individuals after 3 months of growth in soil, with WS2 and *hmg1-1* as controls (**Figure 21, B**). For the twelve candidate lines, *sup* individuals showed a taller size, statistically different from the *hmg1-1* parental line. For C52, Q6.9, and D8.1 lines, *SUP* individuals were also taller than the parental line, but still smaller than the suppressor individuals.

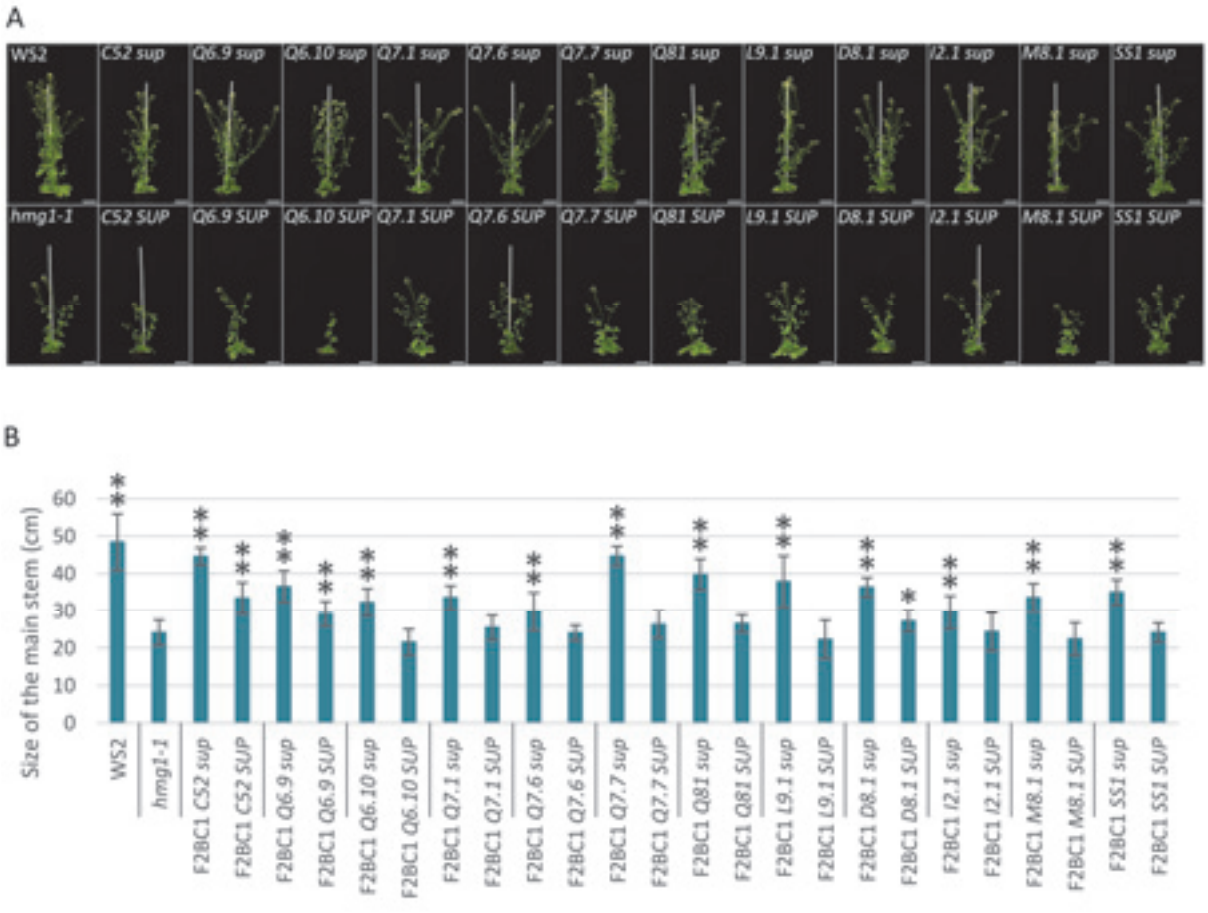

Figure 21. Phenotypes of *Arabidopsis thaliana hmg1-1* suppressor candidates in F2BC1 generations. (**A**), Photographs of 2-month-old *Arabidopsis thaliana hmg1-1* suppressors (*sup*) and non-suppressors (*SUP*) grown in soil, scale bars 5cm. (**B**), Size of the main stem (cm) from *sup* and *SUP* individuals of a F2BC1 population (N_i=15-50). Statistical differences from the value obtained for *hmg1-1* parental line were determined using a pairwise Student t-test, with a p-value<0.05 (single asterisk) or p-value<0.01 (double asterisks). Magnified pictures are available in **Suppl. Figure 1**.

Except for the reduced amount of pollen in the flowers of *hmg1-1*, no other phenotypic difference was observed by comparing the flowers of suppressor and non-suppressor individuals in F2BC1 populations with the flowers of the control lines. Pictures of representative flowers at anthesis are given in **Figure 22, A**. In the same F2BC1 population, the siliques of suppressor individuals were long and large, with a range of different sizes represented in **Figure 22, B**. Some suppressor individuals had siliques almost like the siliques of WS2 wild type, as in Q81 and D8.1 populations. The non-suppressor individuals showed small siliques almost non-filled, as the *hmg1-1* parental line. As long and large siliques were always filled with seeds at maturity, the weight of the mature green siliques after 3 months of growth was considered as representative of the weight of the mature seeds previously measured on smaller populations of plants. The measurements were made on the main stem in F2BC1

populations, siliques were counted and collected to measure their weight, the results are shown in **Figure 22, C**. Except for Q6.10, Q7.1 and L9.1, the number of siliques on the main stem of suppressor individuals was higher than on *hmg1-1* parental line. The weight of the siliques was particularly different between WS2 and *hmg1-1*, and some suppressor individuals showed an equal (C52, SS1) of even higher (Q81, D8.1) weight of siliques on the main stem than the wild type. Suppressor individuals of all the candidate lines showed a higher weight of siliques than *hmg1-1* and non-suppressor individuals. Still, non-suppressor individuals of Q6.9 and D8.1 also showed a higher weight of siliques than *hmg1-1*.

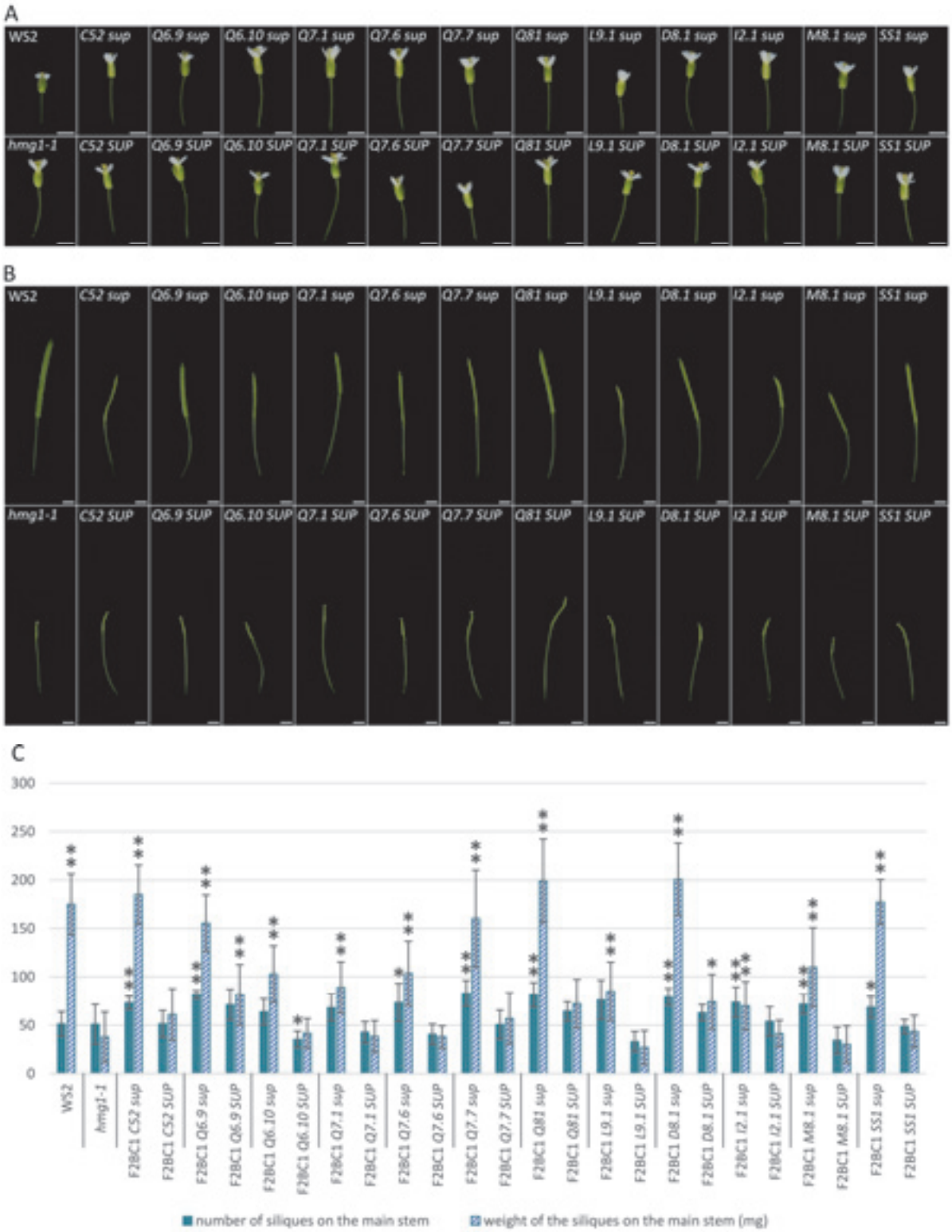

Figure 22. Phenotypes of the flowers and siliques of *Arabidopsis thaliana hmg1-1* suppressors. Pictures of the flowers at anthesis (**A**) and mature green siliques (**B**) of F2BC1 suppressor (*sup*) and non-suppressor (*SUP*) individuals, scale bars 0.2cm. A representative picture is shown for each phenotypic class. (**C**), Number of siliques on the main stem (dark blue bars), and total weight in mg of those siliques of *sup* and *SUP* individuals of a F2BC1 population (N_i=15-50). Statistical difference from the values obtained for *hmg1-1* parental line were determined using a pairwise Student t-test, with a p-value<0.05 (single asterisks) or p-value<0.01 (double asterisks). The weight of the green mature siliques represents a proxy measurement of dry seed weight per plant.

As an increase of the weight of the siliques could be due to more seeds or to bigger seeds in the same amount, phenotypes of the seeds in F2BC1 generation were observed. A representative picture of the seed morphology for each line is given in **Figure 23, A,** and measurements of the seed surface are given in **Figure 23, B**. No phenotypic modification was observed on the seeds by microscopy. Surface measurements show that the seeds of *hmg1-1* and Q81 are slightly smaller, while C52 line has the biggest seeds. The other lines have mean seed surface comparable to WS2.

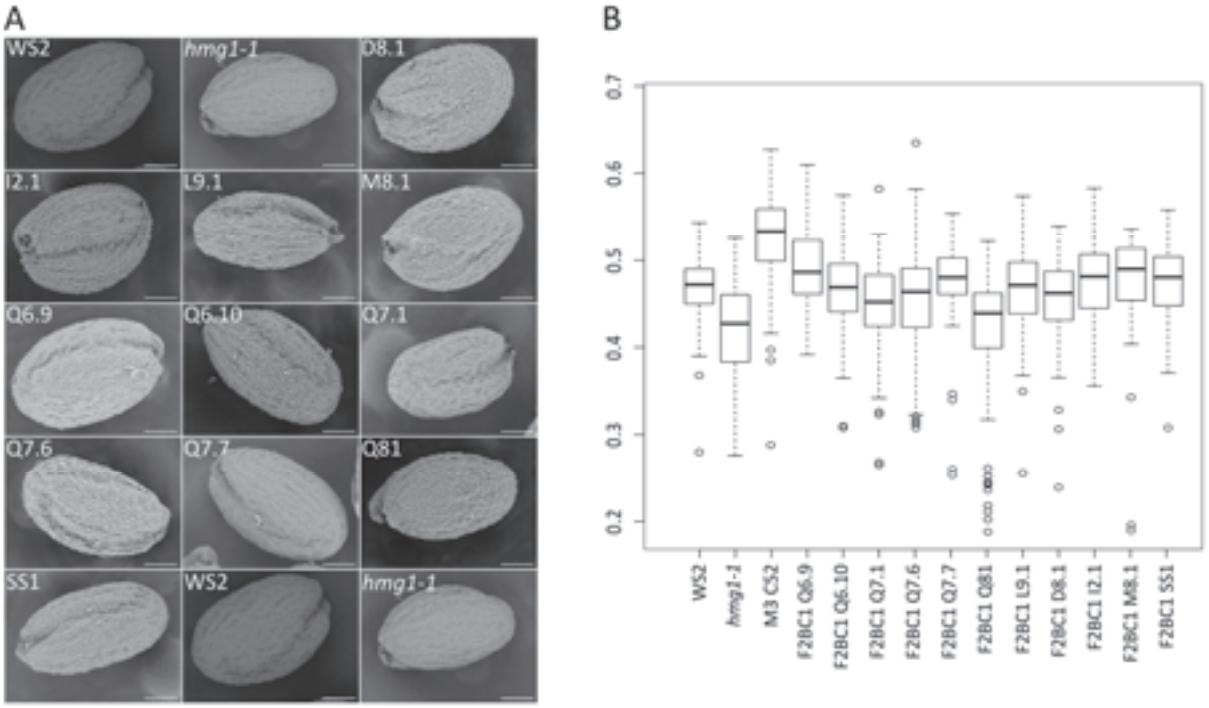

Figure 23. Seeds of *Arabidopsis thaliana hmg1-1* suppressors. Seeds from F1 self-fertilization were sampled in F2BC1 populations (except for the sup^{C52} taken from a M3 generation). (**A**), Pictures were taken with TM-100 electronic tabletop microscope (Hitachi), scale bars 100µm. A representative image is shown for each *hmg1-1* suppressor. For practical reasons, WS2 and *hmg1-1* pictures are presented twice (**B**), Seed size was given by surface measurements in mm^2 using Image J software (Ni>50).

5. Gene expression analysis on MEP and MVA pathways in candidate lines.

The expression of MVA and MEP pathway genes was measured by qPCR (**Figures 8 and 9**). In the analysis of MEP pathway genes expression, three genes have a statistically increased expression in the suppressor lines compared to *hmg1-1*: *DXR* in Q7.7, *HDS* in M5.1 and *HDR* in Q81, L9.1 and M5.1. The expression of all the other genes investigated is not statistically different when comparing the candidate lines to *hmg1-1*.

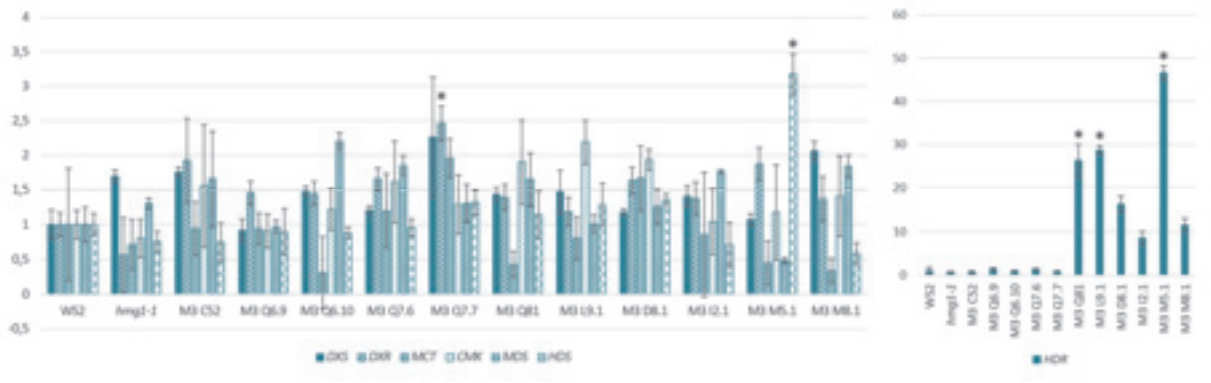

Figure 24. MEP pathway gene expression in *Arabidopsis thaliana hmg1-1* suppressors. *DXS*, 1-deoxy-D-xylulose 5-phosphate synthase; *DXR*, 1-deoxy-D-xylulose 5-phosphate reductoisomerase; *MCT*, MEP cytidyltransferase; *CMK*, 4-(cytidine 5'-diphospho)-2-*C*-methylerythritol kinase; *MDS*, 2-*C*-methylerythritol-2,4-cyclodiphosphate synthase; *HDS*, 4-hydroxy-3-methylbut-2-enyl 4-diphosphate synthase; *HDR*, 4-hydroxy-3-methylbut-2-enyl 4-diphosphate reductase. Technical triplicates were made from one sample. All values are normalized on WS2. Statistical analysis was made with a two-tailed multiple comparison test after Kruskal-Wallis to assess differences between the values obtained for suppressor candidates and *hmg1-1*, with a p-value=0.05 (single asterisk).

As expected, suppressor lines in M3 show a strongly reduced *HMG1* expression as it is the case of the *hmg1-1* parental line, which operates its mevalonate pathway only with *HMG2*. In M5.1 suppressor individuals, *MDC1* and *IDI1* gene expression are increased. In Q6.9 suppressors, *IDI1* gene expression is decreased while *CAS1* is increased compared to *hmg1-1*. In Q7.7 suppressors, *SQS1* and *CAS1* gene expression are both increased. For the other lines and genes considered, no statistical difference in the MVA pathway gene expression was found comparing suppressor individuals with *hmg1-1*.

Figure 25. MVA pathway gene expression in *Arabidopsis thaliana hmg1-1* suppressors. *HMG*, 3-hydroxy-3-methylglutaryl coenzyme A reductase; *MVK*, mevalonate kinase; *PMVK*, 5-phosphomevalonate kinase; *MDC*, mevalonate diphosphate decarboxylase; *IDI*, isopentenyl diphosphate:dimethylallyl diphosphate isomerase; *FDS*, farnesyl diphosphate synthase; *SQS*, squalene synthase; *SQE*, squalene epoxidase; *CAS*, cycloartenol synthase. Technical triplicates were made from one sample. All values are normalized on WS2. Statistical analysis was made with a two-tailed multiple comparison test after Kruskal-Wallis to assess differences between the values obtained for suppressor candidates and *hmg1-1*, with a p-value=0.05 (single asterisk).

6. Sterol content of whole plant extracts.

The *hmg1-1* mutant can fill its siliques after a treatment with squalene, a sterol precursor, thus it was interesting to measure the sterol content in *hmg1-1* suppressor lines. After extraction,

unsaponifiable lipids were analyzed by gas chromatography and mass spectrometry (GC-MS). As all the samples were treated the same way, an approximation of the lipid content in each line can be made by comparing the peak surface obtained for a given molecule. An example of the total ion current (TIC) for an extract is given in **Figure 26, A.** The identification of the different peaks observed on the TIC is made by the observation of the mass spectrum, for example sitosteryl acetate in **Figure 26, B.** The peak areas are given in **Figure 26, C**, showing no statistical difference between WS2, *hmg1-1* and the suppressor individuals in M3 for the studied molecules.

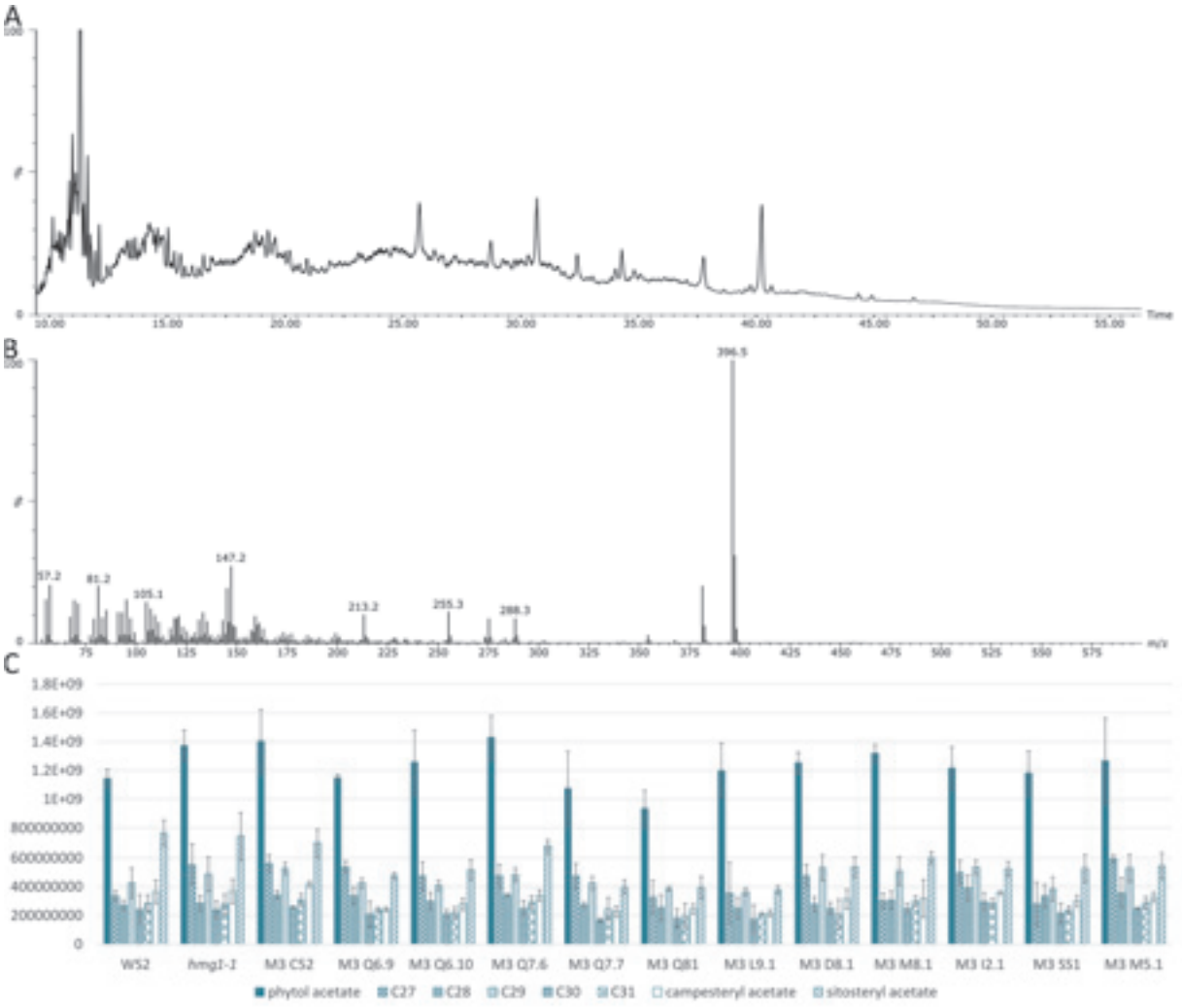

Figure 26. Gas chromatography-mass spectrometry analysis of the unsaponifiable lipids from *Arabidopsis thaliana hmg1-1* suppressor extracts. Lipids were extracted with n-hexane from 50 mg fresh weight of whole plant tissues. (**A**), Total ion current (TIC) chromatogram of extracts. (**B**), Mass spectrum of sitosteryl acetate; mass spectra of other compounds are given in **Suppl. Figure 2**. (**C**), Lipid profiles are given as mean peak areas of biological triplicates. C27 to C31 compounds are stem alcanes. Statistical analysis was made with a Kruskal-Wallis rank sum test, no statistical difference was found between the values obtained for candidate lines and *hmg1-1*.

7. Genetic analysis of suppressor *sup hmg1-1* mutations.

Genetic analysis of suppressor mutations can be performed first with a segregation analysis on F2BC1 populations obtained from a cross between a suppressor candidate as a male and the *hmg1-1-* parental line as a female. As described previously, candidate lines were selected on the basis of a homogenous suppressor population in the M3 generation. M3 plants crossed with *hmg1-1* gave a F1BC1, whose phenotype is unknown because of the treatment of the plants with squalene to obtain enough seeds for the segregation analysis in F2BC1 after selfing of one F1 individual. In F2BC1 populations, the number of suppressor (*sup*) and non-suppressor (*SUP*) plants was recorded to analyze the segregation pattern of one or more mutations causative of the suppressor phenotype. The germination rate of the candidate lines was established on soil and *in vitro*. It shows an overall low germination rate of all lines including the WS2 genetic background. This is most probably not preventing the comparison of results for each line. The type of mutation expected was determined from the segregation analysis, and the best segregation hypothesis was defined using the χ^2 statistical test (full results shown in **Table 6**). The genetic characterization of *hmg1-1* suppressors in the successive generations is summarized in **Table 5.**

Table 5. Genetic characterization of *Arabidopsis thaliana hmg1-1* suppressors. Best segregation hypothesis was determined with χ^2 test (see **Table 6**). All individuals were genotyped to confirm the *hmg1-1*/*hmg1-1* genotype (except WS2 and WS2x*hmg1-1* F1 hybrids).

***hmg1-1* suppressor line**	**% suppressor individuals in M3 N_i=3-8**	**Phenotype of F1BC1 individuals N_i=3-5**	**Phenotypic distribution in a F2BC1**		**Germination rate of the F2BC1 populations**		**Type of mutation**	**Best segregation hypothesis (*sup*:*SUP*)**
			sup	*SUP*	Soil 50 seeds	*in vitro* 100 seeds		
C52	100% *sup*	Unknown	55	24	15%		recessive	2:1
Q6.9	100% *sup*	Unknown	51	105	31%	62%	recessive	1:3?
Q6.10	100% *sup*	Unknown	58	31	35%	78%	recessive	2:1
Q7.1	100% *sup*	Unknown	66	110	34%	46%	recessive	7:9
Q7.6	100% *sup*	Unknown	89	33	37%	71%	dominant	3:1
Q7.7	100% *sup*	Unknown	44	100	39%		recessive	1:3
Q81	100% *sup*	Unknown	40	144	11%	17%	recessive	1:3
L9.1	100% *sup*	Unknown	58	26	26%	43%	recessive	2:1
D8.1	100% *sup*	Unknown	21	124	9%	19%	?	?
I2.1	100% *sup*	Unknown	32	64	28%	65%	recessive	1:3
M8.1	100% *sup*	Unknown	40	41	38%	65%	dominant	1:1
SS1	100% *sup*	Unknown	17	44	6%	5%	recessive	1:3
M74	segregating	Unknown	-	-	-	-	-	-
L51	segregating	Unknown	-	-	-	-	-	-
U21	segregating	Unknown	-	-	-	-	-	-
S61	segregating	Unknown	-	-	-	-	-	-
P9a	segregating	Unknown	-	-	-	-	-	-
WS2x*hmg1-1*	-	Unknown	27 *hmg1-1*	116 WT	31%	-	recessive	1:3
WS2	-	-	-	-	21%	62%	-	-
hmg1-1	-	-	-	-	38%	51%	-	-

The analysis of a WS2 x *hmg1-1* F2BC1 population shows that the *hmg1-1* mutation is recessive (as expected for a biochemical mutant phenotype that is conferred by a T-DNA insertional loss of function allele), with a segregation ratio of 3 suppressors for 1 non-suppressor individuals. In the candidate lines selected, both dominant and recessive mutations have been selected. Three lines show a 3:1 (Q7.6) or 1:3 (Q6.9, Q7.7, Q81, I2.1, SS1) segregation ratio, seven lines

show a 2:1 (C52, Q6.10, L9.1) ratio, and the lines Q7.1 and M8.1 are the only ones to show a 7:9 and 1:1 ratio respectively.

The χ^2 analysis indicates which segregation hypothesis is the most suitable by comparing observed values with theoretical values expected for each hypothesis. The hypothesis is considered as viable if the p-value obtained is bigger than 0.05. If more than one hypothesis is considered as correct, the highest value indicates the most reliable hypothesis.

Table 6. P-values for χ^2 analysis of segregation hypothesis for *Arabidopsis thaliana hmg1-1* suppressor lines in F2BC1. A hypothesis is considered viable if p-value>0.05. If two hypotheses are validated, the best hypothesis selected is the one with the highest p-value. P-values of the selected hypothesis are in bold black, p-values of viable hypothesis are in black, p-values<0.05 are in grey (hypotheses were not considered viable).

Hypothesis *sup:SUP*	**3:1**	**1:3**	**1:1**	**2:1**	**9:7**	**7:9**
WS2x*hmg1-1*	**0,0911**	2,20E-16	9,88E-14	0,0002	2,04E-09	2,20E-16
C52	0,2695	2,20E-16	0,0005	**0,5776**	0,0166	3,57E-06
Q6.9	2,20E-16	**0,0265**	1,54E-05	2,20E-16	3,01E-09	0,0054
Q6.10	0,0322	2,20E-16	0,0042	**0,7643**	0,0899	4,64E-05
Q7.1	2,20E-16	0,0019	0,0009	2,25E-16	5,32E-07	**0,0946**
Q7.6	**0,6012**	2,20E-16	3,98E-07	0,1409	0,0002	7,94E-11
Q7.7	2,20E-16	**0,1237**	3,06E-06	2,20E-16	5,12E-10	0,0014
Q81	2,20E-16	**0,3070**	1,76E-14	2,20E-16	2,20E-16	1,76E-09
L9.1	0,2077	2,20E-16	0,0005	**0,6434**	0,0181	2,96E-06
D8.1	2,20E-16	2,20E-16	2,20E-16	2,20E-16	2,20E-16	1,21E-12
I2.1	2,20E-16	**0,0594**	0,0011	4,26E-12	6,00E-06	0,0397
M8.1	1,01E-07	4,02E-07	**0,9115**	0,0010	0,2128	0,3068
SS1	2,20E-16	**0,6048**	0,0005	1,29E-10	7,88E-06	0,0124

The characterization of suppressor genetics is a precious tool to go further and try to identify the causal mutations by sequencing of the whole genome. At the same time, the classical genetic analysis was pursued by performing a genetic complementation analysis and by further backcrossing *sup hmg1-1* mutants to generate F2BC2 then F2BC3 generations.

8. Identification of causal mutations by next generation sequencing.

Next generation sequencing allows the sequencing of whole genomes, but the quality of the sequencing depends greatly on the quality of the genomic DNA sample preparation. The extraction protocol was developed in order to obtain clean and intact genomic DNA in large amounts for library preparation. The identification of the samples and the concentration of genomic DNA obtained are summarized in **Table 7.** The quality of the genomic DNA (gDNA) was verified by spectrometry, with an $OD_{260/280}$>1.8 for all the samples.

Table 7. Identification and sample quality of gDNA extracts from *Arabidopsis thaliana hmg1-1* suppressor lines sequenced by Illumina. All samples had a value of $OD_{260/280}$>1.8 measured with Nanodrop 2000 (Thermo Scientific).

ID	*hmg1-1* suppressor line	Concentration (ng/µl)	Quantification method	Volume (µl)	Sample type
HTSR15	WS2	41	Qubit	57	gDNA
HTSR16	*hmg1-1*	74	Qubit	57	gDNA
HTSR17	*F2BC1 C52 sup*	37.8	Qubit	58	gDNA
HTSR18	F2BC1 C52 SUP	34.4	Qubit	58	gDNA
HTSR19	*F2BC1 Q6.9 sup*	139.2	Qubit	58	gDNA
HTSR20	F2BC1 Q6.9 SUP	140.8	Qubit	58	gDNA
HTSR21	*F2BC1 Q7.7 sup*	81.4	Qubit	58	gDNA
HTSR22	F2BC1Q7.7 SUP	81	Qubit	58	gDNA
HTSR23	*F2BC1 Q81 sup*	119.4	Qubit	58	gDNA
HTSR24	F2BC1 Q81 SUP	95.6	Qubit	58	gDNA
HTSR25	*F2BC1 D8.1 sup*	50.8	Qubit	58	gDNA
HTSR26	F2BC1 D8.1 SUP	53	Qubit	58	gDNA
HTSR27	*F2BC1 SS1 sup*	42	Qubit	58	gDNA
HTSR28	F2BC1 SS1 SUP	38.4	Qubit	58	gDNA
HTSR29	*F2BC1 Q6.10 sup*	95.6	Qubit	58	gDNA
HTSR30	F2BC1 Q6.10 SUP	115.4	Qubit	58	gDNA
HTSR31	*F2BC1 Q7.6 sup*	53	Qubit	58	gDNA
HTSR32	F2BC1 Q7.6 SUP	50.2	Qubit	58	gDNA
HTSR33	*F2BC1 Q7.1 sup*	110.2	Qubit	58	gDNA
HTSR34	F2BC1 Q7.1 SUP	121.0	Qubit	58	gDNA
HTSR35	*F2BC1 L9.1 sup*	51.8	Qubit	58	gDNA
HTSR36	F2BC1 L9.1 SUP	55.2	Qubit	58	gDNA

HTSR37	*F2BC1 M8.1 sup*	53.4	Qubit	58	gDNA
HTSR38	F2BC1 M8.1 SUP	61	Qubit	58	gDNA
HTSR39	*F2BC1 I2.1 sup*	78.2	Qubit	58	gDNA
HTSR40	F2BC1 I2.1 SUP	85.4	Qubit	58	gDNA

The integrity of the genomic DNA was verified on an electrophoresis gel (**Figure 27, A**) and measured on Covaris (**Figure 27, B**). All samples were non-degraded and could be used for library preparation and sequencing.

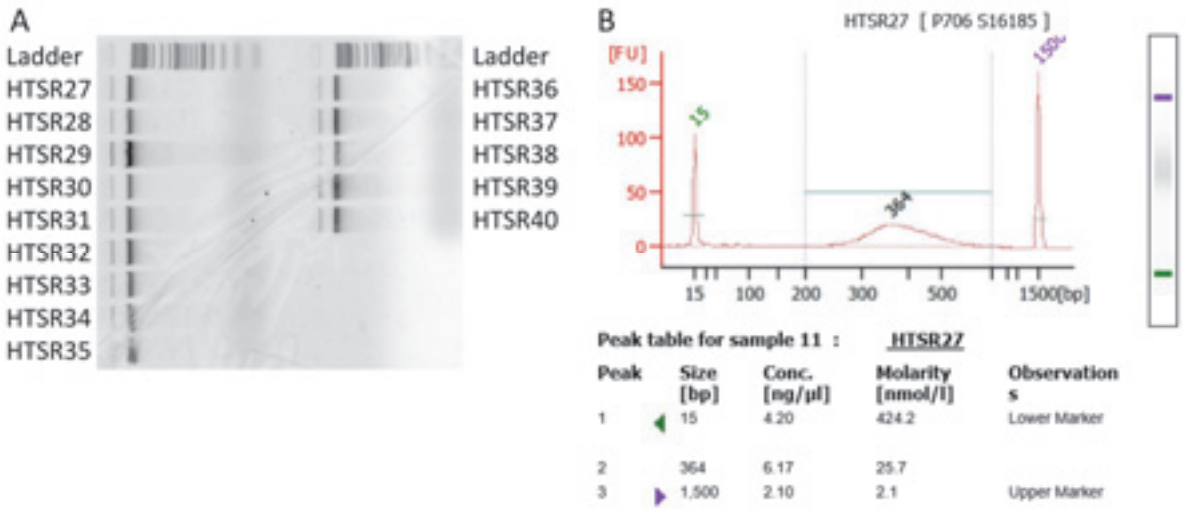

Figure 27. Control of *Arabidopsis thaliana hmg1-1* suppressor lines gDNA sample quality before library preparation and next generation sequencing. (**A**), gDNA integrity was checked on agarose gel and (**B**), quality was controlled on Covaris (Agilent).

Sequencing was performed by the IGBMC Microarray and Sequencing platform (Strasbourg) and bioinformatic analysis was optimized by Sylvain Darnet (Laboratório de Biotecnologia Vegetal, Instituto de Ciências Biológicas, Universidade Federal do Pará (UFPA), Belém, Brazil). The suppressor and non-suppressor individuals were sampled separately, and the non-suppressor sequences obtained served as a blank to eliminate all the non-causal mutations due to the EMS treatment. The theoretical coverage is given by the number of raw reads obtained after sequencing multiplied by 100 (length of a read in base pairs) and divided by the genome size given by databases (TAIR10). During pre-processing, pairing and variant calling, some reads are lost. The final sequencing coverage can be calculated the same way, using the number of reads left after bioinformatic treatment of the data. An example is given in **Table 8** with the analysis of sequencing data obtained for HTSR15 (WS2) sample. The theoretical coverage

calculated from the number of raw reads given after sequencing is 144.78X, and final sequencing coverage indicative of the properly paired sequences is 98.7X.

Table 8. Bioinformatic analysis of HTSR15 (WS2). The number of reads has been recorded after each step of the bioinformatics process and allows the calculation of theoretical and final sequencing coverage of the genome.

HTSR15	Number of reads	% of raw reads
Raw reads	196 428 914	
After pre-processing	194 204 338	98%
Properly paired	172 212 250	88%
After variant calling	133 922 720	77%
Theoretical coverage of the genome	144.78X	
Final sequencing coverage	98.7X	

Raw sequencing data is available for the twelve candidate lines and is being analyzed as described in the bioinformatic analysis section of Materials and Methods.

II. Genetic screening for *chs5* suppressor mutations.

1. Size of the mutagenesis experiment.

Seeds from the *chs5* line (1 gram, approximately 50000 seeds) were treated with EMS as described for the *hmg1-1* mutagenesis. Seedlings were potted in standard soil and grown in a growth chamber under a 12 hours / 12 hours light/dark regime at 21°C during the light period and 19°C during the dark period. A total of 2500 M1 plants were allowed to self in order to generate M2 generations. M2 seeds were harvested per each plant and organized in 125 pools of 20 M2 families, each M2 family being represented by 50 seeds. As for the *hmg1-1* mutagenesis experiment, the screen was conducted by Vincent Compagnon and Hubert Schaller over several months. I joined the laboratory at the time the last batches of M2 pools were screened *in vitro* as described above.

2. Details of screening conditions.

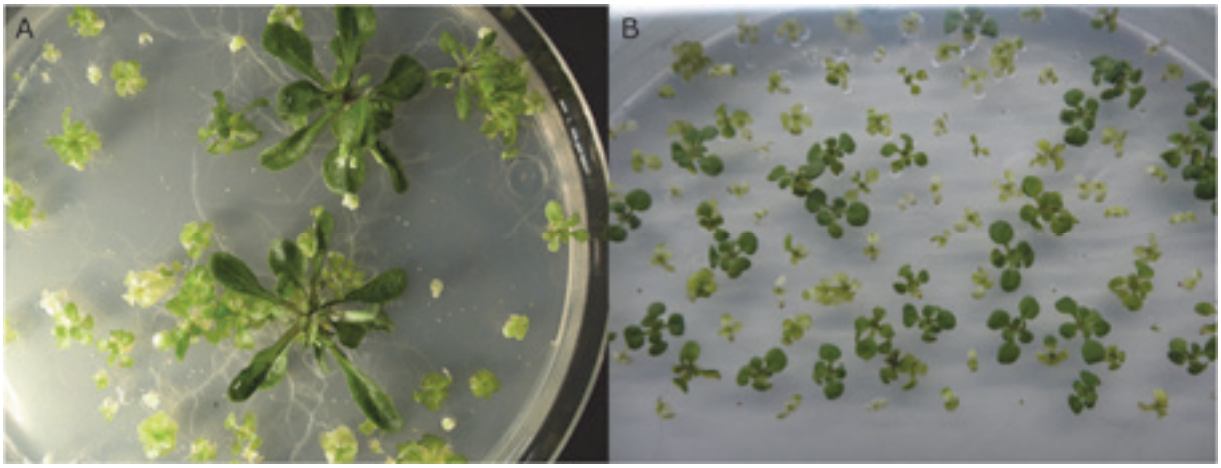

Figure 28. Discrimination between Col-0 and *chs5* phenotypes of seedlings grown *in vitro* on a solid synthetic medium. (**A**), Phenotypes of Col-0 wild type and *chs5* mutant seedlings. Two Col-0 plantlets display normal green leaves and a normal growth, the other plantlets are *chs5* mutants exhibiting a poor growth and chlorotic phenotype (picture and experiment by Vincent Compagnon). (**B**), In a F2BC1 population of suppressor lines, suppressor green plantlets and non-suppressor small and yellow plantlets segregate.

The screening for *chs5* suppressors was performed *in vitro* on a solid synthetic medium (Murashige & Skoog) supplemented with 0.1% sucrose. About 500 seeds were sown per Petri plate (15 cm diameter). These plates were placed for 4 weeks in a Sanyo MLH-51 incubator with the following light and temperature photoperiodic regime: 16 hours light (160µmol photon.s^{-1}.m^{-2}) at 18°C followed by 8 hours light (100µmol photon.s^{-1}.m^{-2}) at 16°C. These growth conditions allowed a very clear discrimination between *chs5* mutant and Col-0 wild type seedlings. In fact, *chs5* seedlings exhibited a very poor growth and chlorotic phenotype, whereas Col-0 displayed a normal photosynthetic growth (**Figure 28, A**). Individuals from M2 *chs5* families that had a wild type-like growth behavior (**Figure 28, B**) were then transferred to soil and grown autotrophically in a growth room. There, the photoperiodic regime was 12 hours light at 18°C and 12 hours dark at 15°C. The temperature record presented in **Figure 29** shows a regular alternation of the temperatures.

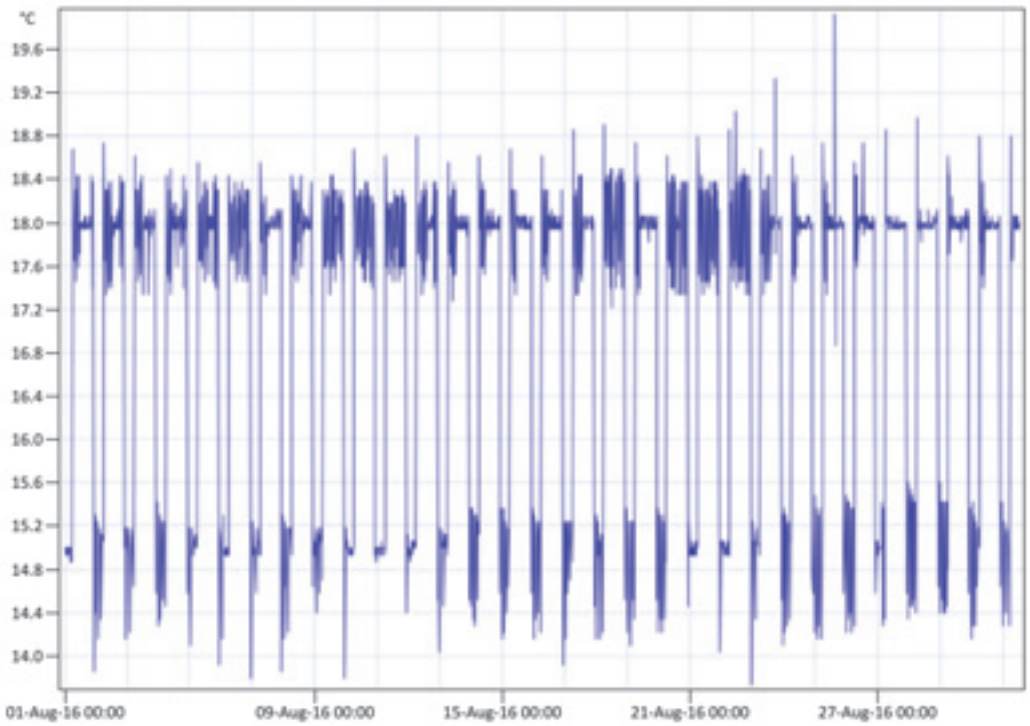

Figure 29. Temperature conditions in the growth room for *Arabidopsis thaliana chs5* suppressor lines.

3. Genotyping of the *chs5* mutation.

The *chs5* mutant is carrying a G to A missense mutation in the exon 8 of the *DXS1* gene, causing a change of an aspartic acid (D) to an asparagine (N) at position 627 (D627N) as represented in **Figure 30, A**. The suppressors (or true revertants) selected in the screen were genotyped for this G to A substitution by PCR amplification, using two distinct reactions. A common reverse primer was used for the two reactions, combined in one case with a forward primer carrying the wild type GAC sequence (DXR-F2N), and in the second case with a forward primer carrying the *chs5* sequence containing an AAC motif (DXR-F2M). The first amplification was selective and gave an amplification product at 213bp in presence of the wild type sequence, the second amplification was quasi-selective and produced an amplification product of 213bp in presence of the *chs5* mutated sequence. The plant DNA was amplified in two separate PCR reactions, and the products were visualized on an electrophoresis gel as seen in **Figure 30, B.** In the case of a *CHS5*/*CHS5* (wild type) plant, only one product was amplified in the reaction with DXR-F2N. Genomic DNA from *CHS5*/*chs5* individuals gave one product in each reaction, thus two bands were visualized on the gel. Finally, amplification of DNA from *chs5*/*chs5* plants gave one product from the reaction with DXR-F2M. At the start of the project, the amplification and

sequencing of an exon 8 PCR product spanning over the GAC>AAC mutation confirmed the SNP between col-0 and *chs5* (Araki et al., 2000).

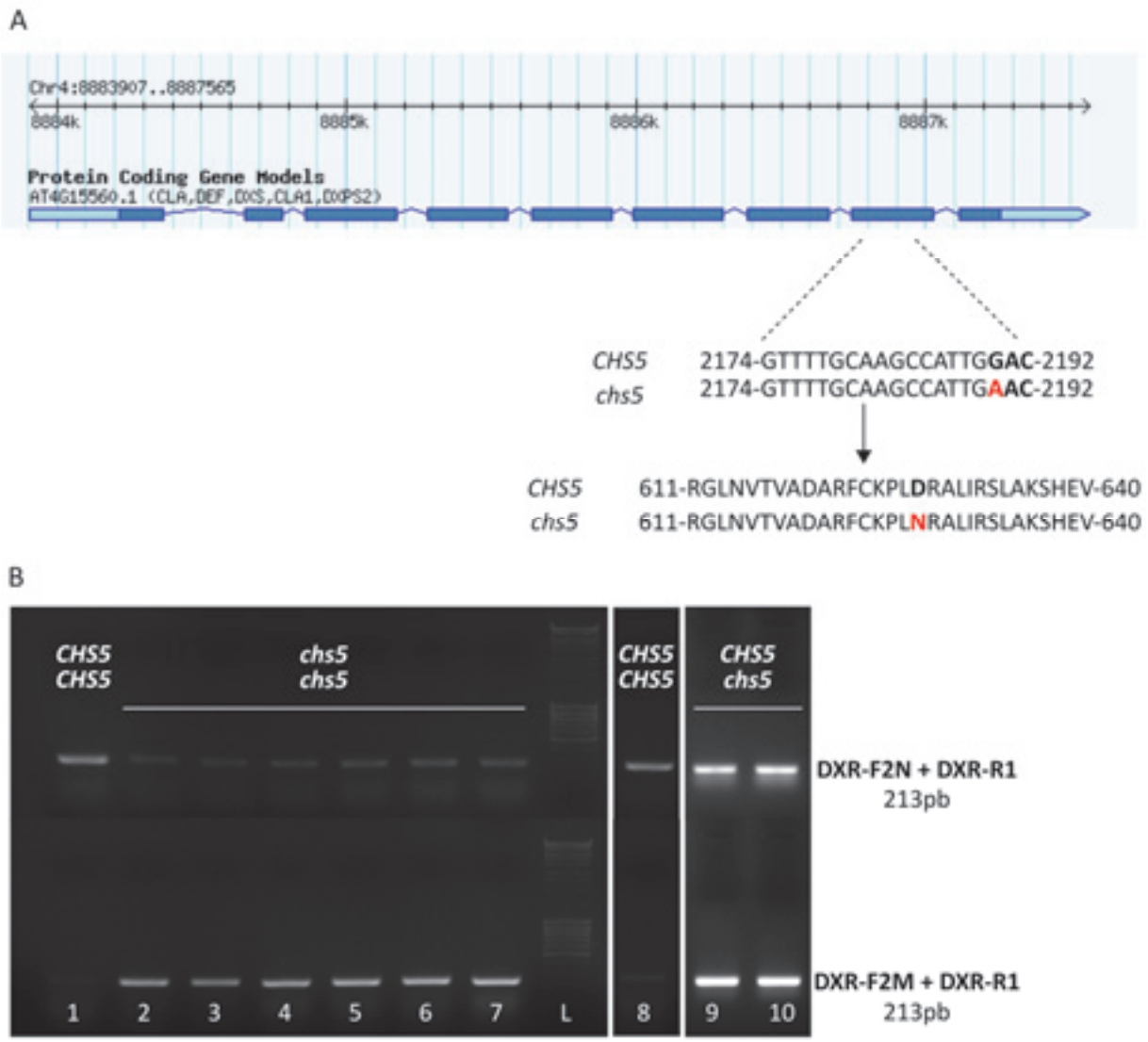

Figure 30. Genotyping of the D627N mutation in the *DXS1*/*CLA1* gene. (**A**), The *Arabidopsis thaliana chs5* mutant is carrying a missense mutation GAC > AAC in the exon 8 of the *DXS1* gene resulting in a substitution of an aspartic acid (D) to an asparagine (N) at position 627 (D627N). Exons are represented as blue boxes, introns as blue lines (Gene map from TAIR, The *Arabidopsis* Information Resource, http://www.*Arabidopsis*.org/). Genotyping of this single nucleotide polymorphism (SNP) was made by selective amplification of two allele-specific PCR products of the same length with a common reverse primer DXS-R1, and a wild type (*CHS5*) allele specific primer DXS-F2N or a *chs5* allele specific primer DXS-F2M that carries an A at nucleotide position 2190 of the genomic sequence instead of a G. (**B**), PCR products visualized by agarose gel electrophoresis discriminated the wild type and mutant DNA due to the selective amplification of wild type DNA with primers F2N + R1 (upper part of the gel), and the quasi-exclusive amplification of mutant DNA with primers F2M + R1 (lower part of the gel). Lane 1, Col-0 wild type *CHS5*/*CHS5* DNA; lane 2, *chs5* mutant *chs5*/*chs5* DNA; lanes 3-7, *chs5* suppressor individuals of *chs5*/*chs5* genotype; lane 8, false positive *chs5* suppressor individual therefore discarded for further experiment; lanes 9-10, *chs5* suppressor individuals of *CHS5*/*chs5* genotype discarded too. L: MassRuler DNA Ladder Mix, Thermo Fischer Scientific.

4. Sequencing of *DXS1*/At4g15560 cDNA in candidate lines.

The aim of this screening was to identify functional suppressors for the analysis of the tremendously important cellular process that is isoprenoid homeostasis. Particularly, the objective was to select intergenic suppressors. Thus, no intragenic suppressors of *DXS1* were expected to be chosen for a further characterization, (although those could be of interest to study an allelic series of *DXS1*). *DXS1* was amplified from cDNA samples of *chs5* and two suppressor candidates (Y50 and Y200), and sequencing was performed on the amplification products obtained. The nucleic sequences obtained were subjected to a basic local alignment tool (BLAST, NCBI, https://blast.ncbi.nlm.nih.gov/Blast.cgi) and matched with *DXS1* sequence from nucleotide position 592 to the end of the sequence. The nucleic sequence was translated using ExPASy Translate tool (http://web.expasy.org/translate/), and protein sequences of *chs5* and candidate lines were compared to the wild type sequence given by The *Arabidopsis* Information Resource (TAIR10, http://www.*Arabidopsis*.org/). Protein sequences matched perfectly from amino acid position 62 to the end of the DXS1 sequence, as shown in **Figure 31**.

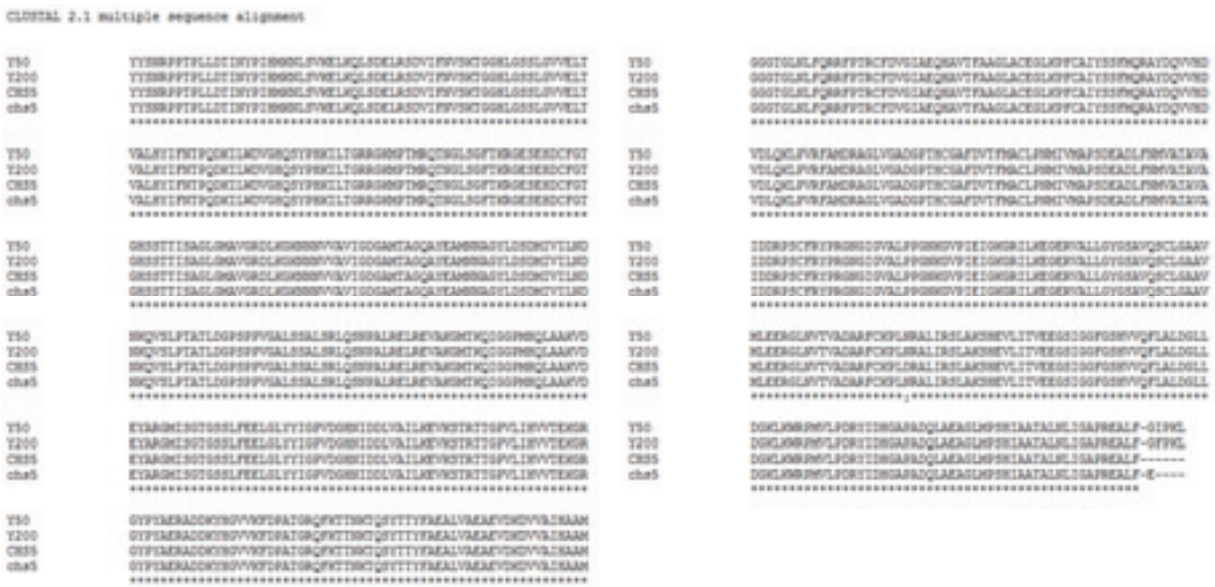

Figure 31. Protein sequence alignment of DXS1. DXS1 sequence was amplified from cDNA samples of *chs5* and suppressor candidates, and the amplification products were sequenced. The nucleic sequences obtained were used for multiple sequence alignment with CLUSTALW (http://www.genome.jp/tools/clustalw/), and then translated with ExPASy Translate tool (http://web.expasy.org/translate/). Protein sequences obtained from *chs5* and suppressor candidates were aligned to the wild type sequence obtained from TAIR (The *Arabidopsis* Information Resource, http://www.*Arabidopsis*.org/). A magnified version of the figure is available in **Suppl. Figure 3**.

5. Phenotypic characterization of *chs5* suppressor in M2, M3 and backcrossed generations.

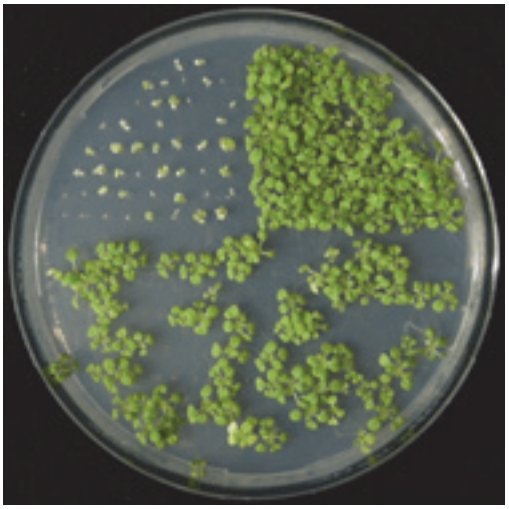

Figure 32. *In vitro* screening for suppressors of *chs5* phenotype. On the same petri plate, M3 generations of suppressor candidates (N_i=150, down) were sown with Col-0 (N_i=50, top right) and *chs5* (N_i=50, top left).

The screening yielded 84 M2 individuals that were selfed (August 2014). M3 generations (N_i=150) were sown together with Col-0 (N_i=50) and *chs5* (N_i=50) on the same Petri plate and grown in selective conditions, as previously defined in order to confirm the suppressor phenotypes for each of these 84 families (**Figure 32**). Of 35 lines that were confirmed, 6 lines were chosen for further studies. The *chs5* suppressor (sup *chs5*) individuals were phenotyped at a young developmental stage, either *in vitro* as seedlings, or in soil at the rosette stage shortly before bolting. A schematic representation of the reference phenotypes is given in **Figure 33**. In soil, *chs5* phenotype is recognized by chlorotic leaves, presenting yellow spots, mainly seen in young tissues. *In vitro*, the cotyledons are generally green and sometimes yellow, and the first pair or leaves is yellow.

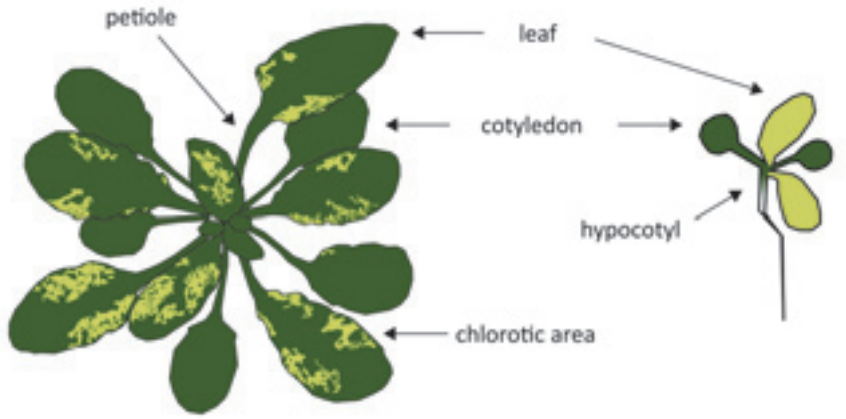

Figure 33. Schematic representation of an *Arabidopsis thaliana* rosette of *chs5* mutant grown in soil (left) and of a seedling grown *in vitro* (right). Seedling size is magnified.

Typical seedling phenotypes of M3 generations are shown in **Figure 34**. Under these conditions, *chs5* individuals presented greenish cotyledons and yellow leaves, while the Col-0 wild type control was fully green. Plantlets were carefully phenotyped after 2 weeks of growth for the 6 *chs5* suppressor lines that were chosen among the candidate lines selected in a M2 generation. Seedlings of the 6 lines exhibited a diversity of phenotypes shown in **Figure 34**. Four lines had fully green leaves of a wild type-like phenotype (G2.10, L8.4, Y50, Y200), one had pale green leaves (LA4) and one had pale green leaves and elongated hypocotyl and petioles (iQ3). Four candidate lines showed a segregation of suppressor (*sup*) and non-suppressor (*SUP*) individuals in a M3 generation, two candidate lines (G2.10 and L8.4) did not show a segregation in this generation.

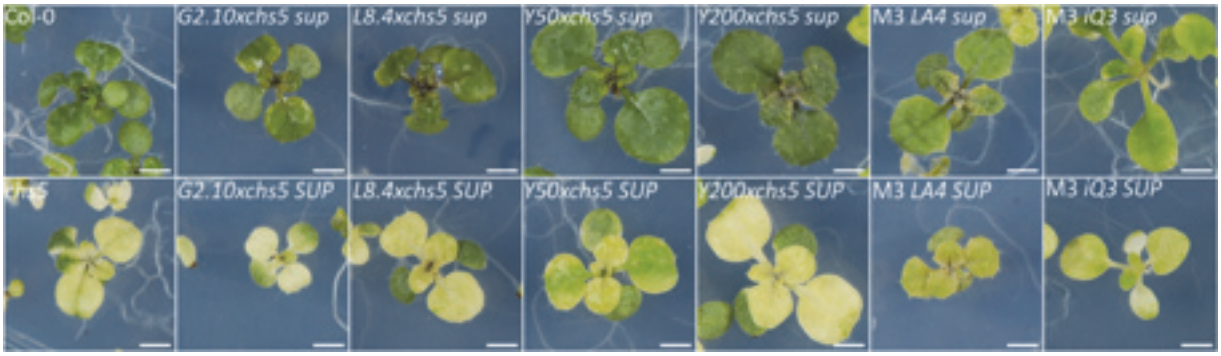

Figure 34. Seedlings of *Arabidopsis thaliana chs5* suppressors grown *in vitro*. Pictures of representative seedlings of suppressor (*sup*) and non-suppressor (*SUP*) phenotypes for the six candidate lines selected after an *in vitro* screening. Seedlings were phenotyped after 2 weeks of growth on synthetic medium at 16°C. Scale bars 0.2cm.

In order to further describe the revertant phenotypes of candidate suppressors and to confirm that reversion in autotrophic conditions, plants were grown in soil according to the conditions described in the Materials and Methods section. Pictures of a representative suppressor and non-suppressor individual for each line are given in Figure 35. Suppressor individuals of the four wild type-like candidates (*sup chs5* G2.10, L8.4, Y50, Y200) presented green leaves and a well-developed rosette after one month of growth. Non-suppressor individuals of these lines had a typical *chs5* phenotype with chlorotic areas on the leaves and smaller rosettes. The *sup chs5* LA4 suppressor showed a pale green rosette, with the center of the rosette being slightly yellow, while non-suppressor individuals clearly exhibited chlorotic areas. The *sup chs5* iQ3 suppressor individuals had a rosette constituted of few pale green leaves, with an elongated petiole, thus partially restoring the slow growth of *chs5* individuals. The non-suppressor *sup chs5* iQ3 individuals showed chlorotic areas and a smaller rosette.

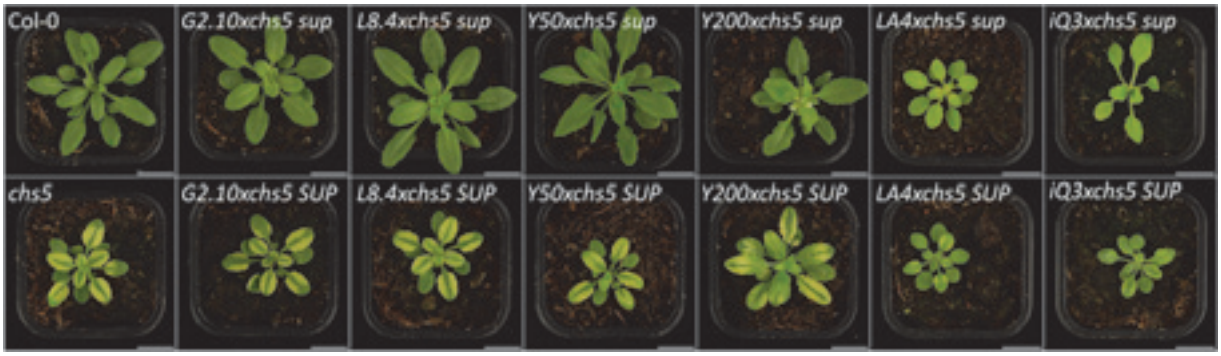

Figure 35. Phenotypes of the rosettes of *Arabidopsis thaliana chs5* suppressors in a F2BC1 generation. F2 seeds of selfed F1 plants obtained from a cross between a suppressor and the parental line (*sup chs5* x *chs5*, F2BC1) were sown on standard soil then a random proportion of the seedling population was potted ($N_i > 30$). Plants were grown as described in Materials and Methods section. Individuals were phenotyped for full green leaves (wild type-like leaves) or partially albino leaves typical of the *CHS5* phenotype after one month of growth. Pictures of the rosettes of F2BC1 *chs5* suppressor (*sup*) and non-suppressor (*SUP*) were taken at this discriminating stage. Scale bars 2cm. Magnified pictures are available in **Suppl. Figure 4**.

The *sup chs5* iQ3 suppressor phenotype was characterized by an elongated hypocotyl seen at the seedling stage *in vitro* and in soil. The long hypocotyl phenotype of *sup chs5* iQ3 seedlings grown in soil is indicated with arrows in **Figure 36, A**. The iQ3 suppressor individuals also presented an early bolting as compared to the Col-0 wild type and *chs5* controls and the other suppressor individuals of the five candidate lines. Non-suppressor individuals of all the candidate lines showed an equivalent developmental stage as the controls (**Figure 36, B**).

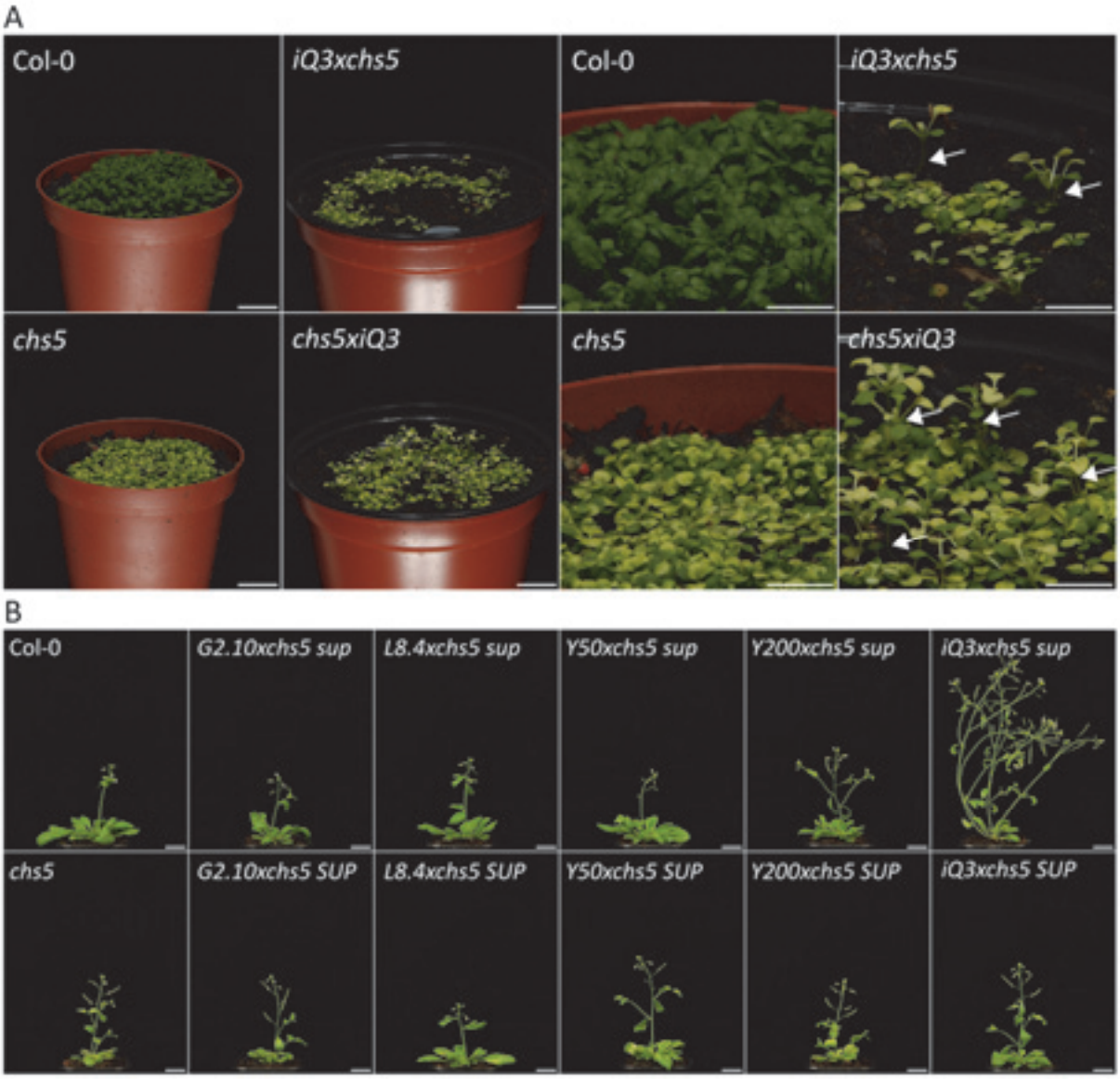

Figure 36. Seedlings and young plants at bolting stage of *Arabidopsis thaliana chs5* suppressors. (**A**), Wild type, *chs5*, and a F2BC1 segregating population of sup^{iQ3} two weeks after sowing. Seedlings are shown as close-up on the right with green cotyledons and white/yellowish first pair of leaves of *chs5* and iQ3 seedlings, arrows indicate the overgrowth of iQ3 hypocotyls compared to Col-0 and *chs5* hypocotyls. (**B**), Growth phenotype of *chs5* suppressors in segregating populations. Scale bars 2cm, 1cm in close up.

The seeds obtained by selfing of M2 suppressors or F1 individuals were observed by electronic microscopy (**Figure 37, A**), and no specific phenotype was described. Seed size was measured on a population of seeds and expressed as a mean value of seed surface in Figure 37, B. The *chs5* parental line exhibited smaller seeds than the wild type. All suppressor lines had seeds presenting approximately the same size as the seeds of Col-0, except for *sup chs5* iQ3 which presents small seeds as *chs5*.

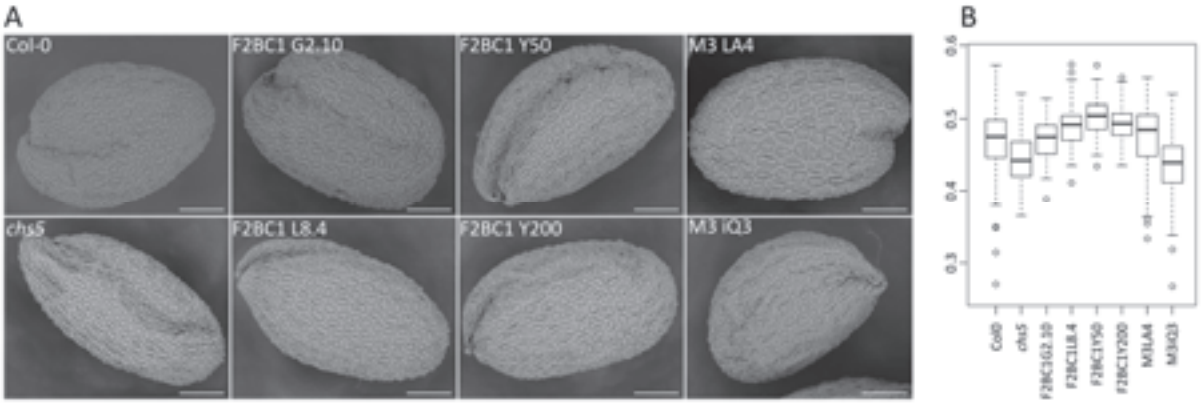

Figure 37. Seeds of *Arabidopsis thaliana chs5* suppressors sampled from F2BC1 or M3 generations. (**A**), TM-100 electronic tabletop microscope (Hitachi) pictures, scale bars 100µm. (**B**), Measurements of seed size expressed as areas (mm^2).

Chlorophyll and carotenoid content in *sup^{chs5}* leaves.

The chlorophylls and carotenoids content in these tissues were measured and expressed as $\mu g.g^{-1}$ fresh weight (FW) in **Figure 38**. No statistical difference was observed in the chlorophyll a, chlorophyll b and carotenoids content between Col-0 and *chs5*. As compared to *chs5*, all suppressor individuals except *sup chs5* iQ3 presented a higher amount of chlorophyll a. The *sup chs5* Y50, Y200, LA4 and iQ3 suppressors had a statistically higher amount of carotenoids in the leaves, and *sup chs5* G2.10 and L8.4 showed a higher carotenoids content.

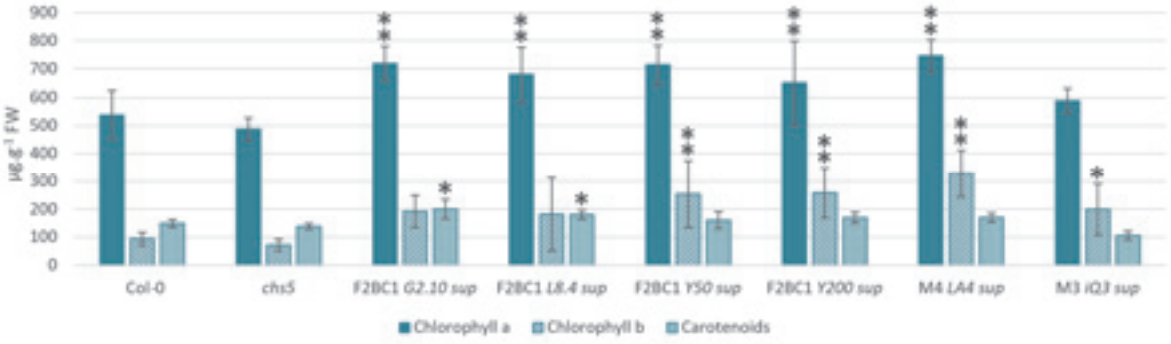

Figure 38. Spectrophotometric measurement of chlorophyll and carotenoid contents in leaves from *Arabidopsis thaliana chs5* suppressor lines. Results are given as $\mu g.g^{-1}$ fresh weight (FW). Statistical differences from the values obtained for *chs5* parental line were determined using a pairwise Student t-test, with a p-value<0.05 (single asterisk) or p-value<0.01 (double asterisks) for the measurement of chlorophyll a and chlorophyll b contents. A two-tailed multiple comparison test after Kruskal-Wallis was applied for the carotenoids content, with a p.value=0.05 (single asterisk).

Measurement of MEP intermediates in rosette leaves.

Biosynthetic intermediates of the MEP pathway were measured in rosette leaves and expressed as pmol.mg^{-1} dry weight (DW) in **Figure 39**. No statistical difference was observed between Col-0 and *chs5* in the quantification of the intermediates, except for a strong accumulation of MEP in *chs5* compared to the wild type. The amount of DXP in *sup chs5* L8.4 suppressors is reduced compared to *chs5*. This reduction is also found for MEcPP in *sup chs5* L8.4 and LA4 suppressors, and IPP and DMAPP in L8.4 suppressors and Y200 non-suppressor individuals.

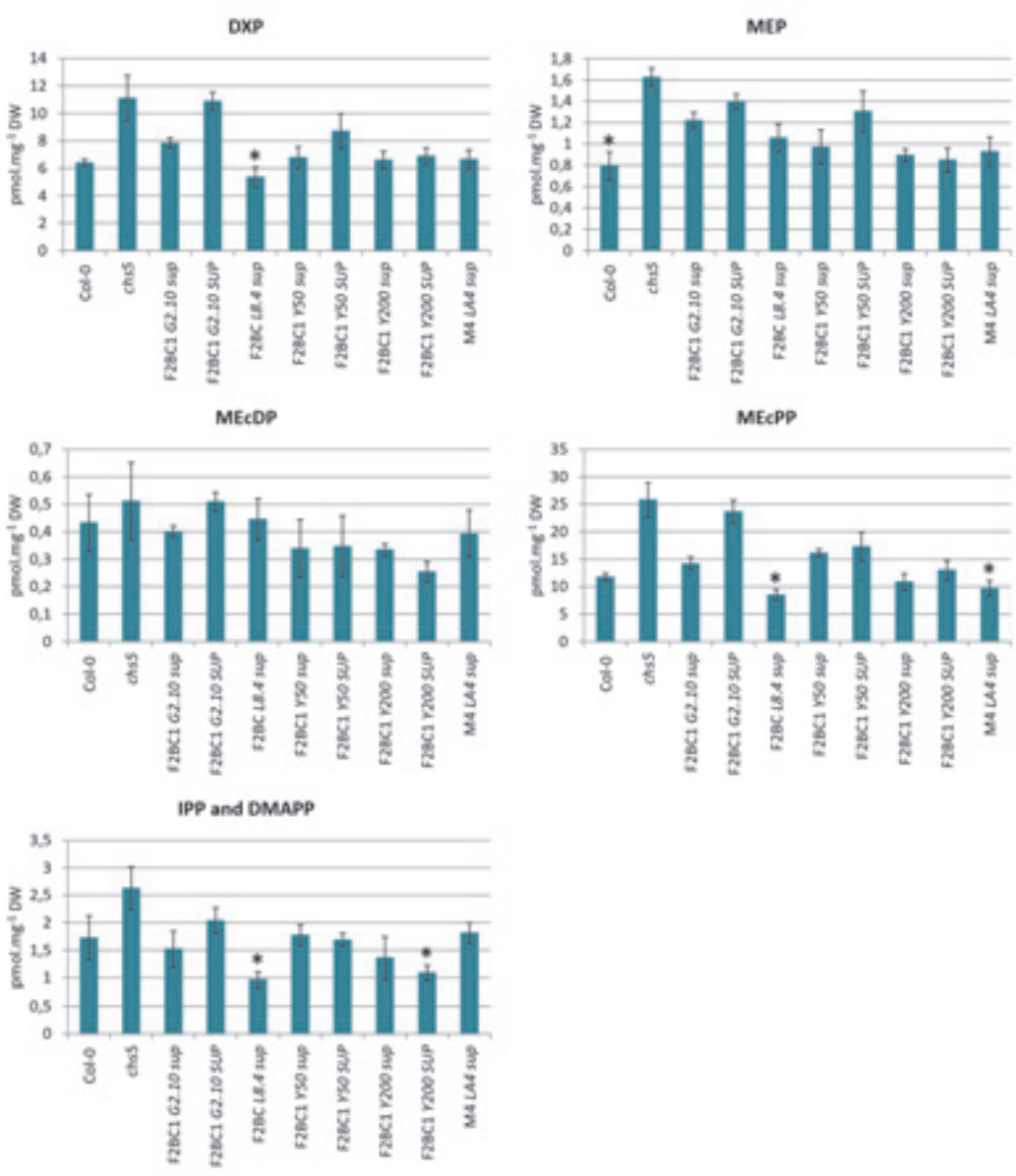

Figure 39. Quantification of MEP pathway intermediates in *Arabidopsis thaliana chs5* suppressor lines. Values are expressed as pmol.mg^{-1} dry weight (DW) of leaf material. DXP, 1-deoxy-D-xylulose 5-phosphate; MEP, 2-*C*-methyl-D-erythritol 4-phosphate ; MEcDP, 2-*C*-methyl-D-erythritol-2,4-cyclodiphosphate; MEcPP, 2-*C*-methylerythritol-2,4-cyclopyrophosphate; IPP, isopentenyl diphosphate; DMAPP, dimethylallyl diphosphate. A two-tailed multiple comparison test after Kruskal-Wallis was applied to search for differences in intermediate measurements with *chs5* as a control, with a p.value=0.05 (single asterisk).

Gene expression analysis on MEP and MVA pathways in candidate lines.

Gene expression analysis of MEP pathway genes is presented in **Figure 40**. No statistical difference was found in the expression of MEP pathway genes comparing *chs5* with the suppressor individuals of the six candidate lines. Only a statistical increase of *MCT* gene expression in L8.4 non-suppressor individuals has been recorded.

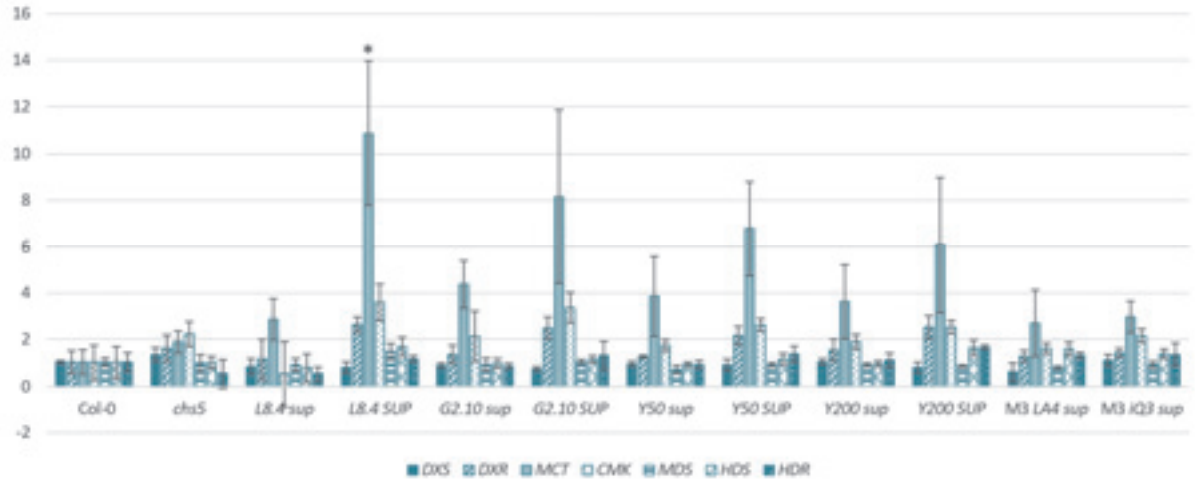

Figure 40. MEP pathway gene expression in *Arabidopsis thaliana chs5* suppressors. *DXS*, 1-deoxy-D-xylulose 5-phosphate synthase; *DXR*, 1-deoxy-D-xylulose 5-phosphate reductoisomerase; *MCT*, MEP cytidyltransferase; *CMK*, 4-(cytidine 5'-diphospho)-2-*C*-methylerythritol kinase; *MDS*, 2-*C*-methylerythritol 2,4-cyclodiphosphate synthase; *HDS*, 4-hydroxy-3-methylbut-2-enyl diphosphate synthase; *HDR*, 4-hydroxy-3-methylbut-2-enyl diphosphate reductase. Three biological replicates were sampled in a F2BC1 population, except for LA4 and iQ3 sampled in M3 generation. All values are normalized on Col-0. A two-tailed multiple comparison test after Kruskal-Wallis was applied to search for differences in gene expression with *chs5* as a control, with a p.value=0.05 (single asterisk).

The expression of MVA pathway genes in *chs5* suppressor candidates was also analyzed, results are presented in **Figure 41**. No statistical difference was shown between the *chs5* parental line and suppressor individuals for the expression of all genes analyzed, except for *SQE5* and *SQE6*. The gene expression of *SQE5* was statistically reduced in L8.4 non-suppressor individuals, and the gene expression of *SQE6* was also reduced in L8.4 non-suppressor and G2.10 suppressor and non-suppressor individuals compared to *chs5*.

Figure 41. MVA pathway gene expression in *Arabidopsis thaliana chs5* suppressors. *HMG*, 3-hydroxy-3-methylglutaryl coenzyme A reductase; *MVK*, mevalonate kinase; *PMVK*, 5-phosphomevalonate kinase; *MDC*, mevalonate diphosphate decarboxylase; *IDI*, isopentenyl diphosphate:dimethylallyl diphosphate isomerase; *FDS*, farnesyl diphosphate synthase; *SQS*, squalene synthase; *SQE*, squalene epoxidase; *CAS*, cycloartenol synthase. Three biological replicates were sampled in a F2BC1 population, except for LA4 and iQ3 sampled in M3 generation. All values are normalized on Col-0. A two-tailed multiple comparison test after Kruskal-Wallis was applied to search for differences in gene expression with *chs5* as a control, with a p.value=0.05 (single asterisk).

6. Genetic analysis of *sup chs5* suppressor mutations.

All the suppressor candidate lines selected presented a segregation in M3 generation sown on petri plates in *in vitro* culture conditions. The number of suppressor (*sup*) and non-suppressor

(*SUP*) individuals in each line was recorded, along with the germination rate, as shown in **Table 9**. Individuals with fully green or pale green leaves were considered as suppressors, plantlets with yellow spots were considered as non-suppressors, with no distinction in the number of spots or the area of the leaf covered with yellow spots.

Table 9. Phenotype selection and *in vitro* segregation in M3 generation in *Arabidopsis thaliana chs5* suppressor lines.

***chs5* suppressor line**	**Phenotype selected in M2**	**Phenotypic distribution in M3**		**Germination rate of the M3 generation (%)**
		sup	*SUP*	
G2.10	Col-0 like	150	0	-
L8.4	Col-0 like	150	0	-
Y50	Col-0 like	88	33	88
Y200	Col-0 like	109	24	90
LA4	Pale green	26	91	82
iQ3	Pale green and long hypocotyl	53	92	99
Col-0	Green leaves	-	-	98
chs5	Yellow leaves	-	-	80

Suppressor individuals selected *in vitro* were transferred to soil to perform a backcross with the *chs5* parental line. The phenotype of the F1 individuals was recorded. One F1 plant of each line was self-fertilized to obtain F2BC1 populations, in which the phenotypic distribution was analyzed to characterize more precisely the genetics of the causative mutation involved in the suppression of *chs5* phenotype. The phenotypes of the F1, the phenotypic distribution in a F2BC1 for each *chs5* suppressor line along with the germination rate in soil are given in **Table 10**. The best segregation hypothesis was chosen according to the results of the statistical χ^2 test, given in **Table 11**. For all the suppressor lines, the number of individuals grown in each generation is given in **Suppl. Figure 5** to **10**.

Table 10. Genetic characterization of *Arabidopsis thaliana chs5* suppressor lines grown *in vitro*. Best segregation hypothesis was determined with χ^2 test with a pvalue > 0.05 (see **Table 11**).

***chs5* suppressor line**	**Phenotype of F1 individuals Ni=10**	**Phenotypic distribution in a F2BC1 *in vitro***		**Germination rate (%) *in vitro***	**Phenotypic distribution in a F2BC1 in soil**		**Germination rate (%) in soil**	**Type of mutation**	**Best segregation hypothesis *in vitro* (*sup*:*SUP*)**
		sup	*SUP*		*sup*	*SUP*			
G2.10	*SUP*	37	117	100	26	69	40	Recessive	1:3
L8.4	*SUP*	44	122	100	43	53	98	Recessive	1:3
Y50	*SUP*	26	124	100	34	63	86	Recessive	1:3 ?
Y200	*SUP*	27	121	99	27	66	52	Recessive	1:3
LA4	*SUP*	-	-	-	-	-	-	Recessive	-
iQ3	*SUP*	18	94	86	-	-	-	Recessive	1:3 ?
Col-0x*chs5*	*SUP*	44	69	82	-	-	-	-	1:3

The χ^2 analysis indicates which segregation hypothesis is the most suitable by comparing observed values with theoretical values expected for each hypothesis. The hypothesis is considered as viable if the p-value is bigger than 0.05. If more than one hypothesis is considered as correct, the highest value indicates the most viable hypothesis.

Table 11. χ^2 analysis of segregation hypothesis for *Arabidopsis thaliana chs5* suppressor lines in a F2BC1. A hypothesis is considered viable if p-value>0.05. If two hypotheses are validated, the best hypothesis selected is the one with the highest p-value. P-values of the selected hypothesis are in bold black, p-values of viable hypothesis are in black, p-values<0.05 are in grey (hypotheses were not considered viable).

Hypothesis *sup:SUP*	**3:1**	**1:3**	**1:1**	**2:1**	**9:7**	**7:9**
G2.10 *in vitro*	2,20E-16	**0,7801**	1,14E-10	2,20E-16	7,57E-16	8,05E-07
L8.4 *in vitro*	2,20E-16	**0,6541**	1,41E-09	2,20E-16	1,12E-14	7,51E-06
Y50 *in vitro*	2,20E-16	0,03012	1,23E-15	2,20E-16	2,20E-16	6,94E-11
Y200 *in vitro*	2,20E-16	**0,05765**	1,10E-14	2,20E-16	2,20E-16	3,97E-10
LA4 *in vitro*						
iQ3 *in vitro*	2,20E-16	0,0291	6,90E-13	2,20E-16	2,20E-16	3,53E-09

Identification of causal mutations by next generation sequencing.

Next generation sequencing was used to search for the causative mutations of a *chs5* suppressor phenotype. The samples were carefully prepared to obtain good quality genomic DNA. For

each line, suppressor individuals and non-suppressor individuals were sampled as pools and identified by a sequencing ID number as described in **Table 12**. All samples had an $OD_{260/280}$>1.8, assessing the good quality of the genomic DNA.

Table 12. Identification and sample quality of gDNA extracts from *Arabidopsis thaliana chs5* suppressor lines sequenced by Illumina. Col-0 and *chs5* individuals were grown in soil, F2BC1 G2.10 and L8.4 were grown and phenotyped *in vitro*. All samples had a value of $OD_{260/280}$>1.8 measured with Nanodrop 2000 (Thermo Scientific).

ID	*chs5* suppressor line	Concentration (ng/µl)	Quantification method	Volume (µl)	Sample type
HTSR13	Col-0	62	Qubit	57	gDNA
HTSR14	*chs5*	75	Qubit	57	gDNA
HTSR5	F2BC1 *G2.10 sup*	183	Qubit	39	gDNA
HTSR6	F2BC1 *G2.10 SUP*	68.6	Qubit	39	gDNA
HTSR7	F2BC1 *L8.4 sup*	157	Qubit	39	gDNA
HTSR8	F2BC1 *L8.4 SUP*	35.2	Qubit	39	gDNA

The integrity of the genomic DNA was verified on an agarose gel as shown in **Figure 42, A**; and measured on Covaris (**Figure 42, B**). The analysis showed no degradation of the DNA that was used for library preparation before sequencing.

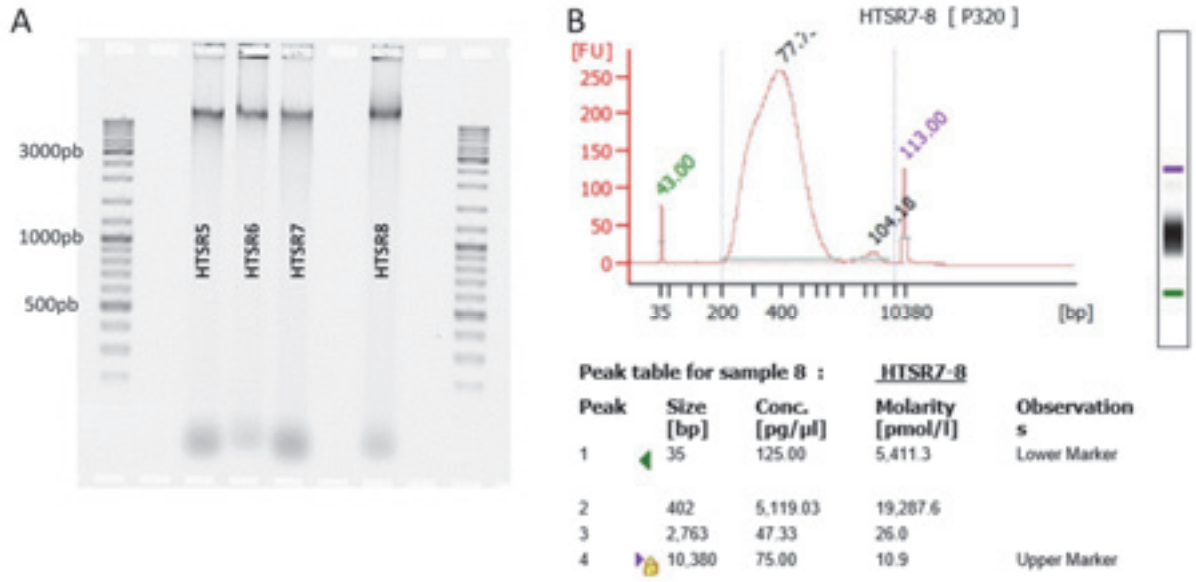

Figure 42. Control of *Arabidopsis thaliana chs5* suppressor lines gDNA sample quality before next generation sequencing. (**A**), gDNA integrity was checked on agarose gel and (**B**), library quality was controlled on Covaris (Agilent).

Sequencing was performed by the IGBMC Microarray and Sequencing platform (Strasbourg) and bioinformatic analysis was optimized by Sylvain Darnet (Laboratório de Biotecnologia Vegetal, Instituto de Ciências Biológicas, Universidade Federal do Pará (UFPA), Belém, Brazil). The suppressor and non-suppressor individuals were sampled separately, and non-suppressor sequences served as a blank to eliminate all the non-causal mutations due to the EMS treatment. The theoretical coverage was given by the number of raw reads obtained after sequencing multiplied by 100bp (length of a read) and divided by the genome size given by databases (TAIR10). During pre-processing, pairing and variant calling, some reads are lost. The final sequencing coverage can be calculated the same way, using the number of reads left after bioinformatic treatment of the data. An example is given in **Table 13** with the analysis of sequencing data obtained for HTSR13 (Col-0) sample. The theoretical coverage calculated from the number of raw reads given after sequencing is 144.4, and final sequencing coverage indicative of the properly paired sequences is 105.1.

Table 13. Bioinformatic analysis of HTSR13 (Col-0). The number of reads has been recorded after each step of the bioinformatics process and allows the calculation of theoretical and final sequencing coverage of the genome.

HTSR13	**Number of reads**	**% of raw reads**
Raw reads	195 914 492	
After pre-processing	193 919 074	98%
Properly paired	181 440 444	93%
After variant calling	142 645 294	78%
Theoretical coverage of the genome	144.4	
Final sequencing coverage	105.1	

A first batch of samples was sequenced and bioinformatic analysis has been done. Individuals of F2BC1 of G2.10 (HTSR5 and 6) and L8.4 (HTSR7 and 8) were sampled after two weeks of *in vitro* cultivation, and separated into suppressor and non-suppressor bulks, each containing 60 plantlets (30 plantlets from a *sup chs5*x*chs5* F2 population, 30 plantlets from a *chs5*x*sup chs5* F2 population) (**Table 14**). Libraries were prepared from genomic DNA and amplified with 10 PCR cycles. For all the libraries, a principal peak was found between 200 and 700bp, with an average of 350bp (**Figure 43**). The size of the inserts was found by subtracting the adapters' size of 120bp. Inserts had a size of approximately 230bp.

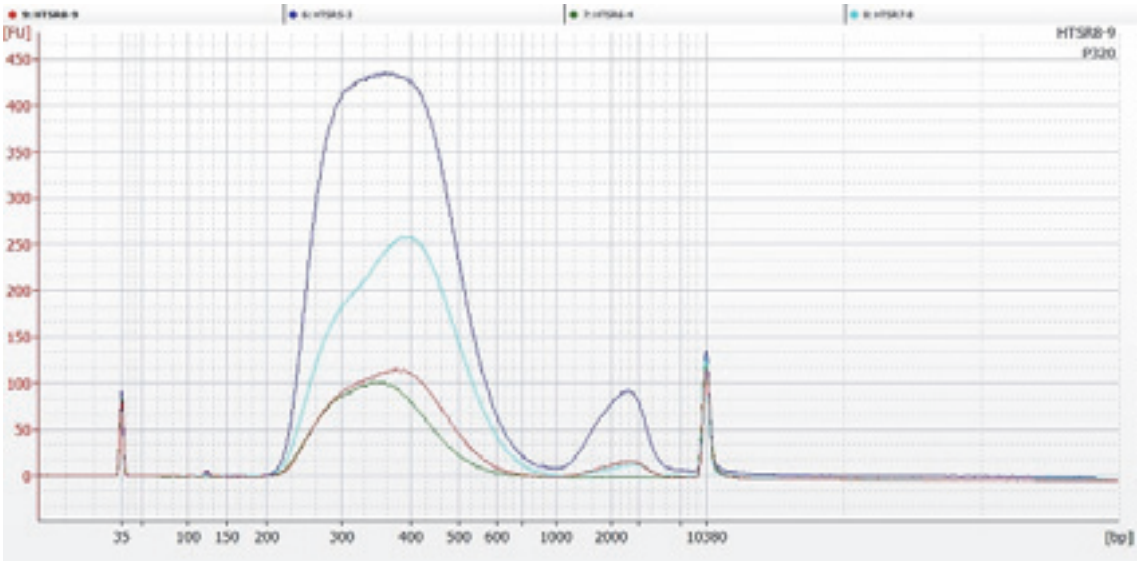

Figure 43. Library profile for HTSR5 to 8. Libraries were prepared by PCR on genomic DNA. The principal peak size was between 200 and 700bp, with an average of 350bp representative of inserts (230bp) and adapters (120bp).

After sequencing, between 41 and 62 million of pairs were obtained as raw reads, which were mapped to *the Arabidopsis thaliana* Col-0 genome. 68 to 77% of the raw reads were properly paired, resulting in a final sequencing coverage of 36 to 59X. Single nucleotide polymorphism (SNPs) and insertions and deletions (INDELS) were detected (**Table 14**). The focus was made on SNPs, described as the type of mutations caused by EMS treatment.

Table 14. Bioinformatic analysis on HTSR5 to 8 done by Sylvain Darnet, UFPA, Brazil.

	HTSR5 G2.10 *sup*	**HTSR6 G2.10 *SUP***	**HTSR7 L8.4 *sup***	**HTSR8 L8.4 *SUP***
Plant set	60 plants	60 plants	60 plants	60 plants
Plant set phenotype	suppressor of *chs5* phenotype (green)	*chs5* phenotype (yellow)	suppressor of *chs5* phenotype (green)	*chs5* phenotype (yellow)
Raw reads	62.4 million of pairs	41.4 million of pairs	45.9 million of pairs	41.6 million of pairs
Mapping on Ath/Col0 genome (gsnap mapper, without PCR duplicates, properly paired)	45.1 million of pairs (72,2%)	28.5 million of pairs (68,9%)	34.8 million of pairs (75,8%)	32.2 million of pairs (77,4%)
Final sequencing coverage (properly paired and mapped reads)	59.9 x	36.7 x	46.9 x	40.5 x
Polymorphism detection (mpileup/bcftools)	total = 33,541 SNPs = 30,128 INDELS = 3,413	total = 32,393 SNPs = 29,282 INDELS = 3,111	total = 32,196 SNPs = 28,916 INDELS = 3,280	total = 31,674 SNPs = 28,630 INDELS = 3,044

The single nucleotide polymorphisms (SNPs) found were mapped on Col-0 reference genome to identify which chromosomes were considered (**Figure 44**). For all the lines, SNPs were found on all the five chromosomes, with a majority of SNPs detected on chromosomes 3 and 5. Most of the SNPs detected were heterozygous (grey), but some homozygous SNPs were also found (black).

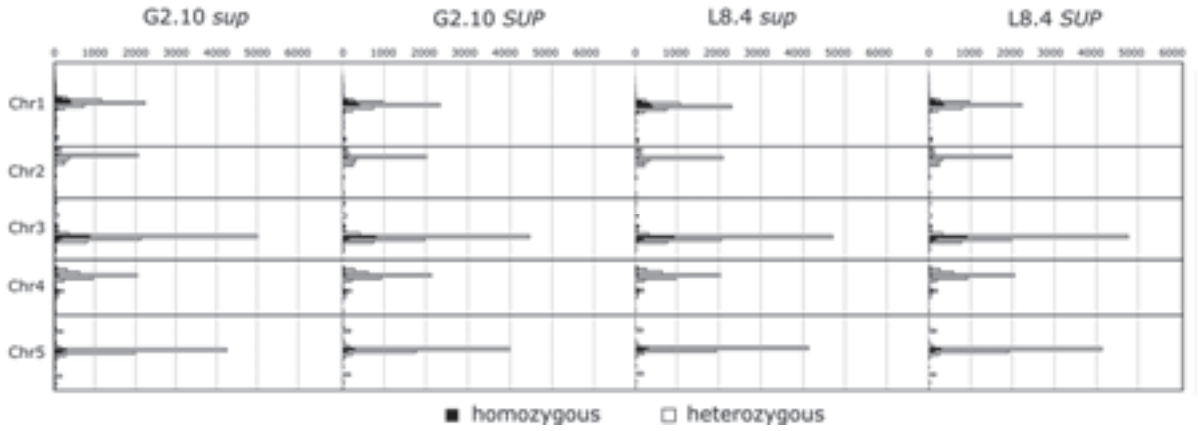

Figure 44. Total SNPs/Mb compared to *Arabidopsis thaliana* Col-0 genome. Mapping was made with gsnap and SNPs calling with Samtools. Chromosomes are indicated on the left, heterozygous SNPs are in grey, homozygous SNPs are in black. Analysis and figure by Sylvain Darnet.

The segregation analysis in a F2BC1 population is essential to guide the bioinformatic analysis in order to identify the causative mutations. The case of a population segregating a recessive mutation is given in **Figure 45**. A suppressor individual is backcrossed with the *chs5* parental line, and a F1 individual is obtained, which is homozygous for the *chs5* mutation and heterozygous for the *sup* mutation. After selfing of one F1 individual, a segregating F2 population is analyzed, in which all the individuals are homozygous for the *chs5* mutation, but the *sup* mutation is segregating. In the case of a recessive mutation, the suppressor phenotype is visible only in the individuals which are homozygous for the *sup* mutation. In the suppressor population, the frequency of *chs5* mutation is one, and the frequency of the *sup* mutation is one. In the non-suppressor population, the *sup* mutation segregates, homozygous and heterozygous individuals are found, along with individuals which do not carry the *sup* mutation anymore. In this population, the frequency of the *chs5* mutation is one, and the frequency of the *sup* mutation is 1/3. Thus, in the study of G2.10 and L8.4 genomes after sequencing, only homozygous SNPs are searched for. Other SNPs were detected, which were not related to the suppressor phenotype, but were either from *chs5* genetic background, or residual non-causative mutations from the EMS treatment.

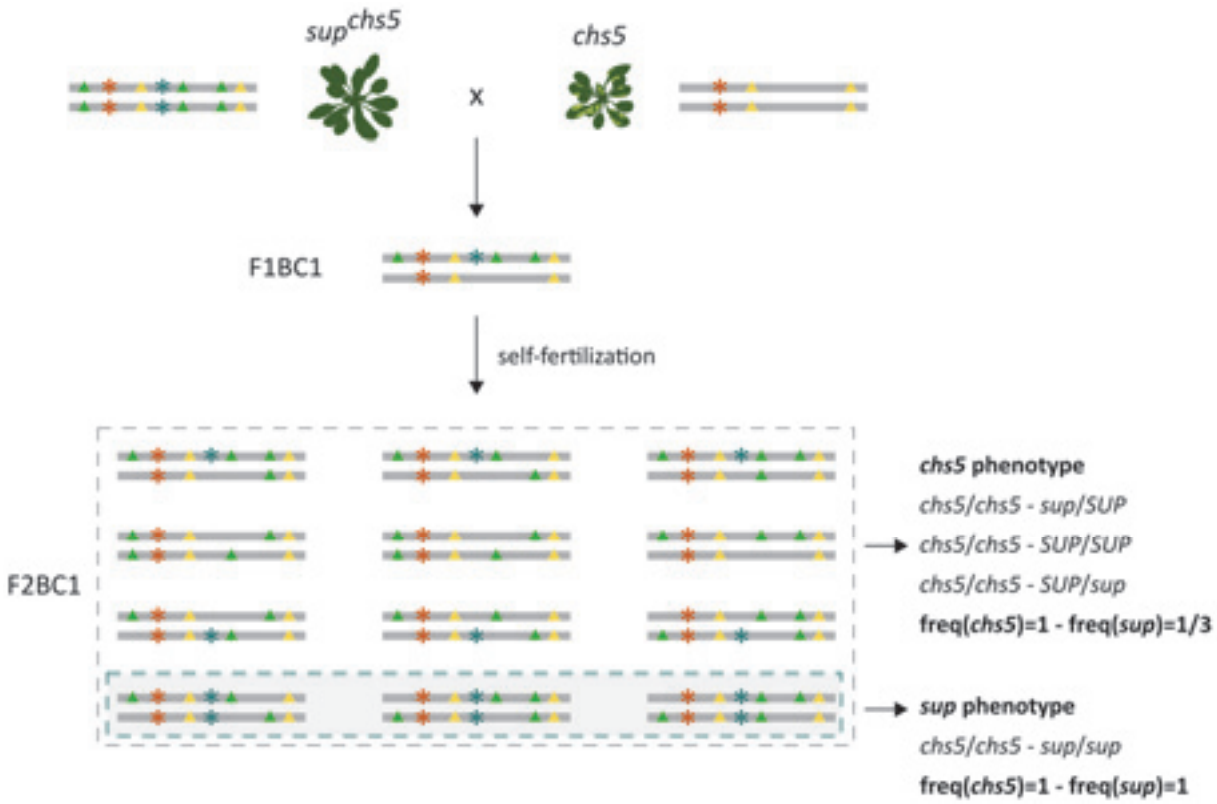

Figure 45. Segregation pattern of *chs5* and *sup* mutations in a F2BC1 generation. Suppressor individuals were crossed with the *chs5* parental line. A F1BC1 individual was self-fertilized to obtain a F2BC1 population in which *chs5* mutation (orange asterisk) and sup mutation (blue asterisk) segregate. Some SNPs were already present in the *chs5* genetic background (yellow triangles) and EMS mutations which are not causative of the suppressor phenotype are present in the suppressor genome (green triangles). Frequencies are presented in the case of a recessive mutation.

A filtering criteria was applied to obtain unique high quality EMS homozygous SNPs. The non-suppressor samples were used as a blank to eliminate all the mutations due to EMS treatment that are not causative of the suppressor phenotype. A common variants subtraction was realized to search for specific mutations only found in G2.10 suppressors or L8.4 suppressors (**Figure 46**). This analysis shows that 108 SNPs are common to all groups, part of the SNPs are specific of G2.10 or to L8.4 but can be found in suppressor and non-suppressor samples. The SNPs of interest are the two found specifically in G2.10 suppressors and the eight found in L8.4 suppressors.

Figure 46. Common variants subtraction between G2.10 and L8.4 suppressor and non-suppressor samples. Non-suppressor samples are used as a blank to eliminate non-causative mutations. Specific SNPs are found only in G2.10 suppressors or L8.4 suppressors.

The unique high quality EMS homozygous SNPs were once again mapped on the Col-0 genome and a more precise analysis of the specific SNPs found only in suppressor samples was made (**Figure 47**). Two SNPs were identified in the G2.10 suppressor sample, a missense mutation (S/F) in *sup*$^{G2.10}$ 01, with a DUF241 domain of unknown function situated on chromosome 2; and a missense mutation (A/V) in *sup*$^{G2.10}$ 02, a transcription factor on chromosome 4. Six SNPs of interest were identified in L8.4 suppressor sample. Five missense mutations: E/K in *sup*$^{L8.4}$ 01, a glucosyl transferase; S/F in *sup*$^{L8.4}$ 02; T/I in *sup*$^{L8.4}$ 03, with DUF716 domain of unknow function; P/L in *sup*$^{L8.4}$ 05, a phosphoinositide-dependent protein kinase; and S/F in *sup*$^{L8.4}$ 06. A splicing modification was found in *sup*$^{L8.4}$ 04, a potassium transporter.

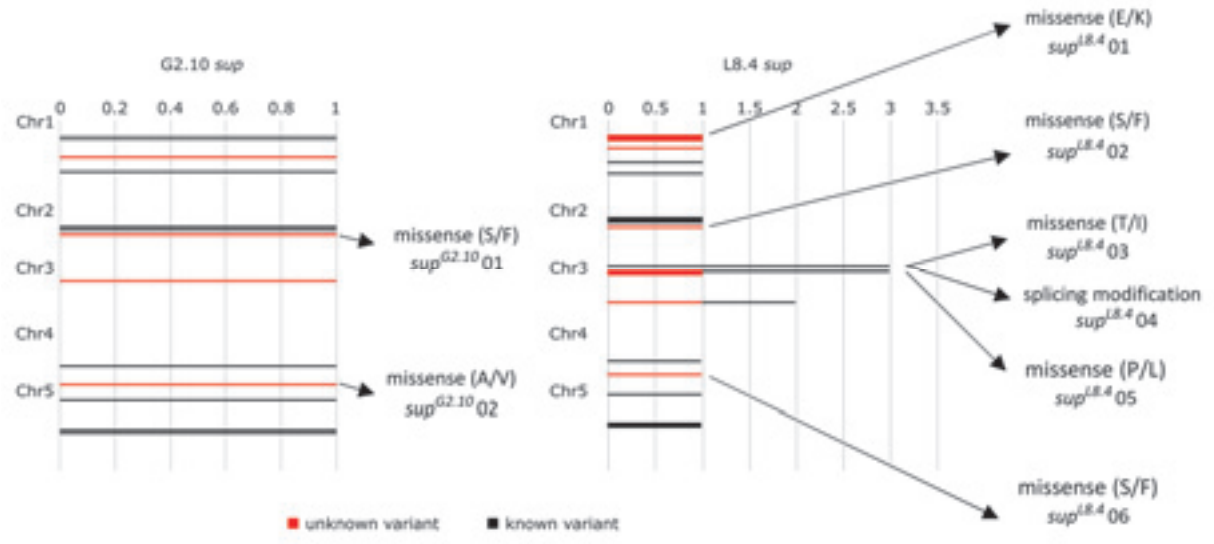

Figure 47. Unique high quality homozygous SNPs obtained in G2.10 suppressor or L8.4 suppressor samples. SNPs were mapped on Col-0 genome.

Sampling has been made for sequencing of the other four candidate lines, which will be performed soon.

Chapter II. Genetic screen for suppressors of growth defects in a brassinosteroid signaling *Hordeum vulgare* mutant.

Materials and Methods

I. Plant material

Barley lines Bowman (wild type) and BW312 (*ert-ii.79/bri1*) were obtained from Carlsberg Reasearch Center, Copenhagen. The semi-dwarf mutant BW312 is a brassinosteroid signaling mutant. It exhibits a double substitution CC>AA at positions 1760 and 1761 of the gene and coding the brassinosteroid receptor HvBRI1 (Gruszka et al., 2011). These substitutions lead to the replacement of a threonine (T) by a lysine (L) at position 573 of in the protein sequence. The mutation is situated on the island domain of the membrane-bound receptor that is necessary for brassinosteroid binding in order to bring the message to the cell. Therefore, BW312 mutant is insensitive to brassinosteroids and exhibits a semi-dwarf phenotype (Dockter et al., 2014).

II. Methods

1. Plant culture conditions in soil

Barley caryopsis were sown in 19cm diameter pots in soil (Surfinia, Havita). Plants were cultivated either in cool conditions in a growth chamber under a 16h light/8h dark regime, at 18°C during the light phase and 15°C during the dark phase, or in standard greenhouse conditions under the same photoperiodic cycle at 22°C during the day and 18°C during the night. Daylight was complemented at the beginning and the end of the light phase (08:00 am to 10:00 pm) with Plantastar 400W artificial light.

2. Crossings

Barley crossings were performed under cool culture conditions (15-18°C maximum). Spikelets were opened by cutting the base of the awn, and stamens were gently removed with forceps before anthesis. After 2 to 6 days of further development and opening of the spikelets, pistils were pollinated by introducing a male stamen in the emasculated spikelets. Spikes were covered with a paper bag until full maturation of the caryopsis.

3. Plant mutagenesis

The mutagenesis of the BW312 (*ert-ii.79*) barley line was made in CRC (Carlsberg Reasearch Center) using sodium azide according to the protocol described by (Owais et al., 1978). In brief, germinated seeds were treated for 2h with 10^{-3}M sodium azide in 0.1M phosphate buffer at pH3.0, then washed several times with tap water. M1 plants were grown in field conditions in New Zealand by Carlsberg company and harvested in January 2014 to generate a bulk M2 population that was send to us for genetic screening purposes.

4. Analysis of mutant populations (screenings)

Suppressor lines of *ert-ii.79* (BW312) were screened in greenhouse conditions, searching for candidates with a tall size as compared to the semi-dwarf parental line. Plants were grown in trays to mimic field conditions in terms of density, and select plants resistant to lodging. The suppressor candidates were genotyped to verify the presence of the CC>AA double substitution in the *BRI1* gene.

5. DNA extraction from leaf material

DNA was extracted from leaf samples. Leaf material was ground in 750µL of grinding buffer with metal beads for 2 minutes on a Tissue Lyser (Quiagen) at 30Hz. Samples were incubated for 30 minutes at 65°C, and extracted with 700µL of chloroform/isoamyl alcohol (24/1, v/v, Carlo Erba Reagents, Merck). After a centrifugation step (5 minutes, 10000rpm, room temperature), aqueous phase was collected and added to 550µL of isopropanol (Carlo Erba Reagents). Precipitated DNA was pelleted by centrifugation (5 minutes at 10000rpm, room temperature) and pellets were washed with 70% ethanol (Sigma Aldrich) and dried at room temperature before resuspension in 20µL of sterile water.

Composition of grinding buffer:
25mL DNA extraction buffer, 25mL Nuclei lysis buffer, 10mL Sarkosyl 5% (Sigma).
DNA extraction buffer: sorbitol 0.35M (Roth), Tris base 0.1M (Sigma), EDTA 0.005M (Euromedex), pH=7.5.
Nuclei lysis buffer: Tris base 0.2M (Sigma), EDTA 0.05M (Euromedex), NaCl 2M (Sigma-Aldrich), CTAB 2% (Sigma).

6. Genotyping by PCR

Plants were genotyped by PCR using the following mix for one sample: 4µL of GoTaq 5X buffer (Promega), 2,4µL of $MgCl_2$ (25mM, Promega), 0,4µL of dNTP (10mM, Promega), 0,48µL of each primer (20µM, Integrated DNA Technologies), 0,24µL of GoTaq (Promega), water up to 19,5µL, and 0,5µL of DNA sample obtained as described. Primers used for each line are listed in **Table 15**.

Table 15. Primers used for genotyping by PCR

Target gene	Primer name	Primer sequence
HvBRI1	BRI FN	GGAGCACAGAGTATACCTTC
	BRI FM	GGAGCACAGAGTATAAATTC
	BRI R	CAGAATGTGACCGGCTATCA

Samples were placed in a thermocycler (Eppendorf Mastercycler) for PCR amplification with a specific cycle (**Table 16**), and placed on a 1% agarose gel (Sigma Life Science) in TAEX1 with Sight DNA stain (Euromedex) for migration at 100V during 30 minutes.

Table 16. PCR cycles used for genotyping of *Hordeum vulgare* suppressor lines.

	HvBRI1		
	Temperature		*Time*
Denaturation	94°C		3min
PCR Cycle	X35	94°C	30sec
		59.6°C	30sec
		72°C	1min
Final elongation	72°C		10min
Hold	4°C		/

7. Hormone extraction from leaf material

Leaf tissues were collected in liquid nitrogen and immediately dried over-night. 20mg of dry material were weighed in a 2mL tube, and ground with metal beads for 4 minutes on a Tissue Lyser (Quiagen) at 30htz. Dry leaf powder was spiked with 3µL of GA3 as internal standard

(500µg.mL^{-1}, Fluka) and extracted with 1,5mL of acetonitrile (Fisher Chemical). Samples were vortexed and shaken for 10 minutes at room temperature, and centrifuged for 5 minutes at 13 000rpm, room temperature. The supernatant was transferred to a glass vial and evaporated with a SpeedVac concentrator (Savant SPD121P, Thermo Fisher) at room temperature. The pellets were extracted twice with 1,5mL acetonitrile, shaken, centrifuged and collected in the same glass vial to be evaporated. After 3 extractions, 6µL of BAP (250µg/mL^{-1}, Sigma Cell Culture) were added to the dried vials, evaporated, and samples were solubilized in 100µL of acetonitrile and placed in glass inserts for injection.

8. Hormone analysis by ultra-performance liquid chromatography and mass spectrometry (UPLC-MS/MS)

The hormone content of the plant extracts was analyzed by ultra-performance liquid chromatography (UPLC) on Acquity ultra performance LC (Waters) coupled with Quattro Premier XE (Micromass technologies) mass spectrometer. The samples were kept at 4°C before injection of 10µL in full loop mode, on a C18 column (Acquity UPLC ® BEH C18 1,7µm 2,1x100mm). Samples were "pushed" through the column following a gradient of solvent A2 (H_2O Direct-Q UV, Millipore; 0,1% formic acid, Sigma) and B2 (acetonitrile, Fisher Chemical; 0,1% formic acid, Sigma). Chromatography was carried out at a flux of 0,300mL/min, starting with 95% A2 and 5% B2 for 2 minutes, reaching 100% B2 at 10 minutes, holding 100% B2 for 3 minutes and coming back to 95% A2 and 5% B2 in 2 minutes, for a total run time of 15 minutes. Hormones were analysed by multiple reaction monitoring (MRM), after determining the retention time, cone voltage, daughter ion and collision energy for each hormone from a standard : abscisic acid (ABA, Sigma), jasmonic acid (JA, OlChemIm), gibberellins A1, A4 and A7 (GA1, GA4, GA7 OlChemIm), indole-3-acetic acid (IAA, Serva), 6-(γ,γ-dimethylallylamino)purine (2iP, Duchefa), 6-furfurylaminopurine (Kinetin, Duchefa), castasterone (CS, OlChemIm), cathasterone (CT, OlChemIm), brassinolide (BR, OlChemIm). Gibberellic acid (GA3, Fluka) and 6-benzylaminopurine (BAP, Sigma Cell Culture) were used as internal standards spiked before and after extraction respectively. Weak solvent (95% H_2O, 5% ACN) and strong solvent (95% ACN, 5% H_2O) were used to wash the syringe. Results were processed using QuanLynx and checked manually.

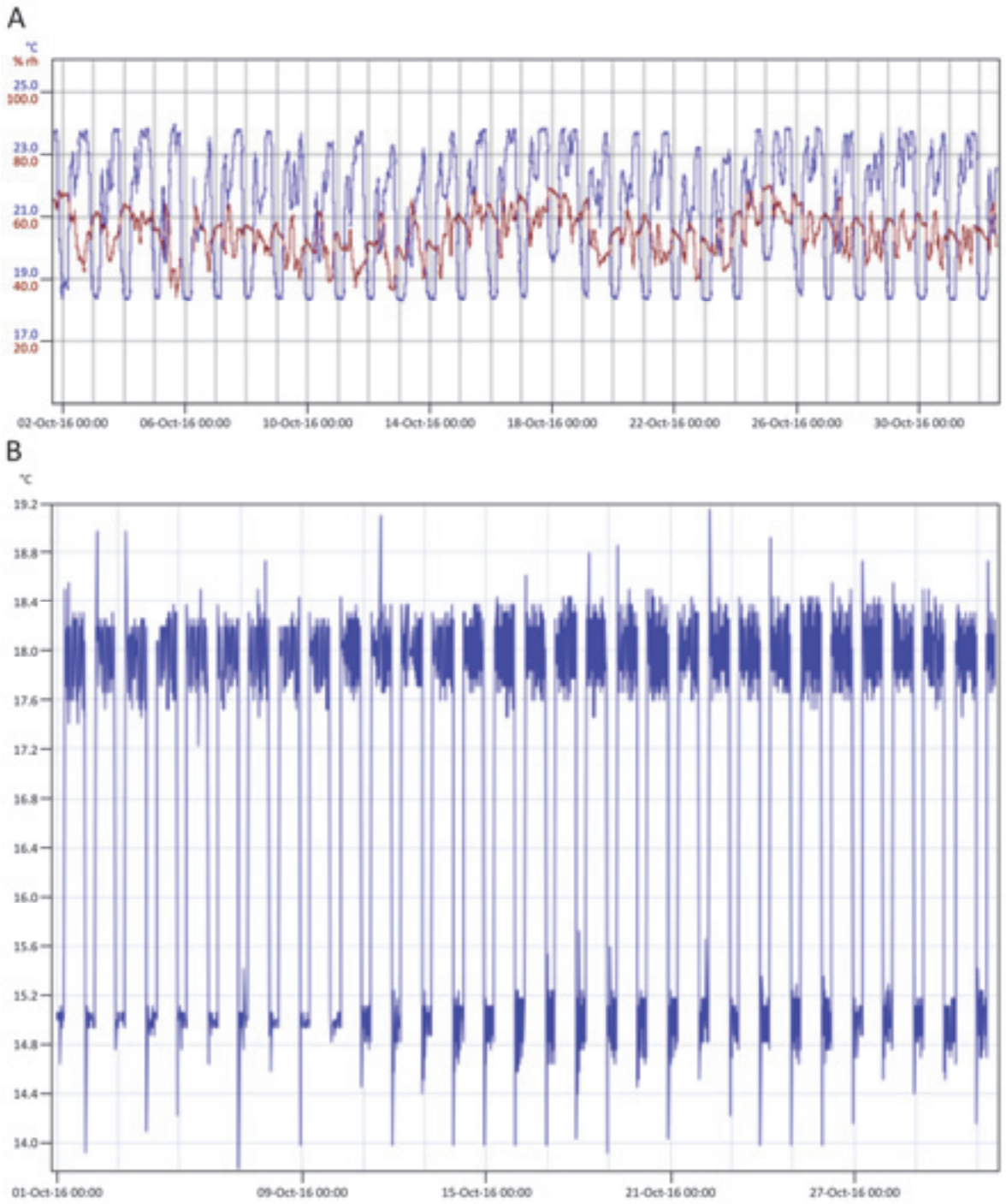

Figure 48. Temperature and humidity conditions at the IBMP plant growth facilities, in the greenhouse (A) or growth room (B) for *Hordeum vulgare ert-ii.79/bri1* (BW312) suppressor lines. Humidity given in % of relative humidity (rh).

Results

1. Barley growth and screening conditions

The screening for barley *ert-ii.79/bri1* suppressors among a population of bulked individuals was done in greenhouse conditions (see Materials and Methods section). Suppressor individuals were grown in standard greenhouse (IBMP roof greenhouse) conditions at 23°C during the light phase (16 hours, complemented light at the start and the end of the light regime, see Materials and Methods) and 19°C during the dark phase (8 hours) (**Figure 48, A**). Alternatively, plants were grown in a growth room at 18°C during the light period and 15°C during the dark period (**Figure 48, B**). As seen in **Figure 48**, the temperature conditions were easier to keep stable in the growth room, but were quite stable in greenhouse, enabling proper barley germination, growth, seed setting and most importantly, genetic crossings.

A batch of seeds (500 grams) of the BW312 mutant line was treated with sodium azide (NaN_3) in the Carlsberg Research Center (CRC, Copenhagen) to induce genetic variability by chemical mutagenesis (Olsen et al., 1993). M1 individuals were grown in field conditions (on a $7m^2$ plot) in New Zealand to generate M2 seeds. Spikes carrying those seeds were shredded to provide 2x2.5kg of seeds. One of these two batches of approximately 56.000 M2 individuals was screened for BW312 suppressor phenotype in a greenhouse with a dense sowing in trays to mimic field conditions, between September 2014 and February 2015. Chlorophyll biochemical mutants, which exhibit a pale green to yellow leaf phenotype or totally albino seedling lethals were estimated at about 1% in the population as a proxy for the efficiency of the mutagenic treatment. Individual plants that displayed a so-called “overgrowth” phenotype defined as an obvious culm size difference with the background population were picked up for further growth in greenhouse conditions. Preliminary assays of comparative barley germinations in greenhouse screening conditions were performed at the start of the project by introducing a few wild type individuals in an *ert-ii.79* sowing (**Figure 49**). This showed a tiny difference between mutant and wild type and let us envisage a very careful survey of the growth of batches of plants grown in the greenhouse for the screening. In fact, the *bri1* semi-dwarf suppressor screening did not

present the characteristics of that reported by Chandler and Harding, 2013, dealing also with "overgrowth" phenotypes in a gibberellin deficiency background.

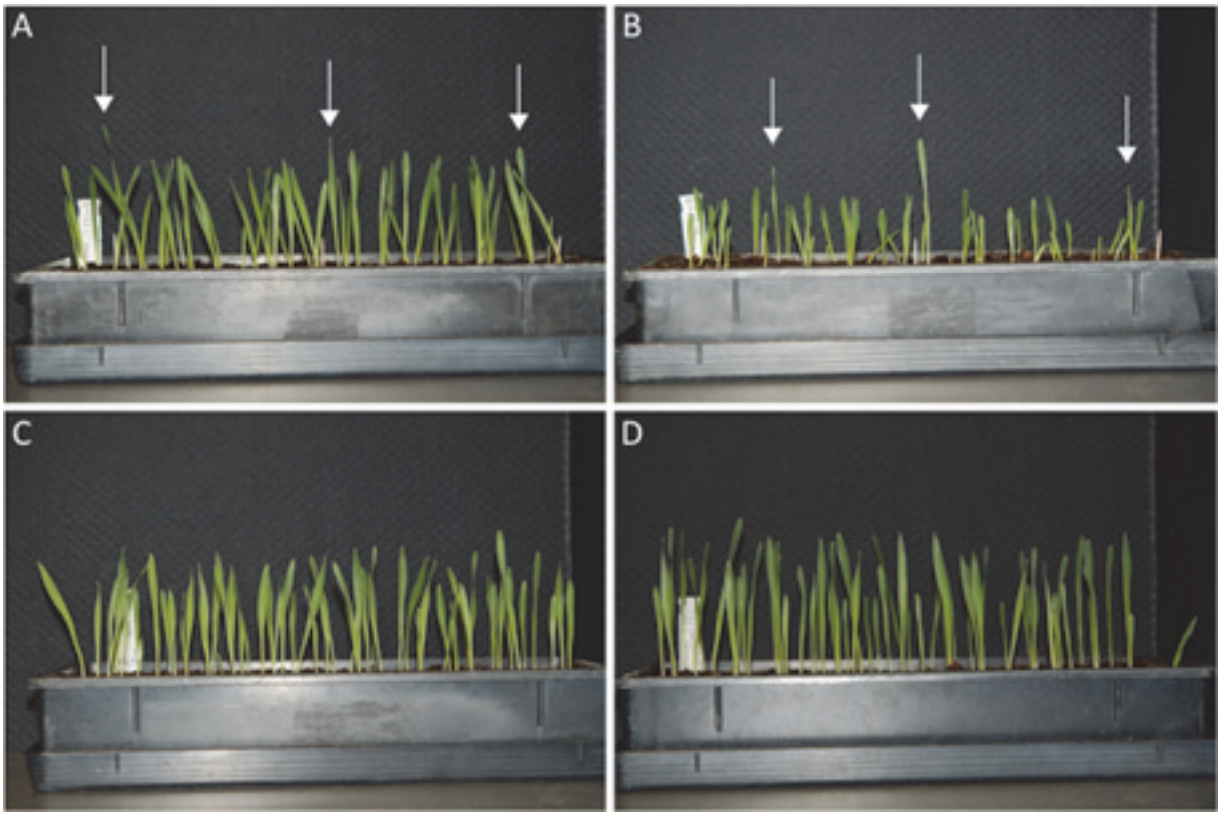

Figure 49. Preliminary assays of comparative barley germinations in greenhouse screening conditions. A few wild type individuals of Explorer cultivar shown by arrows were introduced in an *ert-ii.79* (**A**) or *uzu* (**B**) sowing. Bonus (**C**) and Explorer (**D**) were cultivated as controls.

2. Genotyping of the *ert-ii.79* parental mutation in candidate plants.

The parental line used for this screening is BW312, carrying the *ert-ii.79* mutation in the BRI1 brassinosteroid receptor. The mutant allele is therefore named *bri1*/*ert-ii.79* in a Bowman genetic background, so that the line is called BW312 (Dockter et al., 2014). In fact, the *ert-ii.79* mutant was obtained in 1955 upon mutagenic X-ray treatment of the cultivar Bonus. Later on, *ert-ii.79* that is an *erectoides* mutant was crossed to the Bowman cultivar by Franckowiak J and colleagues to yield BW312 (Mats Hansson, personal communication). This mutation consists of a CC to AA double substitution in the coding sequence of the *BRI1* gene leading to the replacement of a threonine by a lysine at position 573 in the protein sequence (**Figure 50, A**)(Dockter et al., 2014). This double substitution can be detected by PCR amplification of a fragment of the *BRI1* sequence. The gene and primer sequences were provided by Christoph

Dockter (Carlsberg Research Center, Copenhagen). Two separate reactions were performed, with specific primers to amplify wild type or mutant sequence, using forward primer BRI FN carrying the wild type CC sequence or forward primer BRI FM carrying the mutant AA sequence, and a common reverse primer BRI R. Products amplified by PCR reactions were visualized on an agarose gel after electrophoresis (**Figure 50, B**). In presence of the wild type *BRI1*/*BRI1* sequence, one product was amplified with the BRI FN+BRI R reaction mixture. In case of *BRI1*/*bri1* heterozygous individuals, DNA amplification gave two products, while the amplification product obtained from DNA of *bri1*/*bri1* individuals gave only one product with the BRI FM+BRI R reaction mixture. This robust and reliable PCR screening of interesting individuals showing up in the M2 batches permitted to exclude from the candidate list wild type and heterozygous individuals growing taller than the M2 barley canopy. These contaminants were found at an approximate rate of 5-10%. Plants that displayed a confirmed *bri1*/*bri1* genotype (homozygous for the recessive *ert-ii.79/bri1* allele) were grown for further selection and characterization.

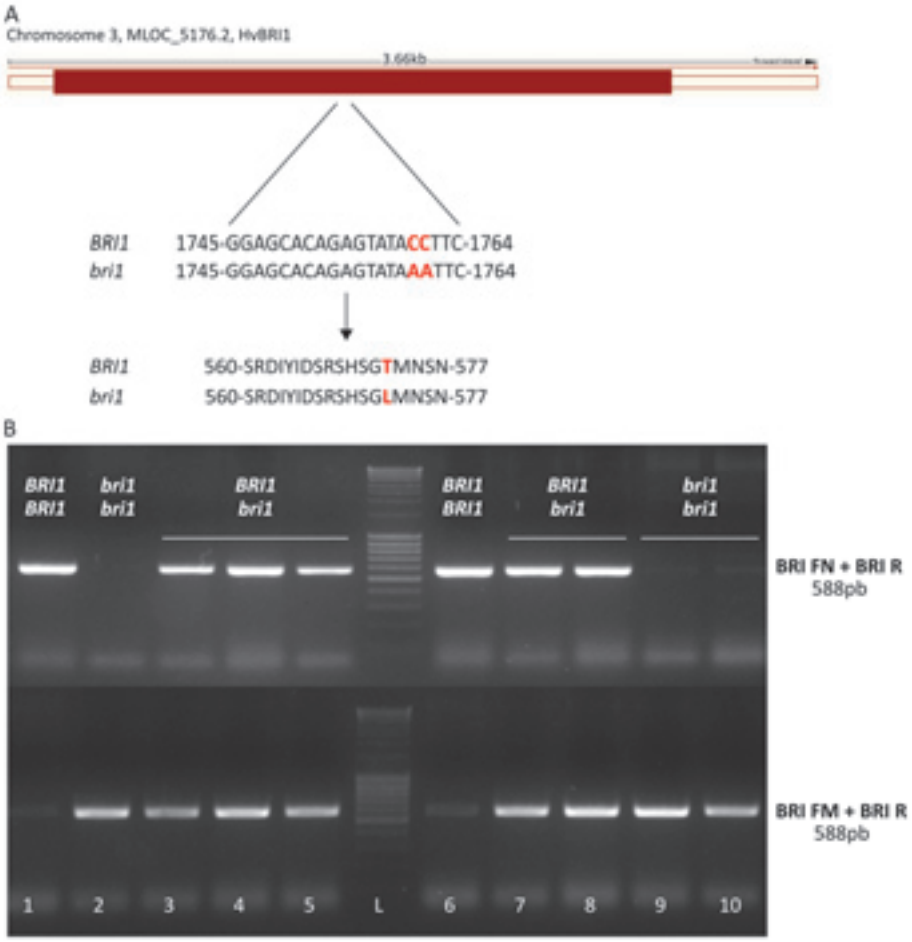

Figure 50. Genotyping of a missense mutation in *Hordeum vulgare* BW312 suppressor and early maturity lines. (**A**), BW312 *Hordeum vulgare* is carrying a CC to AA double substitution in the coding sequence of *BRI1* gene leading to the replacement of a threonine by a lysine at position 573 in the protein sequence. Exon is represented as a red box, introns as red lines (Gene map from Ensembl Plant, http://plants.ensembl.org/index.html). Genotyping was made by PCR with three primers used in two distinct mix to amplify either wild type or mutant sequence. (**B**), Electrophoresis gel shows amplification products obtained from genomic DNA from *BRI1*/*BRI1* wild type (1), *bri1*/*bri1* mutant (2), and homozygous *bri1*/*bri1* (9, 10), heterozygous *BRI1*/*bri1* (3-5, 7,8) or homozygous *BRI1*/*BRI1* (6) suppressor candidates in M2 generation. Sample n°6 was genotyped as wild type and was not selected for further experiment. L: MassRuler DNA Ladder Mix, Thermo Fischer Scientific.

3. Selection of suppressor candidates and phenotypic characterization.

The *ert-ii.79* mutation in *BRI1* is conferring a semi-dwarf phenotype to the line BW312 in Bowman genetic background. Suppressor candidates were selected at a mature stage with the spike out of the flag leaf. Individuals were considered as suppressors (*sup*) when the spike was growing above the canopy of the plant population. In the screen, early maturity (*em*) phenotypes were also found, with plants exhibiting yellow mature spikes when the control lines were only at a flowering stage. Phenotypical traits of barley morphology used in this screen are described in **Figure 51**.

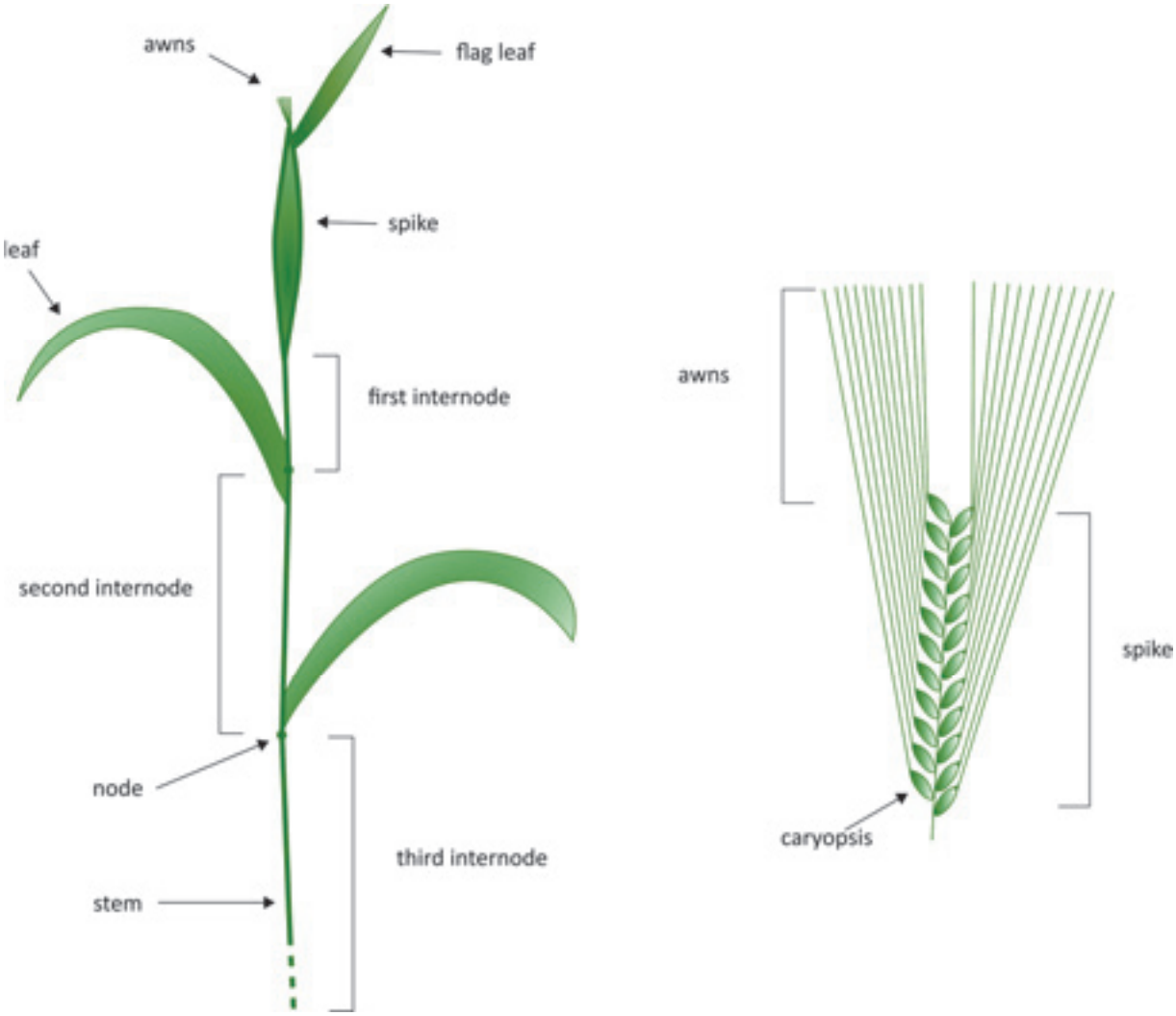

Figure 51. Schematic representation of *Hordeum vulgare* tiller (left) and spike (right). One plant is composed of several tillers, showing lateral leaves and a single spike covered by the last leaf called flag leaf, until maturity. The spike is carrying caryopses prolonged by awns. In this study, the first internode was defined between the basis of the spike and the next node on the tiller. Sizes are not representative; spike drawing is magnified.

After an initial selection of 24 individual plants from the screened M2 bulk population, 11 lines were characterized during this thesis project, as follows. Five suppressor individuals were selected in the screen and self-fertilized to obtain M3 seeds. In the M3 population, suppressor phenotypes were confirmed for four candidate lines (Gi8, Gi15, Gi18, Gi72) by growing 3 to 8 M3 progenies in the screening conditions and comparing morphologies with those of Bowman (wild type) and BW312. The M3 plant with the higher size was allowed to self. Selected lines were further characterized in a segregating M4 population with the measurement of the total plant height on suppressor (*sup*) and non-suppressor (*SUP*) individuals (**Figure 52, A**, no data for Gi72). Bowman (wild type) individuals, Gi8 suppressors and Gi18 suppressors are statistically taller than the BW312 parental line. Gi15 suppressors are slightly taller than

BW312 individuals, but the difference is not statistically significant. Yet, the Gi15 non-suppressor individuals are statistically smaller than the parental line. Six early maturity (*em*) individuals (Gi66, Gi92, EM1, EM2, EM3 and EM4) were picked up during the screening process, and phenotyped by recording the day of maturity of the first spike. The spike was considered mature when all the caryopses were fully yellow, in order to establish a robust criterion from one plant to the other. The early maturity lines had 7 to 26 days of advance in maturity compared to BW312 parental line (**Figure 52, B**). For all the suppressor and early maturity lines, the number of individuals grown in each generation is given in **Suppl. Figure 11** to **20**.

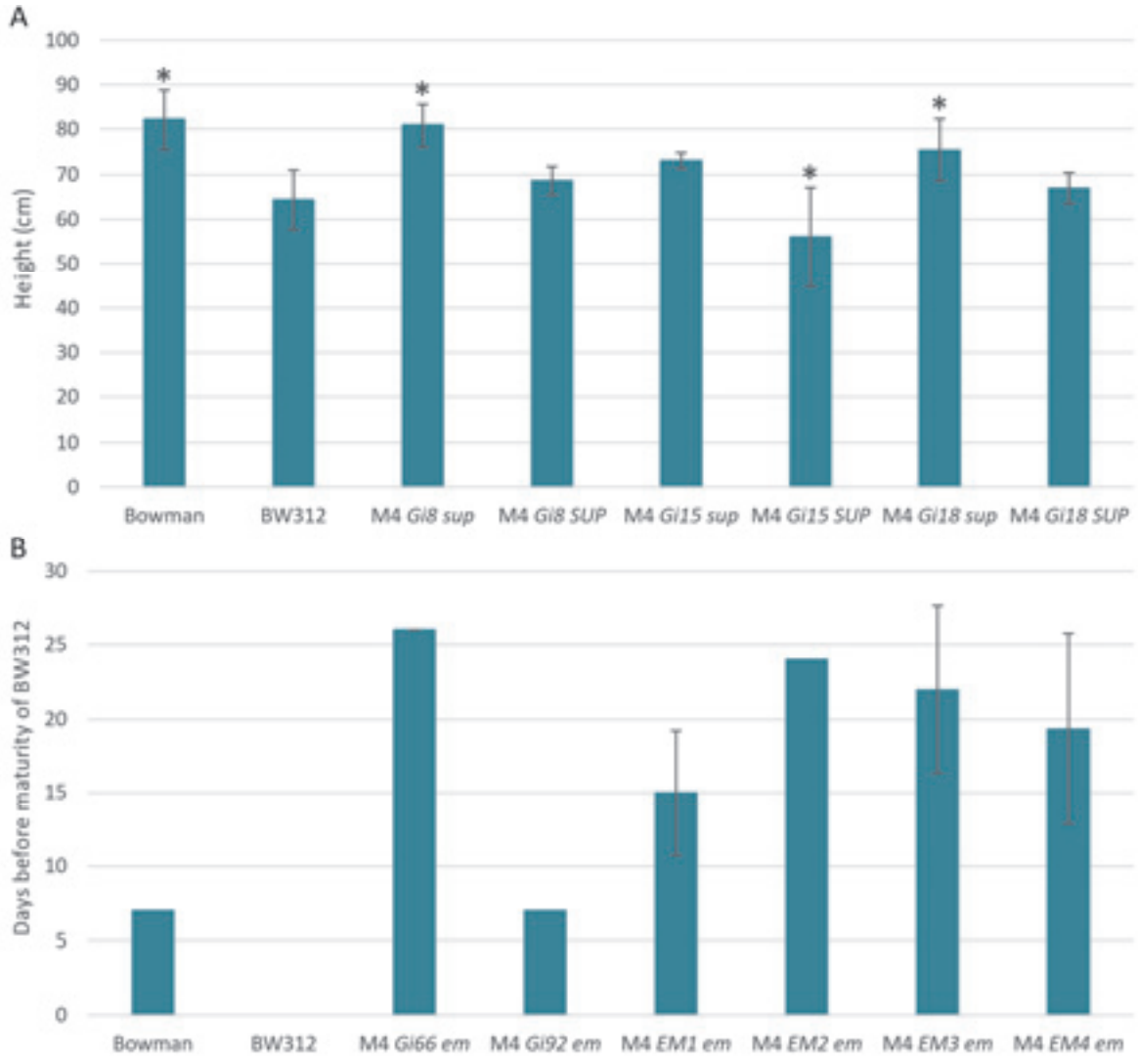

Figure 52. Height and advance in maturity of *Hordeum vulgare* BW312 *ert-ii.79/bri1* suppressor and early maturity individuals in a M4 generation. Plants were distributed in suppressor (*sup*) and non-suppressor (*SUP*) phenotypical classes for size measurement. The date of maturity of the first spike was recorded for early maturity (*em*) individuals and control lines. A two-tailed multiple comparison test after Kruskal-Wallis was applied for the height measurements, with a p-value=0.05 (single asterisk); N_i = 3-16. The date of maturity to obtain the number of days before maturity of BW312 was observed on 1 to 5 individuals per candidate line, no statistical analysis was performed.

Pictures of representative phenotypes of suppressor and early maturity BW312 lines are presented in Figure 53, A in a M5 segregating population, with the measurement of total plant height (**Figure 53, B**). Suppressor individuals have a Bowman like stature, with many tillers and a high size. Gi8, Gi15, Gi18 and Gi72 suppressors are statistically taller than BW312 parental line. No segregation was observed in the Gi18 population. EM1, EM3 and EM4 early maturity phenotypes were lost due to the selection of tall plants at the beginning of the study, which were not of the early maturity phenotype. These phenotypes are still available in a M3 generation. Early maturity phenotypes are characterized by plants of a dwarf or semi-dwarf stature with an early flowering and maturity of the spikes. Gi66 and EM2 candidate lines are the most affected, with a statistically smaller plant size for EM2 early maturity individuals compared to BW312, and present no segregation in a M5 population of 10 to 20 individuals. The other four early maturity candidates segregate *em* and *EM* phenotypes.

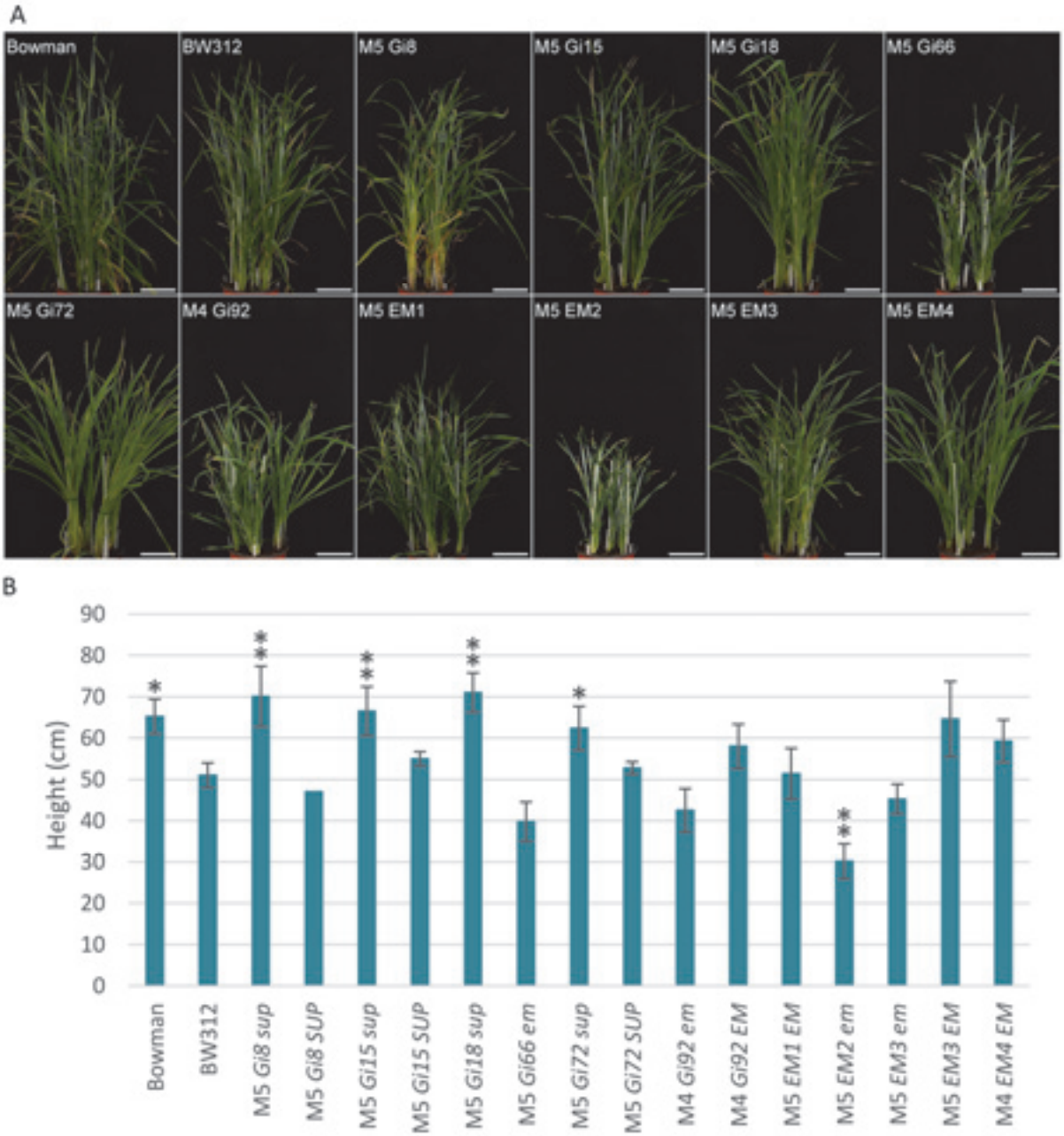

Figure 53. Growth phenotypes of *Hordeum vulgare* BW312 *ert-ii.79/bri1* suppressor and early maturity (*em*) lines in M4 or M5 generations. (**A**), Pictures of M4 or M5 populations, 5 plants sown in the same pot. Scale bars 10cm. (**B**), Measurements of whole plant size (cm) on the segregating populations. Statistical differences from the values obtained for BW312 parental line were determined using a pairwise Student t-test, with a p-value<0.05 (single asterisk) or p-value<0.01 (double asterisks).

For each line of interest, individuals from M3 or M4 generations displaying an *ert-ii.79/bri1* suppressor phenotype, or an *ert-ii.79/bri1* early maturity phenotype were backcrossed to BW312 to obtain F1 seeds. The phenotype of F1 individuals is presented in **Figure 54**. A cross between BW312 and Bowman shows a wild type-like individual. Only one individual was obtained for Gi18 line, showing a semi dwarf parental phenotype. For Gi72 line, the F1 was

homogenous with a semi dwarf parental phenotype. In the F1 generations obtained for early maturity candidate lines, two cases were observed: EM2 presented a homogenous F1 population with early maturity phenotype; Gi66 and EM3 presented a segregating population with half of the individuals exhibiting an early maturity phenotype, and half of the population with a parental-like phenotype. Arrows indicate a mature spike on early maturity individuals.

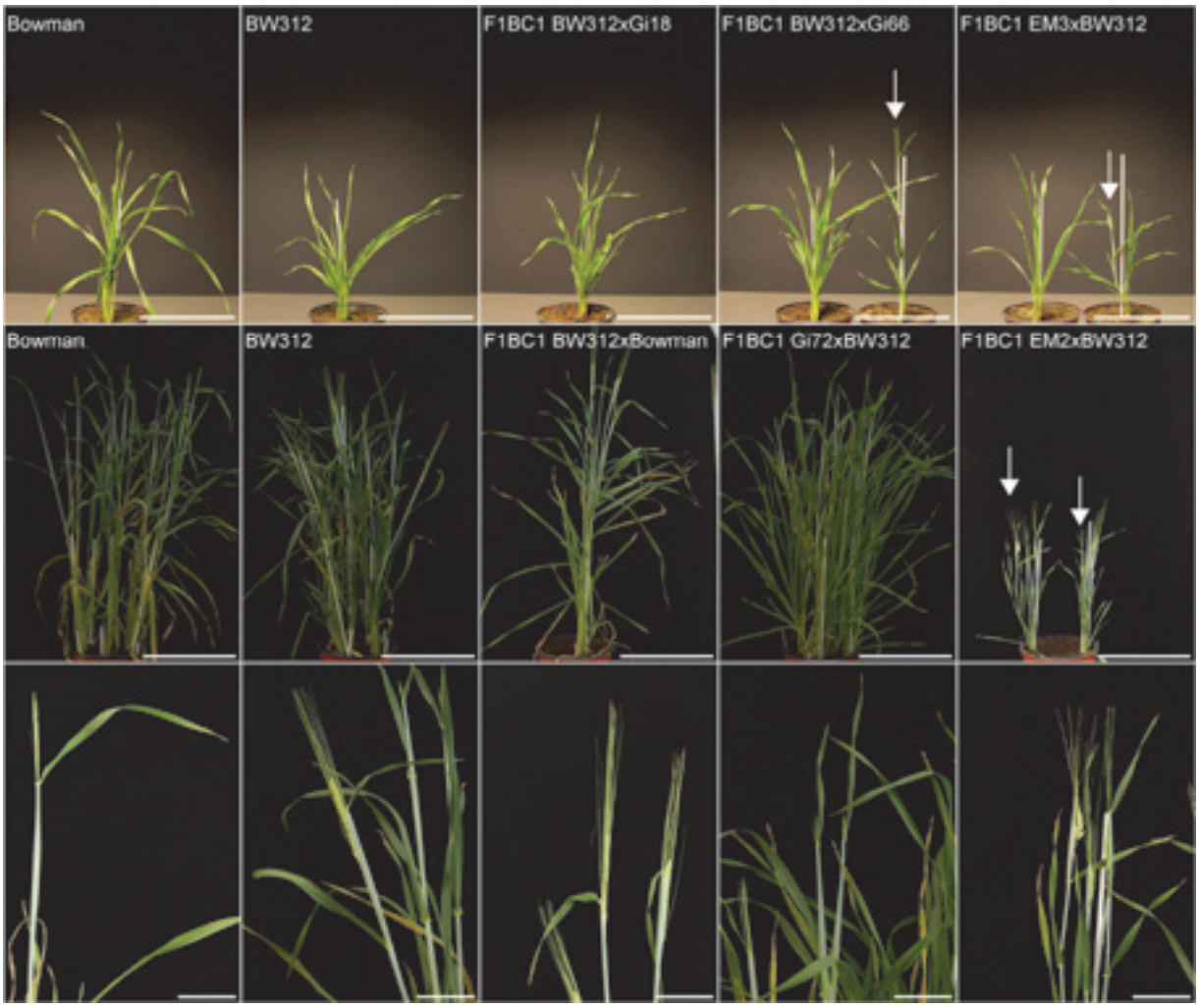

Figure 54. *Hordeum vulgare* BW312 *ert-ii.79/bri1* suppressor and early maturity lines in a F1BC1 generation. Whole plants grown in soil (up) and close-up on the spikes (down). Scale bars 20cm (up) and 2cm (down). First row, 1-month-old plants; second row, 2-month-old plants.

Figure 55 shows representative pictures of the spike morphology (**A**) and leaf angle (**B**) of suppressor or early maturity individuals. Spikes of suppressor individuals are long and carry more than 15 caryopses, while the spikes of BW312 are smaller with less seeds. The typical spikes of early maturity lines are very small, with few caryopses, generally less than 10 per spike. The yellow to brown color of the caryopses shows their maturity, with a spike almost

dry. Gi8 *sup* and Gi66 *em* individuals seem to have a smaller leaf angle compared to the control lines and the other suppressor and early maturity lines, but no measurements were made to assess this observation.

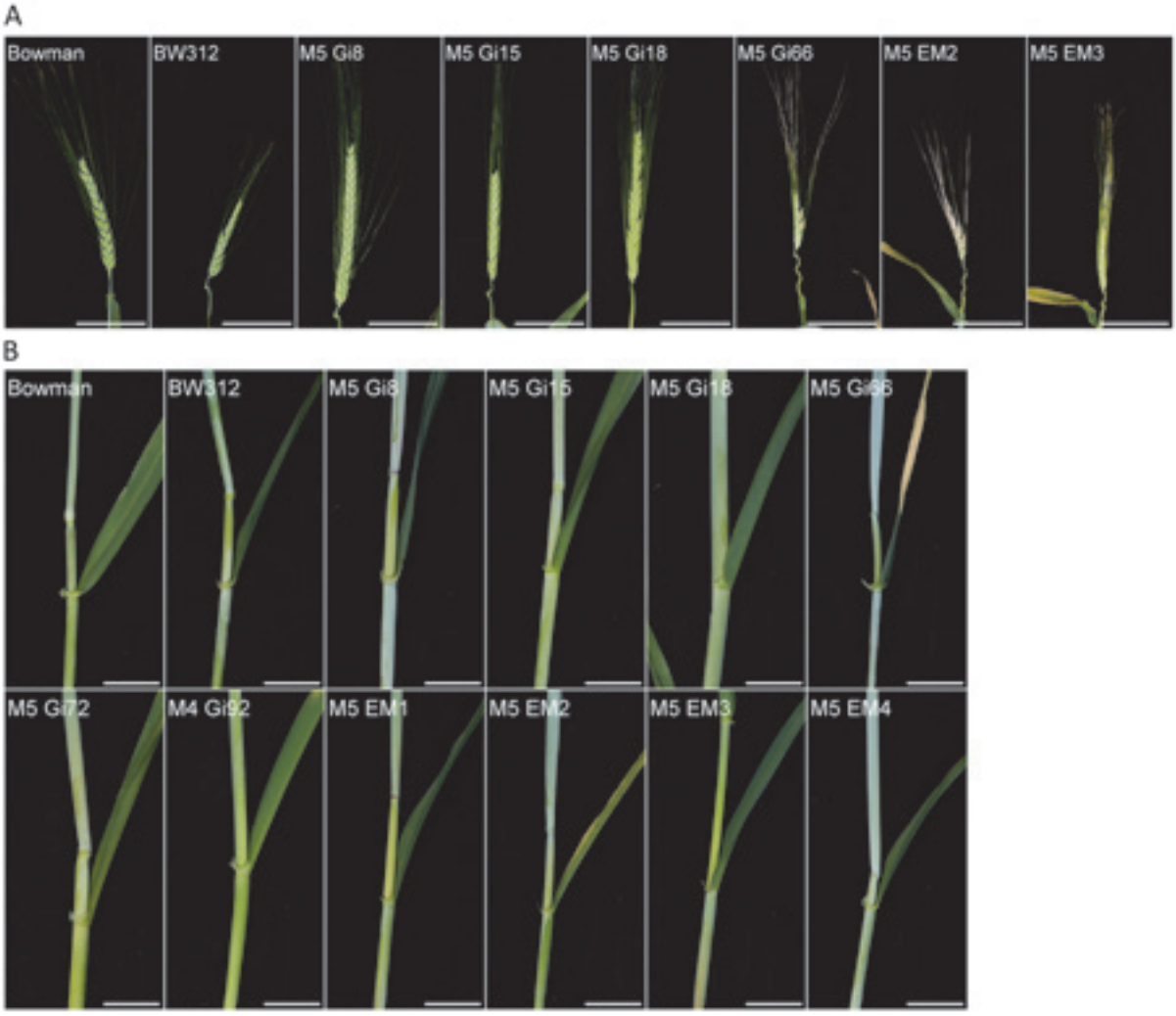

Figure 55. Phenotypic details of *Hordeum vulgare* BW312 *ert-ii.79/bri1* suppressor and early maturity lines. Pictures of spikes (**A**) and leaf angle (**B**) on M5 individuals. Scale bars 5cm (A) and 2cm (B).

From the self-fertilization of one F1 individual (genotyped *bri1*/*bri1*) presenting the suppressor or early maturity phenotype, F2BC1 populations were obtained. Plants were grown in soil as a segregating population, with 5 individuals in the same pot, as shown in **Figure 56**. Suppressor individuals showed a high size and many tillers with tall spikes, early maturity individuals had a dwarf stature with small spikes and few caryopses, while non-suppressor and non-early maturity individuals had a BW312 like phenotype with a semi-dwarf size and a normal maturity cycle. The populations were divided into two phenotypic classes for phenotyping.

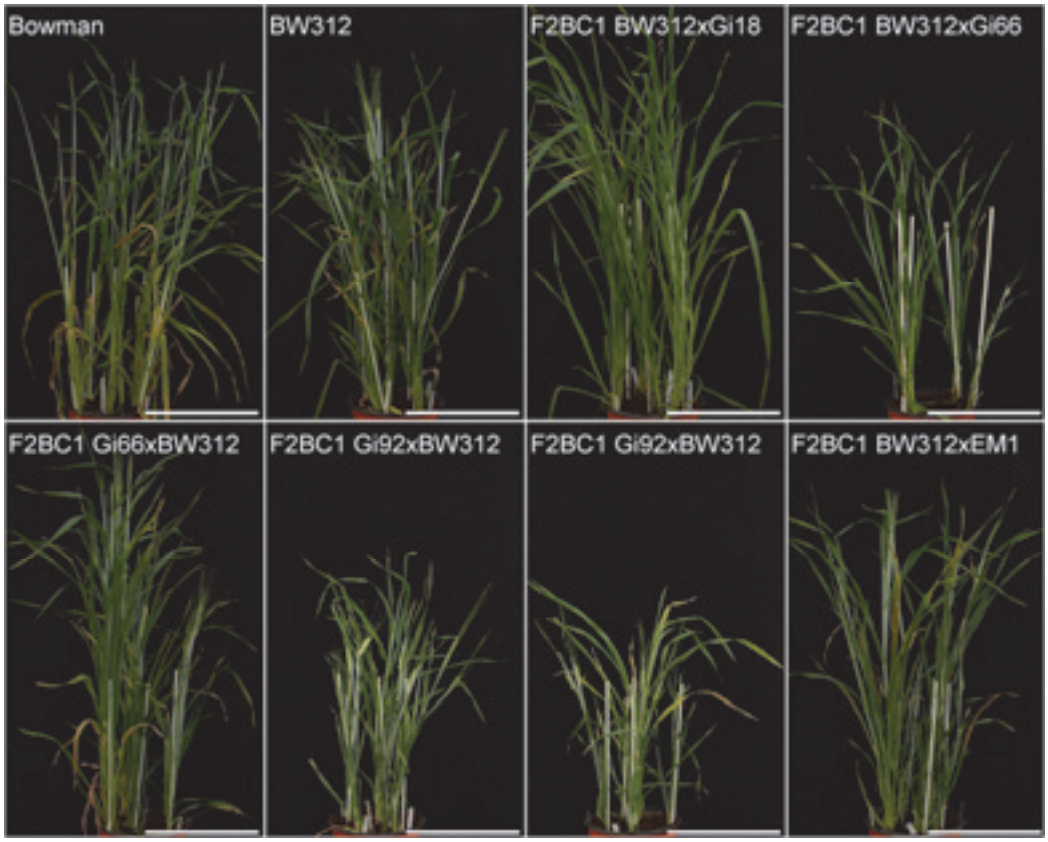

Figure 56. *Hordeum vulgare* BW312 *ert-ii.79/bri1* suppressor and early maturity lines in a F2BC1. Pictures of plant populations grown in soil in greenhouse conditions, five plants per pot. Scale bars 20cm.

The total plant size and the length of the internodes, spikes and awns were recorded for all the individuals of each F2BC1 population (**Figure 57**). For Gi66, reciprocal crosses to BW312 were performed. For Gi92, two distinct F2BC1 populations from independent crossing events were obtained with Gi92 as the pollen donor. Plants from F2 populations were phenotyped with respect to culm size or spike maturity, at first. Suppressor individuals of Gi18 F2 population were statistically taller than BW312, presenting a wild type-like size. The suppressor individuals were easily detected in the greenhouse as a very clear segregation occurred that enabled straight forward categorization of individuals as *sup* or *SUP*, phenotypically. Likewise, EM F2 populations were typically segregating early maturity *em* and *EM* individuals for selected lines, and em individuals were statistically smaller than the parental line (**Figure 57, A**). To further refine the morphometric and phenotypic observations, the size of the three first internodes was measured on each plant of the F2 populations (**Figure 57, B**). BW312 had smaller internodes compared to Bowman, and internodes 2 and 3 of Gi18 suppressors were longer than those of the parental BW312 line. Early maturity individuals of all the selected EM lines displayed smaller internodes than BW312. Gi18 suppressors exhibited statistically longer

spikes and awns compared to the parental line, and longer spikes when compared to Bowman, but smaller awns. All early maturity individuals produced statistically smaller spikes, but the size of their awns was varying. Awns were smaller on Gi66 *em* and EM3 *em* individuals, but got the same size as for BW312 individuals for the other early maturity lines (**Figure 57, C**).

Figure 57. Phenotypic measurements on *Hordeum vulgare* BW312 *ert-ii.79/bri1* suppressor or early maturity individuals in F2BC1 populations. Plant size (**A**), internode length (**B**) and spike and awns sizes (**C**) were measured on suppressor (*sup*), non-suppressor (*SUP*), early maturity (*em*) and non-early maturity (*EM*) individual in F2BC1 populations grown in greenhouse. Statistical differences between the measurements made on BW312 parental line and suppressor candidate lines were determined using a pairwise Student t-test, with a p-value=0.05 (single asterisk) or p-value<0.01 (double asterisks).

4. Hormone content in leaf tissues of *Hordeum vulgare* suppressor and early maturity lines.

The hormone analysis method was set as described in **Table 17** for the determination of the hormone profile in barley leaf tissues at different growth stages. The retention time, molecular ion, daughter ion and ionization mode were obtained from the analysis of hormone standards, to determine the correct parameters for the specific identification of the molecules in a complex extract.

Table 17. Standards used to set the chromatography and mass spectrometry methods for analysis of hormones in leaf samples by UPLC-MS/MS.

Hormone	Molecular weight	Hormone	Molecular weight
ABA	264.32	**KIN**	215.21
GA1	348.39	**CS**	464.68
GA4	332.39	**BR**	480.68
GA7	330.38	**CT**	432.68
JA	210.27	**GA3**	346.37
IAA	175.87	**BAP**	225.25
2iP	203.6		

Leaf tissues were sampled on the same barley plants after one month (**Figure 58, A**) and two months (**Figure 58, B**) of growth in soil in a growth room with cool conditions (15-18°C, M5 individuals), or in the greenhouse (F2 individuals). The eleven hormones presented in **Table 17** were searched for in the extracts. Separation and quantification of peak areas yielded relevant hormone profiles given as percentages of the total hormone content of biological triplicates for each line. For practical reasons, statistical analysis could not be represented on the figure, but statistical difference with the values obtained for BW312 parental line were calculated with a two-tailed multiple comparison test after Kruskal-Wallis, with a p-value=0.05. Statistical analysis was performed on raw peak area data, and in a second time on the values expressed as a percentage of the total hormone content for one barley line. No statistical difference was found between the raw peak areas obtained for all the hormones in BW312 and in the candidate lines at one or two months of growth. When considering the hormonal profile expressed as percentages of the total hormone content for one line, the percentage of abscisic acid (ABA) in M5 Gi8 suppressor individuals was statistically higher than in BW312 control

line cultivated in the same conditions. No other statistical difference in the hormonal profiles has been found. After two months of growth, the hormonal profile of all the lines was modified, gibberellin A4 (GA4) and cathasterone (CT) could be detected in the leaf extracts, with no statistical difference between the lines. All hormones presented in **Table 17** have been searched for, the hormones that are not presented in Figure 58 were under the limit of detection.

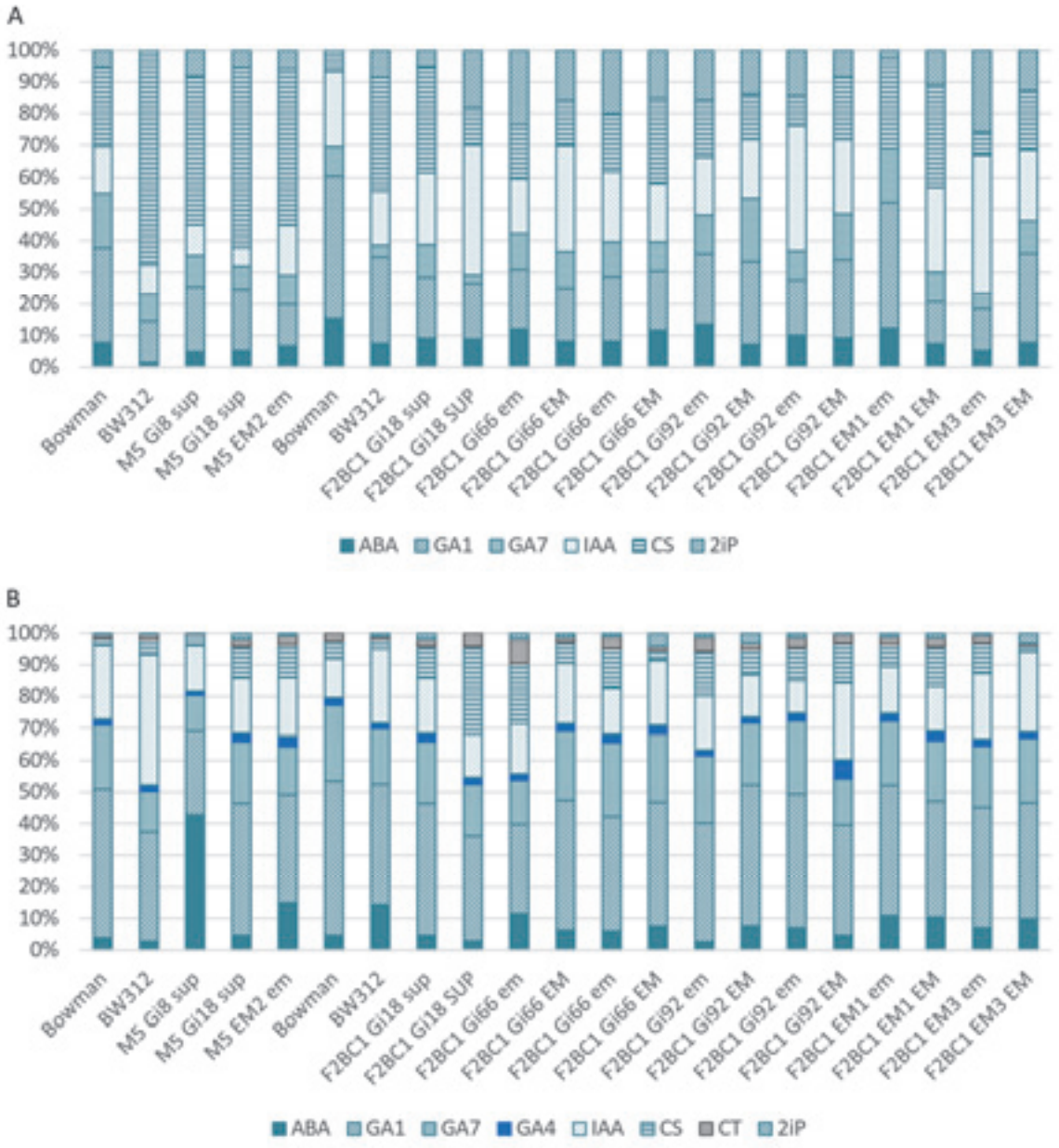

Figure 58. Hormone profile in *Hordeum vulgare* BW312 *ert-ii.79/bri1* suppressor and early maturity lines. Hormone profile in leaf material, expressed as a percentage of the total hormone content, after 1 month (**A**) or 2 months (**B**) of growth in soil. M5 plants were grown under cool conditions (18-15°C), F2BC1 populations were grown in standard greenhouse conditions. Bowman and BW312 control lines are presented for each culture condition. Abscisic acid, (ABA), gibberellins A1 (GA1), A4 (GA4) and A7 (GA7), indole-3-acetic acid (IAA), 6-(γ, γ-dimethylallylamino)purine (2iP), castasterone (CS) and cathasterone (CT) were the hormones detected among the eleven hormones searched in UPLC-MS/MS.

Standard curves were obtained for each hormone detected in the leaf extracts from barley individuals (**Figure 59**). The standard curves are nicely reliable, with a R^2 value between 0.98 and 0.99 and can be used for hormone quantification in the extracts, if the limit of quantification is reached for the molecule considered. The limit of quantification is determined by the ratio between the peak area and the background noise, the peak area has to be 5 times higher than the noise to consider that the molecule of interest can be quantified.

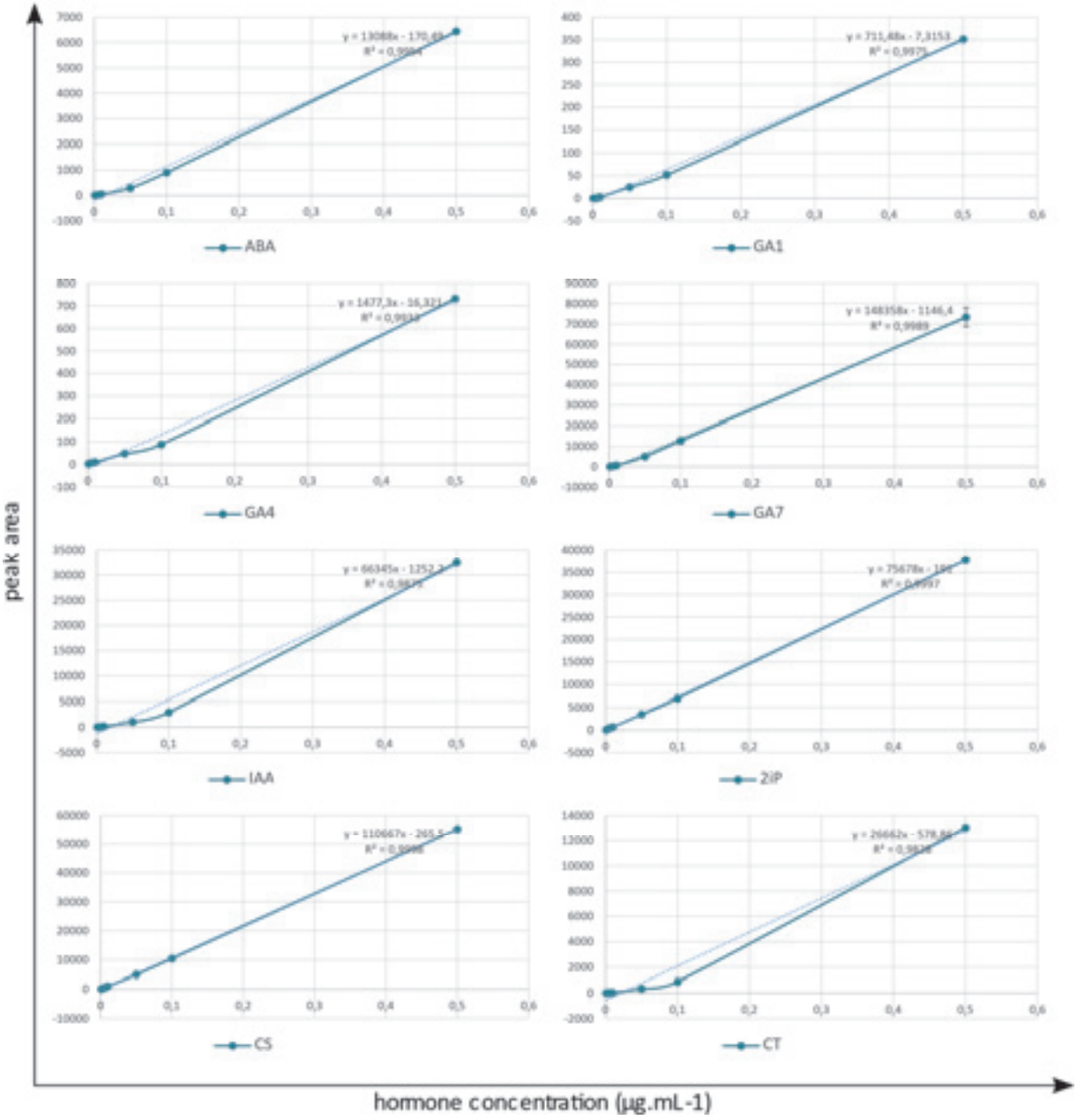

Figure 59. Standard curves for hormones detected in leaf samples of *Hordeum vulgare*. Standard curves were obtained from dilutions of hormones standards, and are presented as hormone concentration (µg.ml^{-1}) per peak area for abscisic acid (ABA), gibberellins A1 (GA1), A4 (GA4) and A7 (GA7), indole-3-acetic acid (IAA), 6-(γ, γ-dimethylallylamino)purine (2iP), castasterone (CS) and cathasterone (CT), which were detected in leaf extracts.

5. Characterization of *ert-ii.79/bri1* suppressor trait inheritance.

The suppressor and early maturity phenotypes segregated in M3 to M5 generations, and individuals of each phenotypic category were counted. The phenotypes selected for each line and the segregation pattern in M generations are summarized in **Table 18**. Suppressor or early maturity individuals in M4 or M5 generation were used for backcrossing to the BW312 parent to generate F1BC1 seeds. F1BC1 individuals were grown and one individual for each line was self-fertilized to obtain F2BC1 populations.

Table 18. Segregation of suppressor (sup) and early maturity (em) phenotypes in *Hordeum vulgare* selected lines.

Name	Phenotype selected in M2	Segregation in M3		Segregation in M4		Segregation in M5	
		sup or *em*	*SUP* or *EM*	*sup* or *em*	*SUP* or *EM*	*sup* or *em*	*SUP* or *EM*
Gi8	*sup*	3	0	7	3	14	0
Gi15	*sup*	3	0	2	0	6	7
Gi18	*sup*	8	0	12	3	11	1
Gi66	*em*	1	1	4	1	9	3
Gi72	*sup*	1	0	-	-	5	0
Gi92	*em*	1	1	8	7	-	-
EM1	*em*	1	2	1	4	1	6
EM2	*em*	1	0	1	0	12	0
EM3	*em*	1	1	2	2	12	2
EM4	*em*	1	3	4	0	1	11

The F1BC1 phenotype of hybrids and the segregation of distinct phenotypes in a mendelian (or possibly non-mendelian) inheritance pattern in F2BC1 populations are important clues to determine the suppressor genetics. A diversity of cases was found in the selected lines, as shown in **Table 19**. The F1 hybrids Gi8xBW312, Gi18xBW312, Gi72xBW312 exhibited the non-suppressor phenotype. F1 hybrids BW312xEM2 had the early maturity phenotype, while Gi66xBW312, Gi92xBW312, EM1xBW312 and EM3xBW312 hybrids were composed of early maturity and non-early maturity individuals. The germination rate in a F2BC1 was good, ranging from 88 to 100%. The best segregation hypothesis was determined using the χ^2 statistical test, full results are shown in **Table 20**.

Table 19. Genetic characterization of *Hordeum vulgare* BW312 *ert-ii.79/bri1* suppressor and early maturity lines. Best segregation hypothesis was determined using the χ^2 test, with a p-value>0.05. Germination rate for Bowman (wild type) and BW312 (parental line) was 100%.

Name	Phenotype in F1BC1	Segregation in a F2BC1		Germination rate in a F1BC1 (%)	Type of mutation	Best segregation hypothesis (*sup*:*SUP* or *em*:*EM*)
		sup or em	*SUP* or *EM*			
Gi8	*SUP*	-	-	100	Recessive	-
Gi18	*SUP*	27	3	100	Recessive	3:1
Gi66	*em/EM*	21	11	100	Dominant	2:1
Gi72	*SUP*	-	-	88	Recessive	-
Gi92	*em/EM*	20	14	100	Dominant	9:7
EM1	*em/EM*	10	9	95	Dominant	1:1
EM2	*em*	-	-	100	Dominant	-
EM3	*em/EM*	12	7	95	Dominant	2:1
BW312xBowman	WT	-	-	100	Recessive	-

Table 20. χ^2 analysis of segregation hypothesis for *Hordeum vulgare* BW312 *ert-ii.79/bri1* suppressor or early maturity lines in a F2BC1. A hypothesis is considered viable if p-value>0.05. If two hypothesis are validated, the best hypothesis selected is the one with the highest p-value. P-values of the selected hypothesis are in bold black, p-values of viable hypothesis are in black, p-values<0.05 are in grey and hypothesis were not considered viable.

Hypothesis *sup*/*SUP* or *em*/*EM*	3:1	1:3	1:1	2:1	9:7	7:9
Gi18	**0.05**	2.2e-16	1.1e-5	0.006	1.9e-4	3.2e-7
Gi66	0.102	9.6e-7	0.157	**0.617**	0.476	0.032
Gi92	0.029	5.2e-6	0.303	0.332	**0.762**	0.076
EM1	0.024	0.005	**0.818**	0.194	0.750	0.435
EM3	0.233	1.2e-4	0.251	**0.745**	0.543	0.088

The genetic analysis performed with recombinant F2BC1 small populations were quite conclusive and will allow the design of molecular genetics experiments for the identification of the mutations responsible for the phenotypes selected in this work. In an attempt to document which signaling or metabolic pathway would be modified in *em* and *sup* mutants, and to finely observe the gene expression networks in BW312 and its selected variants, a transcriptome

analysis will be performed. Sampling of leaf tissues has been made on F2BC1 populations, RNA preparation is currently in progress and a comparison of BW12 and candidate lines transcriptomes is to be done.

Discussion

I. General comments on the genetic screens in *Arabidopsis thaliana* and *Hordeum vulgare*.

The objective of my work was to generate novel biological resources for a comprehensive analysis of isoprenoids homeostasis, and for further understanding of brassinosteroid signaling. I have taken a forward genetic approach for the isolation of *Arabidopsis thaliana* mutants that suppress the phenotypic defects caused by deficient isoprenoid precursor (the C_5 isoprenoid building blocks IPP and DMAPP) pathways. I have taken the same forward genetic approach for the isolation of barley suppressors that overcome a partially deficient brassinosteroid response due to a hypomorphic mutation in the brassinosteroid receptor BRI1. These genetic screening rely solely on the careful examination of growth phenotypes of mutagenized populations, such as a restored photosynthetic capacity, an improved seed setting and filling of siliques, or a moderate but significant overgrowth phenotype in the case of barley. In this thesis work, I have dedicated an important effort to the establishment of such phenotypic measurements and observations. This will serve as a strong basis for the genetic and molecular characterization of many suppressor mutants.

To establish the genetics of the mutations responsible for the suppressor or early maturity phenotypes, a segregation analysis in a F2BC1 is mandatory. After a crossing with the parental line, one or several F1 individuals are obtained, which carry only one allele of the gene affected by the causative mutation(s). Thus, the phenotype of the F1 individual(s) gives the information about the dominance or recessivity of the mutated allele(s) that were selected. If the suppressor or early maturity phenotype is visible, one allele is sufficient to express the phenotype, and the mutation is considered dominant. If the F1 individual has a *SUP* or *EM* phenotype, the mutation is considered recessive, as two alleles are necessary for the phenotype to be seen. In some cases, a segregation is observed in the F1 generation, which means that the suppressor or early maturity parental individual was heterozygous for the mutation(s) of interest (**Figure 60**). In this case, a F1 individual with the suppressor or early maturity phenotype is selected and self-fertilized to obtain a F2 population.

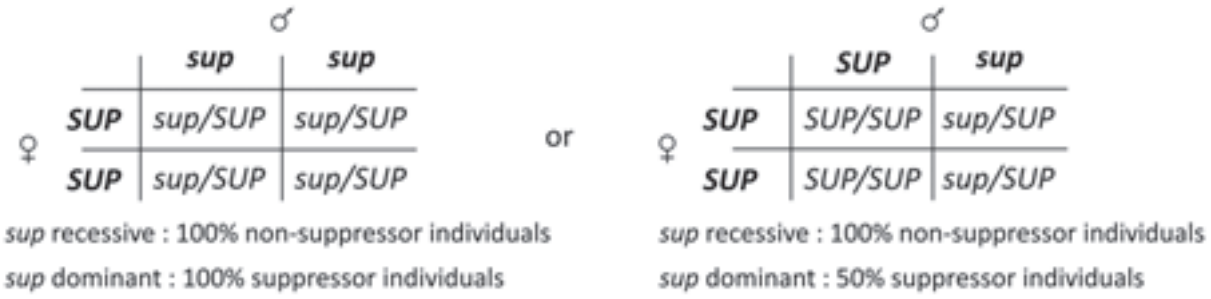

Figure 60. Segregation pattern of *sup* and *SUP* alleles in a F1 generation. Alleles transmitted by the male or the female parent are represented in bold. If the parents are homozygous (left), the F1 population is homogenous and presents the phenotype of the dominant allele. If one parent is heterozygous (right), the F1 population is divided into two phenotypic classes in the case of a *sup* dominant mutation, or shows the wild type phenotype in the case of a *sup* recessive mutation.

In the F2 population, the phenotypes segregate, and the segregation analysis gives the number of genes or loci of interest involved. If only one gene is causative of the suppressor or early maturity phenotype, a typical 3:1 or 1:3 *sup*:*SUP* or *em*:*EM* segregation pattern will be observed, for a dominant allele in the first case, and for a recessive allele in the second case (**Figure 61**).

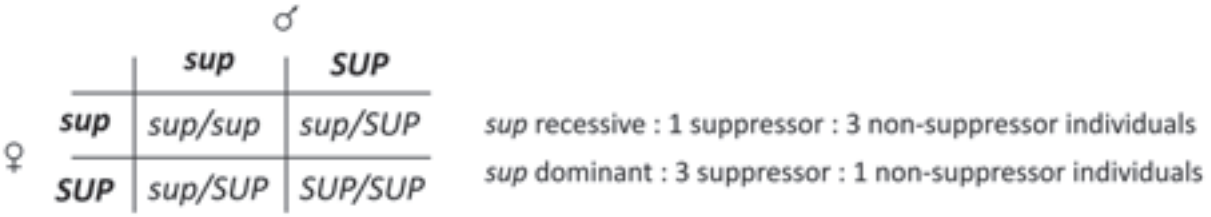

Figure 61. Segregation pattern of *sup* and *SUP* alleles in a F2 generation in the case of monohybridism. Alleles of the F1 individual are represented in bold. In the F2 population, *sup* and *SUP* alleles are segregating and different phenotypic classes can be observed with a 3:1 or 1:3 ratio.

In some cases, a bias from the typical 3:1 or 1:3 ratios of a Mendelian inheritance of characters may be observed. A 1:1 ratio in a F2 population indicates that one of the gametophyte could not transmit the mutated gene to the progeny, which is the case in gametophytic lethality (**Figure 62, A**) that is observed for instance for the *hmg1 hmg2* deficient mutant of *Arabidopsis thaliana* (Suzuki et al., 2009). A 2:1 ratio indicates a recessive lethal allele, which means that homozygous individuals for this allele are not viable (**Figure 62, B**). A 9:3:3:1 ratio is typical of dihybridism, when two distinct genes segregate independently but are responsible for the phenotype when expressed together, with a 7:9 or 9:7 ratio found in the phenotypic classes (**Figure 62, C**).

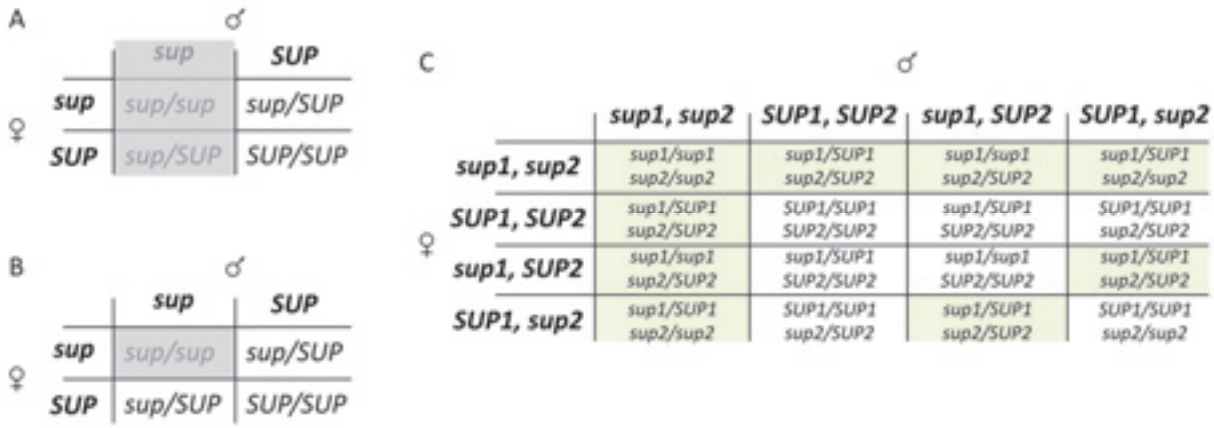

Figure 62. Segregation pattern of *sup* and *SUP* alleles in a F2 generation in specific cases. (**A**), A 1:1 segregation pattern is found when an allele cannot be transmitted to the offspring by one of the parent. (**B**), A 2:1 ratio is typical of a recessive lethal allele. (**C**), A 9:7 or 7:9 ratio indicates dihybridism.

In these screenings, a diversity of segregation patterns has been observed, which means that a diversity of suppressor alleles have most probably been selected. In turn, several suppressing mechanisms are expected after the causative mutations will be identified by Next Generation Sequencing (NGS) strategies.

The choice of the parental lines for EMS (in the case of *Arabidopsis thaliana*) or sodium azide (in the case of barley) mutagenesis was important in order search for regulators of the isoprenoid metabolism that would possibly act as master switches of isoprenoid homeostasis. The *hmg1-1* and *chs5 Arabidopsis thaliana* mutants bear mutations in key genes of the mevalonate and MEP pathways respectively. Indeed, 3-hydroxy-3-methylglutaryl CoA reductase (HMG) and 1-deoxy-D-xylulose 5-phosphate synthase (DXS) are the rate-determining enzymes of the mevalonate and methylerythritol pathways, respectively (Pulido et al., 2012; and for an exhaustive review Hemmerlin et al., 2012). The *bri1* mutant is lacking sensitivity to brassinolide, an important hormone involved in plant growth. The screening for suppressors yielded several mutants of interest that fall into different categories with respect to their detailed phenotypes and genetics. These screenings will be completed soon by a complementation analysis. It is however already clear that the possible redundancy in the selected genetic event will be quite low. The choice of the *Arabidopsis thaliana hmg1-1* and *chs5*, and the barley *ert-ii.79/bri1* mutants is *a posteriori* also totally justified since many gain of function mutants are available and they represent valuable tools for preparing plant breeding strategies.

II. Suppressors of *hmg1-1*.

In the *hmg1-1* suppressor screen, the important part was to establish a good criterion to select suppressor individuals. At the beginning of the screening, the size was the first character considered, as the difference in the size seemed to differentiate the *hmg1-1* mutant from the WS2 wild type. More than the size, the global shape and stature of the plant were easily scorable by eye. As the *hmg1-1* mutant is semi-sterile, the number of siliques and the weight of the seeds were recorded. It was technically not feasible to collect the total seeds of one individual, so these two characters were observed on the main stem, to establish a common basis for all individuals. When analyzing the data obtained after measurement, it appeared that the number of siliques was not a good criterion to discriminate between the *hmg1-1* parental line and WS2 wild type. As the *hmg1-1* mutant produces as many siliques as the wild type, it would not be possible to discriminate between suppressor and non-suppressor individuals considering this criterion. This observation was also made in the F2 populations analyzed later. The size of the plants and the weight of the seeds were the most relevant phenotypic details. A striking example of the non-relationship between the number of siliques and the weight of the seeds is found in the L9.1 candidate line, which produces many siliques that are empty since the weight of the seeds is very small. In a M3 generation, the weight of the seeds could not be measured for all the suppressor candidates, and the number of plants used for this characterization was small, this could explain that no statistical difference was found in the phenotypical measurements made in this generation. This problem was solved in the analysis of F2 populations, with phenotypical measurements made on twenty to fifty individuals, selected in a population of more than a hundred individuals. In such large populations, it was not possible to collect individually the mature siliques on the main stem of each plants to measure the weight of the dry seeds. A good proxy was the measurement of the weight of the siliques, sampled at the same developmental stage for all the lines, when the first siliques of the main stem were dry, and the other siliques of the stem were mature.

In this screen, a challenge was to cross the suppressor lines with the *hmg1-1* parental line. At the beginning of the study, we expected to make the crossings with the suppressor lines as male and as female, to check if the mutation was nuclear and transmitted to the offspring by both male and female parents. The many attempts to use *hmg1-1* as a male failed, certainly due to the semi-sterility of this mutant. The pollen was not available in sufficient amounts, and did not seem viable when observed under magnification as small and dry grains were observed. This

observation was not made for the candidate lines, which presented wild type-like pollen grains. For the candidate lines L92 and M5.1, I could not obtain viable siliques whatever the direction of the crossing. These lines were because of a high the number of siliques on the main stem, but did not produce many seeds, and could be considered as non-suppressors of the semi-sterile *hmg1-1* phenotype, thus explaining the difficulty to perform the crossings.

At the mature seed developmental stage, it was not possible to identify suppressor and non-suppressor individuals. The results of the seeds measurements should then be considered as a mean value for a given population. The *sup hmg1-1* Q81 line showed a strong suppressor phenotype, thus it could be surprising to observe smaller seeds if this criterion were linked to the suppressor phenotype. Since the seed surface measurement is a mean value made on seeds of segregating populations, it is not possible to know if a larger quantity of "non-suppressor" seeds could lead to such a result. The same holds true for *sup hmg1-1* C52, if there are more "suppressor" seeds in the population, the mean value goes higher. The segregation analysis in a F2BC1 gives an answer to this question: Q81 carries a recessive mutation, thus we can expect to have more "non-suppressor" seeds in the bulk. The *sup hmg1-1* C52 is expected to carry a recessive lethal allele coding for a dominant trait with a 2:1 ratio, but the hypothesis of a dominant mutation with a 3:1 ratio is also relevant albeit with a smaller p-value; both could be consistent with the observations made on seeds measurement.

The expression analysis of the MEP pathway genes shows that some suppressor individuals have an increased expression of *DXR* (*sup hmg1-1* Q7.7), *HDS* (*sup hmg1-1* M5.1) and *HDR* (*sup hmg1-1* Q81, L9.1, M5.1). In M5.1, the increased expression of genes coding for the two last enzymes of the MEP pathway could promote the accumulation of the C_5 building blocks, IPP and DMAPP, and from that, to increased levels of pathway end products, however this was not investigated at this stage of the study. It is tempting to speculate that an overexpressed MEP pathway could fuel the cytosolic compartment with IPP and DMAPP otherwise lacking due to the deficiency of the *HMG1* gene, which is confirmed to be less expressed in the *hmg1-1* mutant and all suppressor individuals. Meanwhile, the *HMG2* gene expression is equivalent to that of the wild type in these lines, indicating that no change occurred at the level of HMG2 gene expression. Surprisingly, *sup hmg1-1* Q6.9 and M5.1 exhibited a reduction of *IDI1* gene expression, IDI is the enzyme catalyzing the conversion of IPP into DMAPP. This would decrease the biosynthetic activity in downstream biosynthetic segments leading to pathway end

products, or alternatively would create pools of IPP available for further metabolic processes. Again, at this stage of the project this is not supported by isoprenoid profile measurements. Another interpretation of these results is a feedback regulation of cytokinin synthesis through the regulation of DMAPP synthesis, the precursor of cytokinins (Vranova et al., 2012). Hormone profiles of these lines could be determined to deepen this hypothesis. In the *sup hmg1-1* M5.1 suppressors, the expression of *MDC1* gene is increased, which could favor the production of IPP from its precursor mevalonate-5-diphosphate. In the *sup hmg1-1* Q6.9 suppressors, the expression of the *CAS1* gene encoding the cycloartenol synthase that is the committed step in the sterol biosynthesis, is increased; these individuals could suppress the *hmg1-1* phenotype by directing IPP into the sterol biosynthetic pathway. In the *sup hmg1-1* Q7.7 suppressor individuals, both *SQS1* and *CAS1* gene expressions are increased, thus the hypothesis of plants producing sterols to overcome the *hmg1-1* phenotype could also be pointed. No difference has been detected in the unsaponifiable lipid profile of the suppressors to confirm these hypothesis, but further refined analysis must be done.

Segregation analysis carried out with F2BC1 populations gave rather clear results. Six lines showed a 3:1 (Q7.6) or 1:3 (Q6.9, Q7.7, Q81, I2.1, SS1) segregation of individuals as suppressors *sup* and non-suppressors *SUP* based on the phenotypic criterion already discussed. This demonstrates a Mendelian pattern of inheritance of the characters as single alleles. Three other lines (*sup hmg1-1* C52, Q6.10, L9.1) had a 2:1 ratio of SUP to *sup* individuals that would be in favor of a recessive allele causing lethality in the homozygous state. The candidate lines *sup hmg1-1* Q7.1 and M8.1 are the only lines to show a 7:9 and 1:1 ratio respectively, that do not follow the ratio usually found in classical Mendelian genetic. In the case of *sup hmg1-1* C52 and L9.1, a viable hypothesis according to χ^2 test, indicates a 3:1 or 1:3 Mendelian segregation pattern. For *sup hmg1-1* Q6.10 and Q7.1, the hypothesis of a dihybridism type segregation cannot be rejected. In conclusion, this diversity of segregation patterns will probably unveil a diversity in the causative mutations that have been selected. Most importantly, solid segregation analysis and genetic interpretation of results are the cornerstone of the design of bioinformatics pipelines that are needed to mine whole genome sequencing data and candidate SNP determination. Bulk segregant analysis in the F2BC1 population has been started being largely inspired from James et al., 2013. Illumina sequencing of genomic DNA purified from *sup* and *SUP* bulks has been engaged. The raw sequencing data has been received from the IGBMC platform (Strasbourg University) and is currently being analyzed in

collaboration with Sylvain Darnet (Laboratório de Biotecnologia Vegetal, Instituto de Ciências Biológicas, Universidade Federal do Pará (UFPA), Belém, Brazil).

III. Suppressors of *chs5*.

The screening for *chs5* suppressors was made *in vitro*, and the lines were characterized in soil. The phenotypes were difficult to follow at and adult stage, until I found the good culture conditions, with a specific temperature which allows the phenotype to be more stable during the plant development. In fact, *chs5* mutant is a temperature permissive mutant previously selected as a chilling sensitive mutant (Araki et al., 2000). The other difficulty was the genotyping of the *chs5* mutation, as the amplification was really sensitive to any change in the temperature or the composition of the PCR reaction mix.

I could identify six suppressor lines, four with a wild type-like phenotype (G2.10, L8.4, Y50, Y200), and two mildly suppressing the *chs5* chlorosis and late growth (LA4, iQ3). A diversity of phenotypes could imply a diversity of mechanisms involved in the restoration of the *chs5* phenotype. The four wild type-like phenotypes are difficult to differentiate from each other; it is possible that the same mutation had been selected more than once, this will however be documented soon thanks to genetic complementation assays. The measurement of chlorophylls and carotenoids content is a first clue to assess the phenotypes observed, and to have an idea on how the chlorosis is suppressed. The results show a difference between G2.10 and L8.4 accumulating carotenoids, while Y50 and Y200 accumulate chlorophyll b. This could indicate two different types of suppression mechanisms.

Some metabolic profiling was carried out to measure the levels of MEP pathway intermediates in collaboration with Louwrance Wright (Max Planck Institute for Chemical Ecology, Jena, Germany). In order to get some clues on the metabolic status of the MEP pathway in the *sup chs5* mutant, green suppressor plants were compared with green wild type plants, all grown in autotrophic conditions. Surprisingly, *sup chs5* L8.4 suppressor individuals seem to accumulate less intermediates (DXP, MEcPP, IPP and DMAPP). The *sup chs5* LA4 suppressor individuals only accumulate less MEcPP when compared with the wild type. Two explanations can be discussed: either another gene of the pathway has become deficient due to a mutation and the whole pathway is affected in the accumulation of the intermediates, or the pathway is activated

in these plants to overcome the *DXS1* deficiency and intermediates are used as they are produced. If the turnover is very quick, no accumulation is possible, and the intermediates cannot be detected and quantified. In this second case, an increased gene activity is expected for the MEP pathway genes in *sup chs5* L8.4, it is the case only for *MCT* gene.

In this screening, the most interesting mutants are the intergenic suppressors that will grand access to valuable information about metabolic compensation and crosstalk, pathway interactions and metabolite transport, to speculate just about a few possibilities. To exclude intragenic suppressors (although these might be interesting for another type of study, as for instance DXS structure-activity), second site mutations in the *DXS1* gene of suppressors were surveyed but no one was found. This was done by a bioinformatic analysis of deep-sequencing data, or by RT-PCR cloning and sequencing. Concerning the expression analysis of the mevalonate pathway genes, no significant differences were found in the *chs5* suppressors, indicating that the chlorotic phenotype of *chs5* cannot be suppressed by an apparent activation of the mevalonate pathway. This may be surprising since some complementation of strong *dxs1*/*cla1* deficient mutant could display a restored plastidial pigment accumulation by feeding mevalonate in the seedling growth medium (Nagata et al., 2002).

In the segregation analysis of *sup chs5* M2 and F2 populations, a good *in vitro* germination rate was observed, so no lethal mutation is expected. The phenotypic distribution recorded in soil is different from the distribution observed *in vitro*. This may be due to the fact that in autotrophy (*ie* in soil), the observations were made after a given proportion of seedlings were potted. However, no bias or selection occurred when potting these seedlings. Moreover, the phenotyping in soil was made on smaller populations than for *in vitro* conditions. For this reason, the best segregation hypothesis was chosen from the results obtained *in vitro*. Yet, the segregation patterns observed *in vitro* and in soil were both in favor of a recessive mutation, as confirmed by the *SUP* phenotype observed on F1 individuals.

To come rapidly to the identification of causative mutations of the suppressor phenotypes, a bulk segregant genotyping-by-sequencing strategy was developed, as it is the case for the *hmg1-1* suppressors. Before sequencing, the extraction of pure genomic DNA from the plant samples had to be developed. I already had a gDNA extraction protocol working routinely, but the gDNA obtained also contained RNA and the quantity was not sufficient for sequencing. The

challenge was to obtain enough genomic DNA of good quality from small plant samples since the first samples sequenced were plantlets from *in vitro* cultivation. After development, I could provide good samples, and the first set of data obtained after the bulk sequencing of G2.10 and L8.4 suppressor and non-suppressor individuals was of very good quality. Using the non-suppressor samples as a blank, Sylvain Darnet identified SNPs distributed along all the chromosomes. Thanks to the segregation analysis, the genetics of the mutations of interest was established, and unique high quality EMS homozygous SNPs were filtered from the data. In the common variant subtraction analysis, 108 SNPs are common to all groups, which means that those SNPs are from the *chs5* genetic background. One could wonder if these SNPs have an effect on the *chs5* phenotype, but the analysis of the Col-0x*chs5* and *chs5*xCol-0 F2BC1 populations answers this question. The *chs5* phenotype segregates with a 1 to 3 *chs5*:*CHS5* ratio indicative of a single recessive allele.

The sequencing of *sup chs5* G2.10 and *sup chs5* L8.4 populations allowed the identification of mutations in annotated genes for the suppression of *chs5* phenotype. These mutations were selected according to the segregation analysis made on F2BC1 populations, and homozygous SNPs were sought. Two mutations were found in *sup chs5* G2.10, and six were found in *sup chs5* L8.4. Among these candidates, one is described as located in the chloroplasts, a good lead when dealing with chlorosis suppression. Two candidates are bearing a "domain of unknown functions", which is of interest since they have not yet been described, and could be involved in any pathway or mechanism allowing the compensation of a chlorotic phenotype. The analysis of protein domains is being done to search for features of interest and co-expression patterns. A strategy to select which target gene is involved in the suppression of the *chs5* phenotype is to follow the identified SNPs into further generations of the candidate lines. A second backcross with the parental line has been made, and F2BC2 populations will be available to check which of the target mutations are still present in the suppressor individuals. Crossings have been made between the suppressor candidates to generate complementation groups. The phenotype of the progeny will determine if the suppressor alleles selected so far are able to complement each other, an essential information to avoid the selection of mutations affecting the same gene. To validate the candidate mutation(s), it would be nice to re-introduce the candidate mutation(s) into the *chs5* parental line by knock in with the CRISPR-Cas9 technology. If the selected mutation is causative of the suppressor phenotype, the transformed plants will show a reversion of the leaf chlorosis.

IV. Suppressors of *ert-ii.79/bri1*.

The screening for suppressors of BW312 phenotype in *Hordeum vulgare* aimed at identifying taller plants, which would revert the semi-dwarf parental stature using any other pathway or mechanism to compensate the loss of brassinosteroid sensitivity. In a broader point of view, identifying this type of mechanisms would help in understanding the plant growth mechanisms, and select plants of interest with specific agronomic traits. The size of a plant is important for field cultivation, as a smaller plant will resist to lodging, and avoid a loss of the grains due to contaminations or early germination when caryopses are in contact with the soil. Most importantly, such a suppressor screening has the potential to allow the identification, the characterization and the use of gain-of-function mutations.

A first step in the screening process was to identify culture conditions suitable for barley, which had never been used in the institute. After several tests with the BW312 parental line and Bowman wild type, the greenhouse conditions were chosen. At a later stage in the characterization of candidate lines, crossings appeared to be difficult in these conditions, with approximately 3% of success. Thanks to the advice of Christoph Dockter, plants were then cultivated in cool conditions, and it became possible to obtain F1 seeds, even if barley crossings are still to be improved. Phenotyping is also an important part of the screening, but the physiology and development of *Hordeum vulgare* was not known in the institute. With the advice of Marta Ramel and Richard Wagner, good culture conditions were chosen and I became able to recognize the suppressor and early maturity individuals easily.

In this screening, I was able to identify four lines with a tall size, taller than the semi-dwarf parental line, and six early maturity lines. Even if this trait was not expected in the screening, it appeared to be interesting for agronomical and fundamental reasons and was also selected. Indeed, if the plants are mature earlier in the year, they stay in the field during a shorter period of time, allowing less risks of damage to the culture, and new culture practices. Screening barley and subsequent genetic analysis is quite of a challenge, since the number of individuals in each generation is small (even smaller when talking about early maturity individuals) and the success of the crossings is limited. The small number of individuals can explain why some candidate lines were not confirmed by phenotypic measurements and statistical analysis.

The early maturity phenotype was visible even before the maturation of the spike according to my observations during the course of this thesis work. The early maturity individuals were smaller, with few stems, but the maturation of the first spike was the most reliable character to establish a "date of maturation" and compare the candidate lines with the control lines. Spike morphology and leaf angle were not fully investigated, but these morphological traits could be of interest to further characterize the candidate lines. Indeed, leaf angle is described as related to brassinosteroid and gibberellin sensitivity in crops, and a smaller leaf angle allows planting at a higher density, resulting in a higher grain yield per hectare (Vriet et al., 2012; Tong et al., 2014).

In a recombinant population segregating the phenotypes of interest scored during this work, growth suppressor and non-suppressor, and early maturity and non-early maturity traits were discriminated in a very efficient and robust manner. The size of the plant, either taller or smaller than the BW312 parental line, seems to be linked to the size of the three first internodes. Generally seen, taller individuals (including Bowman wild type control) have longer internodes, and smaller individuals have smaller ones. It would be interesting to investigate whether the internode elongation is due to cell elongation or to a larger number of cells, and the same stands for smaller internodes. Generally, the size of the spike is also related with the size of the plant, and taller plants produce more seeds, but the number of seeds on the spikes was not recorded yet in F2 populations. This characteristic renders the early maturity plants unsuitable for agriculture, but the early maturity trait could eventually be introgressed into barley elite cultivars.

Concerning the analysis of the leaf hormone content, I had to develop the chromatographic and spectrometric methods with hormone standards, and improve the extraction method on tissues from control lines before using tissues from the candidate lines. An interesting thing to observe is the total hormonal profile, more than the real quantification. Indeed, statistical analysis on raw peak area showed no differences between the candidate lines and the parental line grown in the same conditions. The only difference found was by comparing the implication of each hormone in a global hormonal profile for the plant. This is also more efficient in a biological point of view, as the plant growth and life in general is more guided by the hormonal balance than by a real dose effect of each hormone alone. In this state of mind, as a first step, I decided not to quantify the hormones detected in leaf material. Moreover, a part of the hormones

identified showed peak areas above the limit of detection, but below the limit of quantification. Gi8 suppressor plants could compensate the semi-dwarf phenotype with a hormonal balance in favor of abscisic acid, which is known to act on plant growth by regulating cell division and elongation (Finkelstein, 2013).

In this screen, I was able to bring three suppressor lines (overgrowth plants) to a F1BC1 generation, and for all the lines, F1 individuals were non-suppressor, indicating that the mutations of interest causing the suppressor phenotype are recessive. This is consistent with the fact that no non-suppressor individual was seen in a M3 generation, suggesting that the M2 parental individual was homozygous for the *sup* mutation selected. In M4 and M5 generations, the number of non-suppressor individuals is very low and could be false-negatives, ranked as non-suppressor individuals because of the size limit chosen to categorize the plants. As the seeds of all the individuals grown in M1 were bulked, it is possible that the same mutation has been selected several times. This question will find an answer when the segregation analysis of F2BC1 populations will be done. If the segregations are different, the mutations are different; if not, further characterization will be needed. For early maturity candidate lines, EM2 is the only one with a homogeneous F1 population of early maturity individuals, indicative of a dominant mutation. This is also consistent with the fact that no non-early maturity individuals were found in M3 to M5 generations. In Gi66, Gi92, EM1 and EM3 F1 populations, two categories of individuals were found, indicating that the mutations of interest are dominant, but the parental early maturity individual used for the backcross was heterozygous for the mutation(s) selected. As the segregation hypothesis selected for early maturity candidate lines are different, we can expect to have selected different mutational events due to sodium azide treatment, thus different mechanisms leading to early maturity. This phenotype does not seem to be related to the hormonal balance of the plants, as no statistical difference was found between early maturity individuals and BW312 parental line in the total hormone profile. As a first control of this observation, and because known gibberellin mutants are semi-dwarf (Chandler and Robertson, 1999), a treatment of the early maturity individuals with exogenous gibberellins could be done. A positive response to exogenous gibberellins would indicate a gibberellin biosynthetic mutant. Such an hypothesis is certainly realistic since an interaction between brassinosteroids and gibberellins has been described in other plant species (Unterholzner et al., 2015). Furthermore, a sampling has been made in F2BC1 populations of all mutants considered in this work to carry out a transcriptome analysis, in order to get clues

on the mechanisms involved in early maturity and overgrowth. Finally, further backcrosses will be done and a strategy base on genotyping-by-sequencing will be implemented (Mascher et al., 2014).

Chapter III. Pollen specificities in isoprenoid biosynthesis: the case of the sterol pathway.

Introduction

As the male gametophyte of flowering plants, the pollen has to carry the two sperm cells to the embryo sac, the female gametophyte, and for this germinates a pollen tube through the transmitting tract of the pistils. This stage of pollen development encompasses the pollen tube reception by the female gametophyte and the subsequent double fertilization. The pollen tube penetrates one of the synergids of the embryo sac where it discharges its content. During this process, one sperm cell fuses with the egg cell and the second one fuses with the two polar nuclei of the female gametophyte, to produce a diploid embryo and a triploid endosperm, respectively (Mascarenhas, 1989). This fertilization process of Angiosperms has been comprehensively described (Berger et al., 2008; Hamamura et al., 2011; Mori et al., 2006; Sprunck et al., 2012).

Upon landing on the stigma, the pollen grain germinates a pollen tube at a very fast rate to reach the female gametophyte. Such an astoundingly fast cell elongation must require cell wall and membrane formation since pollen grains with a diameter of 20-100 micrometers (depending on the species) produce tubes from a few millimeters (the case of *Arabidopsis thaliana*) to several centimeters (the case of maize). This fast growth requires the deposition of galactolipids at the plasma membrane, an unusual place for these lipids otherwise contained in photosynthetic membranes of plants grown under normal conditions (Botte et al., 2011). Pollen tube growth is polarized and occurs at the tip of the pollen tubes, guided by attraction cues of female gametophytic origin that have been descried in maize (Márton et al., 2005) and in Torenia (Okuda et al., 2009). The lipid biogenesis and membrane homeostasis in growing pollen tubes is an overlooked process in reproductive development of flowering plants.

Whereas a wealth of information related to pollen grain formation (the early stage) and to fertilization (the late stage) has been published in the recent years, little research effort has been devoted to the metabolic biology of the elongating pollen tubes during their journey toward the ovules. Only a role for phosphoinositides (quantitatively minor glycerolipids acting as signaling compounds) has been studied in depth at the level of the pollen tip (Bloch et al., 2016). Phosphoinositides control the directional membrane trafficking required for delivery of

material to the growing tip, but nothing is known on the membrane lipid production required for the growth itself.

At my arrival in the host laboratory, the first observations on *Nicotiana tabacum* and *Arabidopsis thaliana* pollen tubes tended to show that the sterol biosynthetic pathway was truncated in this specific cell type. Then, my first working hypothesis was: if this truncated pathway was of biological meaning, it should be conserved among different species of flowering plants. In order to investigate this hypothesis, I worked on pollen grains and pollen tubes from ten angiosperm species distributed among a variety of families. This work, added to preliminary results in the team, led to the publication of an article in Lipids in 2015.

The preliminary work published in Lipids (2015) showed that cycloeucalenol was the major neosynthesized sterol in pollen tubes, suggesting a truncated pathway at the level of the cyclopropylsterol isomerase (CPI) enzyme. To carry further the investigation of this truncated pathway, I germinated pollen grains in presence of labelled glucose, to identify more precisely which sterols were neosynthesized as compared to the sporophytic pathway. The labelled sterols synthesized in the tubes from the incorporation of labelled glucose were identified by gas chromatography and mass spectrometry (GC-MS). In a subsequent step, I transformed *Nicotiana tabacum* plants with the CPI enzyme fused to a green fluorescent protein (GFP) under the control of the pollen specific promoter LAT52 from *Solanum lycopersicum* (Muschietti et al., 1994). The aim of this experiment was to (*i*) investigate if the sterol composition in the pollen tubes was modified in presence of a functional CPI enzyme, (*ii*) establish the sterol profile of such transformed tubes, and (*iii*) analyze the germination capacity of transformed pollen tubes. The pollen grains from these plants were germinated, and sterols from pollen tubes expressing the LAT52::CPI-GFP (LCG) transgene were identified by the fluorescence conferred by the expression of a functional CPI-GFP fusion.

As the pollen-specific sterol biosynthesis pathway was conserved among various species, a hypothesis was that pollen tubes with a different biosynthesis pathway could have a different capacity to propagate their genetic material to the offspring. Pollen from heterozygous LCG plants was used for crossings with wild type plants and self-fertilization. The LCG construct is linked to glufosinate resistance, thus the LCG progeny could be identified at an early stage when grown in petri plates on a synthetic medium in presence of glufosinate.

Materials and methods

I. Plant material

Pollen samples were collected from different plant speciess. *Nicotiana tabacum* L. (cv xanthi line SH6) is the genotype used in the laboratory (Schaller et al., 1998) and was used for plant transformation. *Nicotiana benthamiana* Domin was obtained from the IBMP horticultural favility. *Wigandia kunthii* Choisy was obtained from the Strasbourg Botanical Garden collection. *Lilium auratum* helvetia L. was bought as a flowering plant and *Papaver rhoeas* L. was grown from seeds collected in the fields close to Strasbourg.

II. Methods

1. Plant culture conditions in soil

Nicotiana tabacum and *Nicotiana benthamiana* plants were grown in soil (Surfinia, Havita) in 13cm diameter pots, in controlled conditions with 16h of light at 24°C and 8 hours of dark at 20°C under fluorescent light (4x Biolux T8, Osram). *Lilium auratum* helvetia L., *Papaver rhoeas* L., *Zea mays* L. were grown in soil (Surfinia, Havita) in a greenhouse with 16h day and 8h night. *Corylus mandshurica* Maxim. was sampled in the botanical garden of Strasbourg, and *Wigandia kunthii* Choisy was cultivated in a greenhouse of the botanical garden of Strasbourg.

2. Plant culture conditions *in vitro*

Nicotiana tabacum

In vitro cultivation of *Nicotiana tabacum* and *Nicotiana benthamiana* plantlets was made on MS growth medium (see II.2.), with 16h of light at 24°C and 8h of dark at 21°C, under 4x Biolux T8 (Osram). Seeds were surface sterilized in 25% bleach with 0,1% SDS (Sodium Dodecyl Sulfate, Euromedex) for 10 minutes, and washed three times with sterile water before sowing. For segregation analysis, 50 seeds were sown in petri plates. For agro-transformation of *Nicotiana tabacum*, leaf disks from *in vitro* grown plants were placed on petri plates, and plantlets obtained from callus were transferred into glass pots to grow before transplanting to soil. The generation of transformants was made with the help of Monique Schmitz (technician

in the laboratory) according to a classical protocol (Schaller et al., 1998) modified from Horsch et al. (1985).

3. Pollen tubes culture conditions

In vitro

Pollen grains were sampled from 1 to 5 flowers at stage 12 right after anthesis (Koltunow et al., 1990). For this, anthers were collected in a 2mL tube, then 1mL of liquid pollen tube growth medium was added. Samples were vortexed to release the pollen grains in the medium. Anthers were removed and pollen tubes were germinated under gentle shaking at 21-24°C for 2 to 24h depending on the experiment. For sterol extraction, pollen tubes were pelleted by centrifugation for 10 minutes at 3000rpm and lyophilized.

Composition of liquid pollen tube growth medium: H_3BO_3 1.62mM (Carlo Erba Analyticals), $Ca(NO_3)_2.4H_2O$ 2mM (Sigma Aldrich), $MgSO_4.7H_2O$ 0.8mM (Merck), KNO_3 1mM (Duchefa), glucose 54g.L^{-1} (Sigma), pH=5.9. Solid pollen tube growth medium: Add agar 4g.L^{-1} (Bio-Rad).

Semi *in vivo* germination of pollen tubes

The apical ends of elongating pollen tubes were collected in a semi *in vivo* experimental design. For this, emasculated flowers at stage 11 (Koltunow et al., 1990) were hand pollinated with given pollen samples. Flowers were kept closed and sampled 5h after pollination. Pistils were dissected by cutting the style off the top of the ovary and placed in a petri dish on solid pollen tube growth medium to be incubated in saturated humidity conditions in the IBMP *in vitro* culture room (16h light at 24°C, 8h dark at 21°C) until the pollen tubes reached the sectioned bottom of the styles and grow out of it.

4. Crossings

Crossings in *Nicotiana tabacum* were performed by emasculating before anthesis (stage 11) the flower taken as a female and pollinating by hand with fresh pollen grains taken from the plant

selected as male. Flowers were labelled in order to collect the seeds after full repining of the capsules.

5. Cloning of LAT52::CPI-GFP and LAT52::GFP constructs

LAT52::CPI-GFP and LA52::GFP constructs were cloned using the pBASTA (Compagnon et al., 2009) plasmid that carries a marker gene conferring glufosinate resistance to the transformed plants. pLAT52 is a pollen specific promoter cloned from *Solanum lycopersicum* gDNA by H. Schaller based on a published sequence (Twell et al., 1989; Muschietti et al., 1994). CPI cDNA sequence was cloned from *Arabidopsis thaliana*. Clonings were made from two plasmids already available in the laboratory (B. Grausem): one carrying pLAT52::CPI, the other carrying CPI-GFP fusion protein. The pLAT52::CPI plasmid was linearized by enzymatic digestion with BamHI and SpeI to remove the CPI insert, according to the FastDigest protocol (Thermo Scientific). The CPI-GFP cDNA insert was amplified by PCR to add BamHI restriction site at 5' end with primer BO2CV32 (5'- GGATCCATGTCAGGATC -3') and SpeI restriction site at 3' end with primer BO2BG66 (5'- GGACTAGTTTATTTGTATAGTTCATCCATGCC-3'). The GFP insert was amplified the same way to add BamHI (primer BO2CV31, 5'-GGATCCATGAGTAAAGGA-3') and SpeI (primer BO2BG66, 5'- GGACTAGTTTATTTGTATAGTT CATCCATGCC-3') restriction sites. The reaction mixture for PCR was composed of 4µL of GoTaq 5X Green Buffer (Promega), 2.4µL of $MgCl_2$ (25mM, Promega), 0.4µL of dNTP (10mM, Promega), 0.48µL of each primer (20µM, Integrated DNA Technologies), 0.24µL of GoTaq (Promega), water to 19µL and 1µL of template plasmid. The program used for amplification was as follows: 94°C/1.5min; 40x(94°C, 30s; 56°C, 1min; 72°C, 1,5min); 72°C 10min. The fragments obtained were purified on NucleoSpin Gel and PCR Clean Up columns (Macherey-Nagel) according to the proposed protocol, and digested with BamHI and SpeI using the FastDigest protocol (Thermo Scientific). Formated BamHI-CPI-GFP-SpeI and BamHI-GFP-SpeI fragments were individually ligated to the linearized pBASTA-LAT52 plasmid using Rapid DNA ligation kit (Thermo Scientific) according to the instructions. The constructs were checked by enzymatic digestion and PCR before sequencing.

6. Plant transformation with LAT52::CPI-GFP and LAT52::GFP constructs

Agrobacterium tumefaciens LBA4404 transformed with LAT52::CPI-GFP and LAT52-GFP constructs respectively were grown for one night at 28°C in liquid LB medium supplemented with kanamycin (50mg.mL^{-1}, Euromedex) and rifampicin (100mg.mL^{-1}, Sigma). Cells were pelleted by centrifugation at 3 000rpm for 10 minutes and washed three times with $MgSO_4$ 10mM (Fluka). Leaf disks from *in vitro* grown *Nicotiana tabacum* or *Nicotiana benthamiana* plants were prepared and placed in liquid medium for co-culture with the transformed *Agrobacterium* for 20 minutes to 2h. Leaf disks were then dried on a sterile paper and placed on solid medium containing ANA (0.1mg.mL^{-1}, Sigma) and BAP (1mg.mL^{-1}, Sigma Cell Culture). After three days of incubation, leaf disks were transferred to the same solid medium complemented with glufosinate (4mg.mL^{-1}, Sigma Aldrich) and cefotaxim (500mg.mL^{-1}, Duchefa Biochemie) to obtain callus and plantlets.

Composition of liquid medium for co-culture: Murashige & Skoog Medium M0221 (Duchefa Biochemie) 4.4g.L^{-1}, glucose 30g.L^{-1} (Sigma), myo-inositol 100mg.L^{-1} (Duchefa Biochemie), thiamine HCl 0.5mg.L^{-1} (Duchefa), pyridoxine HCl 0.5mg.L^{-1} (Duchefa), nicotinic acid 0.5mg.L^{-1} (Duchefa), glycine 2mg.L^{-1} (Duchefa), pH=5.7. For solid medium: Add agar 8g.L^{-1} (X).

7. DNA extraction

From plant material for PCR genotyping

DNA was extracted from leaf samples in 750µL of grinding buffer. Fresh leaves were ground with metal beads for 2 minutes on a Tissue Lyser (Quiagen) at 30hHz and incubated for 30 minutes at 65°C. Samples were extracted with 700µL of chloroform/isoamyl alcohol (24/1, v/v, Carlo Erba Reagents, Merck) and centrifuged for 5 minutes at 10000rpm, room temperature. Aqueous phase was collected and DNA was precipitated with 550µL of isopropanol (Carlo Erba Reagents) and centrifugation for 5 minutes at 10000rpm, room temperature. Pellets were washed with 70% ethanol (Sigma Aldrich) and dried at room temperature before resuspension in 20µL of sterile water.

8. Genotyping by PCR

Plants were genotyped by PCR using the following mix for one sample: 4µL of GoTaq 5X buffer (Promega), 2.4µL of $MgCl_2$ (25mM, Promega), 0.4µL of dNTP (10mM, Promega), 0.48µL of each primer (20µM, Integrated DNA Technologies), 0.24µL of GoTaq (Promega), water up to 19.5µL, and 0.5µL of DNA sample obtained as described. Primers used are the same as for the cloning. PCR amplification was performed in a thermocycler (Eppendorf Mastercycler) as described in **Table 21**, and samples were placed on a 1% agarose gel (Sigma Life Science) in TAEX1 with Sight DNA stain (Euromedex) for migration at 100V during 30 minutes.

Table 21. PCR cycle used for genotyping of *Nicotiana tabacum* transformants.

	Temperature		*Time*
Denaturation	94°C		1.5min
PCR Cycle	40x	94°C	30sec
		56°C	1min
		72°C	1.5min
Final elongation	72°C		10min
Hold	4°C		/

9. RNA extraction

Plant material was ground into liquid nitrogen before adding 1mL of Trizol (Molecular Research Center). Samples were incubated at room temperature for 4 minutes and centrifuged for 10 minutes at 13500rpm, 4°C. The supernatant was collected and added to 200µL of chloroform (Carlo Erba Reagents) for incubation at room temperature during 4 minutes. Aqueous phase was collected after centrifugation (10 minutes at 13500rpm, 4°C), mixed with 500µL isopropanol (Carlo Erba Reagents) and incubated at room temperature for 10 minutes. The RNA pellets were obtained after centrifugation for 10 minutes, 13500rpm, 4°C and washed with 70% ethanol (Sigma Aldrich) before resuspension in 10 to 50µL of water. Samples were stored at -20°C.

10. Reverse transcription

RNA samples were quantified on a NanoDrop 2000 (Thermo Scientific) and diluted to obtain a 1µg.µL^{-1} solution in water. DNA from 1µL of sample was digested with 2µL of DNAse (Thermo Scientific, diluted to 1/50) at 37°C for 15 minutes. On ice, 1µL of random primers (200ng.µL^{-1}, Promega), 1µL of dNTP (10mM, Promega) and 10µL of RNAse-free water were added. Samples were incubated at 65°C for 5 minutes, and put back at 4°C. Then, 4µL of RT buffer 5X (Invitrogen) and 1µL of reverse transcriptase (Super Script III, Invitrogen) were added to the samples, placed in a thermocycler for 10 minutes at 25°C, 30 minutes at 50°C and 5 minutes at 85°C to obtain cDNA samples.

11. qPCR analysis of sterol pathway genes expression in *Nicotiana tabacum* tissues

cDNA samples were filled up to 100µL with water. On a 96 wells plate, each sample was prepared as follows: 5µL of cDNA solution, 7.5µL of primer pool (1µM, Integrated DNA Technologies), 12.5µL of SYBR Green (Roche). The plate was sealed and centrifuged for 10 minutes at 3000rpm before reading on light cycler 480 (Roche) following the cycle : denaturation (95°C, 5min, 4.8°C/s), PCR 45 x (95°C, 10s, 4.8°C/s ; 60°C, 15s, 2.5°C/s ; 72°C, 15s, 4.8°C/s), melting curve (95°C, 5s, 4.8°C/s ; 55°C, 1min, 2.5°C/s ; 95°C, 0.11°C/s, 5 acquisitions/°C), cooling (40°C, 30s, 2.5°C/s). Primers used for each specific gene are listed in table **Table 22**.

Sterol pathway genes expression was analyzed in leaves, corolla, anthers and pollen tubes germinated *in vitro* from wild type (SH6), control (LAT52::GFP) and LCG plants. One biological sample was analyzed in technical triplicate for leaves, corolla and anthers, two biological replicates were analyzed in technical triplicate for pollen tubes.

Table 22. Primers used for qPCR analysis of gene expression in *Nicotiana tabacum*.

Target gene	Primer name	Primer sequence
AtCPI	ACPIF	CATTACTCTTCGGAGGCTACGC
	ACPIR	CCATGCAGCCTCAAAACACC
mGFP5	PGFPF	CCATGCCTGAGGGATACGTG
	PGFPR	TGTAGTTCCCGTCGTCCTTGAA
NtCAS1	NCASF	TGCAACTAATCGTCTTTCGTGGT

	NCASR	TCCCTCCCAACTAATGAAGGAAA
NtSMT1-1	NSMT11F	AGCTGCAGAAGGTCTTGTCG
	NSMT11R	GCTTGCGAACCACGAAGAAG
NtSMT1-2	NSMT12F	GTCTCCGCACTTGAATTCGT
	NSMT12R	GAAACCTTGAACCCTTTGACTACC
NtCPI	NCPI1F	CCCTAGCAAGAGATGGGGTGA
	NCPI1R	GAGCTTATACGGGACGACAACA
	NCPI2F	CGAGAATATTCAGTGGGCCTTC
	NCPI2R	TGGAAATAGCTAATGTCTCCAAATAAG
NtCYP51	NCYP1F	CCAGAAGTGTCGGCCCATTT
	NCYP1R	TGATAAACCTCTTGTTGACTGAGATCG
	NCYP2F	CAGATGCATAAAGGAAGTCCTGA
	NCYP2R	TGCGAACTACGTAGAAGCATTATCA
NtSMT2	NSMT2F	TGCGAGCTATCGCAGCTCAT
	NSMT2R	GGCCCGGTTTACTTGGTATTCA
NtSMT3	NSMT3F	CGAGAAAGAGAATGTCCAAGACAA
	NSMT3R	CGGCGGTTTCGATTTCTTT
Nt5DES1	NDES1F	TTCAGGGATGGCTCCGTAAC
	NDES1R	GCACCAGAGGAAACCGGAGA
Nt5DES2	NDES2F	TGGTTTTCTTTGGTGCTTCTACA
	NDES2R	TGAAGGGATGGCATCTTTAGGG
Nt Actin (Tob103)	NACTF	TCGACACACTGGCGTTATGG
	NACTR	GCTTCGTCACCCACATAGGC
	NACT2F	TCTTGCTGGCCGTGACCTAA
	NACT2R	TGGATCCTCCGATCCAGACA
Nt Elongation factor 1 alpha	NEF1F	CAACCCTGACAAGATCCCCTTT
	NEF1R	TCGAGCATGTTGTCACCTTCC
	NEF2F	CCCCTTTGTCCCCATCTCTG
	NEF2R	AGCAACAAACCCACGCTTGA

12. Confocal microscopy on pollen grains and pollen tubes

In vitro cultures of pollen tubes

Pollen tubes cultivated *in vitro* were observed on LSM780 confocal microscope (Zeiss) under white light and 488nm excitation laser to check for a GFP signal in the transformed LCG pollen tubes.

Semi *in vivo* cultures of pollen tubes

Pollen tubes cultivated in semi *in vivo* conditions were observed under an Axio Zoom V16 microscope (Zeiss) to visualize and measure the growth of pollen tubes coming out of the style.

Use of probes on *in vitro* pollen tubes

Two ratiometric lipid probes provided by Andrey Klymchenko (Laboratoire de biophotonique, UMR 7213, Faculté de Pharmacie, Université de Strasbourg) were used to specifically target the outer leaflet of cell membranes (Nile Red, **NR**12S, Darwich et al., 2012) or the plasma membrane and the intracellular membranes (Push-pull pyrene, **PA**, Niko et al., 2016). Pollen tubes were grown for 4 hours as previously described before treatment with probes. For each sample, 4µL of probe (20µM) were diluted in 200µL of liquid medium, before adding 200µL of pollen tubes culture. Samples were homogenised by inverting the tubes and few microliters were placed on a glass slide with a coverslip. The laser used for excitation was set on 488nm for NR probe and GFP track, and 405nm for PA probe. For NR probe, fluorescence was observed at two spectral ranges, 553-597nm (green channel) and 600-705nm (red channel), and GFP was observed at 500-540nm. For PA probe, spectral ranges used were 450-550nm (blue channel) and 555-700nm (red channel), together with GFP channel set at 500-550nm. For the two probes, transmitted light was also recorded from 410 to 695nm.

Images were processed with ImageJ, using a macro provided by Andrey Klymchenko, to generate a ratiometric image from the division of the images from the green channel by the red channel for NR and images from the red channel by the blue channel for PA. A color scale indicates the ratio obtained.

13. Extraction of total sterols, sterol esters, fatty acids from plant tissues

Total extracts from pollen tubes

Lyophilised pollen tubes were saponified in 12.5mL of 6% KOH in methanol (Carlo Erba) at 75°C for 2h under hot air stream. After addition of water to 15mL total volume, samples were extracted 3 times with 15mL *n*-hexane (Roth). The hexane phase was evaporated, and acetylation was performed on the dried residue with 50µL of toluene (Carlo Erba), 30µL of acetic anhydride (Fluka) and 20µL of pyridine (Fluka) in a glass vial at 70%C for 30 minutes. The extracts were spiked with lupenyl-3,28-diacetate (20µg, Sigma) as a standard for chromatography, and resuspended in 300µl of *n*-hexane.

Sterol fractions from pollen grains

Pollen grain samples were collected in 2ml tubes and saponified with 0.5ml of 6% KOH in methanol (Carlo Erba) at 75°C for 2h. After addition of 0.5 volume of water, the unsaponifiable compounds were extracted with 3 volumes of *n*-hexane (Roth). The dried residue was then subjected to an acetylation reaction in 50µl of toluene (Carlo Erba) with 30µl of acetic anhydride (Fluka) and 20µl of pyridine (Fluka) in a glass vial with a PFTE screw cap, at 70%C for 30 minutes. The reagents were dried under a hot air stream. The extracts were spiked with lupenyl-3,28-diacetate (20µg, Sigma) as a standard for chromatography, and the total was resuspended in 300µl of n-hexane. The isolation of free sterols and steryl esters from a dichloromethane/methanol (2/1, v/v) extract of a given sample was carried out by TLC (20x20cm, silica gel, 60 F_{254}, Merck) using dichloromethane (Sigma Aldrich) as developing solvent. Desmethyl sterols, 4α-methyl sterols and 4,4-dimethyl sterols were scraped off the plate to form one free sterol fraction. Steryl esters were scraped off the plate, saponified and treated as above.

14. Sterol analysis by gas chromatography and mass spectrometry (GC-MS)

Plant extracts were analyzed by gas chromatography (GC instrument, Agilent 6890) and mass spectrometry (MS analyzer, Agilent 5973) to identify the different sterol species in their composition. A HP-5MS column (5% PhenylMethyl Siloxane, 30mx250µmx0.25µm, Agilent J&W) was used, on which 2µL of sample were injected and transported with a helium flux of 1mL.min^{-1}. The column temperature was hold at 60°C for 1min, heated to 200°C at 30°C.min^{-}

[1] before reaching a maximum of 300°C at 2°C.min^{-1}, for a total run time of 56,33min per sample. The separated molecules were ionized by electronic impact at 70eV. The identification of each species was made by the detection of specific daughter ions obtained after ionization.

15. Bioinformatic analysis of publicly available datasets

Sterol pathway genes orthologs

Orthologs of *Arabidopsis thaliana* sterol pathway genes were searched for in the OrthoMCL database (http://orthomcl.org) based on the EC (Enzyme Commission) number obtained from UniProt database (http://www.uniprot.org/) for each gene. Data thus obtained were checked and completed using PicoPlaza database (http://bioinformatics.psb.ugent.be /plaza/versions/pico-plaza/). Terpene synthases could not be identified separately in orthologs databases. For the organisms of interest, protein sequences were compared to *Arabidopsis thaliana* sequences using BLASTP (NCBI). Specific databases were used to obtain the sequences from organisms of interest (AlcoDB, http://alcodb.jp).

Specific expression of cyloeucalenol cycloisomerase (CPI) gene

Publicly available data were used to analyse gene expression profiles in dry pollen and pollen tubes grown for different times in different conditions, in comparison to sporophytic tissues (leaves and root hairs). The Gene Expression Omnibus (NCBI) provided two sets of data, GSE17343 for pollen tissues in *Arabidopsis thaliana* and GSE38486 for sporophytic tissues. A heatmap was generated from these data using GenePattern (Broad Institute).

Results

A simplified plant sterol biosynthesis pathway is presented **Figure 63**. Sterols are derived from C_5 isoprene units produced *via* the mevalonate pathway from acetyl-CoA. Six units are condensed to form squalene, which is further oxidized in squalene oxide, later cyclized in cycloartenol, the 9β,19-cyclopropylsterol committed precursor of plant sterols. Several methylation, desaturation, reduction and demethylation enzymatic steps are necessary for the production of the three major end products found in sporophytes: campesterol, sitosterol and stigmasterol. As to pollen, the working hypothesis that supports the sets of experiments presented here is the presence of a biosynthetic pathway that is truncated at the level of the CPI enzyme.

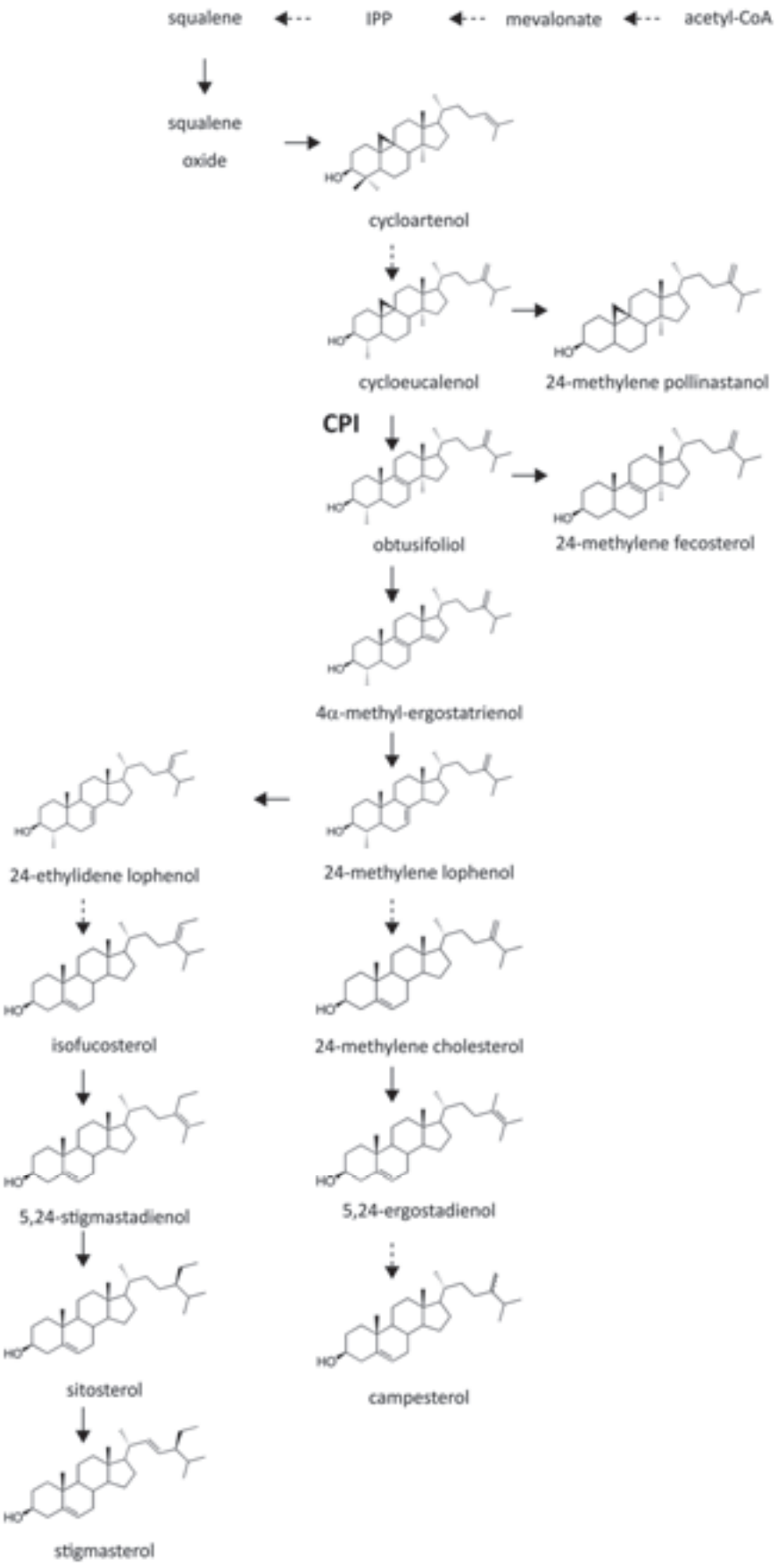

Figure 63. Simplified plant sterol biosynthetic pathway. CPI: cyclopropylsterol isomerase. Full arrows indicate single steps, dashed arrows indicate multiple steps. Adapted from Caroline Mercier, 2016.

As mentioned in the general introduction, the CPI enzyme is necessary for the normal development of plants including *Arabidopsis thaliana* plants. Indeed, *cpi1-1 Arabidopsis thaliana* mutants cultivated *in vitro* show an extreme dwarf phenotype (**Figure 64, b**) and do not develop correctly to complete the plant life cycle. To investigate the involvement of CPI enzyme in pollen tubes, the sterol profile of *in vitro* germinating pollen tubes was determined by gas chromatography and mass spectrometry (GC-MS). Fresh pollen was collected from *Nicotiana tabacum* flowers at anthesis (**Figure 64, a**) and germinated in a synthetic liquid medium (**Figure 64, d**). In order to identify the compounds that are neo-synthesized in the pollen tubes during their growth, ^{13}C labelled glucose was added to the germination medium. After extraction, sterols were identified and the enrichment factor was calculated for each sterol (**Figure 64, c**). As a control, the same experiment was done with MM2 *Arabidopsis thaliana* cells, which exhibit a sporophytic sterol biosynthesis. In wild type pollen tubes, cycloartenol and cycloeucalenol are synthesized from carbon precursors provided by glycolysis, which is shown by an increase of the calculated isotopic enrichment factor to approximately 25% when pollen tubes were cultivated with ^{13}C labelled glucose. The enrichment factor obtained for the samples cultivated with ^{12}C glucose is in agreement with the natural abundance of ^{13}C glucose. In 24-methylene cholesterol and sitosterol, no difference was found in the isotopic enrichment when comparing pollen tubes cultivated in the presence of ^{12}C and ^{13}C glucose. In MM2 cells, all sterols considered had an isotopic enrichment factor varying from approximately 8% to 13% in the presence of ^{13}C labelled glucose in the medium.

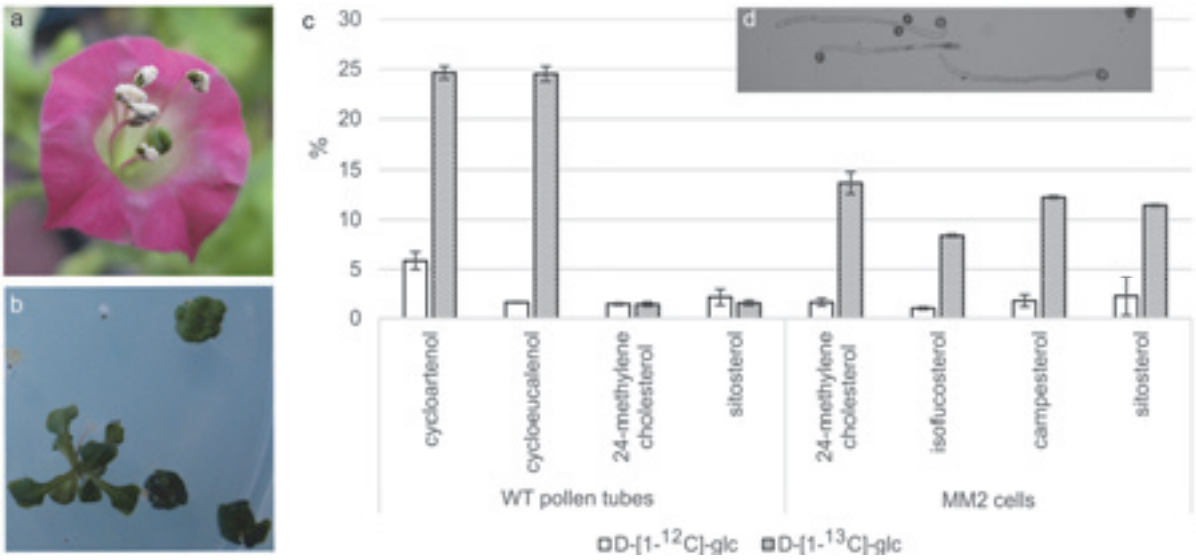

Figure 64. Sterol biosynthesis in the pollen tube. (**a**), picture of a flower of *Nicotiana tabacum* at anthesis, from the top. Anthers are opened, releasing the pollen grains. (**b**), picture of WT (left) and *cpi* mutants of *Arabidopsis thaliana* seedlings cultivated on synthetic medium. (**c**), isotopic enrichment (%) in cyclopropylsterols and sterols from WT pollen tubes and MM2 *Arabidopsis* cells in biological triplicates. (**d**), picture of germinating pollen tubes of *Nicotiana tabacum*. Isotopic enrichment in fatty acids is given in **Suppl. Figure 23**. Isotopic enrichment in cyclopropylsterols and sterols from other species is given in **Suppl. Figure 22**. Mass spectra and isotopic enrichment calculation are given in **Suppl. Figure 21**.

In the previous experiment, samples of *in vitro* germinating pollen tubes were composed of pollen tubes, but also pollen grains. In order to avoid the presence of pollen grains, and to get closer to physiological conditions, pollen tubes were germinated in semi *in vivo* conditions. Flowers of *Nicotiana tabacum* were selected before anthesis, at stage 12 defined by Koltunow et al. (1990), and dissected to remove the anthers. Fresh pollen of the plant of interest was applied on the stigma, and flowers were closed. A longitudinal view of an entire flower is given in **Figure 65, a**. After several hours of incubation on the plant, flowers were removed and styles were placed on solidified pollen tube germinating medium. After germinating through the transmitting tract, pollen tubes were able to continue their growth on the solid medium (**Figure 65, b**) and were collected. Lipids were extracted from these samples; GC-MS analysis of the extracts enabled to identify the sterols that were specific of the pollen tubes. In wild type pollen tubes (**Figure 65, c**), cycloeucalenol (2) and its C_4 demethylated metabolite 24-methylene pollinastanol (1) were identified. In pollen tubes expressing the CPI-GFP enzyme (**Figure 65, d**), obtusifoliol (4) and its C_4 demethylated metabolite 5,24 methylene-fecosterol (3) were identified.

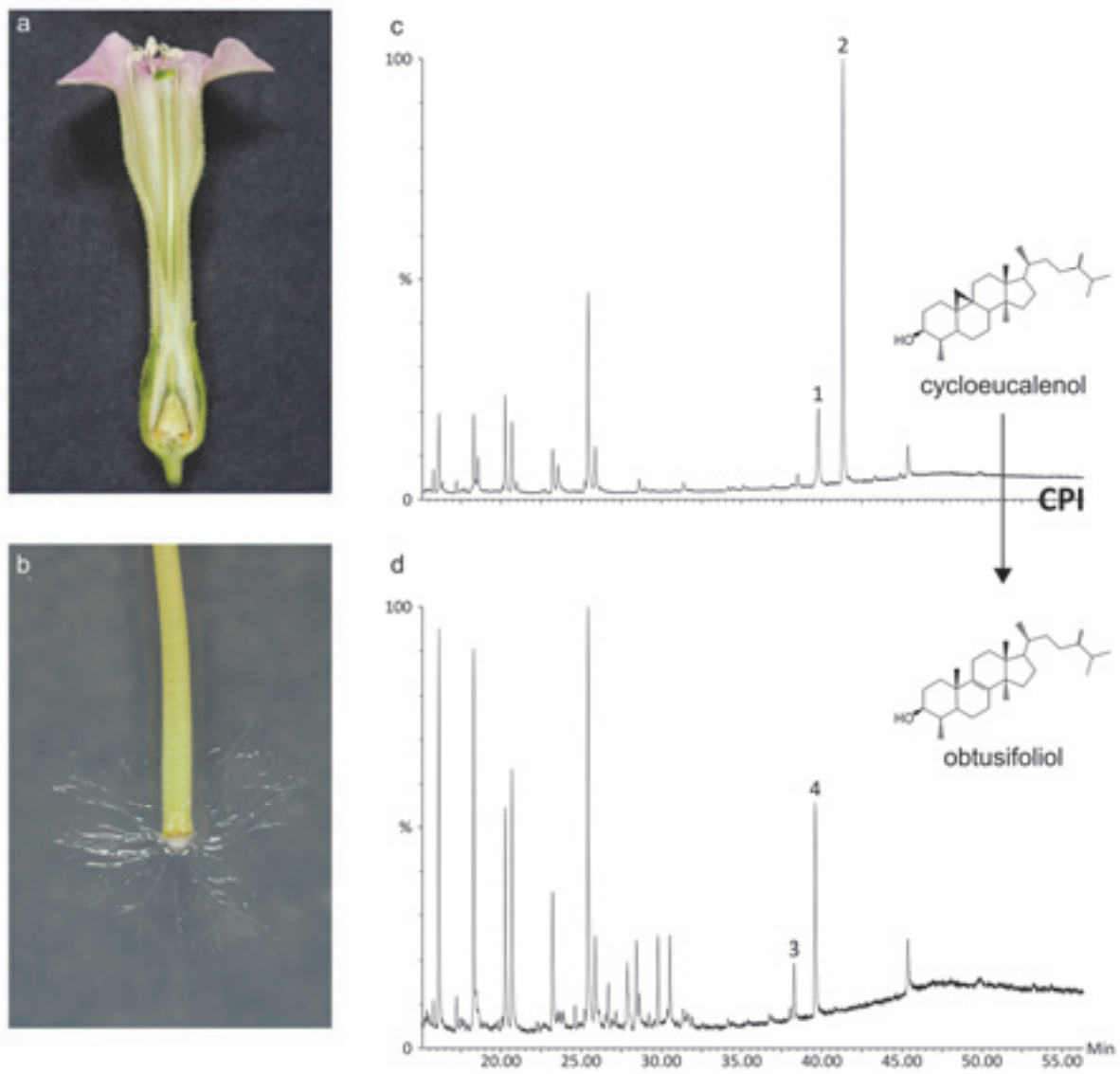

Figure 65. Pollen specific expression of CPI. (**a**), longitudinal section of a *Nicotiana tabacum* flower at anthesis; (**b**), picture of pollen tubes coming out of the style after semi *in vivo* cultivation. Sterol profile of WT (**c**) and LCG (**d**) pollen tubes cultivated semi *in vivo*. 1, 24-methylene pollinastanol; 2, cycloeucalenol; 3, 5,24 methylene-fecosterol; 4, obtusifoliol. Mass spectra are given in **Suppl. Figure 24**.

The growth of pollen tubes carrying the CPI-GFP transgene was compared to the growth of wild type pollen tubes in semi *in vivo* conditions. Plants transformed with a LAT52::GFP transgene served as a control. Pollen from heterozygous plants (*gfp*/+) was applied on the stigma of wild type flower. Fresh pollen was applied on the stigma of wild type flowers, and pollen tubes were observed when growing out of the stigma after germinating through the transmitting tract (**Figure 66**). To help the observation, the last row of this figure **Figure 66** shows as a white line the extent of the growth of non-GFP pollen tubes, and as a green line the extent of the growth of GFP pollen tubes. Wild type and control LG pollen tubes show a similar

growth. For LG control line, the maximum growth of GFP and non-GFP pollen tubes was the same. For LCG line, the GFP pollen tubes carrying a CPI enzyme showed a shorter length compared to non-GFP pollen tubes which do not carry the CPI enzyme.

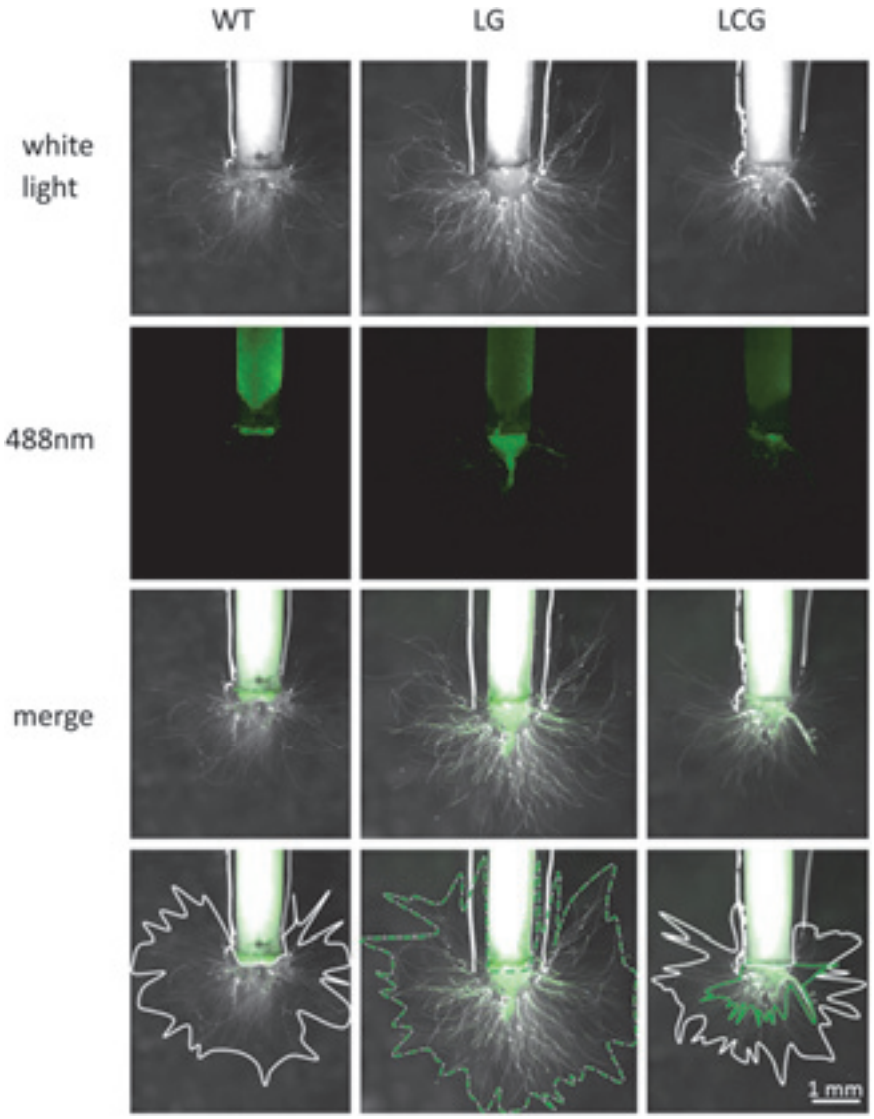

Figure 66. Semi *in vivo* analysis of pollen tube growth in the transmitting tract. Pollen grains from wild type (WT), LAT52::GFP (LG) and LAT52::CPI-GFP (LCG) were placed on the stigma of wild type emasculated flowers. Styles were collected and incubated on a pollen tube growth medium. White and green lines represent the growth extent of non-GFP and GFP pollen tubes, respectively. Adapted from Caroline Mercier, 2016.

The LAT52::CPI-GFP transgene carries as a T-DNA construct a marker gene that confers glufosinate resistance (p35S::BASTA) to sphorophytic tissues (for example, seedlings). In order to see if a bias in the transmission of this marker gene to the progeny of the crosses described above is observable, I have germinated seeds obtained from another series of crosses in which LCG pollen from homozygous (*gfp/gfp*) or heterozygous (*gfp/+*) plants of 3 distinct

lines (LCG8, LCG9, LCG25) was deposited on wild type styles. Seeds obtained from these crossings were cultivated in petri plates in presence of glufosinate, and the resistant and sensitive plantlets were counted to define the segregation pattern (**Table 23**). When pollen from homozygous plants was used, all the plantlets were resistant to glufosinate. When pollen from heterozygous plants was used, many sensitive plantlets were accounted for. The experiment was made twice for each line and gave different results, with segregation patterns ranging from 1:1 to 1:3 resistant to sensitive ratios.

Table 23. Effect of the CPI-GFP transgene on the segregation of the resistance to glufosinate character. χ^2 value was set at 3.84. Adapted from Caroline Mercier, 2016.

pollen genotype	resistant plantlets	sensitive plantlets	non-germinated seeds	total	χ^2	segregation hypothesis
WT	0	99	1	100	-	-
LCG8 (*gfp/gfp*)	96	0	4	100	-	-
	71	4	25	100	-	-
LCG8 (*gfp/*+)	31	63	6	100	0.01	1:2
	42	56	2	100	2.00	1:1
LCG9 (*gfp/gfp*)	99	0	1	100	-	-
	95	0	5	100	-	-
LCG9 (*gfp/*+)	26	69	5	100	0.28	1:3
	39	56	5	100	2.55	1:2
LCG25 (*gfp/gfp*)	90	2	8	100	-	-
	99	0	1	100	-	-
LCG25 (*gfp/*+)	46	51	3	100	0.26	1:1
	37	58	5	100	1.35	1:2

These results indicate that pollen tubes are able to germinate and achieve fertilization whether they have cycloeucalenol or obtusifoliol in their sterol profile. However, tubes bearing obtusifoliol exhibited a slower rate of germination, possibly indicative of modified membrane properties. In a first attempt to characterize the lipid order in the membranes of germinating pollen tubes, ratiometric probes were used, in collaboration with Andrey Klymchenko (laboratoire de biophotonique, UMR 7213, Faculté de Pharmacie, Université de Strasbourg). Preliminary results were obtained in the case of wild type pollen tubes and showed that those probes are compatible with the survival and growth of pollen tubes *in vitro*. Nile Red (**Figure 67, a**) probe targets the outer leaflet of cell membranes, and push-pull pyrene probe (**Figure 67, b**) targets the intracellular membranes. Further experiments are to be performed to conclude on this subject.

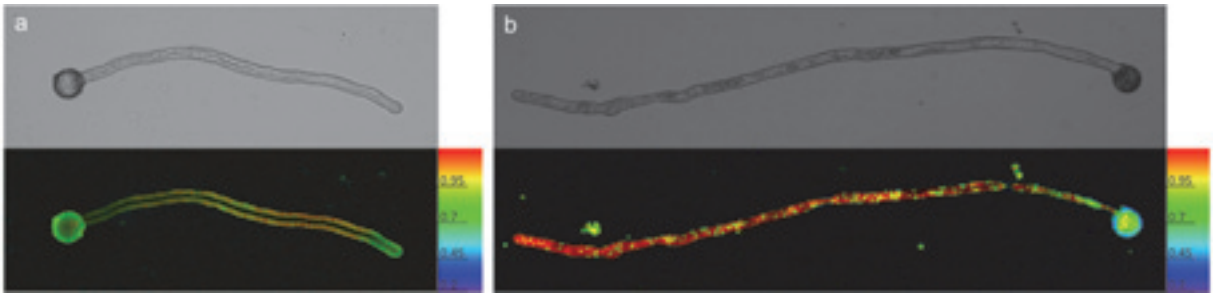

Figure 67. Use of ratiometric probes on wild type pollen tubes of *Nicotiana tabacum* cultivated *in vitro*. (**a**) Nile Red probe (Darwich et al., 2012) targets the outer leaflet of cell membranes; (**b**), Push-pull pyrene probe (Niko et al., 2016) targets the intracellular membranes.

Discussion

In pollen tubes, I have shown that cycloartenol and cycloeucalenol, two 9β,19-cyclopropylsterols, are neosynthesized. This experiment demonstrates that the sterol pathway in the male gametophyte is in fact a cyclopropylsterol pathway, since no further enzymatic conversion of cycloeucalenol is detected. This holds true for other species (see **Suppl. Figure 22**). Based on the semi *in vivo* pollen tube germination experiment, it was clear that downstream metabolites of cycloeucalenol, such as small amounts of sitosterol identified in sterol extracts of pollen grains germinated *in vitro*, are of maternal origin and are part of the pollen grains. In fact, these compounds are not found in sterol extracts from pollen tubes grown semi *in vivo*. Indeed, this culture system grants access to the apical part of pollen tubes only. This kind of sampling is certainly much more difficult and time-consuming than the *in vitro* germination of pollen grains, but should be absolutely preferred in further work. Indeed, this is physiologically relevant.

When transforming *Nicotiana tabacum* plants with a LAT52::CPI-GFP transgene, the CPI enzyme is catalyzing the conversion of cycloeucalenol into obtusifoliol in the growing pollen tubes. This change in the sterol biosynthesis still allows the pollen tubes to grow, as they are able to germinate through the transmitting tract semi *in vivo* and also to achieve fertilization. However, pollen tubes carrying a CPI enzyme and showing fluorescence seem to be shorter. This would mean that the production of obtusifoliol in the pollen tubes is not in favor of their rapid growth. A 1:1 ratio of resistant to sensitive seedlings is expected in the segregation of the herbicide marker gene in the progeny of wild type plants fertilized by LAT52::CPI-GFP *gfp*/+ pollen. As a bias in the favor of more sensitive plantlets is observed, the modified composition of the pollen tubes seems to be a handicap for the delivery of the sperm cells to the female gametophyte. This would explain that a cyclopropylsterol pathway was selected and conserved among Angiosperms. This cyclopropylsterol pathway in the male gametophyte appears as a truncated sporophytic pathway. Such a specific sterol pathway is therefore optimal for pollen tube growth. The impact of a modified sterol content of pollen tubes membranes will be investigated further with the use of ratiometric lipid probes.

Concluding remarks

This work led to the isolation of precious novel plant lines for a further characterization with the aim of dissecting biological processes such as isoprenoid homeostasis and brassinosteroid signaling.

Twelve *Arabidopsis thaliana* suppressor lines in the *hmg1-1* genetic background have been brought to a F2BC1 generation, sampled as bulks of suppressor and non-suppressor individuals, and sequenced by Illumina technology. This work allowed a collaboration with Sylvain Darnet (Laboratório de Biotecnologia Vegetal, Instituto de Ciências Biológicas, Universidade Federal do Pará (UFPA), Belém, Brazil) and I could be trained to the bioinformatics process for the analysis of whole genome datasets. Six *Arabidopsis thaliana* suppressor lines in the *chs5* genetic background were brought to a F2BC2 generation, and two lines were sequenced. This resulted in a first set of candidate mutations for the suppression of the chlorotic phenotype of *chs5* parental line. The four lines remaining have been sampled and will be sequenced (IGBMC sequencing platform, Illkirch, France) for genotyping according to a bulk segregant analysis.
Genetic screens in *Arabidopsis thaliana* represent a powerful tool to unveil and characterize mutants and genes of interest (Page and Grossniklaus, 2002). Genomic resources for *Arabidopsis thaliana* are massively available, as for instance the full genome sequence frequently updated: the current version known as TAIR10 (https://www.*Arabidopsis*.org/) has a size of 135Mbp of DNA that constitutes 5 chromosomes of the most documented model plants. Thus, next generation sequencing supported by mapping on a reference genome is accessible. User guides and analytic pipelines have been developed over the last years (Zuryn et al., 2010; James et al., 2013; Allen et al., 2013) and can be easily handled from platforms such as Galaxy (https://usegalaxy.org/), The frequency of mutations (especially SNPs) of interest in large sequence datasets is based on the segregation pattern of a trait of interest in recombinant populations (as an example, Pacurar et al., 2014). Then, a functional *in silico* analysis of genes identified by their alleles that carry the mutations of interest can be performed: gene expression pattern in plant tissues (http://bar.utoronto.ca/), co-expression of sets of genes (http://atted.jp/), or protein domain analysis (http://uniprot.org/).
In a very near future, the *hmg1-1* and *chs5* suppressor mutations tentatively identified by the Next-Generation-Sequencing strategy will be confirmed as causative mutations provided they strictly co-segregate with the suppressor phenotypes in succeeding recombinant generations (*ie* two additional backcrosses will be done, and the effect of the selected mutations introduced in different genetic backgrounds will be monitored. Alternatively, emerging tools like the

CRISPR-Cas9 genome editing technique can be used to specifically induce a given mutation in parental lines, and check if the suppressor phenotype is conferred by this mutation.

I have taken up the challenge of barley cultivation and genetics, since eight lines characterized by an "overgrowth" or "early maturity" phenotype could be selected then analyzed as recombinant populations. The analysis of their hormone content in leaves will be further developed, and a metabolomic approach could be designed to hunt down differences between the mutant and the parental lines. The identification of early maturity phenotypes during the screening was not expected but should certainly be of interest as this trait could be useful in agriculture. *Hordeum vulgare* is widely cultivated across the different regions of the world, therefore a great diversity of mutants is available. Most of these mutants or cultivar have been morphologically and genetically characterized and carefully maintained in repositories. A great effort was made to obtain mutant alleles in nearly isogenic lines in the cultivar Bowman background to help comparing mutants of interest (Mascher et al., 2014; Druka et al., 2011), providing precious genetic material. Until recently, the development of genomics on barley was difficult due to the large size of the genome and the presence of repetitive DNA sequences. The lack of genomic resources did not allow the fast and easy breeding of crops with improved characteristics, relying solely on laborious map-based cloning (Feuillet et al., 2012). Recently, the genome of the cultivar Morex has been sequenced and almost fully assembled, with a size of approximately 5.1Gbp in 7 chromosomes (Mayer et al., 2012). This genome is a precious tool to accelerate fundamental research and breeding processes, allowing structural and functional studies of genes of interest. The availability of the genome sequence allows the use of bioinformatics tools and emerging techniques as mapping-by-sequencing (Mascher et al., 2014), which requires a reference genome. This technique can be implemented using a recombinant F2 population (after backcrossing a mutant of interest with the parental line) for the analysis of the distribution of allele frequencies in phenotypic bulks. As barley genome is one of the largest diploid genomes sequenced, exome capture is rather developed (Mascher et al., 2013). This technique targets mRNA-coding exomes, and reduces the genome complexity (50-fold), and consequently the sequencing and data analysis efforts. These tools now allow a faster and easier identification of genes of interest, for fundamental research and breeding purposes, to obtain new varieties with selected traits. This will be considered in further studies with the valuable *ert-ii.79/bri1* suppressors in the BW312 background.

Genetic screens designed to ultimately find out novel genes acting on metabolic pathways were of paramount interest in this thesis work. The functional analysis of a specific biosynthetic pathway, namely, sterol biosynthesis, was also of very high value. The work carried out on sterol profiles pollen grains and germinating pollen tubes aimed at investigating the *raison d'être* of the specific biosynthetic detour occurring in the plant sterol pathway. The identification of 9β,19-cyclopropylsterols as end products accumulated in elongating pollen tubes established a gametophytic truncated, compared to the sporophytic pathway, never described so far. This feature was conserved among Angiosperm species, and should confer an advantage in the capability of the pollen tubes to transmit the genetic material to the progeny. The mandatory neosynthesis of 9β,19-cyclopropylsterols in pollen tubes explains the biosynthetic detour through these cyclopropanic intermediates that plants take to produce their sterols, whereas other organisms (fungi, mammals) do not. Tools available for the identification of metabolites by mass spectrometry are in constant evolution, allowing a precise identification of the products of interest. The recent development of mass spectrometry imaging could allow the localization of compounds of interest in biological objects, providing valuable functional informations. This could possibly apply to refining the sterol distribution in pollen tubes, together with other lipids.

Summary of the thesis work (in French).

Introduction générale

Les isoprénoïdes sont retrouvés dans la diversité du monde vivant, depuis les bactéries jusqu'aux animaux en passant par les champignons, algues et plantes. Ils ont des fonctions en tant que produits de fin de chaine biosynthétique, comme les stérols dans les membranes (cholestérol, phytostérols, ergostérol…), ou les hormones (oestradiol, brassinostéroïdes, ecdysone). Quelques-uns de ces produits de fin de chaine peuvent également pour partie servir comme précurseurs pour la synthèse de composés oxydés issus du métabolisme appelé « secondaire ». Par exemple, le cholestérol abondant dans les solanacées, sert de précurseur pour la biosynthèse d'alcaloïdes comme la solanine.

Mon projet a porté sur les isoprénoïdes de plantes, dont la structure et la nomenclature sont décrits par l'IUPAC (Union of Pure and Applied Chemistry). Tous les isoprénoïdes ont comme élément de base à leur structure une unité à 5 atomes de carbone, et dérivent de l'isopentenyl diphosphate (IPP) et de son isomère le dimethyllalyl diphosphate (DMAPP). Selon le nombre de carbones composant le squelette des différents isoprénoïdes, ils sont classés en différentes familles : monoterpenes (C_{10}), diterpenes (C_{20}), sesterterpenes (C_{25}) triterpenes (C_{30}), tetraterpenes (C_{40}) ou polyterpenes pour les molécules à plus de 40 atomes de carbone.

Les isoprénoïdes de plantes jouent un rôle dans les interactions plante-environnement, l'attraction des pollinisateurs ou dans la protection contre les herbivores et pathogènes. Ces fonctions ont été valorisées par l'homme en cosmétique (parfums), pharmacie (molécules actives) ou dans l'industrie (caoutchouc). Au sein de la plante elle-même, les isoprénoïdes sont par exemple des constituants membranaires (stérols), qui s'intercalent dans la bicouche phospholipidique pour la maintenir dans un état de fluidité optimal. Ils s'insèrent entre les phospholipides, avec le groupement hydroxyle face à l'environnement hydrophile et la chaine latérale à l'intérieur de la structure hydrophobe. Ils aident ainsi à ordonner les membranes.
La structure des stérols se compose de 4 cycles (A, B, C, D), portant un groupement hydroxyle sur le carbone 3, et une chaine latérale sur le carbone 17. La numérotation des carbones est définie par l'IUPAC.

Beaucoup d'organismes présentent un produit de fin de chaine unique dans la voie de biosynthèse des stérols. Chez les plantes, un mélange de différents stérols de fin chaine est retrouvé, dont la composition varie selon les espèces. Les stérols majoritaires retrouvés dans toutes les espèces sont le campesterol, le sitosterol et le stigmasterol.

Le campestérol peut en partie être utilisé comme précurseur pour la production d'hormones végétales, les brassinostéroïdes. D'autres hormones végétales font partie de la famille des isoprénoïdes, ce sont les gibbérellines et l'acide abscissique. Ces hormones sont impliquées dans la croissance et le développement des plantes pour les premières, et dans la tolérance aux stress pour la dernière. Des plantes affectées dans la synthèse ou la signalisation de brassinostéroïdes présentent des phénotypes nains ou semi-nains.

D'autres isoprénoïdes importants sont les composés de la machinerie photosynthétique : les chlorophylles et caroténoïdes. Ces molécules sont impliquées dans l'absorption de la lumière solaire dans les photosystèmes, et dans la protection des plantes contre les rayonnements et la formation nocive d'espèces réactives de l'oxygène pendant la photosynthèse.

Cette diversité de composés est obtenue *via* deux voies de biosynthèse distinctes. La voie du mévalonate (MVA) se déroule dans le cytoplasme, tandis que la voie du méthylérythritol phosphate (MEP) a lieu dans les plastes. Cette particularité n'est retrouvée que dans les plantes. Les gènes et enzymes impliquées dans la biosynthèse d'isoprénoïdes par ces deux voies sont connus et ont été décrits. Cependant, les éléments concernant la régulation de l'homéostasie des isoprénoïdes sont encore manquants. C'est dans ce contexte que se place mon travail. Afin d'étudier ces mécanismes de régulation sans cibler un gène ou une voie de biosynthèse en particulier, j'ai réalisé des criblages de suppresseurs de défaut de croissance chez deux lignées d'*Arabidopsis thaliana* affectées dans la synthèse d'isoprénoïdes, et une lignée d'orge (*Hordeum vulgare*) affectée dans la signalisation des hormones brassinostéroïdes.
Par ailleurs, je me suis concentrée sur l'étude du type cellulaire particulier qu'est le grain de pollen ou gamétophyte mâle, dans lequel la voie de biosynthèse des stérols est originale. En effet, elle ne met pas en jeu les produits de fin de chaine observés dans les tissus sporophytiques, mais semble tronquée. J'ai vérifié cette hypothèse dans plusieurs espèces végétales, et entrepris de caractériser cette particularité métabolique plus précisément par l'utilisation d'un précurseur

marqué (^{13}C-glucose) dans le milieu de culture de tubes polliniques en germination. Le but de cette démarche est de comprendre l'implication d'une voie de biosynthèse de stérols tronquée dans la germination des tubes polliniques, caractérisée par une croissance rapide et polarisée. Pour ce faire, j'ai utilisé une approche génétique et métabolomique.

Démarche expérimentale

Chez *Arabidopsis thaliana*, j'ai réalisé les criblages génétiques de suppresseurs de défaut de croissance après mutagenèse de deux fonds génétiques particuliers. Le premier, le mutant *hmg1-1*, est porteur d'un T-DNA inséré dans le gène codant pour l'enzyme HMG-CoA reductase (HMGR1), responsable de la production de mévalonate dans le cytoplasme. Cela engendre un défaut de synthèse d'isoprénoïdes via la voie du MVA confère aux plantes une taille réduite et une stérilité partielle. Le mutant *chs5* est porteur d'un allèle faible récessif codant une isoforme de la deoxy xylulose 5-phosphate synthase (DXS1), ce qui ralentit le développement des plantes et leur donne un phénotype de chlorose foliaire. Ce phénotype est conditionnel, s'exprimant principalement dans les tissus jeunes et à des températures inférieures à 18°C. La lignée BW312 dans *Hordeum vulgare* présente une mutation ponctuelle dans le gène codant pour le récepteur de brassinostéroïdes *BRI1*. Ce mutant présente une réponse aux brassinostéroïdes altérées et un phénotype semi-nain en comparaison de plantes sauvages.

Les graines des lignées parentales ont été traitées à l'EMS pour *Arabidopsis thaliana* et à l'azide de sodium pour *Hordeum vulgare*, dans le but de générer des mutations aléatoires sur tout le génome. Les graines ainsi mutagénisées ont été semées et ont composé la génération M1 de plantes, autofécondées pour constituer des populations M2. Le criblage de suppresseurs a consisté à chercher dans ces populations des plants présentant une croissance restaurée. Les individus suppresseurs ont été identifiés visuellement en comparant leur phénotype aux contrôles parentaux et sauvages semés dans les mêmes conditions. Pour *hmg1-1*, la grande taille des plantes et le remplissage des siliques, critère indiquant une restauration de la fertilité, ont été recherchés. Pour *chs5*, un développement normal et un reverdissement des feuilles ont été ciblés, le criblage a été réalisé en conditions *in vitro* et à température fraiche. Chez l'orge, une restauration de la taille des plantes a été recherchée. Lors de ce criblage, un phénotype de maturité précoce a également pu être observé et a été sélectionné. Les plantes candidates sélectionnées en M2 ont été autofécondées afin de valider les phénotypes en génération M3.

Douze individus suppresseurs du phénotype *hmg1-1* ont été sélectionnés après validation du phénotype en M3. A chaque étape, la présence du T-DNA dans le gène *HMG1* a été vérifiée afin de confirmer le fond génétique des individus sélectionnés. Les plantes sélectionnées ont été croisées avec la lignée parentale, afin d'éliminer (par backcross successifs) une partie des mutations générées par le traitement EMS mais ne causant pas le phénotype suppresseur. Les graines issues du croisement ont permis de générer des plantes F1, autofécondées pour obtenir des populations F2 dans lesquelles les phénotypes suppresseur et non-suppresseur ségrégent. Les phénotypes ont été caractérisés précisément par la mesure de la taille totale des plantes, du nombre et du poids des siliques de la hampe principale, sur 20 à 50 individus de chaque catégorie phénotypique par lignée sélectionnée. L'expression des gènes de la voie du MVA et de la voie du MEP dans les individus suppresseurs a été analysée par qPCR, et le contenu en stérols a été évalué par chromatographie gazeuse couplée à la spectrométrie de masse (GC-MS). Ainsi, les individus suppresseurs sélectionnés ont été caractérisés d'un point de vue phénotypique, biochimique et métabolique. La caractérisation génétique des lignées sélectionnée a été réalisée par l'analyse en ségrégation des populations F2. Cette analyse a permis d'identifier des mutations dominantes et récessives, présentant des types de ségrégation différents, laissant penser que différentes mutations ont pu être sélectionnées lors de ce crible. L'échantillonnage d'individus suppresseurs et non-suppresseurs a été réalisé afin d'extraire de l'ADN génomique pour séquençage complet du génome selon la technique émergente du « Next Generation Sequencing (NGS) ». Les données brutes ont été obtenues et sont en cours d'analyse en collaboration avec Sylvain Darnet (Laboratório de Biotecnologia Vegetal, Instituto de Ciências Biológicas, Universidade Federal do Pará (UFPA), Belém, Brazil).

Six individus suppresseurs du phénotype *chs5* ont été sélectionnés en conditions *in vitro*. Différents phénotypes ont été sélectionnés : reverdissement complet des feuilles de la rosette (4 lignées), reverdissement partiel et homogène (vert clair, 1 lignée), reverdissement partiel (vert clair) et hypercroissance de l'hypocotyle (1 lignée). Pour chaque individu, la présence de la mutation ponctuelle (SNP) dans le gène *DXS1* conférée par le fond génétique parental a été vérifiée. Pour quelques lignées, le séquençage du gène a été réalisé afin de vérifier qu'aucune mutation intragénique n'a été sélectionnée. Les individus sélectionnés *in vitro* ont été transférés en terre afin de réaliser un croisement avec la lignée parentale et générer des graines F1. Les individus F1 ont été phénotypés, permettant de définir la dominance ou la récessivité des mutations sélectionnées. Après autofécondation des F1, des populations F2 ont été obtenues,

dans lesquelles ségrégent des phénotypes suppresseurs et non-suppresseurs. Le dosage de chlorophylles et caroténoïdes a été réalisé dans les jeunes feuilles de ces individus, afin de caractériser plus finement le reverdissement sélectionné visuellement. L'expression des gènes de la voie du MVA et de la voie du MEP a également été analysée par qPCR dans ces individus. Un dosage d'intermédiaires de la voie du MEP a été réalisé en collaboration avec l'équipe de Louwrance Wright (Max Planck Institute for Chemical Ecology, Biochemistry Department, Jena, Allemagne). La caractérisation génétique de ces lignées a été réalisée par l'observation des phénotypes des individus F1, puis la ségrégation des individus suppresseurs et non-suppresseurs au sein des familles F2. Pour deux lignées, le séquençage profond du génome par NGS a pu être réalisé, et apporte une première série de gènes candidats pour la suppression du phénotype *chs5*.

La culture d'orges a été mise en place *de novo* à l'IBMP, et a nécessité une mise au point des méthodes et conditions de culture, en particulier dans le but de développer des criblages génétiques. L'objectif de cette partie de la thèse est de mieux comprendre la réponse aux brassinostéroïdes chez l'orge. J'ai développé un criblage génétique visant à identifier *in fine* à identifier des mutations gain de fonction en recherchant dans une population M2 des individus supprimant le caractère semi-nain de la lignée parentale. Des orges présentant une maturité précoce de l'épi ont également été observées durant ce criblage, et sélectionnées pour la suite du travail. Au total, 4 suppresseurs de taille et 6 plantes à maturité précoce ont été sélectionnés. Les phénotypes ont été caractérisés par la mesure de la taille totale des plantes, mais également de la taille des entrenœuds, épis et barbes. La date de maturité du premier épi a été notée, comme critère déterminant la maturité précoce ou non des plantes par rapport à la lignée parentale et au fond génétique sauvage. Les orges précoces ont toutes montré un phénotype nain. Dans ces orges suppresseurs ou à maturité précoce, la présence de la mutation *bri1* a bien été vérifiée.
Les hormones étant des régulateurs essentiels de la croissance, j'ai mis en place une méthode d'analyse d'hormones à partir de feuilles d'orges a été mise au point, en utilisant la chromatographie liquide ultra performance couplée à la spectrométrie de masse (UPLC-MS). Cette méthode a permis de doser 8 hormones dans les feuilles d'orges, et de réaliser un profile hormonal pour chaque lignée étudiée. Les orgess suppresseurs ou précoces ont été croisées avec la lignée parentale BW312 afin de générer des caryopses F1. La caractérisation génétique des lignées sélectionnées a été faite par l'observation des phénotypes des individus F1, puis de la ségrégation des phénotypes dans les populations F2 obtenues par autofécondation des F1. Ce

travail chez l'orge est plus long que chez *Arabidopsis thaliana*, du fait d'un cycle de vie plus long de l'orge et de la difficulté à réaliser les croisements.

A côté de cette étude génétique du métabolisme d'isoprénoïdes, je me suis aussi concentrée sur des aspects spécifiques de ce métabolisme en étudiant la voie de biosynthèse de stérols spécifique des tubes polliniques en germination. Ce type cellulaire particulier a pour fonction d'amener les gamètes jusqu'au gamétophyte femelle, pour y réaliser la fécondation. Cette étape de la reproduction des plantes à fleur est donc essentielle. J'ai étudié les tubes polliniques de plusieurs espèces végétales, afin de vérifier que cette voie de biosynthèse était sélectionnée de façon généralisée dans différentes familles. Des grains de pollen frais ont été prélevés et placés en culture dans un milieu liquide adapté à chaque espèce. Après germination des tubes polliniques, les stérols ont été extraits et analysés en chromatographie gazeuse couplée à la spectrométrie de masse (GC-MS). Ces analyses montrent que les tubes polliniques de toutes les espèces analysées accumulent des 9β,19-cyclopropyl stérols, habituellement décrits comme intermédiaires de biosynthèse dans les tissus sporophytiques. D'autres stérols ont également été détectés dans les cultures de tubes polliniques. Afin d'identifier quels stérols sont néosynthétisés durant la croissance des tubes polliniques, du glucose marqué (^{13}C) a été utilisé dans le milieu de culture. L'analyse des spectres de masse obtenus pour les différents stérols permet de calculer un enrichissement isotopique si les produits sont synthétisés à partir de catabolites marqués du glucose. Les 9β,19-cyclopropyl stérols produisent des spectres de masse montrant une abondance d'isotopomères lourds, ce qui n'est pas le cas des autres produits. Par conséquent, ces derniers proviennent très probablement d'un apport maternel à la biogenèse des grains de pollen. Ces expériences montrent une synthèse inédite de 9β,19-cyclopropyl stérols comme produits finaux du métabolisme stérolique chez le pollen. Pour confirmer cette synthèse de 9β,19-cyclopropyl stérols dans les tubes polliniques, ceux-ci ont été isolés *in vivo*. Pour cela, des fleurs sont pollinisées puis les styles dans lesquels les tubes polliniques s'allongent sont placés sur milieu solide jusqu'à ce que les tubes polliniques en sortent, poursuivant ainsi leur germination sur le milieu au cours de leur germination. Ces tubes ont été récoltés et leur profil stérolique analysé. Ce profil indique la présence unique de 9β,19-cyclopropyl stérols dans les extraits.

Ces travaux montrent que la voie de biosynthèse des stérols dans les tubes polliniques en germination est stoppée au niveau de l'enzyme cyclopropylsterol isomérase (CPI), capable

d’ouvrir le 9β,19-cycloprane. Cela montre de façon originale la présence d’une voie de synthèse particulière des 9β,19-cyclopropylstérols chez le pollen. La suite des travaux a consisté à transformer des plantes de *Nicotiana tabacum* avec un cDNA codant l’enzyme CPI couplée à une protéine fluorescente verte (GFP), sous contrôle du promoteur spécifique du pollen LAT52. Les plantes ainsi transformées présentent des tubes polliniques fluorescents, et capables de synthétiser de l’obtusifoliol, produit de l’isomérisation du cycloeucalénol par l’enzyme CPI. L’impact d’un profil stérolique modifié de ces tubes polliniques est une capacité modifiée à transmettre leur patrimoine génétique. Une série d’expériences est en cours afin de préciser les propriétés de ces tubes polliniques.

Supplemental figures

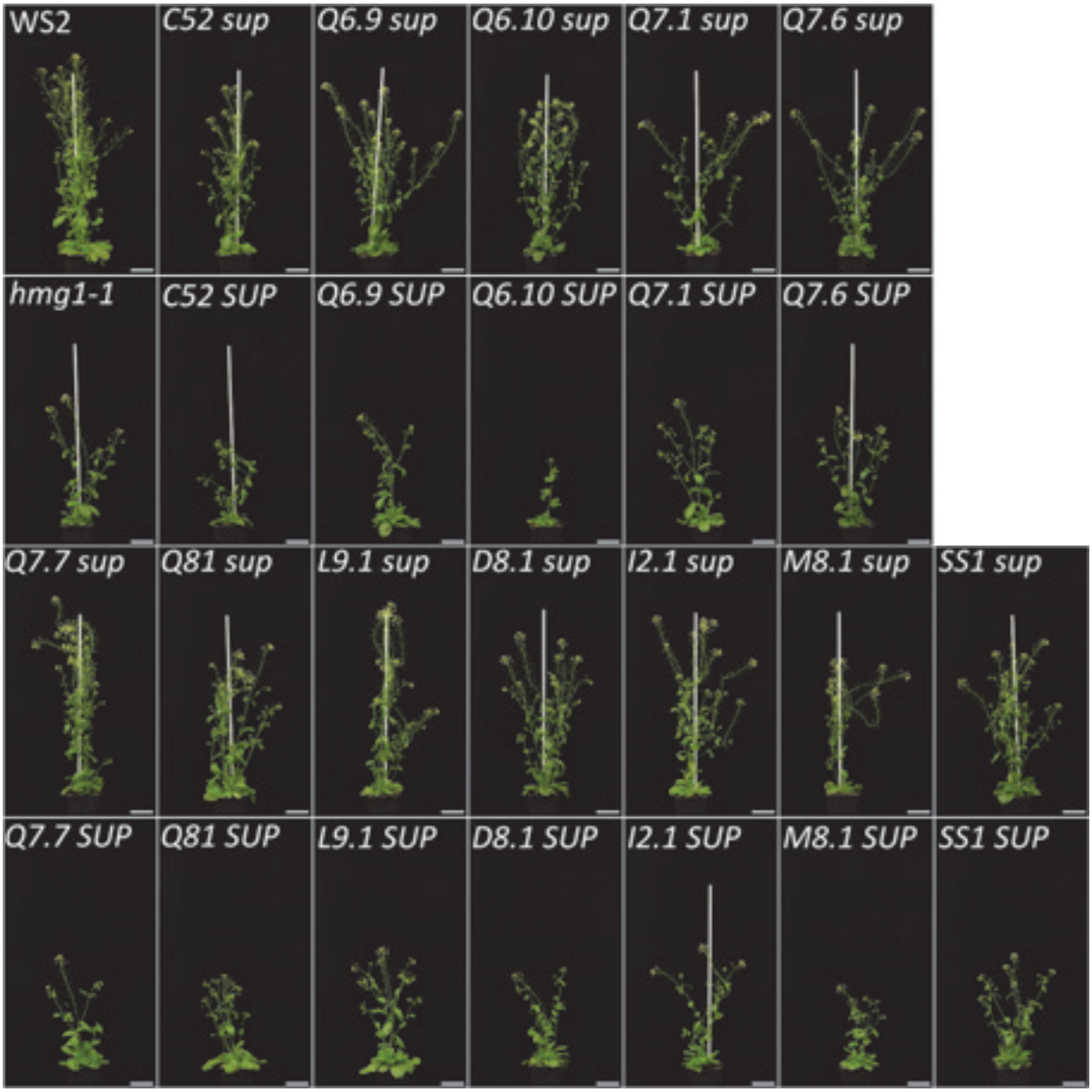

Suppl. Figure 1. Magnified pictures of *hmg1-1* suppressor and non-suppressor phenotypes in a F2BC1. Scale bars 5cm.

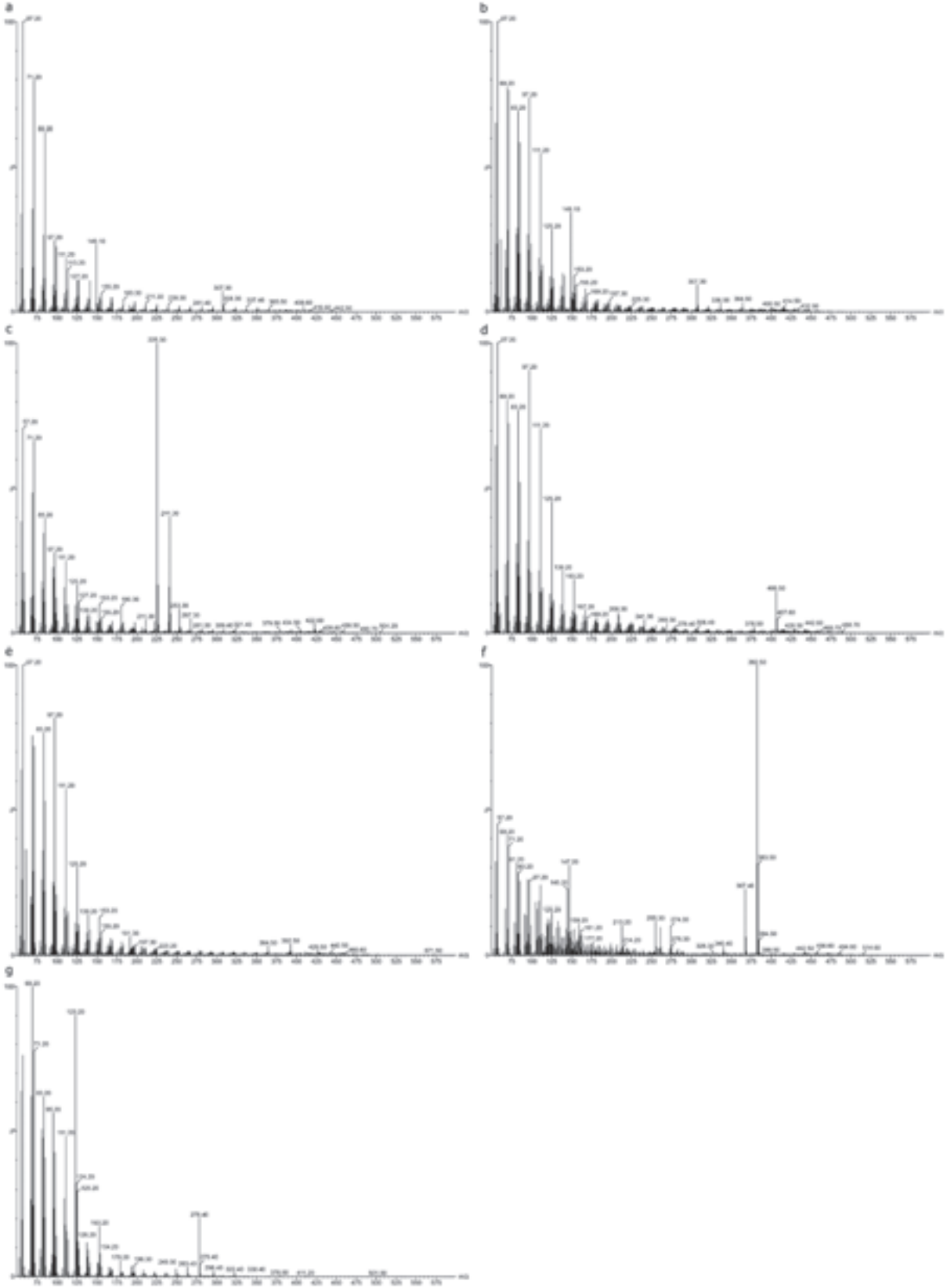

Suppl. Figure 2. Mass spectra of unsaponifiable lipids identified in *hmg1-1* suppressors. a, C27 heptacosane acetate; b, C28 octacosane acetate : c, C29 nonacosane acetate; d, C30 ; e, C31; f, campesteryl acetate ; g, phytol acetate.

Suppl. Figure 3. Magnified view of DXS1sequence alignment.

Suppl. Figure 4. Magnified pictures of *chs5* suppressor and non-suppressor phenotypes. Scale bars 2cm.

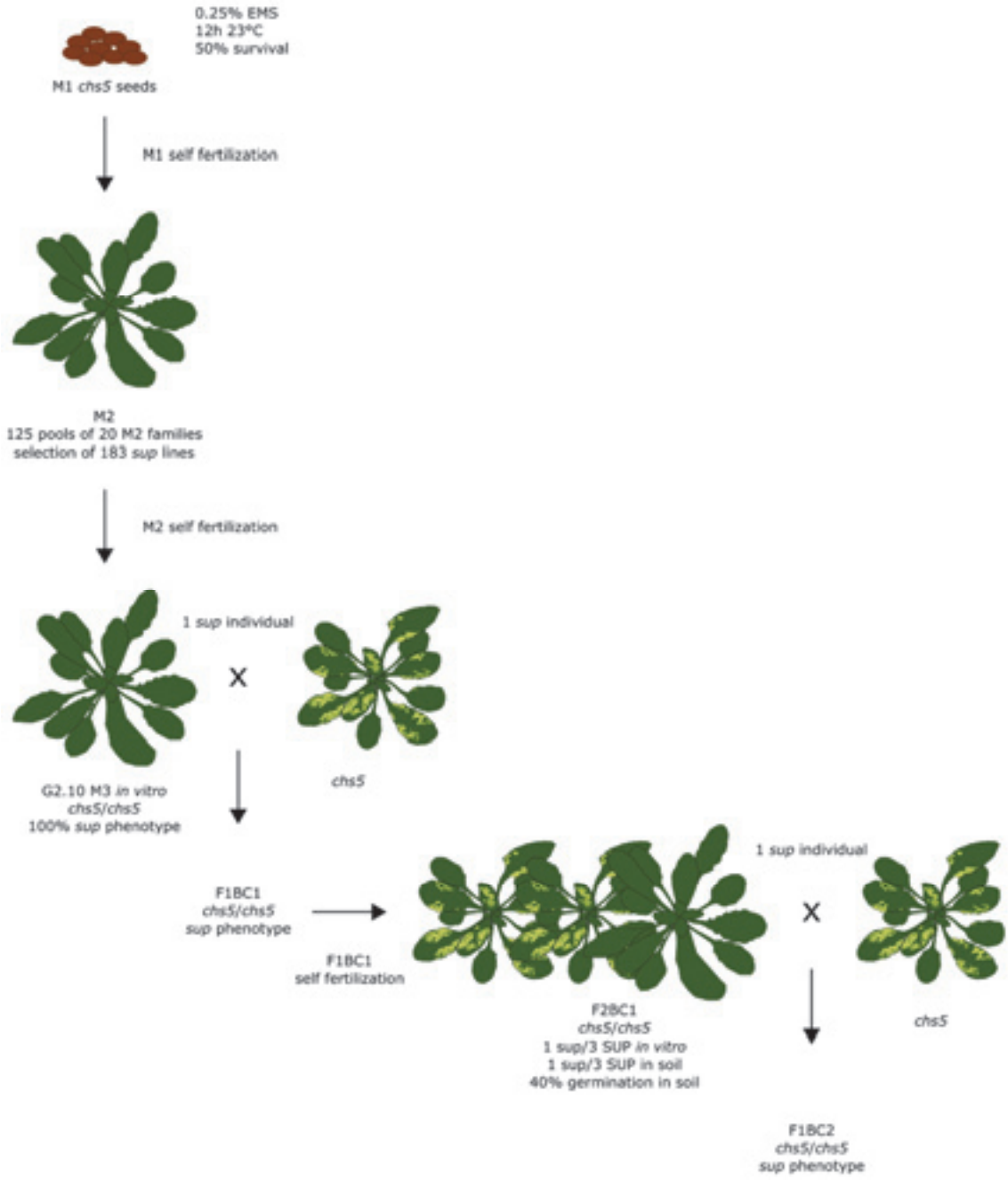

Suppl. Figure 5. Selection process of *Arabidopsis thaliana sup chs5* G2.10 line.

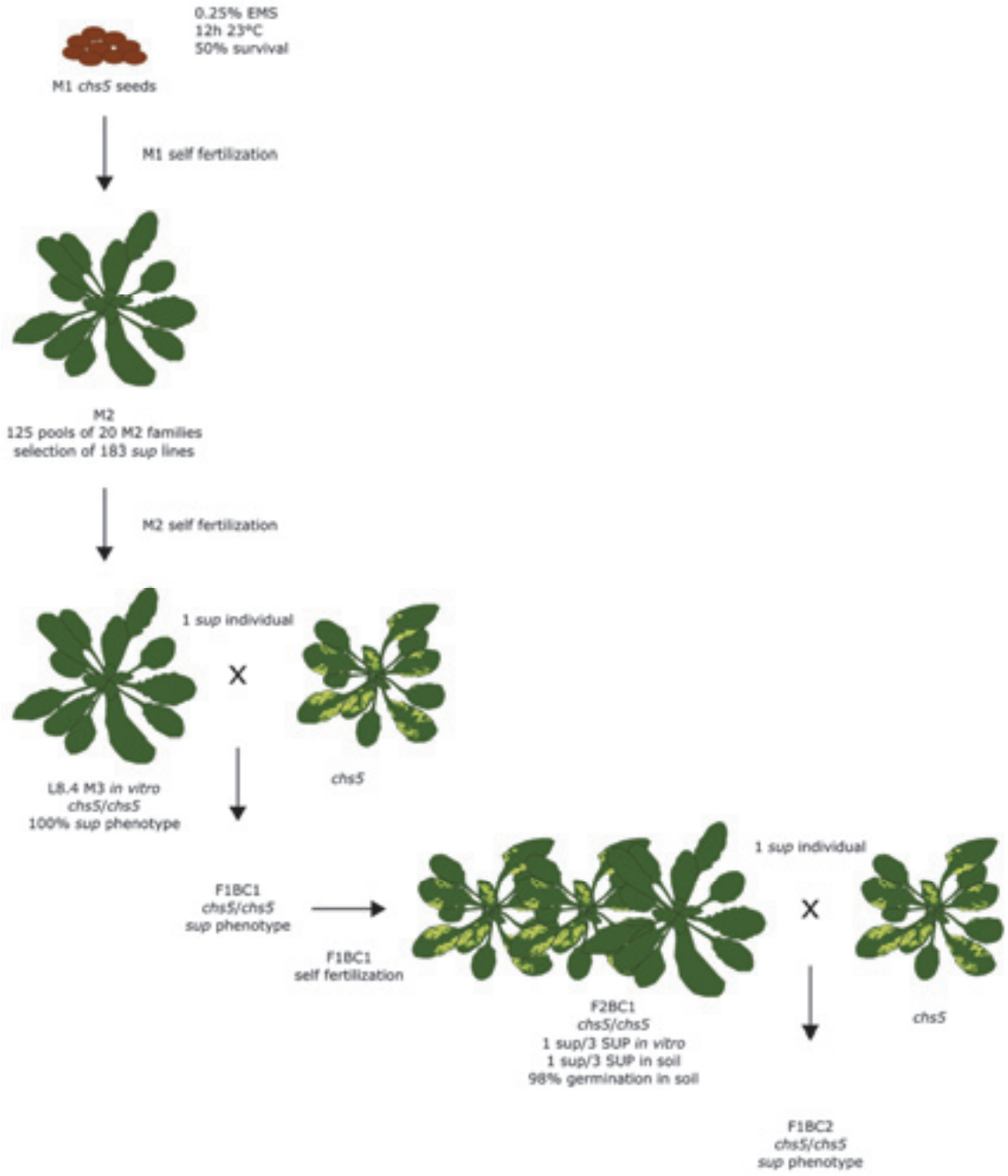

Suppl. Figure 6. Selection process of *Arabidopsis thaliana sup chs5* L8.4 line.

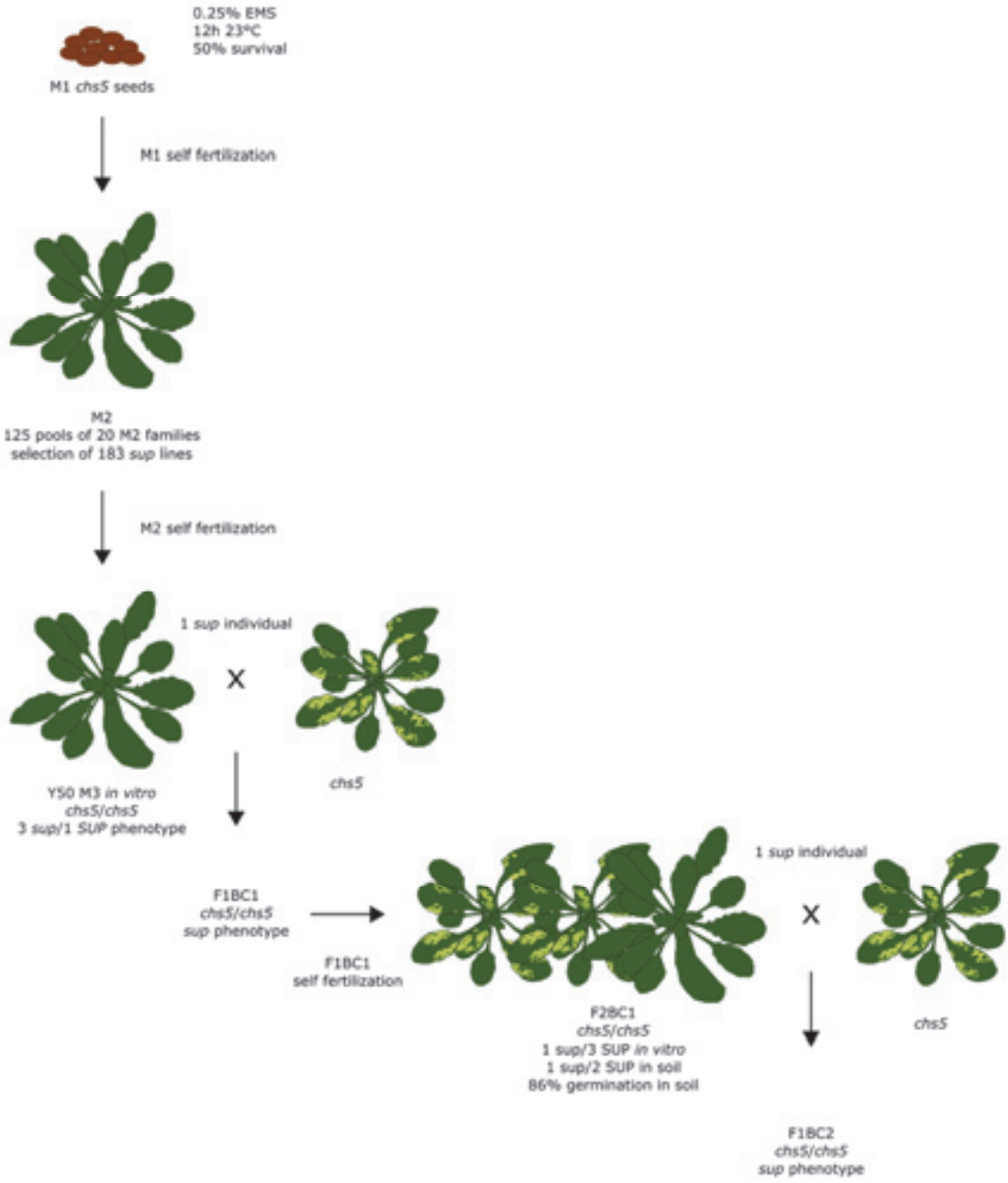

Suppl. Figure 7. Selection process of *Arabidopsis thaliana sup chs5* Y50 line.

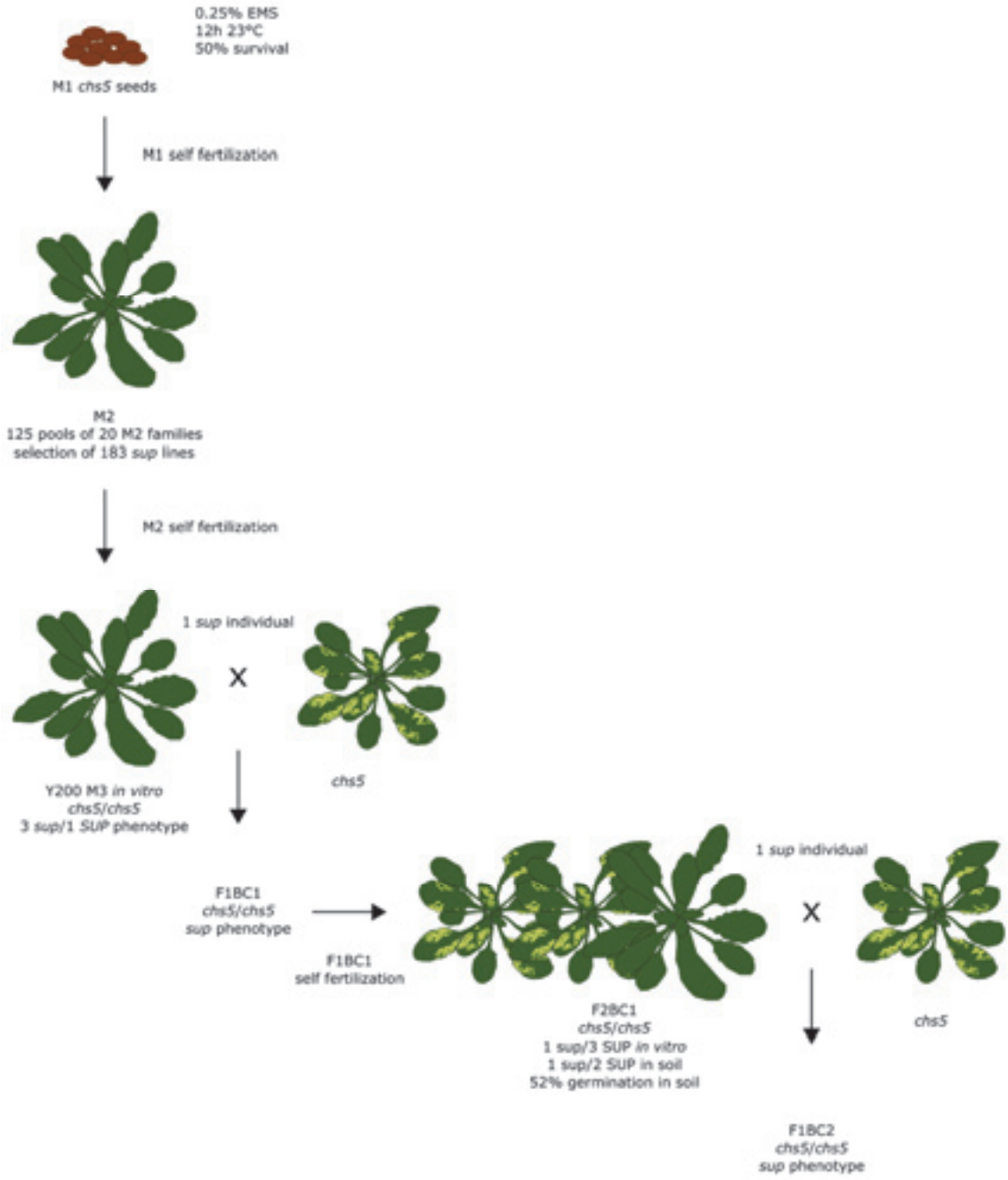

Suppl. Figure 8. Selection process of *Arabidopsis thaliana sup chs5* Y200 line.

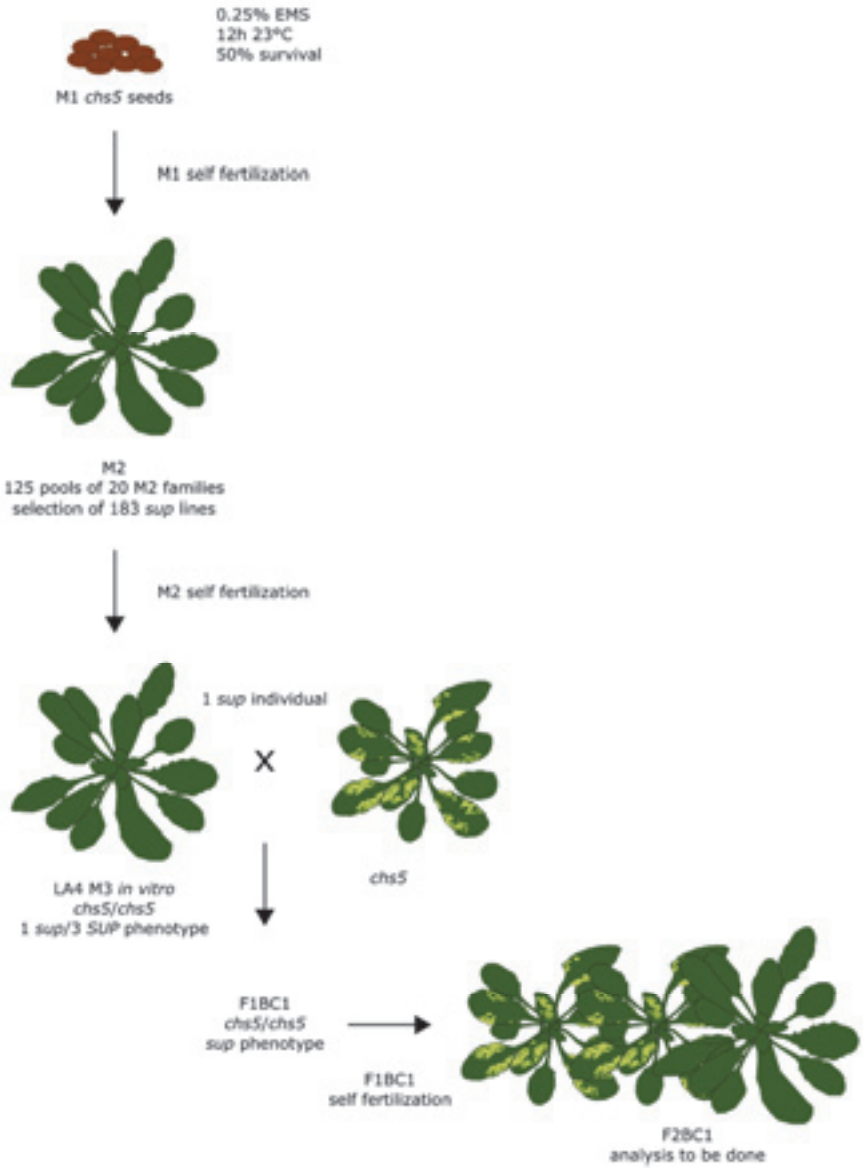

Suppl. Figure 9. Selection process of *Arabidopsis thaliana sup chs5* LA4 line.

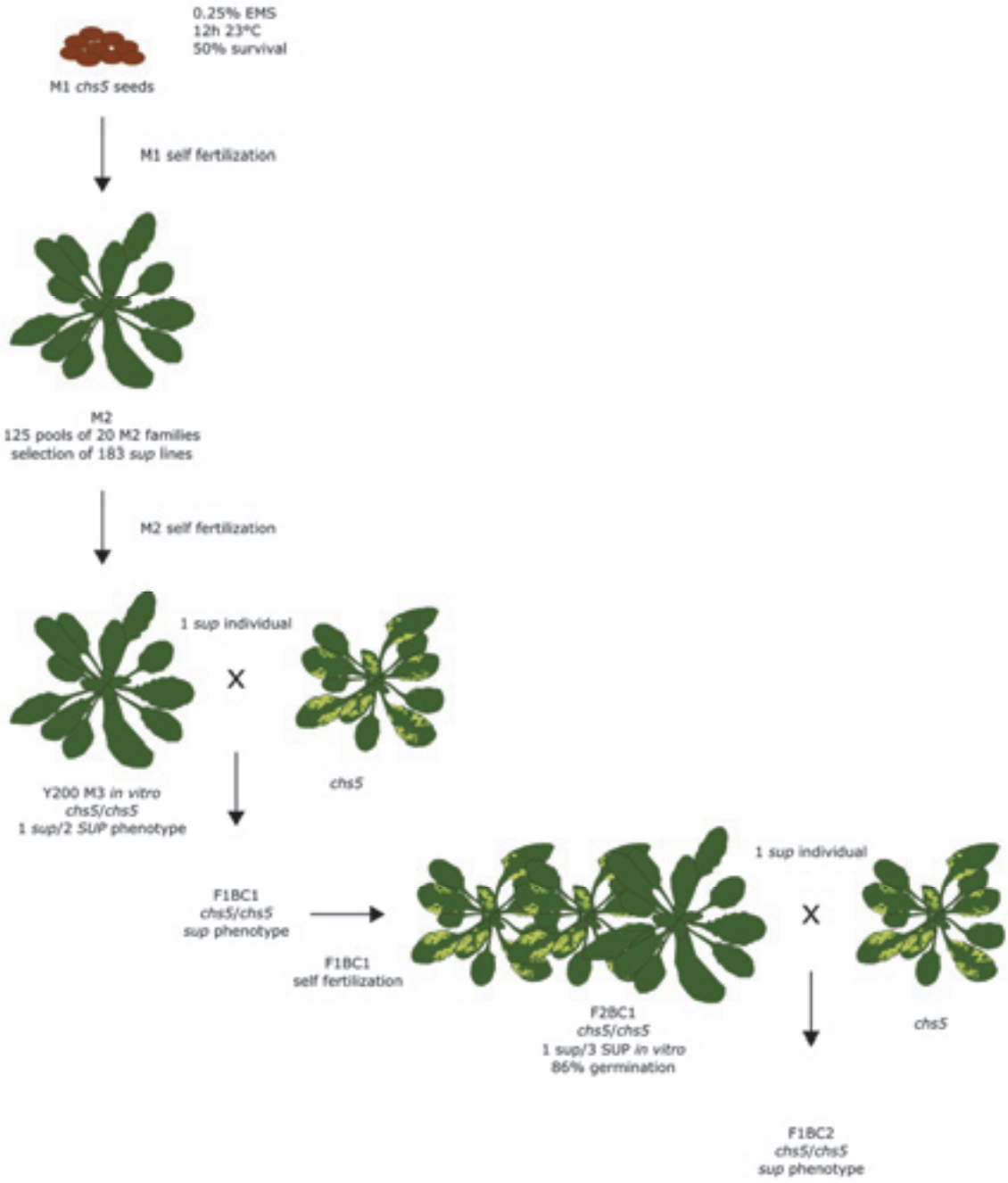

Suppl. Figure 10. Selection process of *Arabidopsis thaliana sup chs5* iQ3 line.

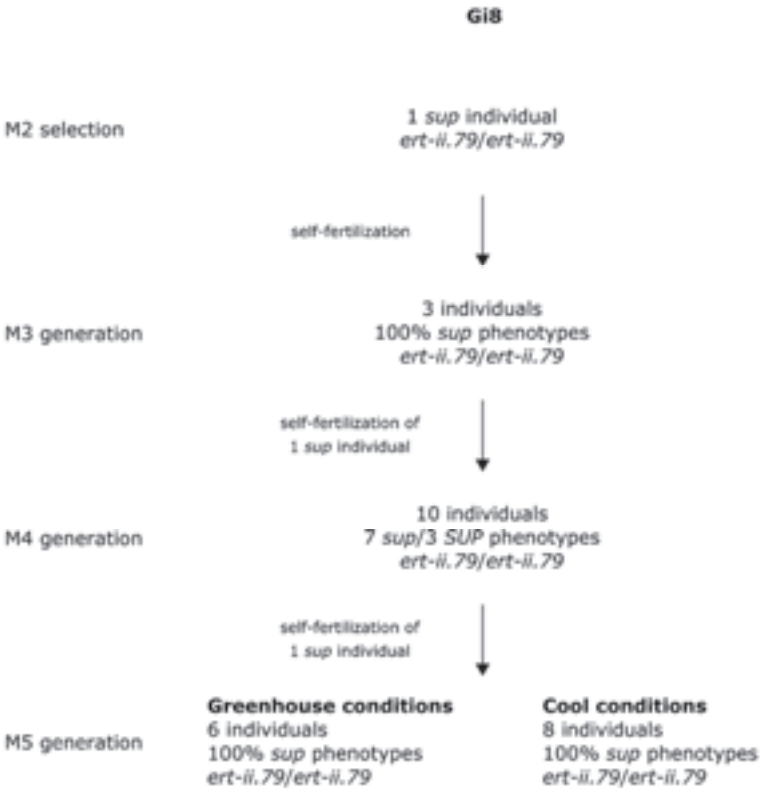

Suppl. Figure 11. Selection process of *Hordeum vulgare ert-ii.79/bri1* Gi8 suppressor (*sup*) line.

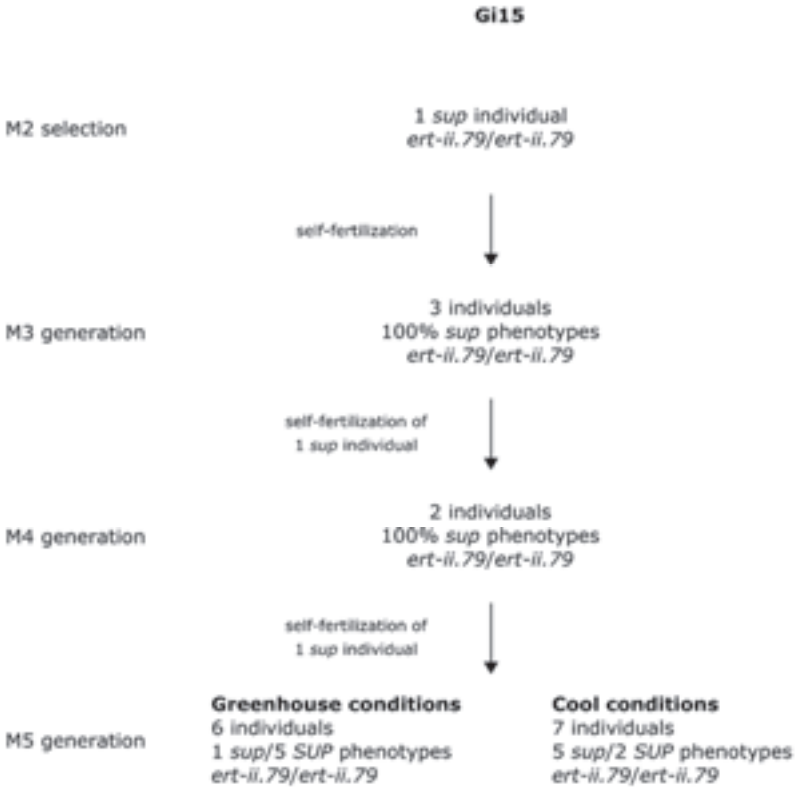

Suppl. Figure 12. Selection process of *Hordeum vulgare ert-ii.79/bri1* Gi15 suppressor (*sup*) line.

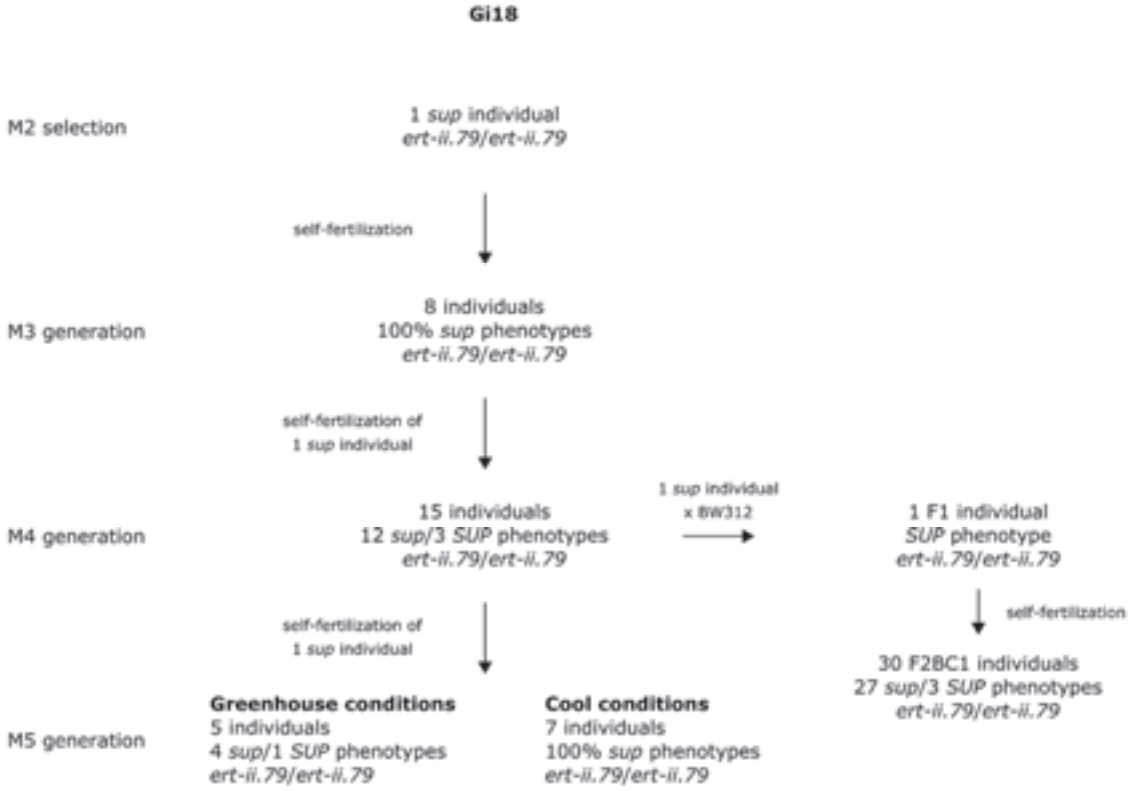

Suppl. Figure 13. Selection process of *Hordeum vulgare ert-ii.79/bri1* Gi18 suppressor (*sup*) line.

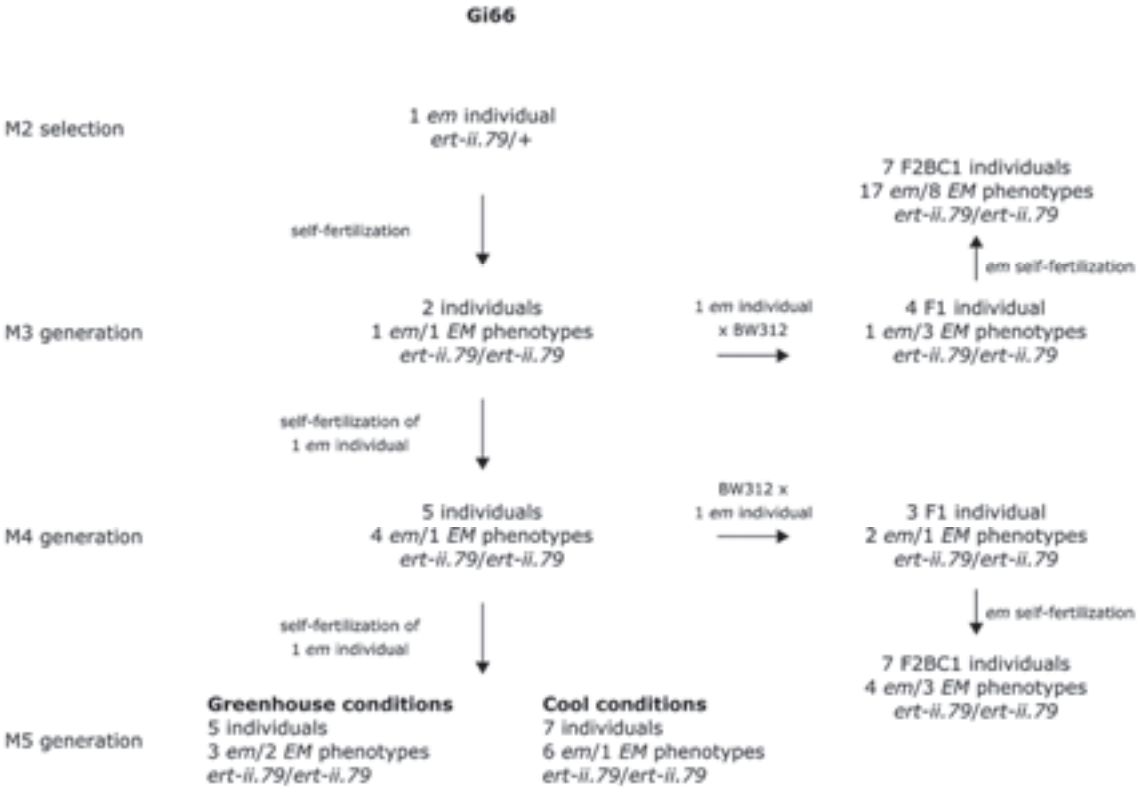

Suppl. Figure 14. Selection process of *Hordeum vulgare ert-ii.79/bri1* Gi66 early maturity (*em*) line.

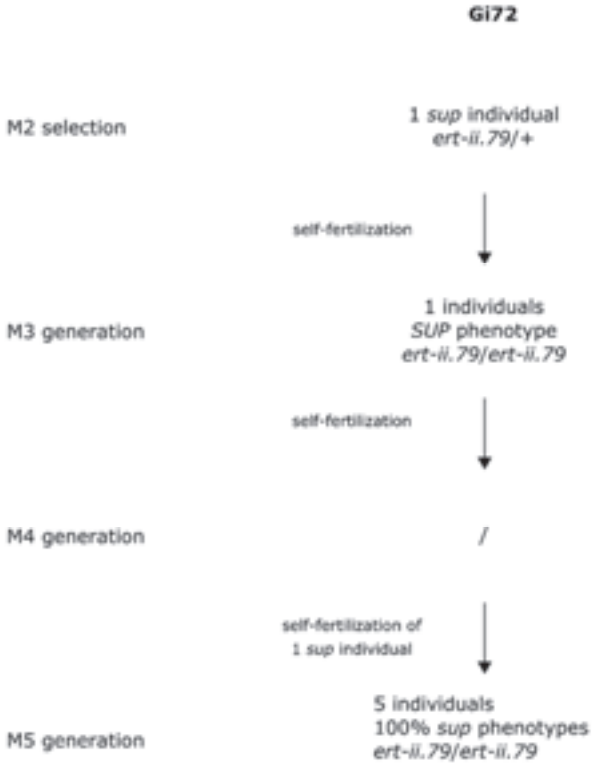

Suppl. Figure 15. Selection process of *Hordeum vulgare ert-ii.79/bri1* Gi72 suppressor (*sup*) line.

Suppl. Figure 16. Selection process of *Hordeum vulgare ert-ii.79/bri1* Gi92 early maturity (*em*) line.

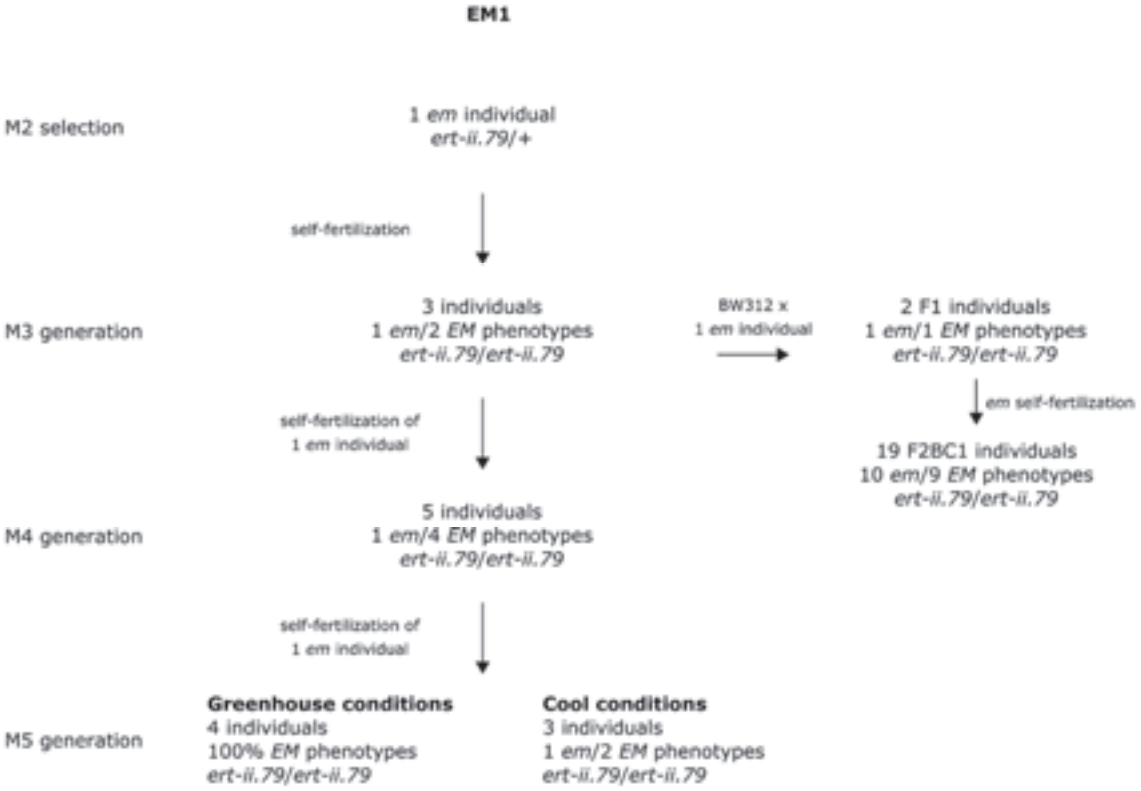

Suppl. Figure 17. Selection process of *Hordeum vulgare ert-ii.79/bri1* EM1 early maturity (*em*) line.

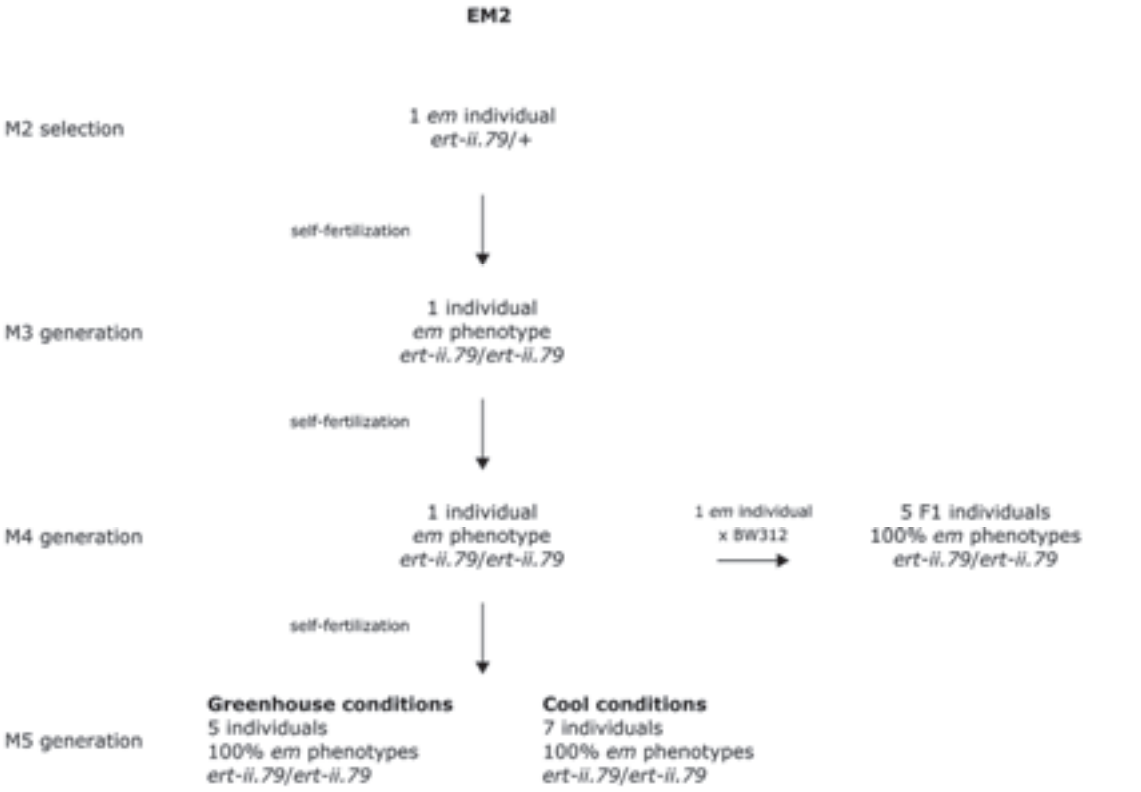

Suppl. Figure 18. Selection process of *Hordeum vulgare ert-ii.79/bri1* EM2 early maturity (*em*) line.

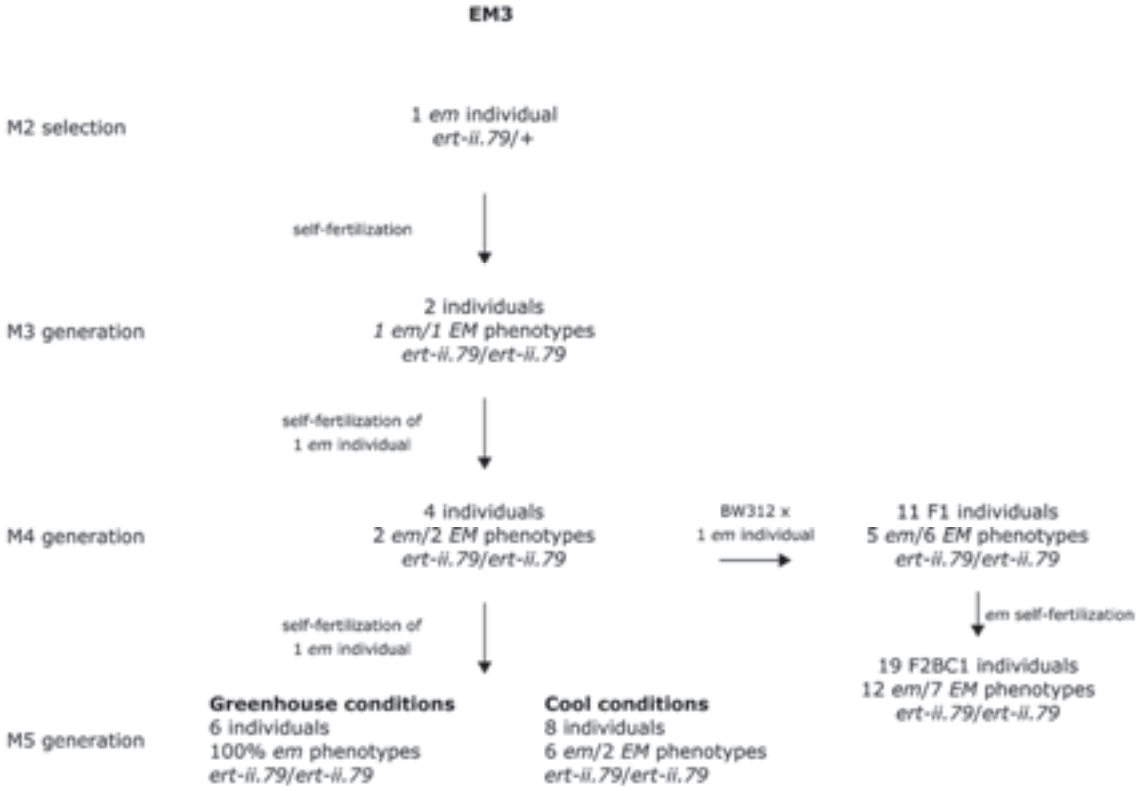

Suppl. Figure 19. Selection process of *Hordeum vulgare ert-ii.79/bri1* EM3 early maturity (*em*) line.

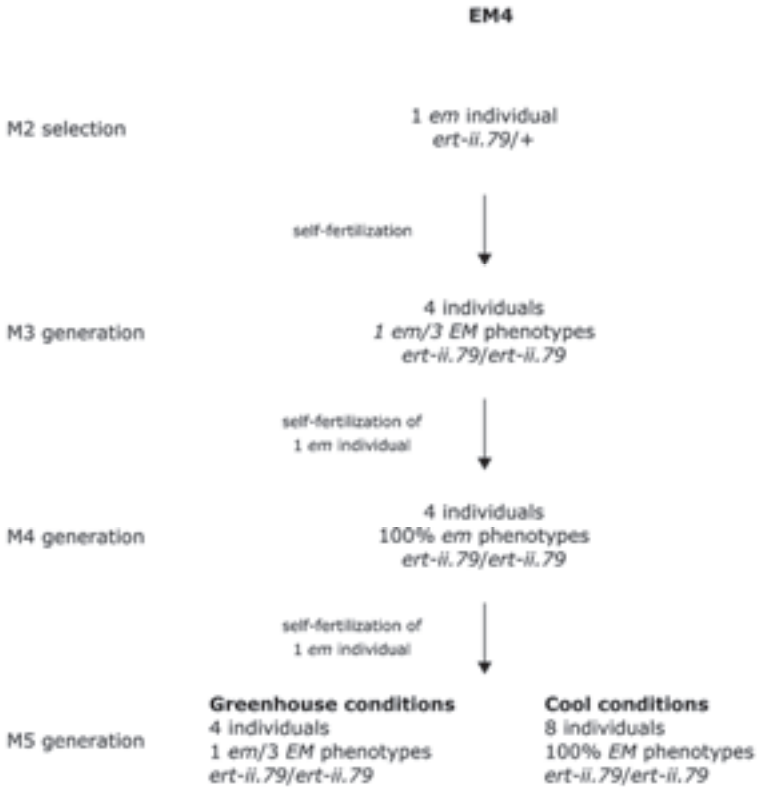

Suppl. Figure 20. Selection process of *Hordeum vulgare ert-ii.79/bri1* EM4 early maturity (*em*) line.

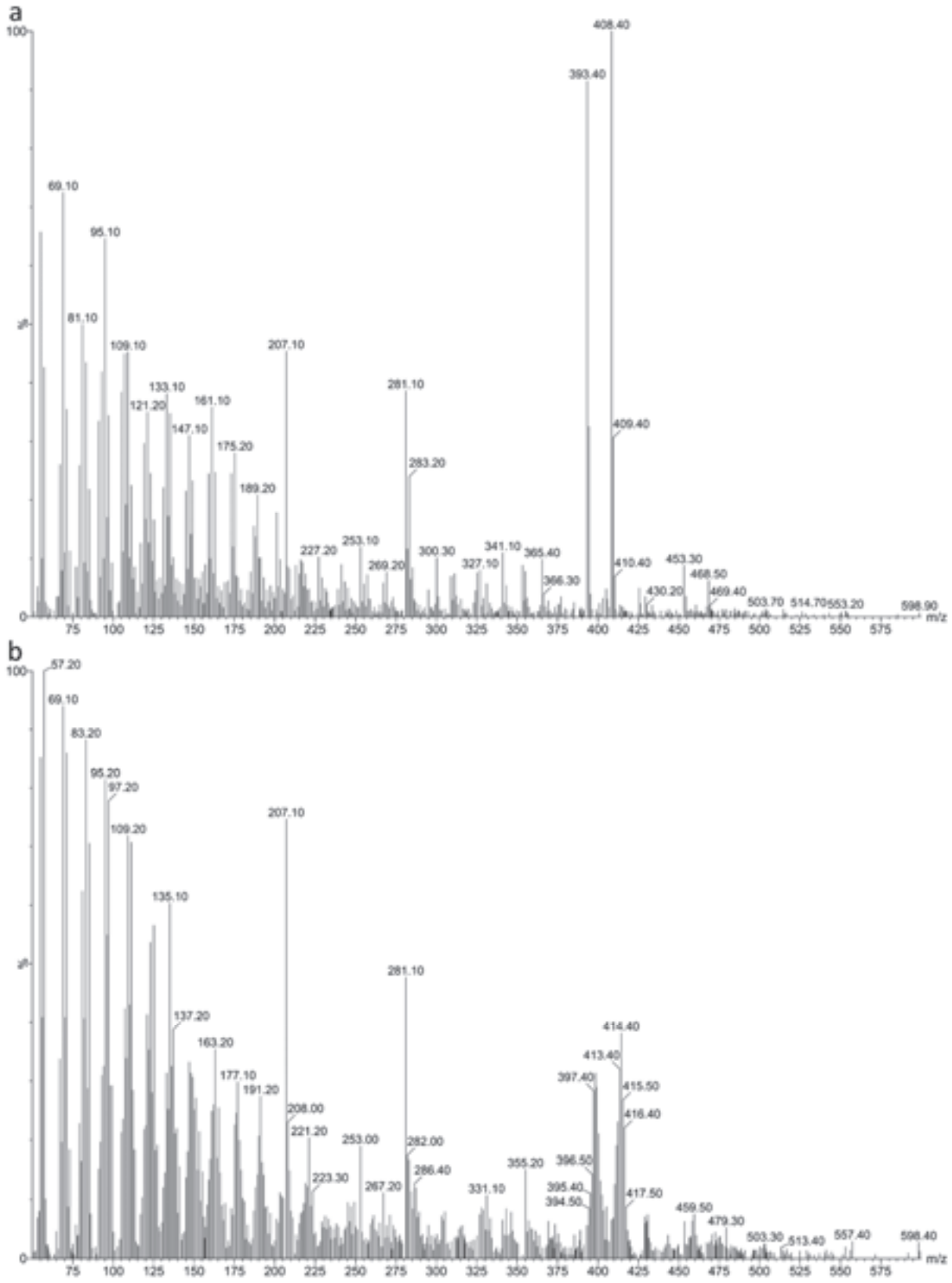

Suppl. Figure 21. Full mass spectra of ^{12}C (a) and ^{13}C-enriched (b) cycloeucalenol identified in lipid extracts from pollen tubes of *Nicotiana tabacum*.

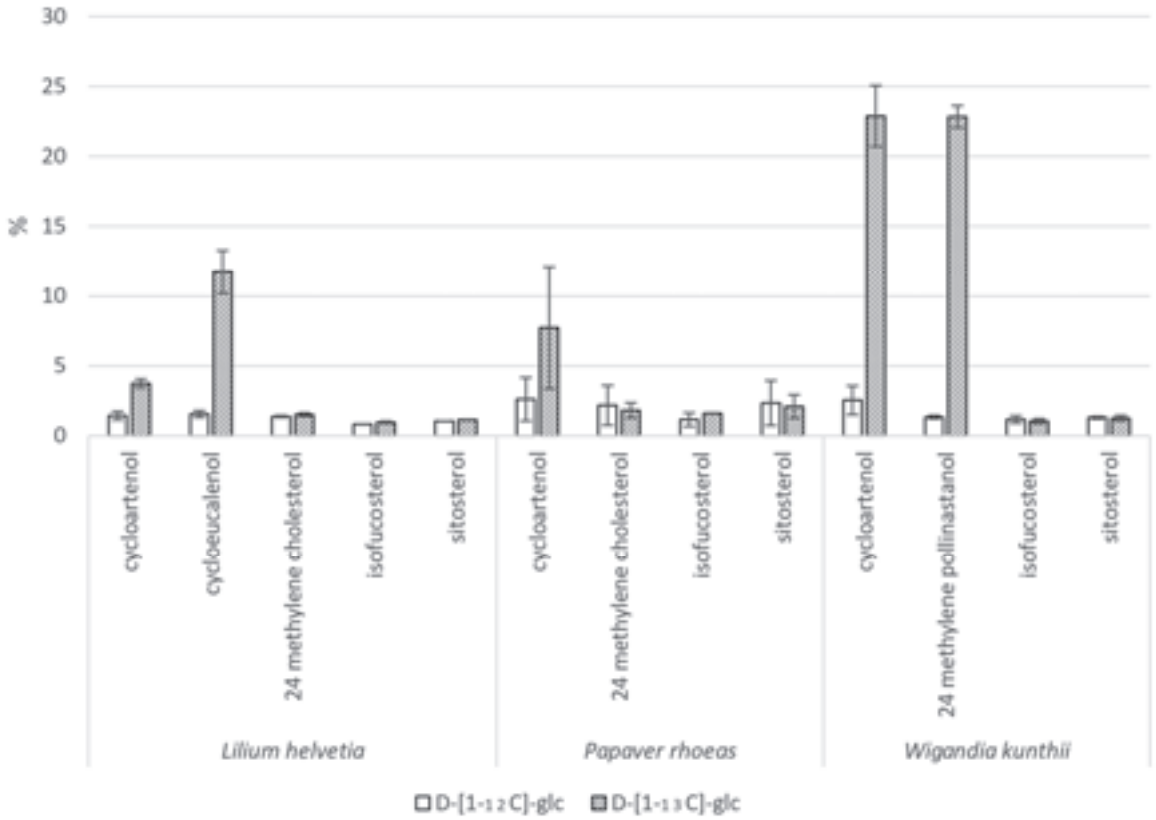

Suppl. Figure 22. Isotopic enrichment (%) in cyclopropylsterols and sterols from pollen tubes of other species. Pollen grains of *Lilium helvetia*, *Papaver rhoeas* and *Wigandia kunthii* were germinated *in vitro* in presence of ^{12}C or ^{13}C labelled glucose.

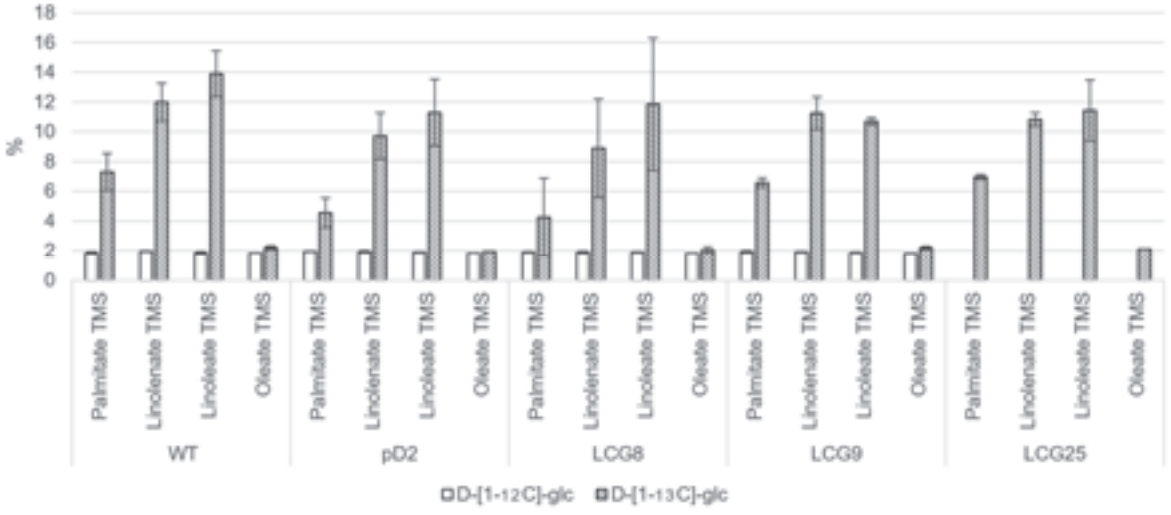

Suppl. Figure 23. Isotopic enrichment (%) in fatty acids from *in vitro* grown pollen tubes of *Nicotiana tabacum*.

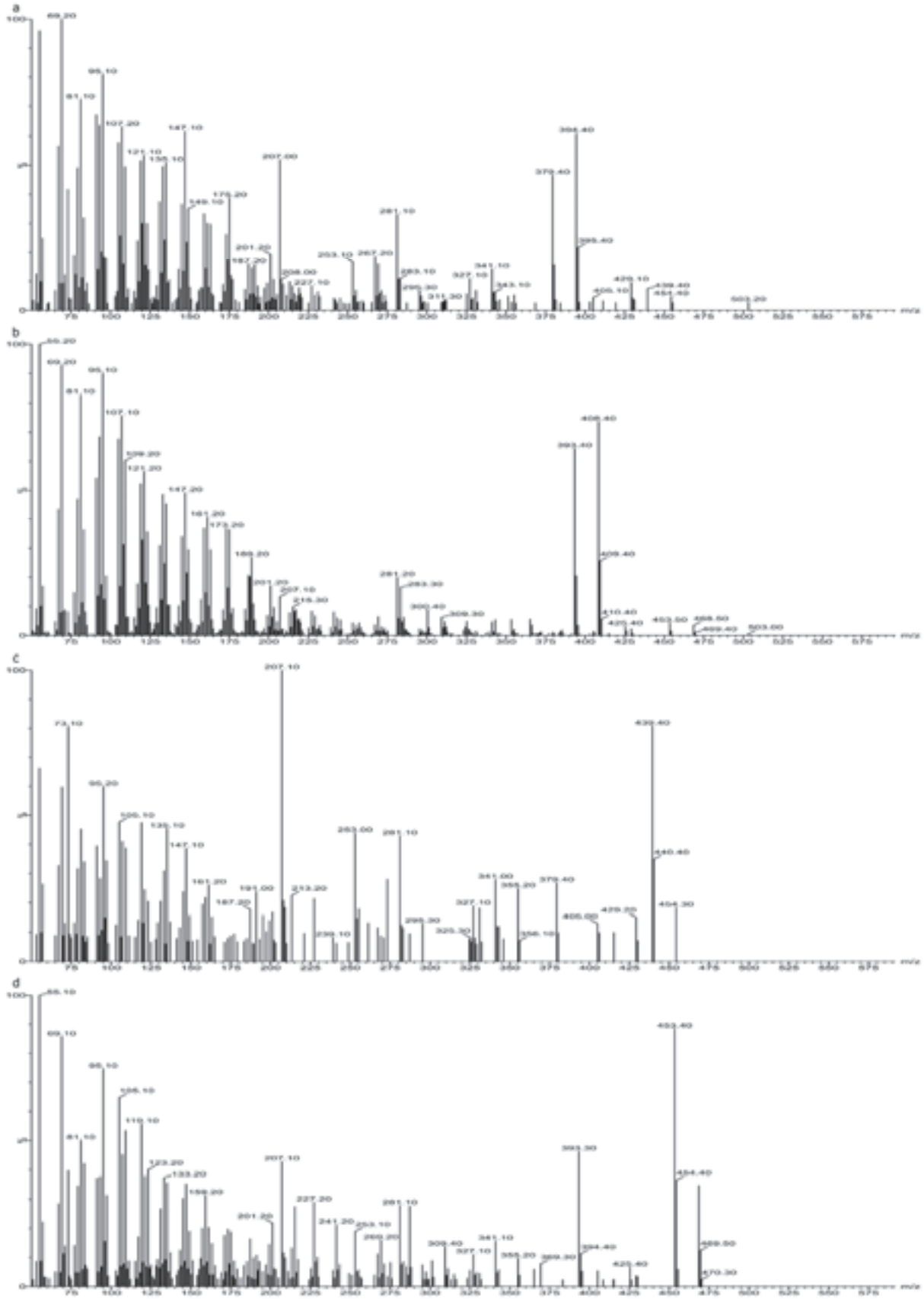

Suppl. Figure 24. Mass spectra of sterols identified in semi *in vivo* pollen tubes of *Nicotiana tabacum*. a, 24-methylene pollinastanol; b, cycloeucalenol; c, 5,24 methylene-fecosterol; d, obtusifoliol.

Bibliography

Allen, R.S., Nakasugi, K., Doran, R.L., Millar, A. a., and Waterhouse, P.M. (2013). Facile mutant identification via a single parental backcross method and application of whole genome sequencing based mapping pipelines. Front. Plant Sci. **4**: 362.

Antolín-Llovera, M., Leivar, P., Arró, M., Ferrer, A., Boronat, A., and Campos, N. (2011). Modulation of plant HMG-CoA reductase by protein phosphatase 2A. Plant Signal. Behav. **6**: 1–5.

Araki, N., Kusumi, K., Masamoto, K., Niwa, Y., and Iba, K. (2000). Temperature-sensitive *Arabidopsis* mutant defective in 1-deoxy-d-xylulose 5-phosphate synthase within the plastid non-mevalonate pathway of isoprenoid biosynthesis. Physiol Plant **108**: 19–24.

Babiychuk, E., Bouvier-Navé, P., Compagnon, V., Suzuki, M., Muranaka, T., Van Montagu, M., Kushnir, S., and Schaller, H. (2008). Allelic mutant series reveal distinct functions for *Arabidopsis* cycloartenol synthase 1 in cell viability and plastid biogenesis. Proc. Natl. Acad. Sci. U. S. A. **105**: 3163–8.

Bajguz, A. (2007). Metabolism of brassinosteroids in plants. Plant Physiol. Biochem. **45**: 95–107.

Berger, F., Hamamura, Y., Ingouff, M., and Higashiyama, T. (2008). Double fertilization - caught in the act. Trends Plant Sci. **13**: 437–443.

Bishop, G.J. and Koncz, C. (2002). Brassinosteroids and Plant Steroid Hormone Signaling. Plant Cell **Volume 14**: 97–110.

Bloch, D., Pleskot, R., Pejchar, P., Potocký, M., Trpkošová, P., Cwiklik, L., Vukašinović, N., Sternberg, H., Yalovsky, S., and Žárský, V. (2016). Exocyst SEC3 and Phosphoinositides Define Sites of Exocytosis in Pollen Tube Initiation and Growth. Plant Physiol. **172**: 980–1002.

Bolger, A.M., Lohse, M., and Usadel, B. (2014). Trimmomatic: A flexible trimmer for Illumina sequence data. Bioinformatics **30**: 2114–2120.

Botte, C.Y. et al. (2011). Chemical inhibitors of monogalactosyldiacylglycerol synthases in *Arabidopsis thaliana*. Nat Chem Biol **7**: 834–842.

Bouhss, A., Trunkfield, A.E., Bugg, T.D.H., and Mengin-Lecreulx, D. (2008). The biosynthesis of peptidoglycan lipid-linked intermediates. FEMS Microbiol. Rev. **32**: 208–233.

Bouvier-Navé, P., Berna, A., Noiriel, A., Compagnon, V., Carlsson, A.S., Banas, A., Stymne, S., and Schaller, H. (2010). Involvement of the phospholipid sterol

acyltransferase1 in plant sterol homeostasis and leaf senescence. Plant Physiol. **152**: 107–119.

Bouvier, F., Rahier, A., and Camara, B. (2005). Biogenesis , molecular regulation and function of plant isoprenoids. Prog. Lipid Res. **44**: 357–429.

Brian, P.W. (1959). Effects of Gibberellins on Plant Growth and Development. Biol. Rev. **34**: 37–77.

Carretero-Paulet, L., Cairó, A., Talavera, D., Saura, A., Imperial, S., Rodríguez-Concepción, M., Campos, N., and Boronat, A. (2013). Functional and evolutionary analysis of DXL1, a non-essential gene encoding a 1-deoxy-D-xylulose 5-phosphate synthase like protein in *Arabidopsis thaliana*. Gene **524**: 40–53.

Chandler, P. and Robertson, M. (1999). Gibberellin dose-response curves and the characterization of dwarf mutants of barley. Plant Physiol. **120**: 623–32.

Chandler, P.M. and Harding, C.A. (2013). “Overgrowth” mutants in barley and wheat: new alleles and phenotypes of the “Green Revolution” DELLA gene. J. Exp. Bot. **64**: 1603–13.

Clouse, S.D. (2011). Brassinosteroid signal transduction: from receptor kinase activation to transcriptional networks regulating plant development. Plant Cell **23**: 1219–30.

Compagnon, V., Diehl, P., Benveniste, I., Meyer, D., Schaller, H., Schreiber, L., Franke, R., and Pinot, F. (2009). CYP86B1 Is Required for Very Long Chain w-Hydroxyacid and a,w-Dicarboxylic Acid Synthesis in Root and Seed. Plant Physiol. **150**: 1831–1843.

Croce, R., Amerongen, H. Van, van Amerongen, H., and Amerongen, H. Van (2014). Natural strategies for photosynthetic light harvesting. Nat. Chem. Biol. **10**: 492–501.

Darwich, Z., Klymchenko, A.S., Kucherak, O.A., Richert, L., and Mély, Y. (2012). Detection of apoptosis through the lipid order of the outer plasma membrane lea fl et. Biochim. Biophys. Acta **1818**: 3048–3054.

Dockter, C. et al. (2014). Induced Variations in Brassinosteroid Genes Define Barley Height and Sturdiness, and Expand the Green Revolution Genetic Toolkit. Plant Physiol. **166**: 1912–1927.

Dresselhaus, T. and Márton, M.L. (2009). Micropylar pollen tube guidance and burst:

adapted from defense mechanisms? Curr. Opin. Plant Biol. **12**: 773–80.

Druka, A., Franckowiak, J., Lundqvist, U., Bonar, N., Alexander, J., Houston, K., Radovic, S., Shahinnia, F., Vendramin, V., Morgante, M., Stein, N., and Waugh, R. (2011). Genetic dissection of barley morphology and development. Plant Physiol. **155**: 617–27.

Enfissi, E.M. a, Fraser, P.D., Lois, L.-M., Boronat, A., Schuch, W., and Bramley, P.M. (2005). Metabolic engineering of the mevalonate and non-mevalonate isopentenyl diphosphate-forming pathways for the production of health-promoting isoprenoids in tomato. Plant Biotechnol. J. **3**: 17–27.

Feuillet, C., Stein, N., Rossini, L., Praud, S., Mayer, K., Schulman, A., Eversole, K., and Appels, R. (2012). Integrating cereal genomics to support innovation in the Triticeae. Funct Integr Genomics **12**: 573–583.

Finkelstein, R. (2013). Abscisic Acid synthesis and response. *Arabidopsis* Book **11**: 1–36.

Fujioka, S. and Yokota, T. (2003). Biosynthesis and metabolism of brassinosteroids. Annu. Rev. Plant Biol. **54**: 137–64.

Gaber, R.F., Copple, D.M., Kennedy, B.K., Vidal, M., and Bard, M. (1989). The yeast gene *ERG6* is required for normal membrane function but is not essential for biosynthesis of the cell-cycle-sparking sterol. Mol. Cell. Biol. **9**: 3447–3456.

Greene, E.A., Codomo, C.A., Taylor, N.E., Henikoff, J.G., Till, B.J., Reynolds, S.H., Enns, L.C., Burtner, C., Johnson, J.E., Odden, A.R., Comai, L., and Henikoff, S. (2003). Spectrum of chemically induced mutations from a large-scale reverse-genetic screen in *Arabidopsis*. Genetics **164**: 731–740.

Grove, M.D., Spencer, G.F., Rohwedder, W.K., Mandava, N., Worley, J.F., Warthen Jr, J.D., Steffens, G.L., Flippen-Anderson, J.L., and Cook Jr, J.C. (1979). Brassinolide, a plant growth-promoting steroid isolated from Brassica napus pollen. Nature **281**: 216–217.

Gruszka, D., Szarejko, I., and Maluszynski, M. (2011). New allele of *HvBRI1* gene encoding brassinosteroid receptor in barley. J. Appl. Genet. **52**: 257–268.

Hamamura, Y., Saito, C., Awai, C., Kurihara, D., Miyawaki, A., Nakagawa, T., Kanaoka, M.M., Sasaki, N., Nakano, A., Berger, F., and Higashiyama, T. (2011). Live-cell imaging reveals the dynamics of two sperm cells during double fertilization in *Arabidopsis thaliana*. Curr. Biol. **21**: 497–502.

Hartmann, M. (1998). Plant sterols and the membrane environment. Trends Plant Sci. **3**: 170–175.

Hauser, F., Waadt, R., and Schroeder, J. (2011). Evolution of abscisic acid synthesis and signaling mechanisms. Curr. Biol. **21**.

Hedden, P. and Sponsel, V. (2015). A century of gibberellin research. J. Plant Growth Regul. **34**: 740–760.

Heintz, D., Gallien, S., Compagnon, V., Berna, A., Suzuki, M., Yoshida, S., Muranaka, T., Van Dorsselaer, A., Schaeffer, C., Bach, T.J., and Schaller, H. (2012). Phosphoproteome exploration reveals a reformatting of cellular processes in response to low sterol biosynthetic capacity in *Arabidopsis*. J. Proteome Res. **11**: 1228–1239.

Hemmerlin, A., Harwood, J.L., and Bach, T.J. (2012). A *raison d'être* for two distinct pathways in the early steps of plant isoprenoid biosynthesis? Prog. Lipid Res. **51**: 95–148.

Hemmerlin, A., Hoeffler, J.F., Meyer, O., Tritsch, D., Kagan, I.A., Grosdemange-Billiard, C., Rohmer, M., and Bach, T.J. (2003). Cross-talk between the cytosolic mevalonate and the plastidial methylerythritol phosphate pathways in tobacco bright yellow-2 cells. J. Biol. Chem. **278**: 26666–26676.

Horsch, R.B., Fry, J.E., Hoffmann, N.L., Eichholtz, D., Rogers, S.G., and Fraley, R.T. (1985). A simple and general method for hybridization revealed the expected. Science (80-.). **227**: 1229–1231.

Huang, Z.R., Lin, Y.K., and Fang, J.Y. (2009). Biological and pharmacological activities of squalene and related compounds: Potential uses in cosmetic dermatology. Molecules **14**: 540–554.

Hugly, S. and Somerville, C. (1992). A role for membrane lipid polyunsaturation in chloroplast biogenesis at low temperature. Plant Physiol. **99**: 197–202.

Jain, S., Caforio, A., and Driessen, A.J.M. (2014). Biosynthesis of archaeal membrane ether lipids. Front. Microbiol. **5**: 1–16.

James, G.V., Patel, V., Nordström, K.J. V, Klasen, J.R., Salomé, P. a, Weigel, D., and Schneeberger, K. (2013). User guide for mapping-by-sequencing in *Arabidopsis*. Genome Biol. **14**: R61.

Jende-Strid, B. (1993). Genetic control of flavonoid biosynthesis in barley. Hereditas **119**: 187–204.

Kannenberg, E.L. and Poralla, K. (1999). Hopanoid biosynthesis and function in bacteria. Naturwissenschaften 86: 1168–179.

Kashman, Y. and Rudi, A. (2004). On the biogenesis of marine isoprenoids. Phytochem. Rev. **3**: 309–323.

Kim, T.-W. and Wang, Z.-Y. (2010). Brassinosteroid signal transduction from receptor kinases to transcription factors. Annu. Rev. Plant Biol. **61**: 681–704.

Kim, Y., Schumaker, K.S., and Zhu, J.-K. (2006). EMS mutagenesis of *Arabidopsis*. Methods Mol. Biol. **323**: 101–103.

Koga, Y. and Morii, H. (2007). Biosynthesis of ether-type polar lipids in Archaea and evolutionary considerations. Microbiol. Mol. Biol. Rev. **71**: 97–120.

Koltunow, A.M., Truettner, J., Cox, K.H., Wallroth, M., and Goldberg, R.B. (1990). Different temporal and spatial gene-expression patterns occur during anther development. Plant Cell **2**: 1201–1224.

Kumari, P., Kumar, M., Reddy, R.K., and Jha, B. (2013). Algal lipids, fatty acids and sterols. In Functional Ingredients from Algae for Foods and Nutraceuticals, H. Dominguez, ed. Elsevier, pp. 87–134.

Lange, B.M., Rujan, T., Martin, W., and Croteau, R. (2000). Isoprenoid biosynthesis: The evolution of two ancient and distinct pathways across genomes. Proc. Natl. Acad. Sci. U.S.A. **97**: 13172–13177.

Lees, N.D., Skaggs, B., Kirsch, D.R., and Bard, M. (1995). Cloning of the late genes in the ergosterol biosynthetic pathway of Saccharomyces cerevisiae-A review. Lipids **30**: 221–226.

Li, H., Handsaker, B., Wysoker, A., Fennell, T., Ruan, J., Homer, N., Marth, G., Abecasis, G., and Durbin, R. (2009). The sequence alignment/map format and SAMtools. Bioinformatics **25**: 2078–2079.

Lichtenthaler, H.K. and Buschmann, C. (2001). Chlorophylls and carotenoids: measurement and characterization by UV-VIS spectroscopy. Curr. Protoc. Food Anal. Chem.: F4.3.1-F4.3.8.

Lundqvist, U. (1992). Mutation research in barley.

Maluszynski, M. and Szarejko, I. (2005). Induced mutations in the Green and Gene Revolutions. In Tuberosa R., Phillips R.L., Gale M (eds.). Proceedings of the International Congress "In the Wake of the Double Helix: From the Green Revolution to the Gene Revolution", 27-31 May 2003, Bologna, Italy, pp. 403–425.

Maresca, J.A., Graham, J.E., and Bryant, D.A. (2008). The biochemical basis for structural diversity in the carotenoids of chlorophototrophic bacteria. Photosynth. Res. **97**: 121–140.

Márton, M.L., Cordts, S., Broadhvest, J., and Dresselhaus, T. (2005). Micropylar pollen tube guidance by egg apparatus 1 of maize. Science. **307**: 573–576.

Mascarenhas, J.P. (1989). The male gametophyte of flowering plants. Plant Cell **1**: 657–664.

Mascher, M. et al. (2013). Barley whole exome capture: a tool for genomic research in the genus *Hordeum* and beyond. Plant J. **76**: 494–505.

Mascher, M., Jost, M., Kuon, J.-E., Himmelbach, A., Aßfalg, A., Beier, S., Scholz, U., Graner, A., and Stein, N. (2014). Mapping-by-sequencing accelerates forward genetics in barley. Genome Biol. **15**: R78.

Mayer, K.F.X., Waugh, R., Brown, J.W.S., Schulman, A., Langridge, P., Platzer, M., Fincher, G.B., Muehlbauer, G.J., Sato, K., Close, T.J., Wise, R.P., and Stein, N. (2012). A physical, genetic and functional sequence assembly of the barley genome. Nature **491**: 711–716.

Men, S., Boutté, Y., Ikeda, Y., Li, X., Palme, K., Stierhof, Y.-D., Hartmann, M.-A., Moritz, T., and Grebe, M. (2008). Sterol-dependent endocytosis mediates post-cytokinetic acquisition of PIN2 auxin efflux carrier polarity. Nat. Cell Biol. **10**: 237–44.

Miller, M.B., Haubrich, B. a, Wang, Q., Snell, W.J., and Nes, W.D. (2012). Evolutionarily conserved Delta(25(27))-olefin ergosterol biosynthesis pathway in the alga *Chlamydomonas reinhardtii*. J. Lipid Res. **53**: 1636–45.

Moreau, R., Whitaker, B.D., and Hicks, K.B. (2002). Phytosterols, phytostanols, and their conjugates in foods: structural diversity, quantitative analysis, and health-promoting uses. Prog. Lipid Res. **41**: 457–500.

Mori, T., Kuroiwa, H., Higashiyama, T., and Kuroiwa, T. (2006). *GENERATIVE CELL SPECIFIC 1* is essential for angiosperm fertilization. Nat. Cell Biol. **8**: 64–71.

Moss, G.P. (1989). The nomenclature of steroids. Pure Appl. Chem. **61**: 1783–1822.

Muschietti, J., Dircks, L., Vancanneyt, G., and McCormick, S. (1994). LAT52 protein is essential for tomato pollen development : pollen expressing antisense *LAT52* RNA hydrates and germinates abnormally and cannot achieve fertilization.

Plant J. **6**: 321–338.

Nagata, N., Suzuki, M., Yoshida, S., and Muranaka, T. (2002). Mevalonic acid partially restores chloroplast and etioplast development in *Arabidopsis* lacking the non-mevalonate pathway. Planta **216**: 345–350.

Niko, Y., Didier, P., Mely, Y., Konishi, G., and Klymchenko, A.S. (2016). Bright and photostable push-pull pyrene dye visualizes lipid order variation between plasma and intracellular membranes. Sci. Rep. **6**: 1–9.

Okuda, S. et al. (2009). Defensin-like polypeptide LUREs are pollen tube attractants secreted from synergid cells. Nature **458**: 357–361.

Olsen, O., Wang, X., and von Wettstein, D. (1993). Sodium azide mutagenesis: preferential generation of A.T-->G.C transitions in the barley *Ant18* gene. Proc. Natl. Acad. Sci. U. S. A. **90**: 8043–7.

Owais, W.M., Zarowitz, M.A., Gunovich, R.A., Hodgdon, A.L., Kleinhofs, A., and Nilan, R.A. (1978). A mutagenic *in vivo* metabolite of sodium azide. Mutat. Res. **53**: 355–358.

Pacurar, D., Pacurar, M., Pacurar, A., Gutierrez, L., and Bellini, C. (2014). A novel viable allele of *Arabidopsis* CULLIN1 identified in a screen for superroot2 suppressors by next generation sequencing-assisted mapping. PLoS One **9**: e100846.

Page, D.R. and Grossniklaus, U. (2002). The art and design of genetic screens: *Arabidopsis thaliana*. Nat. Rev. Genet. **3**: 124–36.

Palanivelu, R. and Preuss, D. (2006). Distinct short-range ovule signals attract or repel *Arabidopsis thaliana* pollen tubes *in vitro*. BMC Plant Biol. **6**: 7.

Phillips, M.A., León, P., Boronat, A., and Rodríguez-Concepción, M. (2008). The plastidial MEP pathway: unified nomenclature and resources. Trends Plant Sci. **13**: 619–623.

Pulido, P., Llamas, E., Llorente, B., Ventura, S., Wright, L.P., and Rodríguez-Concepción, M. (2016). Specific Hsp100 chaperones determine the fate of the first enzyme of the plastidial isoprenoid pathway for either refolding or degradation by the stromal Clp protease in *Arabidopsis*. PLoS Genet. **12**: 1–19.

Pulido, P., Perello, C., and Rodríguez-Concepción, M. (2012). New insights into plant Isoprenoid metabolism. Mol. Plant **5**: 964–967.

Qin, Y. and Yang, Z. (2011). Rapid tip growth: insights from pollen tubes. Semin. Cell

Dev. Biol. **22**: 816–24.

Rahier, A. and Benveniste, P. (1989). Mass spectral identification of phytosterols. in analysis of sterols and other biologically significant steroids, pp. 223–250.

Rédei, G.P. and Koncz, C. (1992). Classical mutagenesis. In Methods in *Arabidopsis* Research, Koncz C., Chua N.-H. and Schell, J. (eds). World Scientific Publishing Co Inc., pp. 16–82.

Rodríguez-Concepción, M. and Boronat, A. (2015). Breaking new ground in the regulation of the early steps of plant isoprenoid biosynthesis. Curr. Opin. Plant Biol. **25**: 17–22.

Rohmer, M. (2007). Diversity in isoprene unit biosynthesis: The methylerythritol phosphate pathway in bacteria and plastids. Pure Appl. Chem. **79**: 739–751.

Rohmer, M. (1999). The discovery of a mevalonate-independent pathway for isoprenoid biosynthesis in bacteria, algae and higher plants. Nat. Prod. Rep. **16**: 565–574.

Sáenz, J.P., Grosser, D., Bradley, A.S., Lagny, T.J., Lavrynenko, O., Broda, M., and Simons, K. (2015). Hopanoids as functional analogues of cholesterol in bacterial membranes. Proc. Natl. Acad. Sci. U. S. A. **112**: 11971–6.

Salvi, S., Druka, A., Milner, S.G., and Gruszka, D. (2014). Induced genetic variation, TILLING and NGS-based cloning. In Biotechnological Approaches to Barley Improvement, J. Kumlehn and N. Stein, eds, Biotechnology in Agriculture and Forestry. (Springer Berlin Heidelberg), pp. 287–310.

Schaeffer, A., Bronner, R., Benveniste, P., and Schaller, H. (2001). The ratio of campesterol to sitosterol that modulates growth in *Arabidopsis* is controlled by STEROL METHYLTRANSFERASE 2;1. Plant J. **25**: 605–615.

Schaller, H. (2003). The role of sterols in plant growth and development. Prog. Lipid Res. **42**: 163–75.

Schaller, H., Bouvier-Navé, P., and Benveniste, P. (1998). Overexpression of an *Arabidopsis* cDNA encoding a sterol-C24(1)-methyltransferase in tobacco modifies the ratio of 24-methyl cholesterol to sitosterol and is associated with growth reduction. Plant Physiol. **118**: 461–469.

Schaller, H., Grausem, B., Benveniste, P., Chye, M., Tan, C., Song, Y., and Chua, N.-H. (1995). Expression of the Hevea brasiliensis (H.B.K.) Müll . Arg . 3-hydroxy-3-methylglutaryl-coenzyme A reductase 1 in tobacco results in sterol

overproduction. Plant Physiol **109**: 761–770.

Schneider, J.C., Suzanne, H., and Somerville, C.R. (1995). Chilling-sensitive mutants of *Arabidopsis*. Plant Mol. Biol. Report. **13**: 11–17.

Shi Ni Loo, C., Siu Kei Lam, N., Yu, D., Su, X., and Lu, F. (2016). Artemisinin and its derivatives in treating protozoan infections beyond malaria. Pharmacol. Res. **117**: 192–217.

Sonawane, P.D. et al. (2016). Plant cholesterol biosynthetic pathway overlaps with phytosterol metabolism. Nat. Plants **3**: 16205.

Sprunck, S., Rademacher, S., Vogler, F., Gheyselinck, J., Grossniklaus, U., and Dresselhaus, T. (2012). Egg Cell-Secreted EC1 triggers sperm cell activation during double fertilization. Science. **338**: 1093–1097.

Strobel, G.A., Stierle, A., and Hess, W.M. (1993). Taxol formation in yew - *Taxus*. Plant Sci. **92**: 1–12.

Sun, H. and Schneeberger, K. (2015). SHOREmap v3.0: fast and accurate identification of causal mutations from forward genetic screens. In Methods in Molecular Biology Vol. 1284 (Alonso, J.M. and Stepanova, A.N. eds., Springer Science+Business Media New York), pp. 381–395.

Suzuki, M., Kamide, Y., Nagata, N., Seki, H., Ohyama, K., Kato, H., Masuda, K., Sato, S., Kato, T., Tabata, S., Yoshida, S. and Muranaka, T. (2004). Loss of function of *3-hydroxy-3-methylglutaryl coenzyme A reductase 1 (HMG1)* in *Arabidopsis* leads to dwarfing, early senescence and male sterility, and reduced sterol levels. Plant J. **37**: 750–761.

Suzuki, M., Nakagawa, S., Kamide, Y., Kobayashi, K., Ohyama, K., Hashinokuchi, H., Kiuchi, R., Saito, K., Muranaka, T., and Nagata, N. (2009). Complete blockage of the mevalonate pathway results in male gametophyte lethality. J. Exp. Bot. **60**: 2055–64.

Takahagi, K., Uehara-Yamaguchi, Y., Yoshida, T., Sakurai, T., Shinozaki, K., Mochida, K., and Saisho, D. (2016). Analysis of single nucleotide polymorphisms based on RNA sequencing data of diverse bio-geographical accessions in barley. Sci. Rep. **6**: 33199.

Tong, H., Xiao, Y., Liu, D., Gao, S., Liu, L., Yin, Y., Jin, Y., Qian, Q., and Chu, C. (2014). Brassinosteroid regulates cell elongation by modulating gibberellin metabolism in rice. Plant Cell **26**: 4376–4393.

Twell, D., Wing, R., Yamaguchi, J., and McCormick, S. (1989). Isolation and expression of an anther-specific gene from tomato. Mol. Gen. Genet. **217**: 240–5.

Unterholzner, S.J., Rozhon, W., Papacek, M., Ciomas, J., Lange, T., Kugler, K.G., Mayer, K.F., Sieberer, T., and Poppenberger, B. (2015). Brassinosteroids are master regulators of gibberellin biosynthesis in *Arabidopsis*. Plant Cell **27**: 1–13.

Urich, K. (2013). Comparative Animal Biochemistry (Springer-Verlag Berlin Heidelberg GmbH).

Verma, V., Ravindran, P., and Kumar, P.P. (2016). Plant hormone-mediated regulation of stress responses. BMC Plant Biol. **16**: 86.

Verslues, P.E. (2016). ABA and cytokinins: challenge and opportunity for plant stress research. Plant Mol. Biol. **91**: 629–640.

Vranová, E., Coman, D., and Gruissem, W. (2012). Structure and dynamics of the isoprenoid pathway network. Mol. Plant **5**: 318–333.

Vriet, C., Russinova, E., and Reuzeau, C. (2012). Boosting crop yields with plant steroids. Plant Cell **24**: 842–57.

Wang, P. and Grimm, B. (2015). Organization of chlorophyll biosynthesis and insertion of chlorophyll into the chlorophyll-binding proteins in chloroplasts. Photosynth. Res. **126**: 189–202.

Wilkinson, S., Kudoyarova, G.R., Veselov, D.S., Arkhipova, T.N., and Davies, W.J. (2012). Plant hormone interactions: Innovative targets for crop breeding and management. J. Exp. Bot. **63**: 3499–3509.

Wollam, J. and Antebi, A. (2011). Sterol regulation of metabolism, homeostasis, and development. Annu. Rev. Biochem. **80**: 885–916.

Wu, T.D. and Nacu, S. (2010). Fast and SNP-tolerant detection of complex variants and splicing in short reads. Bioinformatics **26**: 873–881.

Xing, S., Miao, J., Li, S., Qin, G., Tang, S., Li, H., Gu, H., and Qu, L.-J. (2010). Disruption of the 1-deoxy-D-xylulose-5-phosphate reductoisomerase (DXR) gene results in albino, dwarf and defects in trichome initiation and stomata closure in *Arabidopsis*. Cell Res. **20**: 688–700.

Yates, A. et al. (2016). Ensembl 2016. Nucleic Acids Res. **44**: D710–D716.

Zhai, S., Xia, X., and He, Z. (2016). Carotenoids in staple cereals: Metabolism, regulation, and genetic manipulation. Front. Plant Sci. **7**: 1–13.

Zuryn, S., Le Gras, S., Jamet, K., and Jarriault, S. (2010). A strategy for direct

mapping and identification of mutations by whole-genome sequencing. Genetics **186**: 427–430.

Claire VILLETTE

Isoprenoid biosynthesis, specificities and homeostasis in plants. Genetic approach for the identification of regulators by screening for suppressors of growth defect.

Résumé

Les plantes produisent une grande diversité de produits naturels parmi lesquels les isoprénoïdes prédominent. Ces molécules ont des fonctions essentielles pour la croissance et le développement : hormones végétales, régulateurs de croissance comme les brassinostéroïdes, pigments photosynthétiques, tous agissant sur des processus biologiques majeurs. Ainsi, la germination, la floraison, la tolérance aux stress thermiques et hydriques, ou la production de semences, sont contrôlées par l'action d'isoprénoïdes. Le but de mon projet est d'identifier par une sélection génétique les éléments régulateurs de l'homéostasie des isoprénoïdes. Pour cela, j'ai réalisé le criblage de suppresseurs de défaut de croissance dans deux mutants de biosynthèse d'isoprénoïdes chez *Arabidopsis thaliana* et un mutant de signalisation de brassinostéroïdes chez *Hordeum vulgare*. J'ai par ailleurs étudié la voie de biosynthèse de stérols spécifique ayant lieu dans un type cellulaire particulier, le tube pollinique en croissance.

Mots clés : Isoprénoïdes, stérols, homéostasie, criblage de suppresseurs, *Arabidopsis thaliana*, *Hordeum vulgare*, pollen.

Summary

Plants produce a great diversity of natural compounds, among which isoprenoids prevail. These molecules have essential functions for growth and development: plant hormones, growth regulators as brassinosteroids, photosynthetic pigments, acting on major biological processes. Thus, germination, flowering, heat and draught stress tolerance, or seed production are controlled by the action of isoprenoids. The aim of my project is to identify by genetic selection the regulators of isoprenoid homeostasis. For this, I carried out genetic screens for suppressors of growth defects in two isoprenoid biosynthesis deficient *Arabidopsis thaliana* mutants and a brassinosteroid signaling *Hordeum vulgare* mutant. The second part of my project was focused on the specific sterol biosynthetic pathway occurring in a specialized cell type, the germinating pollen tube.

Keywords: Isoprenoids, sterols, homeostasis, suppressor screen, *Arabidopsis thaliana*, *Hordeum vulgare*, pollen.